DISCLAIMER NOTICE

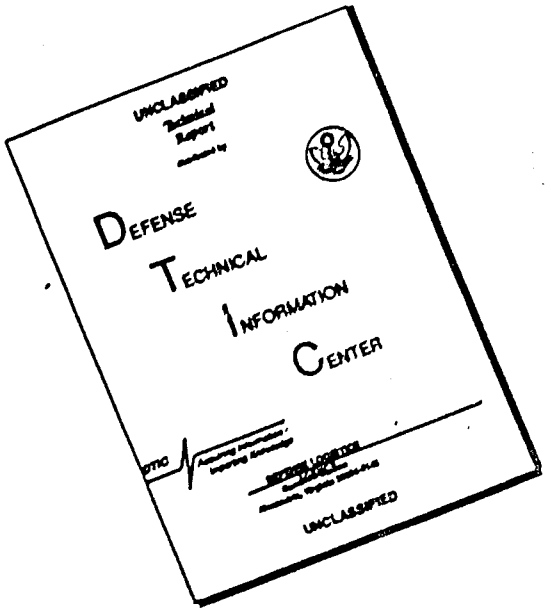

THIS DOCUMENT IS BEST QUALITY AVAILABLE. THE COPY FURNISHED TO DTIC CONTAINED A SIGNIFICANT NUMBER OF PAGES WHICH DO NOT REPRODUCE LEGIBLY.

RADC-TDR-63-37

January 1963

[illegible] ANALYSIS STUDY

[illegible] SUMMARY

[illegible] & BAILEY,
[illegible] Corporation
[illegible], D.C. Alexandria, Va.

[illegible] CONTRACT AF [illegible]02)-2665

Prepared for
Rome Air Development Center
Air Force Systems Command
UNITED STATES AIR FORCE
Griffiss Air Force Base, New York

RADC-TDR-63-37

Interference Analysis Study

PUBLICATION REVIEW

This report has been reviewed and is approved.

Approved:
HOLLIS J. HEWITT
Task Engineer
Applied Research Branch

Approved:
SAMUEL D. ZACCARI, Chief
Electromagnetic Vulnerability Lab
Directorate of Communications

RADC-TDR-63-37 January 1963

INTERFERENCE ANALYSIS STUDY
INTERIM SUMMARY

JANSKY & BAILEY
A Division of Atlantic Research Corporation
Washington, D.C. Alexandria, Va.

CONTRACT NUMBER AF 30(602)-2665

Prepared for
Rome Air Development Center
Air Force Systems Command
UNITED STATES AIR FORCE
Griffiss Air Force Base, New York

Jansky & Bailey

A Division of Atlantic Research Corporation

Alexandria, Va.
Contract Number AF 30(602)-2665

DISTRIBUTION LIST FOR CONTRACT REPORTS

	No. of Copies
RADC (RAUMA ATTN: Mr. H.J. Hewitt) Griffiss AFB, NY	5
RADC (RAAPT) Griffiss AFB, NY	1
RADC (RAALD) Griffiss AFB, NY	1
GEEIA (ROZMCAT) Griffiss AFB, NY	1
RADC (RAIS, ATTN: Mr. Mallcy Griffiss AFB, NY	1
US Army Electronics R&D Labs Liaison Officer RADC Griffiss AFB, NY	1
AUL (3T) Maxwell AFB, Ala	1
ASD (ASAPRD) Wright-Patterson AFB, Ohio	1
Air Force Field Representative Naval Research Lab. ATTN: Code 1010 Washington 25, D.C.	1
Commanding Officer US Army Electronics R&D Labs. ATTN: SELRA/SL-ADT Ft. Monmouth, NJ	1
RTD (RTGS) Bolling AFB Washington 25, D.C.	1
AFSC (SCSE) Andrews AFB Washington 25, D.C.	1
Commanding General US Army Electronics Proving Ground ATTN: Technical Documents Library Ft. Huachuca, Arizona	1

Bureau of Naval Weapons
Main Navy Bldg.
Washington 25, D.C.
ATTN: Technical Librarian, DLl-3 1

NAFEC Library
Bldg. 3
Atlantic City, NJ 1

Georgia Institute of Technology
ATTN: Mr. Bruce Warren
Atlanta 13, Georgia 1

University of Pennsylvania
ATTN: Prof. O.D. Salati
34 Walnut Street
Philadelphia 4, Pennsylvania 1

USASRDL (Mr. S. Weitz)
Ft. Monmouth, NJ 1

ESD (ESRDV, Mr. Dix)
L.G. Hanscom Field
Bedford, Mass. 1

National Security Agency
ATTN: Mr. J.C. McKinney (R-312)
Fort George G. Meade, Maryland 1

RTD (RTHE, Mr. Tepper)
Bolling AFB
Washington 25, D.C. 1

Electro-Mechanics Co.
ATTN: Dr. F.J. Morris
P.O. Box 802
Austin 64, Texas 1

U.S. Department of Commerce
National Bureau of Standards
Boulder Laboratories
Boulder, Colorado
ATTN: A. V. Corrny 1

Ohio State University
Dept. of Electrical Engineering
Antenna Laboratory (Mr. L. Peters, Jr.)
Columbus 10, Ohio 1

Armour Research Foundation
of Illinois Institute of Technology
ATTN: Mr. B. Ebstien
Technology Center
Chicago 16, Illinois 1

Radiation Incorporated
ATTN: Mr. W.F. Quinlivan
P.O. Box 37
Melbourne, Florida 1

ASTIA (TISIA-2) Arlington Hall Station Arlington 12, VA.	10
Airborne Instruments Laboratory ATTN: Mr. Stanley Becker Deer Park, Long Island, NY	1
Frederick Research Corporation ATTN: Mr. A.H. Sullivan, Jr. 2601 University Boulevard, West Wheaton, Maryland	1
RTD (RTHE, Co. O.J. Schulte) Bolling AFB Washington 25, D.C.	1
Commanding Officer & Director U.S. Navy Electronics Lab. (Lib) San Diego 52, Calif.	1
ASD (ASRNC-2 Mr. H. Bartman) Wright-Patterson AFB, Ohio	1
Electromagnetic Compatibility Analysis Center ATTN: Mr. B. Lindeman U.S. Naval Engineering Experimental Station Annapolis, Maryland	2
RADC (RAUMM, Mr. Porter) Griffiss AFB, NY	1
Navy Air Navigation Electronic Project Weapons System Test Division (Mr. O.D. Stewart) Naval Air Test Center Patuxant River, Maryland	1
Melpar, Inc. ATTN: Mr. W. Myers Falls Church, Virginia	1

ABSTRACT

The accompanying report describes a portion of the work undertaken by Jansky & Bailey, A Division of the Atlantic Research Corporation, under Contract AF 30(602)-2665 with the Rome Air Development Center. This report is an interim summary for the period May 1962 to December 1962.

Emphasis is upon new material, with review of the highlights of previous work where necessary. A summary of the basic prediction methods is given along with a detailed sample prediction. The results of the latest prediction validation experiment are presented.

Methods for handling all transmitter outputs except non-harmonically related spurious outputs common to such output devices as magnetrons have been developed. A statistical model for the magnetron is presented, and a basic study of magnetron output frequency relationships is summarized.

The fundamental receiver analysis functions are reviewed. Methods for handling the nonlinear characteristics of the receiver mixer stages have been reviewed extensively in the past. In this report, sample pre-mixer and post-mixer selectivity analyses are presented in detail for several sample radar transmitters.

A complete pattern distribution function analysis for a typical radar antenna is presented. Pattern distribution function variations for various elevation angles are examined. In addition, a site effect statistic which has been developed and is currently in use is presented.

Approved: Kenneth G. Heisler, Jr.
Kenneth G. Heisler, Jr.
Project Manager

Approved: Delmer C. Ports
Delmer C. Ports
Technical Director

The work reported herein was carried out by the following members of the staff of Jansky & Bailey, A Division of Atlantic Research Corporation, Shirley Highway and Edsall Road, Alexandria, Virginia:

Thomas E. Baldwin, Jr.
William G. Duff
Frank E. Ferrante
Kenneth G. Heisler, Jr.
A. Ray Howland
James P. Kallenborn
James T. Luck
Delmer C. Ports
Dr. Henry R. Reed
Charles E. Sampson
William P. Seneker
Jack R. Vaill

TABLE OF CONTENTS

LIST OF ILLUSTRATIONS

LIST OF TABLES

Section 1

INTRODUCTION

This technical note is an interim summary for contract AF 30(602)-2665. This project is a fourth phase continuation of an interference prediction and analysis study originally conducted under contract AF 30(602)-1934. During the previous contract an interference prediction process was developed and applied to provide interference predictions for a number of existing equipment complexes. The input functions required by the prediction process were also the subject of extensive study during the previous contract. Mathematical forms consistent with the needs of the prediction process were derived and in turn evaluated for large classes of equipment now in use.

Emphasis during the current work is upon updating the interference prediction methods themselves and upon enlarging the range of available input functions so that an ever-increasing panorama of interference situations may be considered. Particular emphasis is upon those potential interference problems associated with complexes containing large high-powered equipments.

A continuous validation of the prediction methods and each of the inputs which are generated is a constant theme throughout the project. Attention is also directed toward formalization of the prediction methods which have been developed to date so that they may eventually be used by engineers in "handbook" fashion.

It is not possible to adequately review here all of the results that have been accomplished to date which serve as background to the material presented in the following pages. However, the remainder of this introduction will serve as a very brief resume of past results with an emphasis upon the major problem areas which still remain. For more detailed background, the reader is referred to the following report and the references contained therein.

Interference Analysis Study, Jansky & Bailey , A Division of Atlantic Research Corporation, Alexandria, Virginia RADC-TDR-61-312, Contract No. AF 30(602)-1934; January, 1962.

In addition a two-volume propagation handbook which presents propagation data for interference analysis has been completed.

> Propagation Data for Interference Analysis, Jansky & Bailey, A Division of Atlantic Research Corporation, Alexandria, Virginia, Vols. I and II, RADC-TDR-61-313, Contract No. AF 30(602)-1934; January, 1962.

These two volumes contain the methods and input data required to compute the propagation function for all common types of propagation up to 100 kMc.

The pertinent performance characteristics for transmitters, receivers, antennas and propagation phenomena have been studied in detail. In addition adequate methods for combining the functional representations of these performance parameters to provide the means for interference prediction and analysis have been developed.

Large uncertainties are inherent to each of the required prediction parameters. In most cases, these uncertainties can only be handled mathematically in a statistical sense. Thus each of the input functions in some respect is statistically defined and the interference prediction process includes elements of statistical analysis.

The statistical nature of transmitter output spectra has been studied in detail, both analytically and with the aid of measured data. Statistical representations for the harmonic outputs of transmitters have been developed and actual numerical values have been tabulated for a significant number of equipments. A graphical numerical method has been developed for predicting the harmonic output levels from tube-type transmitters. The statistical representations employed provide adequate detail for the amplitude of undesired output from transmitters at all spurious output frequencies, both harmonically related and nonharmonically related. For nonmicrowave transmitters almost all spurious outputs occur at either a harmonic of the operating frequency or a harmonic of the master oscillator frequency. Thus a statistical representation of the possible output amplitudes coupled with the regular harmonic pattern of possible output frequencies provides the means of completely specifying mathematically the output spectra from nonmicro-

wave transmitters.

For most microwave tubes, except such devices as the magnetron, the predominant spurious outputs occur at frequencies which are harmonically related to the operating frequency. Thus, except for the magnetron and a few related devices, an adequate representation for the spurious output levels and frequencies is already established. A recent analysis, leading toward a representation of the output spectra for magnetron devices is presented in Section 3 of this report.

In addition to the spurious output levels and frequencies from transmitters, the modulation envelope about each possible transmitter output is also important. The fundamental frequency of a transmitter has energy representing modification distributed about the carrier frequency. In addition, each spurious output from the transmitter, whether harmonically related to the fundamental or not, has some distribution of energy about it. An adequate representation of these modulation envelopes about the fundamental frequency and each spurious output has been the subject of extensive study. A function representing the interaction between the energy distributed about any particular spurious output from a transmitter and any particular spurious response of a receiver has been developed. This function is called the "bandwidth" function and is currently used in the prediction process.

Most significant spurious response frequencies for superhetrodyne receivers can be predicted from the p-q equation which is as follows.

$$f_i = \frac{\left| pf_{LO} \pm f_{IF} \right|}{q}$$

where

f_i = the spurious response frequencies
f_{LO} = the local oscillator frequency
f_{IF} = the intermediate frequency of the receiver
p and q = any positive integers.

Although the p-q equation serves to predict the major spurious response frequencies for superhetrodyne receivers, the prediction of the spurious response amplitudes is far more complicated. Mathematical forms, similar to those used to represent the spurious output levels from transmitters have been developed to represent the spurious response amplitudes for receivers. These mathematical forms have been evaluated for a significant number of receivers and are currently in use in the prediction process. Section 4 of this report discusses the receiver functions in more detail and contains a sample analysis for a radar receiver.

For antennas, the three parameters used for interference prediction and analysis are the pattern distribution functions, the major-lobe gain of the antenna and the site effect. For the purpose of analyzing the pattern behavior of antennas, all antennas have been divided into several generic classes. Because of large statistical uncertainties which are inherent to the transmitter and receiver functions and the propagation mechanism, pattern distribution functions for the lower gain and more nearly nondirectional antennas are of minor importance. However, the highly directional, high-gain antennas such as the feed plus reflector types and the large array antennas are of primary importance. A great deal of insight into the pattern distribution function for these large antennas at both fundamental and spurious frequencies has been obtained through the thorough analysis of antenna pattern measurements available through the current spectrum signature collection program. The most recent analyses are presented in Section 5 of this report. The site effect statistic which is currently in use is also presented in Section 5.

Section 2 of this report presents a sample interference prediction using the methods which have been developed for interference prediction and analysis. The methods themselves are described in the final report for contract AF 30(602)-1934 which was referenced at the beginning of this introduction. The sample calculation which is presented is for an actual equipment configuration which exists at the U.S. Air Force Test Facility in Verona, New York. The prediction results are compared to actual interference measurements which were made by Air Force personnel at the Verona Test Facility.

In addition to over-all interference measurements the strength of the predominant environmental components were measured. These latter measurements provide the basis for an independent validation of the propagation statistics and transmitter output representations currently in use.

Section 2
INTERFERENCE PREDICTION

2.1 Introduction

Before presenting the details of a sample prediction, the highlights of the prediction process which was used will be reviewed. Additional detail may be obtained by consulting the final report for Phase II of the work now under discussion.[1] The general discussion of the process, coupled with actual details of a specific sample problem should give the reader a valuable insight into the fundamental features of the prediction process. The exposition of the prediction process will be begun by introducing the functional forms that are used for each of the input functions. Next, how these functional forms are combined to produce a rapid culling result will be presented. Then the process of frequency culling will be discussed, and finally, the translation from frequency cull answer to the probability of interference will be presented.

2.2 General Form of the Input Functions

2.2.1 Transmitter Power Output, P_T

For the rapid culling step, the most efficient approximation to the transmitter output function has been shown to be a linear relationship between transmitter power output expressed in decibels and the logarithm of frequency. The output power expressed in this manner represents a level which is not exceeded with a probability of 90 percent.

The rapid cull procedure involves adding five statistical numbers to obtain a measure in decibels of the interference. For the particular types of statistical distributions involved, if five statistical numbers are added together and if it is 90 percent probable that each of them is not exceeded, then it is 99.9 percent probable that the sum is not exceeded. Thus, the cases that do not pass the rapid cull can be eliminated with a 99.9 percent

1. Interference Analysis Study, Jansky & Bailey, A Division of Atlantic Research Corporation, Alexandria, Va., Vol. I-2, Chap. 3, RADC TR-61-15A, Contract No. AF-30(602)-1934; January, 1961.

certainty that no case of interference is ignored.

To simplify the computations, power output and frequency are normalized to the tuned frequency characteristics. This is shown in Eqs. 1 and 2 for the rapid cull estimate of the power output from a transmitter. Equation 1 is used for frequencies above the fundamental frequency of the transmitter and 2 is used for frequencies below the fundamental frequency:

$$P_T = P_O - \left[A \log \frac{f}{f_o^t} + B \right] \quad \text{for } f_o^t < f < f_u^t \tag{1}$$

$$P_T = P_O - \left[A' \log \frac{f}{f_o^t} + B' \right] \quad \text{for } f_\ell^t < f < f_o^t \tag{2}$$

where

P_O = fundamental power output of the transmitter

f_o^t = tuned frequency of the transmitter

f_u^t = highest frequency which need be considered

f_ℓ^t = lowest output frequency which need be considered

A, A', B, B' = arbitrary constants whose value depends upon the particular transmitter under consideration.

The function represented by Eqs. 1 and 2 are shown graphically in Figure 2-1. The geometrical interpretation of the constants A,A',B and B' can be seen from Figure 2-1. The upper and lower frequency bounds can be determined in the following way. The lowest output frequency which need be considered, f_ℓ^t, may be taken as the master oscillator frequency for those equipments which use a master oscillator. In the absence of any information at all, the general rule-of-thumb has been adopted that f_ℓ^t will be taken as $0.01\ f_o^t$, and f_u^t, the highest output frequency which need be considered as $100\ f_o^t$. For systems employing waveguides the f_ℓ^t is taken to be the waveguide cutoff frequency.

If desired, more than two straight lines can be used to approximate the power output from a transmitter. Each line is used in the prediction and the answers derived from each line are

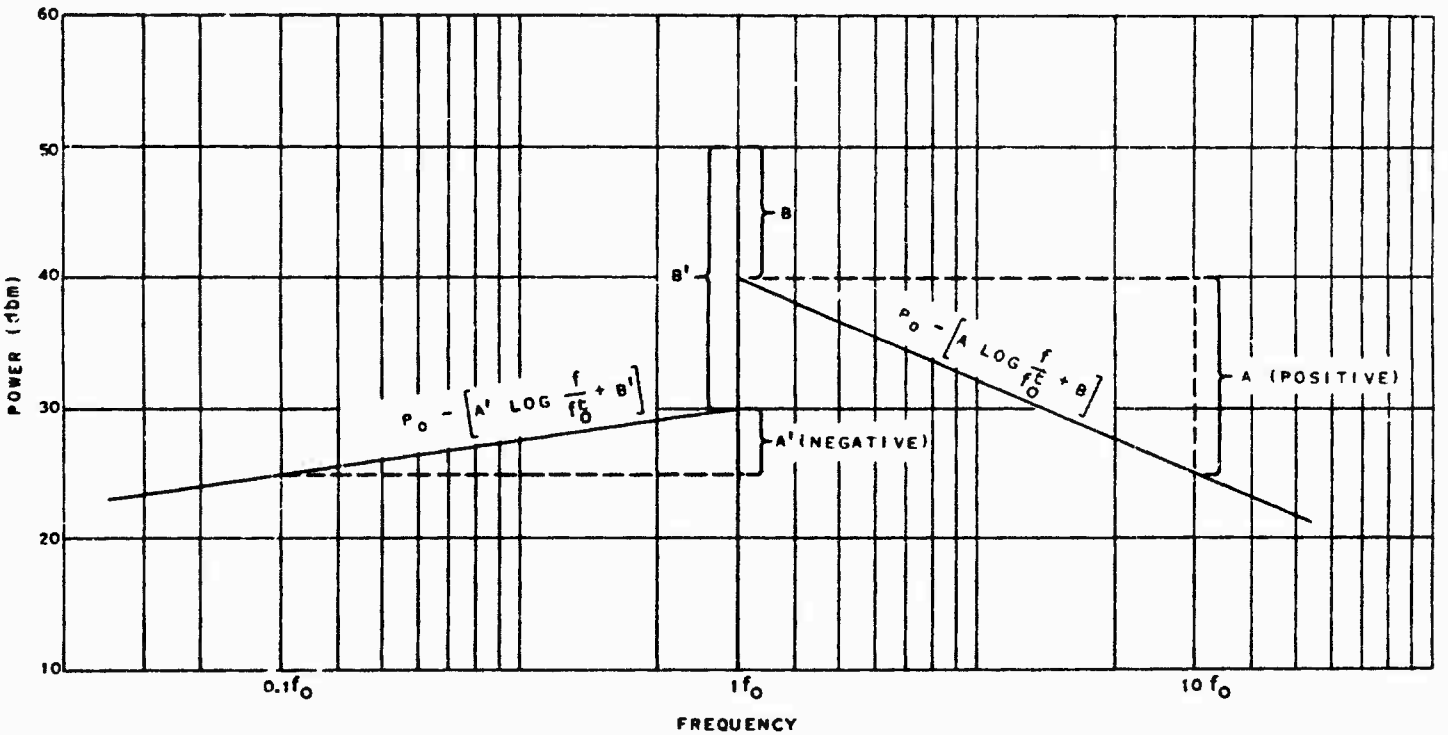

Figure 2-1. Illustration of the Rapid Cull Estimate to P_T.

applied to those cases for which the line is valid.

2.2.2 Power Required to Interfere with the Receiver, P_R

The receiver functions are treated in a manner analogous to the transmitter functions and are defined by Eqs. 3 and 4. Equation 3 applies to the frequencies above the tuned frequency of the receiver and Eq. 4 applies to the frequencies below the tuned frequency of the receiver. The receiver function is normalized to the fundamental sensitivity of the receiver S_o, and the fundamental frequency of the receiver, f_o^r.

$$P_R = S_o + I \log \frac{f}{f_o^r} + J \quad \text{for } f_o^r < f < f_u^r \tag{3}$$

$$P_R = S_o + I' \log \frac{f}{f_o^r} + J' \quad \text{for } f_\ell^r < f < f_o^r \tag{4}$$

where

S_o = maximum sensitivity of the receiver

f_o^r = tuned frequency of the receiver

f_u^r = highest frequency for which spurious responses need be considered

f_ℓ^r = lowest frequency for which spurious responses need be considered

I, I', J, J' = arbitrary constants whose value depends upon the particular receiver under study.

It may be desirable to use several straight lines for the receiver function. If so, then each line is used in the prediction process and the answer obtained is used for those cases to which the particular line applies. A separate line is conveniently used for each q of the p - q equation.[2] The line associated with the q=2 responses is generally taken to be a constant 15 db below the q=1 responses, and q=3 and 4 responses are generally taken to be 20 db below the q=1 responses. This rule allows a simple correction factor to be applied directly in the final stages of the frequency cull to account for these less important responses.

2. See Section 2.4.

2.2.3 Antenna Gain

The antenna function is chosen as the best straight-line fit to a plot of maximum or main-lobe antenna gain versus the logarithm of frequency. The working form of the antenna approximation is consistent with that for the transmitter or receiver and is given by Eqs. 5 and 6 for the transmitting antenna and by Eqs. 7 and 8 for the receiving antenna. The antenna function is normalized to the main-lobe gain of the antenna at the fundamental frequency of its companion transmitter or receiver. The antenna function is also normalized to the fundamental frequency of the companion transmitter or receiver.

$$G_T = Y_o^t - \left[C \log \frac{f}{f_o^t} + D\right] \text{ for } f_o^t < f < f_u^t \tag{5}$$

$$G_T = Y_o^t - \left[C' \log \frac{f}{f_o^t} + D'\right] \text{ for } f_\ell^t < f < f_o^t \tag{6}$$

where

Y_o^t = maximum lobe gain of the transmitting antenna at f_o^t

C, C', D, D' = arbitrary constants whose value depends upon the specific antenna under study

and f_o^t, f_u^t, f_ℓ^t are as defined for the transmitter.

$$G_R = Y_o^r - \left[G \log \frac{f}{f_o^r} + H\right] \text{ for } f_o^r < f < f_u^r \tag{7}$$

$$G_R = Y_o^r - \left[G' \log \frac{f}{f_o^r} + H'\right] \text{ for } f_\ell^r < f < f_o^r \tag{8}$$

where

Y_o^r = maximum lobe gain of the receiving antenna at f_o^r

G,G',H,H' = arbitrary constants whose value depends upon the particular antenna under study

and f_o^r, f_ℓ^r, f_u^r are as defined for the receiver.

2.2.4 Propagation Loss

For closely spaced equipments (i.e., line-of-sight) the median propagation function has been found to be one that is similar to the function for free-space transmission loss. The function is considered to have a normally distributed statistic associated with it. The function is linear in the logarithm of frequency and the logarithm of distance. The function is given by Eq. 9.

$$L = 20(\log f + \log d) + 37 \qquad (9)$$

where

f = radio frequency in megacycles

d = distance in miles between the potentially interfering transmitter and its victim receiver.

2.3 Rapid Cull

The rapid cull separates those situations that pass the criteria for interference from those that do not when upper estimates are used for the intput functions. The condition for interference is

$$P_T - P_R + G_T + G_R - L > 0 \qquad (10)$$

and the rapid cull is concerned with the sum on the left in the above inequality. Reviewing the functional forms that have just been introduced for each of the terms in Eq. 10, one readily sees that the sum will take the form

$$N \log f + M \qquad (11)$$

where N and M are independent of the radio freuqncy, f.

By collecting all of the approriate terms concerned with the frequency range above both the transmitter and receiver fundamental frequency the M and N are given by Eqs. 12 and 13.

$$M = P_o + A \log f_o^t - B - S_o + I \log f_o^r - J + Y_o^t + C \log f_o^t - D$$

$$+ Y_o^r + G \log f_o^r - H - 20 \log d - 37 \qquad (12)$$

$$N = - A - C - G - I - 20 \qquad (13)$$

For the region below both the transmitter and receiver fundamental frequencies, M and N are denoted as M' and N' and are given by Eqs. 12 and 13 with A,B,C,D,G,H, I and J replaced by their corresponding primed values. For the region between the two fundamental frequencies, M and N are denoted as M° and N° and are given by Eqs. 12 and 13 with G,H, I and J replaced by their corresponding primed values if $f_o^r > f_o^t$ and with A,B,C and D replaced by their corresponding primed values if $f_o^t > f_o^r$.

For ease in computation, M is divided into a contribution from the receiver and its antenna, M_r; a contribution from the transmitter and its antenna, M_t; and a contribution which is independent of the equipments used, M_c The N in Eq. 12 is similarly divided into N_r, N_t and N_c. Then

$$M_r = -S_o + I \log f_o^r - J + Y_o^r + G \log f_o^r - H \qquad (14)$$

$$M_t = P_o + A \log f_o^t - B + Y_o^t + C \log f_o^t - D \qquad (15)$$

$$M_c = -20 \log d - 37 \qquad (16)$$

$$N_r = - G - I \qquad (17)$$

$$N_t = - A - C \qquad (18)$$

$$N_c = -20. \tag{19}$$

The factors M_r', M_t', N_r', and N_t' are defined by replacing appropriate constants by their primed values.
By definition

$$M = M_r + M_t + M_c \tag{20}$$

$$N = N_r + N_t + N_c \tag{21}$$

$$M' = M_r' + M_t' + M_c \tag{22}$$

$$N' = N_r' + N_t' + N_c \tag{23}$$

$$\left.\begin{aligned} M^\circ &= M_r + M_t' + M_c \qquad (24)\\ N^\circ &= N_r + N_t' + N_c \qquad (25)\end{aligned}\right\} \text{if } f_o^t \geq f_o^r$$

$$\left.\begin{aligned} M^\circ &= M_r' + M_t + M_c \qquad (26)\\ N^\circ &= N_r' + N_t + N_c \qquad (27)\end{aligned}\right\} \text{if } f_o^r \geq f_o^t$$

Equations 14 through 27 are all of the equations necessary to compute the expression

$$N \log f + M \tag{28}$$

for any situation. The sum in Eq. 28 is defined as the "interference margin". Since Eq. 28 represents the sum on the left of Eq. 10, and since Eq. 10 represents the condition for interference, then the circumstances where the interference margin (Eq. 10) is less than zero may be discarded as noninterfering. For those circumstances in which the interference margin is positive, the case must be con-

sidered to be potential interference and must be carried on to the next stage of analysis.

Once all of the appropriate M's and N's have been determined, the problem is to determine the frequency ranges over which the interference margin is positive. Only the positive ranges are carried forward to the frequency cull for further analysis. If the interference margin is nowhere positive for a particular transmitter and receiver under consideration, that potentially interfering pair may be immediately dropped from consideration as noninterfering.

In general, there will be three frequency ranges that must be considered in the frequency cull. These are (1) the region above both the transmitter and receiver fundamental frequencies, (2) the region between the fundamentals, and (3) the region below both fundamentals. The M's and N's for the three regions are: M and N are used for the region above fundamentals; M° and N° for the region between fundamentals; and M' and N' are used in the region below both fundamentals.

The above frequency regions are illustrated in Figure 2-2. The upper plot on Figure 2-2 is a plot of a typical transmitter output spectrum in the frequency domain only. Figure 2-2 shows that the transmitter output is defined by one function from a lower frequency limit to the fundamental frequency of the transmitter and then is defined by another function from the transmitter fundamental to an upper frequency limit. The middle curve on Figure 2-2 shows, in a similar manner, that the receiver is defined by one function from a lower frequency limit to its fundamental frequency and follows a second function from its fundamental to an upper frequency limit.

The lower curve on Figure 2-2 shows the three separate frequency ranges that result from combining the receiver and transmitter functions. First there is that frequency range above both fundamentals, in this case the frequency range above the receiver fundamental which combines the receiver function above its fundamental and the transmitter function above its fundamental. Next, there is the region between fundamentals, where, in the case shown the transmitter and receiver functions are defined above and below their fundamental, respectively.

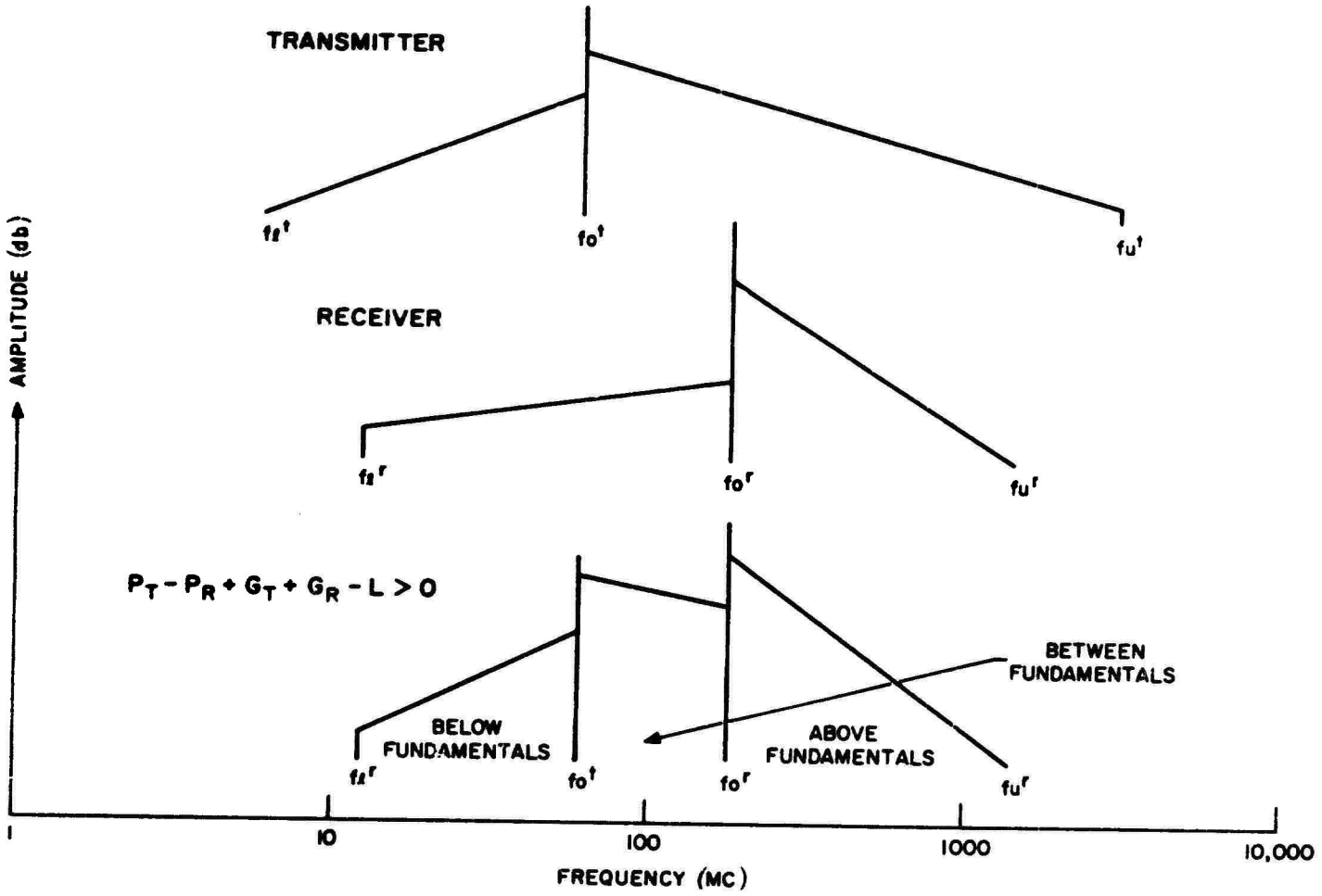

Figure 2-2. Frequency Regions.

Finally, there is the third region that exists below both equipment fundamentals for which both functions are defined below their respective fundamentals.

The region above fundamentals will be considered as an example of determining the frequency range used in the frequency cull. The interference margin is represented by Eq. 28. When Eq. 28 is zero the interference margin passes from positive to negative, hence Eq. 29 must be solved for f.

$$N \log f + M = 0 \tag{29}$$

The general solution is

$$f = \text{antilog} \frac{-M}{N} \tag{30}$$

where f is the frequency in megacycles at which Eq. 28 crosses the zero interference margin. If N is a positive quantity, the line represented by Eq. 28 increases with increasing f and hence the frequency bound represented by Eq. 28 is a lower frequency bound. The upper frequency bound would be the lowest upper bound on the range of definition of the input functions (i.e., in general the lower of f_u^t or f_u^r).

If N is a negative quantity, the line represented by Eq.28 decreases with increasing f and hence the frequency found by Eq.28 represents an upper frequency bound. The lower frequency bound in this latter case would be the greatest lower bound on the range of definition of the input functions (i.e., in general the greater of f_o^r or f_o^t). By the methods just described an upper and lower frequency bound can be found for each region. The regions thus defined represent that portion of the problem that must be carried forward to the frequency cull for further analysis.

The fundamental output of the transmitter and the fundamental response of the receiver are the two most likely sources of interference in general and are treated as special cases. The transmitter fundamental interference level (TFIL) is defined as the interference margin at the fundamental frequency of the trans-

mitter and may be computed directly from Eq. 31. The receiver fundamental interference level (RFIL) is defined as the interference margin at the fundamental frequency of the receiver and may be computed directly from Eq. 32.

$$TFIL = P_o + Y_o^t + M_r + N_r \log f_o^t + M_c + N_c \log f_o^t \text{ if } f_o^r < f_o^t \quad (31)$$

M_r' and N_r' are used if $f_o^t < f_o^r$.

$$RFIL = -S_o + Y_o^r + M_t + N_t \log f_o^r + M_c + N_c \log f_o^r \text{ if } f_o^r > f_o^t \quad (32)$$

and M_t' and N_t' are used if $f_o^r < f_o^t$.

If the receiver-tuned frequency equals the transmitter-tuned frequency (i.e., $f_o^r = f_o^t$), then

$$TFIL - RFIL = P_o - S_o + Y_o^t + Y_o^r - 20 \log d - 20 \log f_o^t - 37 \quad (33)$$

2.4 Frequency Cull

The frequency culling step consists of comparing all transmitter output frequencies with all receiver spurious response frequencies within the range of possible interference as determined by the rapid cull. The separation between each pair of frequencies compared must be correlated with a composite of the bandwidth of the receiver and the bandwidth of the transmitted signal. This correlation will yield an amplitude correction factor for the interference margin as determined in the rapid cull. Also, the exact frequencies of interference are generated, thus identifying the transmitter harmonic and receiver response to which interference reduction techniques should be applied.

The primary output frequencies of a transmitter can in general be represented as

$$f_t = nf_o^t \quad (34)$$

where

f_t = the output frequencies of the transmitter
n = any positive integer
f_o^t = fundamental frequency of the transmitter.

If one is concerned with harmonics of the transmitter master oscillator, f_{mo}, the master ocillator frequency is substituted for f_o^t in Eq. 34. If one is concerned with outputs which are not harmonically related, f_t, the frequency of the output, is used directly and Eq. 34 is no longer useful.

The receiver spurious response frequencies can in general be represented by

$$f_r = \frac{\left| pf_{\ell o} \pm f_{if} \right|}{q} \tag{35}$$

where

f_r = the response frequency of the receiver
$f_{\ell o}$ = the local oscillator frequency of the receiver
f_{if} = the intermediate frequency of the receiver
p, q = any positive integers.

The problem is then to find the receiver response that is closest in frequency to each transmitter output. Any frequency close to f_r, the receiver response frequency, can be represented as

$$\frac{\left| (p + \Delta p)\, f_{\ell o} \pm f_{if} \right|}{q} \tag{36}$$

where p is the same as that defined for Eq. 35 and Δp is an arbitrary fraction between zero and one. For any specific harmonic n, it is necessary to compute the nearest receiver response p and q. This may be accomplished with the aid of Eq. 37:

$$nf_o^t = \frac{\left| (p + \Delta p)\, f_{\ell o} \pm f_{if} \right|}{q} \tag{37}$$

Solve Eq. 37 for (p + Δp), and obtain

$$(p + \Delta p) = \frac{\left| qn\, f_o^t \pm f_{if} \right|}{f_{\ell o}} \qquad (38)$$

For each particular n and q, a (p + Δp) may be found from Eq. 38. The closest receiver response is obtained when the magnitude of Δp is a minimum. The difference in frequency, Δf, between the transmitter harmonic, n, and the closest receiver response as determined by Eq. 38 may be computed most simply from Eq. 39:

$$\Delta f = \frac{f_{\ell o} \left| \Delta p \right|}{q} \qquad (39)$$

If Δf is zero, the transmitter output and receiver response exactly match in frequency. If the two exactly match in frequency, the interference margin computed in the rapid cull is directly applicable. The condition of zero frequency difference is shown by the dotted curve on Figure 2-3a.

For most cases Δf will not be zero. The nonzero condition is shown by the solid curves on Figure 2-3a. When the transmitter output is separated from the receiver response by some Δf, the transmitter power can be increased by a number of db before interference will occur. The apparent increase in transmitter power output that could be tolerated is treated as a bandwidth factor that may be subtracted from the interference margin provided by the rapid cull. The magnitude of the bandwidth factor is taken to be the minimum difference between the two solid curves of Figure 2-3a when their centers are separated by a frequency of Δf. As Δf is allowed to vary, the bandwidth factor is generated as a function of Δf. A typical curve representing the bandwidth factor is shown in Figure 2-3b.

The rapid cull concerns itself with the envelope of receiver responses that are predicted by the p - q equation with q=1. All other responses are below the level of the q=1 responses. Hence, whenever a response is considered in the frequency cull that is different from a q=1 response, an additional bandwidth factor

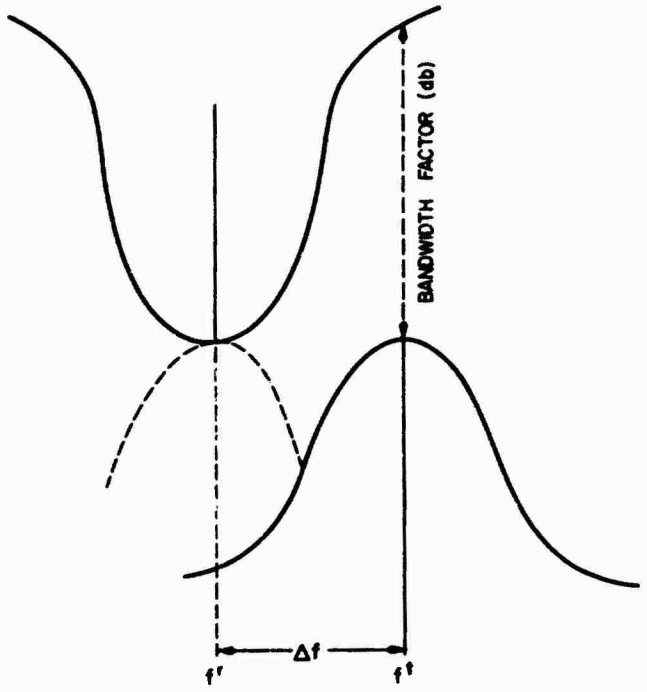

Figure 2-3a. Bandwidth Adjustment Process.

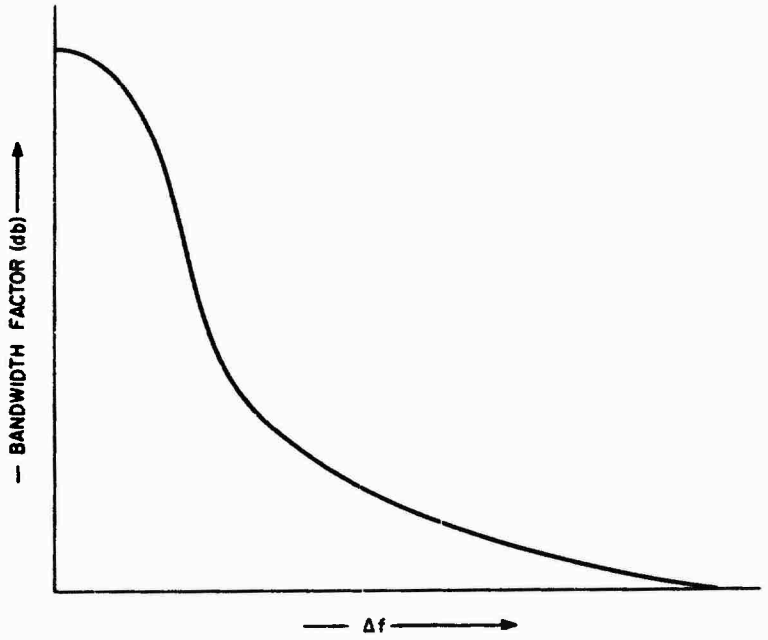

Figure 2-3b. Combined Receiver and Transmitter Bandwidth Adjustment Factor.

is applied. The additional bandwidth factors used are 15 db for a q=2 response and 20 db for a q=3 or q=4 response.

For most receivers the bandwidth function is the bandwidth of the first intermediate frequency stage and is independent of the order of the response. For transmitters the output envelope about each spurious output is a function of the particular output which is being considered. This means that in general a separate curve of the type shown in Figure 2-3b must be used for each transmitter output. However, a general rule-of-thumb has been adopted to relate the modulation envelope about each harmonic to the modulation envelope about the fundamental. The rule is that the bandwidth goes up directly with the harmonic number. This means that a curve of the type shown in Figure 2-3b for the bandwidth function about the fundamental is expanded by a factor equal to the harmonic number of the particular transmitter output under consideration.

The methods for obtaining the interference margin and all additional factors to be added to the interference margin have been discussed. Once the final interference margin has been determined, it represents the level which is not exceeded with a probability of 99.9 percent. The final question to be answered is, what is the probability of interference? The condition for interference is that the interference margin exceed zero. Therefore, the probability of interference is simply the probability that the interference margin exceed zero. Since each of the input statistical distributions is known, the statistical distribution of the sum of all input functions is known.[3] The standard deviation of the sum is also known.[4] The amplitude associated with the 99.9 percent probability level is known, since this amplitude is simply the corrected interference margin. To completely specify a statistical distribution it is only necessary to know the type of statistical distribution, its standard deviation and one point on the distribution. Hence the complete

---

3. Interference Analysis Study, Jansky & Bailey, A Division of Atlantic Research Corporation, Alexandria, Va., Vol. I-2, Chap. 3, Sec. 3.3.3 ("Combination of Statistical Terms") RADC TR 61-15A, Contract No. AF 30(602)-1934; January, 1961.

4. Ibid.

statistical distribution for the interference margin is known and the probability of interference (i.e., the probability that the interference margin is greater than zero) may be determined directly.

Figure 2-4 is a plot of the cumulative probability distributions that are typical of the type used in the prediction carried out to date. Figure 2-4 has been plotted in such a way that the interference margin may be found on the vertical scale; the horizontal scale will give the probability of interference directly.

In Figure 2-4 several curves which translate the interference margin into the probability of interference are shown. The curve marked with "TFIL = RFIL", is used when the interference margin has been determined to be at or near the tuned frequency of the receiver by the fundamental output of the transmitter. The curve marked "RFIL" is used when interference from any source enters the receiver at or near its tuned frequency. The curve marked "TFIL" is used when interference is caused by the fundamental output of the transmitter. The curve marked " Off Fundamentals" is used when neither the receiver response nor the interfering transmitter emission are at the tuned frequencies of their respective equipments. As the curves of Figure 2-4 indicate, there exists a wide difference in the spread of the statistical distributions depending upon whether or not both fundamentals, one fundamental or no fundamentals are involved in the particular situation under investigation. The wider spread of the statistical distributions at other than design frequencies reflects the fact that the uncertainties are small at the design frequencies and are large at frequencies other than the design or tuned frequencies.

2.5 Sample Problem

2.5.1 Definition of the Problem

The following problem is an example of the interference prediction process, which was applied to an electromagnetic complex at the RADC Test Facility, Verona, New York. This complex contained radar receivers and transmitters for both search and tracking, a communications receiver in the UHF band, and ECM equipment.

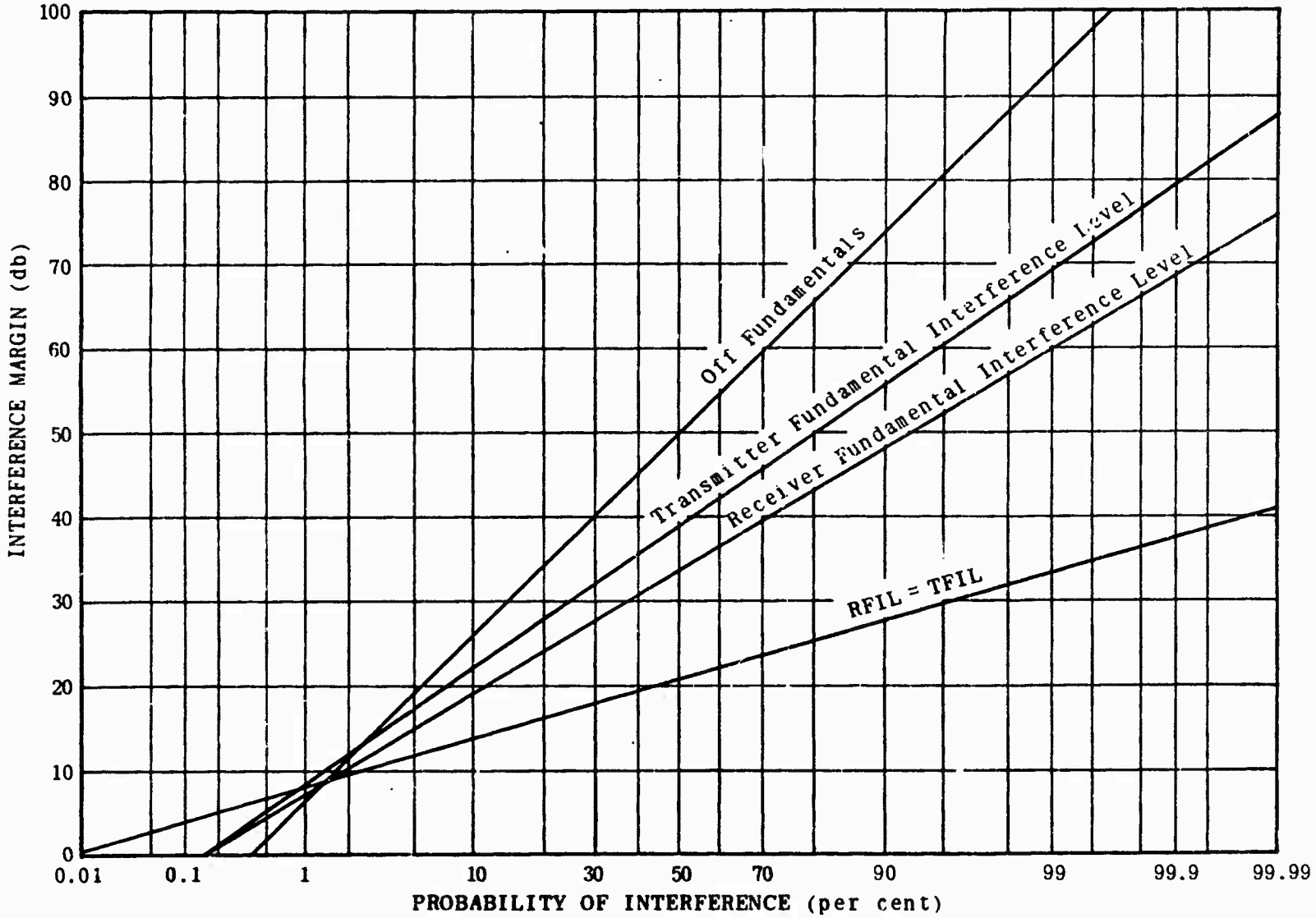

Figure 2-4. Typical Relations Between Interference Margin and Probability of Interference.

The complex involves three transmitter-receiver systems, and two transmitters and four receivers operating independently. Each system contains one antenna, one transmitter, and one receiver which are tuned to the same frequency and which are not operated simultaneously. Therefore, no interference is possible between equipments within the same system.

Preliminary information available to define the given complex is shown in Table 2-1 for the receiving equipment and in Table 2-2 for the transmitting equipment.

Table 2-1

RECEIVER OPERATIONAL CHARACTERISTICS

Receiver	Operating Frequency (Mc)	Operating Sensitivity (dbm)	Antenna Type	Antenna Gain (db)
R_1	2810	-100	G_1	39
R_2	5497	-100	G_2	33
R_3	154.8	- 95	G_3	2
R_4	394.8	- 92	G_4	7
R_5	8600	-100	G_5	40
R_6	2860	- 95	G_6	2
R_7	1338	-100	G_7	32

Table 2-2

TRANSMITTER OPERATIONAL CHARACTERISTICS

Transmitter	Operating Frequency (Mc)	Power Output (dbm)	Antenna Type	Antenna Gain (db)
T_1	2810	97	G_1	39
T_2	5497	90	G_2	33
T_3	2854	84	G_8	35
T_4	3254	90	G_9	35
T_5	8600	84	G_5	40

Next, information forms are filled out for the equipment in the complex. Data required on the forms are generally obtainable from either the specifications of the equipment or the technical manuals for the equipment. Tables 2-3 and 2-4 show the information for receivers and transmitters, respectively.

Table 2-3

EQUIPMENT CHARACTERISTIC FORM FOR RECEIVERS

Characteristic	Description			
	R_1	R_2	R_3	R_4
Nomenclature	*	*	*	*
Frequency Range	2700-2900 Mc	5450-5825	100-156 Mc	225-399 Mc
Mode of Operation	Pulse Radar	Pulse Radar	AM	AM
Max. Sensitivity	-102 dbm	-109 dbm	-95 dbm	-92 dbm
Input Impedance	50 ohms		70 ohms	52 ohms
IF Frequencies	30 Mc	30 Mc	12 Mc	1st: 40-49.9 Mc 2nd: 9-9.9 Mc 3rd: 2.05 Mc
Osc. Frequencies	2670-2870 Mc	5480-5855 Mc	88-144 Mc	1st L.O.: 180-350 Mc 2nd L.O.: 31-40 Mc 3rd L.O.: 6.95-7.85 Mc
Specified Image Rejection	60 db		70 db	60 db
Receiver Bandwidths	3 db: 600 Mc	3db: 3 Mc	6 db: 140 Mc	6 db: 85 kc 60 db: 225 kc
No. RF Resonant Circuits	None		1 Single-Tuned 1 Double-Tuned	Three
No. RF Amplifier Stages	None		One	Two
Type of Mixer	Crystal	Crystal	Pentode	Pentode, L.O. in Cathode
Trans. Line			RG-8	Coaxial
Max. Antenna Gain			2 db	7 db

* The nomenclatures for these equipments are classified.

Table 2-3 (cont'd)

EQUIPMENT CHARACTERISTIC FORM FOR RECEIVERS

Characteristic	Description		
	R_5	R_6	R_7
Nomenclature	*	*	*
Frequency Range	8500-9600 Mc	1000-10,850 Mc	1220-1350 Mc
Mode of Operation	Pulse Radar		Pulse Radar
Max. Sensitivity	-100 dbm	-95 dbm	-100 dbm
Input Impedance			50 ohms
IF Frequencies	60 Mc	160 Mc	60 Mc
Osc. Frequencies	8440-9540 Mc	1160-2760 Mc 2140-4290 Mc 4460-7510 Mc 6890-10,590 Mc	1280-1410 Mc
Specified Image Rejection			60 db
Receiver Bandwidths	3 db: 10 Mc		3 db: 1 Mc
No. RF Resonant Circuits			2 cavities
No. RF Amplifier Stages			None
Type of Mixer	Crystal		Triode
Trans. Line Max. Antenna Gain			

* The nomenclatures for these equipments are classified.

Table 2-4

EQUIPMENT CHARACTERISTIC FORM FOR TRANSMITTERS

Characteristic	T_1	T_2	T_3	T_4	T_5
Nomenclature	*	*	*	*	*
Frequency Range	2810 Mc	5497 Mc	2700-2900 Mc	3100-3500 Mc	8500-9600 Mc
Mode of Operation	Pulsed	Pulsed	Pulsed	Pulsed	Pulsed
Power Output	97 dbm	90 dbm	84 dbm	90 dbm	84 dbm
Output Generator	Magnetron	Magnetron	Magnetron	Magnetron	Magnetron
Output Circuit	Cavity	Cavity	Cavity	Cavity	Cavity
Class of Operation of Output Stage	-	-	-	-	-
Output Frequency Generated by Fundamental M.O.	Output Generator	Output Generator	Output Generator	Output Generator	Output Generator
Frequencies	Output Frequency	Output Frequency	Output Frequency	Output Frequency	Output Frequency
Transmission line	Waveguide	Waveguide	Waveguide	Waveguide	Waveguide
Max. Antenna Gain	42 db	33 db	35 db	35 db	40 db

* The nomenclatures for these equipments are classified.

2.5.2 Rapid Cull for Sample Problem

2.5.2.1 Tabulation of Constants

The receiver constants required for the rapid cull are tabulated in Table 2-5. Receiver R_1 is used as an example of the available methods for deriving the constants. Similar procedures may be used for R_2, R_3, R_4, R_5, R_6, and R_7. To obtain the constants tabulated in Table 2-5, the following steps were followed.

1. f_o^r = 2810 Mc = operating frequency of R_1 as specified in Table 2-1
2. f_ℓ^r = 30 Mc = lowest intermediate frequency used in R_1 as specified in Table 2-3
3. f_r^u = 10 kMc = the frequency arbitrarily chosen as the highest frequency at which R_1 is susceptible to interference
4. S_o = -100 dbm = maximum sensitivity of R_1 as specified in Table 2-3
5. The constants I=0 and J=60 were selected from Table 2-6 by multiplying the standard deviation by 1.3 and adding this value to the corresponding intercept
6. The constants I'=-241 and J'-100 were selected from a Table similar to Table 2-6
7. Log f_o^r in megacycles = 3.45 (f_o^r from step 1)
8. I log f_o^r = 0 (I from step 5)
9. I' log f_o^r = -831 (I' from step 6)
10. f_ℓ^r = 0.0107 f_o^r. This factor is computed from steps 1 and 2 to aid in the determination of antenna constants
11. f_u^r = 3.56 f_o^r. This factor was computed from steps 1 and 3 to aid in the determination of antenna constants
12. Y_o^r = 39 db = maximum antenna gain from Table 2-3
13. G = 0, H = 0
14. G' = -21, H' = 0
15. G log f_o^r = 0 (G from step 13)
16. G' log f_o^r = -72.4 (G' from step 14).

Table 2-5

RECEIVER CONSTANTS

Step No.		R_1	R_2	R_3	R_4	R_5	R_6	R_7
1	f_o^r Mc	2810	5497	154.8	394.8	8600	2860	1338
2	f_ℓ^o	30	30	12	44.8	60	160	60
3	f_u^r	10,000	10,000	3000	5000	10,000	10,000	10,000
4	S_o dbm	-100	-100	-85	-92	-100	-95	-100
5	I	0	0	37	30	0	0	0
6	I'	-241	-241	-40	0	-241	0	-241
	J	60	60	41	62	60	40	60
	J'	100	100	38	80	100	40	100
7	log f_o^r	3.45	3.74	2.19	2.59	3.93	3.46	3.13
8	I log f_o^r	0	0	81	77.7	0	0	0
9	I' log f_o^r	-831	-901	-87.6	0	- 947	0	-755
10	f_ℓ^r	$0.0107f_o^r$	$0.0546f_o^r$	$0.1135f_o^r$	$0.1135f_o^r$	$0.00698f_o^r$	$0.056f_o^r$	$0.0449f_o^r$
11	f_u^r	$3.56f_o^r$	$1.82f_o^r$	$19.4f_o^r$	$2.65f_o^r$	$1.16f_o^r$	$3.5f_o^r$	$7.49f_o^r$
12	Y_o^r db	39	33	2	7	40	2	32
13	G	0	0	-2	-23	0	0	0
14	G'	-21	0	-1	-4	0	0	-16
	H	0	0	-5	0	0	0	0
	H'	0	0	0	0	0	0	0
15	G log f_o^r	0	0	-4.36	-59.5	0	0	0
16	G' log f_o^r	-72.4	0	-2.19	-10.36	0	0	-50.1

Table 2-6

DESCRIPTIVE CONSTANTS FOR RECEIVER SPURIOUS RESPONSES

Nomenclature	Intercept	Slope	Standard Deviation
R-836/ARN-51	107	0.1	14
R-174/URR	105	11	11.9
AN/FPS-6	76	0	12
RT-175/PRC-9	47	178	2
RT-323/VRC-24	66	66	18.7
R-391/URR	114	14	13.6
Mod III	76	0	12
R-394/U	112	5	16.8
R-274-A/FRR	94	8	14.2
R-125/GRC	97	12	9.6
Nike Ajax Track	76	0	12
R-390A/URR	92	9	17.7
RT-70/GRC	540	48	26.2
RT-66/GRC	84	36	22.2
BC-689	57	37	12
AN/GRC-27	78	30	12
R-108/GRC	122	14	17.7
R-392/URR	103	8	16.4
R-388/URR	103	2	17.9
AN/TPS-1D	76	0	12
RT-77A/GRC-9	100	18	12.5
BC-342D	108	12	15.4
RT-294/ARC-44	11	84	9.1
AN/APR-9	56	0	12

The transmitter constants required for the rapid cull are tabulated in Table 2-7. Transmitter T_1 is used as an example of the available methods for deriving the constants. Similar procedures may be used for T_2, T_3, T_4, and T_5. To obtain the constants listed in Table 6 for T_1, the following steps were followed:

1. f_o^t = 2810 Mc = operating frequency of T_1 as specified in Table 2-2
2. f_ℓ^t = 2810 Mc = waveguide cut-off frequency for T_1
3. f_u^t = 10 kMc = highest frequency at which harmonic output need be considered for this case
4. P_o = 97 dbm = maximum power output from T_1 as specified in Table 2-4
5. The constants A=30 and B=56 were selected from Table 2-8 by multiplying the standard deviation by 1.3 and adding this value to the corresponding intercept
6. A'=0, B'=0, since there is no significant spurious output below the fundamental
7. Log f_o^t in megacycles = 3.45 (f_o^t from step 1)
8. A log f_o^t = 103.5 (A from step 5)
9. A' log f_o^t = 0 (A' from step 6)
10. $f_\ell^t = 1.0\ f_o^t$. This factor was computed to aid in the computation of antenna constants
11. $f_u^t = 3.56\ f_o^t$. This factor was computed to aid in the computation of antenna constants
12. Y_o^t = 39 db = maximum antenna gain from Table 2-4
13. C = -20, D = 0
14. C' = 0, D' = 0
15. C log f_o^t = -69 (C from step 13)
16. C' log f_o^t = 0 (C' from step 14).

Table 2-7

TRANSMITTER CONSTANTS

Step No.	Term	T_1	T_2	T_3	T_4	T_5
1	f_o^t Mc	2810	5497	2854	3245	8600
2	f_ℓ^t Mc	2810	5497	2854	3254	8600
3	f_u^t Mc	10,000	10,000	10,000	10,000	10,000
4	P_o dbm	97	90	84	90	84
5	A	30	30	30	30	30
6	A'	0	0	0	0	0
	B	56	56	56	56	56
	B'	0	0	0	0	0
7	log f_o^t	3.45	3.74	3.46	3.51	3.93
8	A log f_o^t	103.5	112.2	103.8	105.3	117.9
9	A'log f_o^t	0	0	0	0	0
10	f_ℓ^t	$1.0f_o^t$	$1.0f_o^t$	$1.0f_o^t$	$1.0f_o^t$	$1.0f_o^t$
11	f_u^t	$3.56f_o^t$	$1.82f_o^t$	$3.5f_o^t$	$3.08f_o^t$	$1.16f_o^t$
12	Y_o^t db	39	33	35	35	40
13	C	-20	0	0	0	0
14	C'	0	0	0	0	0
	D	0	0	0	0	0
	D'	0	0	0	0	0
15	C log f_o^t	-69	0	0	0	0
16	C'log f_o^t	0	0	0	0	0

Table 2-8

DESCRIPTIVE CONSTANTS FOR
TRANSMITTER OUTPUT SPECTRA

Nomenclature	Intercept	Slope	Standard Deviation
T-638/URT	57	34	8.7
T-195/GRC-19	49	45	9.8
T-213/GRC-26	36	43	9.5
T-417/GR	76	23	7.2
AM-415/GR	80	22	6.3
AM-494/GR	83	20	-
AN/MSQ-1A	70	30	10.0
RT-66/GRC-3	31	52	10.4
T-235/GRC-10	59	23	11.8
T-352	25	33	-
RT-70/GRC-3	33	56	6.7
T-278/VRC-19	70	16	-
RT-77/GRC-9	24	51	11.2
T-416/GR	84	18	-
BC-610C	24	53	10.6
T-1580/FRT	23	46	14.2
Mod III	70	30	10.0
BC-339N	6	63	12.0
AN/FPS-7	36	42	9.9
AN/UST-2	25	45	10.0
AN/FPS-8	15	55	10.0
AN/FPS-20	25	45	10.0
Nike Ajax	70	30	10.0
SCR-270	8	40	10.0
AN/TPS-1D	15	55	10.0
AN/FPS-6	70	30	10.0
AN/FPS-15	70	40	10.0
AN/GRC-27	27	60	10.0
BC-640	22	43	6.6

2.5.2.2 Intermediate Computations

Next, the appropriate constants from Table 2-5 are entered in the indicated receiver spaces in Tables 2-9 and 2-10. Likewise, the appropriate constants from Table 2-7 are entered in the indicated transmitter spaces in Tables 2-11 and 2-12. To obtain M_r, M'_r, N_r, N'_r, M_t, M'_t, N_t and N'_t, add each column in Tables 2-9 through 2-12. The resulting values for M_r, M'_r, N_r, and N'_r, are entered in the indicated rows in Table 2-13 for the corresponding receiver. The resulting values for M_t, M'_t, N_t and N'_t are entered in the indicated columns in Table 2-13 for the corresponding transmitters. From Tables 2-5 and 2-7, enter in the designated locations on Table 2-13 the values of f_o^t and f_o^r.

Each system has been defined as having the receiver and transmitter tuned to the same frequency and not operating simultaneously. Therefore in Table 2-13 for the cases where $f_o^r = f_o^t$ (i.e., for combinations of R_1 and T_1, R_2 and T_2, and R_5 and T_5), cross out the intersecting rows and columns since these cases need not be considered.

Further examination of Table 2-13 is necessary before computing M, M°, M', N, N°, and N'. Check each of the remaining receiver-transmitter pairs for the condition that $f_o^t > f_o^r$ or $f_o^r > f_o^t$, and note which statement is incorrect. Cross out the M° and N° cases in the column under the incorrect statement as determined above. A sample block of Table 2-13 is shown in Figure 2-5 for R_2 and T_1.

In Figure 2-5 the condition $f_c^t > f_o^r$ is false and therefore the M° and N° cases in the $f_o^t > f_o^r$ columns are crossed out. For all valid sets of intersecting M, M', N, N' rows and columns, numerically add the values that head each row and column and enter as shown in Figure 2-5. The corresponding answers for determining the range of interference between T_1 and R_2 are $M = M_r + M_t = 187.5$ above fundamentals, $M° = M'_r + M_t = -751.5$ between fundamentals, and $M' = M'_r + M'_t = 730$ below fundamentals. Similarly, $N = -10$ above fundamentals, $N° = 231$ between fundamentals, and $N' = 241$ below fundamentals.

	R_1		R_2		R_3		R_4		R_5	
	M_r	M_r'	M_r	M_r'	M_r	M_r'	M_r	M_r'	M_r	M_r'
$-J$	-60		-60		-41		-62		-60	
$I \log f_o^r$	0		0		81.4		77.7		0	
$-H$	0		0		5		0		0	
$G \log f_o^r$	0		0		-4.36		-59.5		0	
$-S_o$	100	100	100	100	95	95	92	92	100	100
Y_o^r	39	39	33	33	2	2	7	7	40	40
$-J'$		-100		-100		-38		-80		-100
$I' \log f_o^r$		-82.8		-899		-87.6		0		-947
$-H'$		0		0		0		0		0
$G' \log f_o^r$		-72.4		0		-2.19		-10.36		0
TOTAL	79	-116.2	73	-866	138	-30.8	55.2	8.6	80	-907

Table 2-9. Form for Computation of M_r and M_r'

	R_6		R_7		R		R		R	
	M_r	M'_r	M_r	M'_r	M_r	M'_r	M_r	M'_r	M_r	M'_r
$-J$	-40		-60							
$I \log f_o^r$	0		0							
$-H$	0		0							
$G \log f_o^r$	0		0							
$-S_o$	95	95	100	100						
Y_o^r	2	2	32	32						
$-J'$		-40		-100						
$I' \log f_o^r$		0		-755						
$-H'$		0		0						
$G' \log f_o^r$		0		-50.1						
TOTAL	57	57	72	-773.1						

Table 2-9 (cont'd). Form for Computation of M_r and M'_r.

N_r'	R_1		R_2		R_3		R_4		R_5	
	N_r	N_r'	N_r	N_r'	N_r	N_r'	N_r	N_r'	N_r	N_r'
-G	0		0		2		23		0	
-I	0		0		-37		-30		0	
-G'		21		0		1		4		0
-I'		241		241		40		0		241
TOTAL	0	262	0	241	-35	41	-7	4	0	241

Table 2-10. Form for Computation of N_r and N_r'.

N_r'	R_6 N_r	R_6 N_r'	R_7 N_r	R_7 N_r'	R N_r	R N_r'	R N_r	R N_r'	R N_r	R N_r'
-G	0		0							
-I	0		0							
-G'		0		16						
-I'		0		241						
TOTAL	0	0	0	257						

Table 2-10 (cont'd). Form for Computation of N_r and N_r'.

	T_1		T_2		T_3		T_4		T_5	
	M_t	M_t'	M_t	M_t'	M_t	M_t'	M_t	M_t'	M_t	M_t'
-B	-56		-56		-56		-56		-56	
A LOG f_o^t	103.5		112.2		103.8		105.3		117.9	
-D	0		0		0		0		0	
C LOG f_o^t	-69		0		0		0		0	
P_o	97	97	90	90	84	84	90	90	84	84
Y_o^t	39	39	33	33	35	35	35	35	40	40
-B'		0		0		0		0		0
A' LOG f_o^t		0		0		0		0		0
-D'		0		0		0		0		0
C' LOG f_o^t		0		0		0		0		0
TOTAL	114.5	136	179.2	123	166.8	119	174.3	125	185.9	124

Table 2-11. Form for Computation of M_t and M_t'.

	T_1		T_2		T_3		T_4		T_5	
	N_t	N_t'	N_t	N_t'	N_t	N_t'	N_t	N_t'	N_t	N_t'
-A	-30		-30		-30		-30		-30	
-C	20		0		0		0		0	
-A'		0		0		0		0		0
-C'		0		0		0		0		0
TOTAL	-10	0	-30	0	-30	0	-30	0	-30	0

Table 2-12. Form for Computation of N_t and N_t'.

			T_1 $f_o^t=2810$				T_2 $f_o^t=5497$				T_3 $f_o^t=2854$				T_4 $f_o^t=3254$				T_5 $f_o^t=8600$			
			$f_o^r>f_o^t$	$f_o^t>f_o^r$	$f_o^r>f_o^t$	$f_o^t>f_o^r$	$f_o^r>f_o^t$	$f_o^t>f_o^r$	$f_o^r>f_o^t$	$f_o^t>f_o^r$	$f_o^r>f_o^t$	$f_o^t>f_o^r$	$f_o^r>f_o^t$	$f_o^t>f_o^r$	$f_o^r>f_o^t$	$f_o^t>f_o^r$	$f_o^r>f_o^t$	$f_o^t>f_o^r$	$f_o^r>f_o^t$	$f_o^t>f_o^r$	$f_o^r>f_o^t$	$f_o^t>f_o^r$
			M_t	M'_t	N_t	N'_t	M_t	M'_t	N_t	N'_t	M_t	M'_t	N_t	N'_t	M_t	M'_t	N_t	N'_t	M_t	M'_t	N_t	N'_t
			114.5	136	-10	0	179.2	123	-30	0	166.8	119	-30	0	174.3	125	-30	0	185.9	124	-30	0
R_1	M_r	79					258.2	202			245.8	198			253.3	204			264.9	203		
	M'_r	-116.2						6.8				2.8				8.8				7.8		
$f_o^r=2810$	N_r	0							-30	0			-30	0			-30	0			-30	0
	N'_r	262								262				262				262				262
R_2	M_r	73	187.5								239.8				247.3				258.9	197		
	M'_r	-866	-751.5	-730							-699.2	-747			-691.7	-741				-742		
$f_o^r=5497$	N_r	0			-10								-30				-30				-30	0
	N'_r	241			231	241							211	241			211	241				241
R_3	M_r	138	252.5	274			317.2	261			304.8	257			312.3	263			323.9	262		
	M'_r	-30.8		105.2				92.2				88.2				94.2				93.2		
$f_o^r=154.8$	N_r	-35			-45	-35			-65	-35			-65	-35			-65	-35			-65	-35
	N'_r	41				41				41				41				41				41
R_4	M_r	55.2	169.7	191.2			234.4	178.2			222	174.2			229.5	180.2			241.1	179.2		
	M'_r	8.6		144.6				131.6				127.6				133.6				134.6		
$f_o^r=394.8$	N_r	-7			-17	-7			-37	-7			-37	-7			-37	-7			-37	-7
	N'_r	4				4				4				4				4				4
R_5	M_r	80	194.5				259.2				246.8				254.3							
	M'_r	-907	-792.5	-771			-727.8	-784			-740.2	-788			-732.7	-782						
$f_o^r=8600$	N_r	0			-10				-30				-30				-30					
	N'_r	241			231	241			211	241			211	241			211	241				

Table 2-13. Form for Computation of M, M^o, M′, N, N^o and N′.

			T_1, $f_o^t = 2810$			
			$f_o^r > f_o^t$	$f_o^t > f_o^r$	$f_o^r > f_o^t$	$f_o^t > f_o^r$
			M_t	M_t'	N_t	N_t'
			114.5	136	-10	0
R_6	M_r	57	171.5			
	M_r'	57	171.5	193		
$f_o^r = 2860$	N_r	0			-10	
	N_r'	0			-10	0
R_7	M_r	72	186.5	208		
	M_r'	-773.1		-637.1		
$f_o^r = 1338$	N_r	0			-10	0
	N_r'	257				257
R	M_r					
	M_r'					
$f_o^r =$	N_r					
	N_r'					
R	M_r					
	M_r'					
$f_o^r =$	N_r					
	N_r'					
R	M_r					
	M_r'					
$f_o^r =$	N_r					
	N_r'					

		T_2, $f_o^t = 5497$			
		$f_o^r > f_o^t$	$f_o^t > f_o^r$	$f_o^r > f_o^t$	$f_o^t > f_o^r$
		M_t	M_t'	N_t	N_t'
		179.2	123	-30	0
R_6	M_r	236.2	180		
	M_r'		180		
$f_o^r = 2860$	N_r			-30	0
	N_r'				0
R_7	M_r	251.2	195		
	M_r'		-650.1		
$f_o^r = 1338$	N_r			-30	0
	N_r'				257
R	M_r				
	M_r'				
$f_o^r =$	N_r				
	N_r'				
R	M_r				
	M_r'				
$f_o^r =$	N_r				
	N_r'				
R	M_r				
	M_r'				
$f_o^r =$	N_r				
	N_r'				

		T_3, $f_o^t = 2854$			
		$f_o^r > f_o^t$	$f_o^t > f_o^r$	$f_o^r > f_o^t$	$f_o^t > f_o^r$
		M_t	M_t'	N_t	N_t'
		166.8	119	-30	0
R_6	M_r	223.8			
	M_r'	223.8	176		
$f_o^r = 2860$	N_r			-30	
	N_r'			-30	0
R_7	M_r	238.8	191		
	M_r'		-654.1		
$f_o^r = 1338$	N_r			-30	0
	N_r'				257
R	M_r				
	M_r'				
$f_o^r =$	N_r				
	N_r'				
R	M_r				
	M_r'				
$f_o^r =$	N_r				
	N_r'				
R	M_r				
	M_r'				
$f_o^r =$	N_r				
	N_r'				

		T_4, $f_o^t = 3254$			
		$f_o^r > f_o^t$	$f_o^t > f_o^r$	$f_o^r > f_o^t$	$f_o^t > f_o^r$
		M_t	M_t'	N_t	N_t'
		174.3	125	-30	0
R_6	M_r	231.3	182		
	M_r'		182		
$f_o^r = 2860$	N_r			-30	0
	N_r'				0
R_7	M_r	246.3	197		
	M_r'		-646.1		
$f_o^r = 1338$	N_r			-30	0
	N_r'				257
R	M_r				
	M_r'				
$f_o^r =$	N_r				
	N_r'				
R	M_r				
	M_r'				
$f_o^r =$	N_r				
	N_r'				
R	M_r				
	M_r'				
$f_o^r =$	N_r				
	N_r'				

		T_5, $f_o^t = 8600$			
		$f_o^r > f_o^t$	$f_o^t > f_o^r$	$f_o^r > f_o^t$	$f_o^t > f_o^r$
		M_t	M_t'	N_t	N_t'
		185.9	124	-30	0
R_6	M_r	242.9	181		
	M_r'		181		
$f_o^r = 2860$	N_r			-30	0
	N_r'				0
R_7	M_r	257.9	196		
	M_r'		-649.1		
$f_o^r = 1338$	N_r			-30	0
	N_r'				257
R	M_r				
	M_r'				
$f_o^r =$	N_r				
	N_r'				
R	M_r				
	M_r'				
$f_o^r =$	N_r				
	N_r'				
R	M_r				
	M_r'				
$f_o^r =$	N_r				
	N_r'				

Table 2-13 (cont'd). Form for Computation of M, M^O, M', N, N^O and N'.

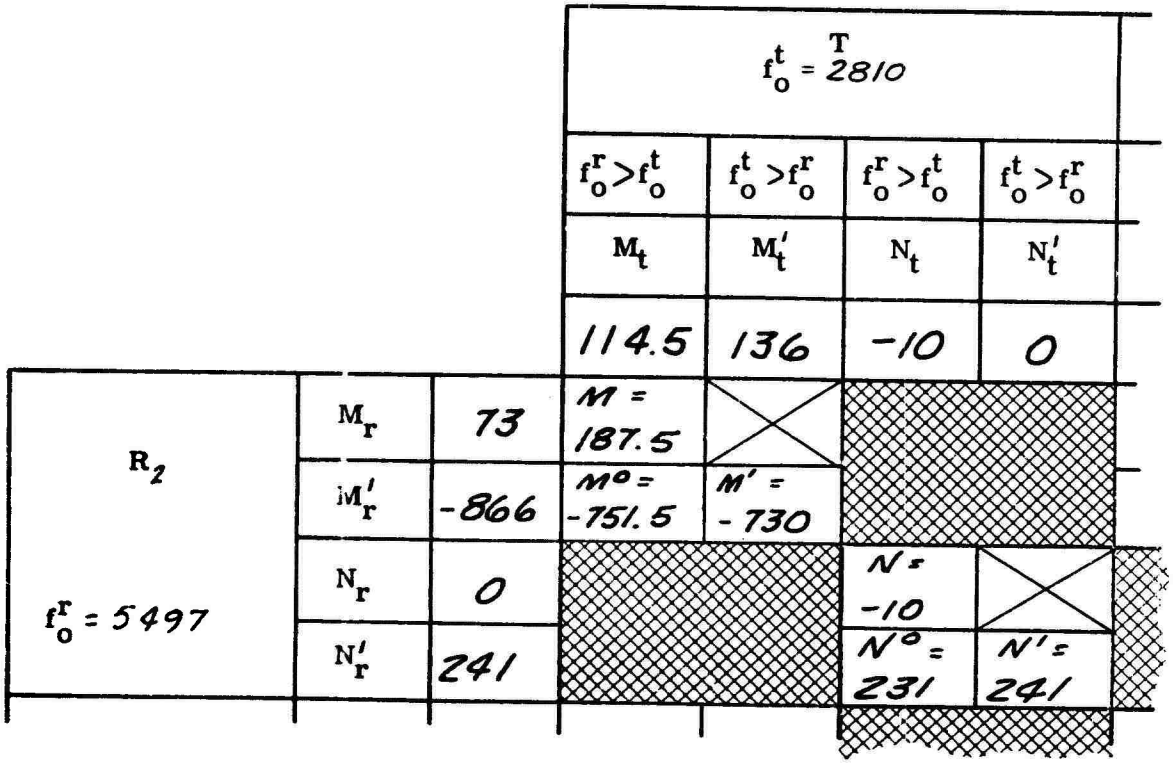

Figure 2-5. Sample Block from Table 2-13.

2.5.2.3 Distance Matrix and Associated Constants

Obtain the distances in miles between each possible combination of receiver and transmitter and enter these values in Table 2-14. The R and T pairs belonging to the same system are not considered (as in the discussion of Table 2-13) and those cases are crossed out. In order to compute M_c, it is necessary to perform the operations indicated in Table 2-14.

2.5.2.4 Frequency Comparison Scheme

Table 2-15 establishes the frequency ranges which exist between all receiver and transmitter combinations. By using the following procedure, some cases of interference are eliminated before any frequency calculations are made. Also, the defined range of frequencies is reduced for many cases before any frequency calculations are made.

Enter in Table 2-15 the values of f_u^t, f_o^t and f_ℓ^t, from Table 2-7 in the columns for the corresponding transmitters. Also enter in Table 2-15 the values of f_u^r, f_o^r and f_ℓ^r from Table 2-5 in rows for the corresponding receivers. The procedure for computing the limits of the frequency ranges is outlined in the following steps. A sample block from Table 2-15 is shown in Figure 2-6.

1. In Table 2-15 for each possible receiver-transmitter combination, check for the conditions $f_\ell^t > f_u^r$ and $f_\ell^r > f_u^t$. These conditions void that receiver-transmitter combination from the need for further analysis. Each voided combination is crossed out.

2. At the intersection of each f_u^r row and f_u^t column, enter the lower of the two values f_u^r or f_u^t. This number as shown in Figure 2-7 will be called f_u, the present upper frequency limit for the defined region above the transmitter and receiver fundamental frequencies.

3. At the intersection of each f_ℓ^r row and f_ℓ^t column, enter the higher of the two values f_ℓ^r or f_ℓ^t. This number as shown in Figure 2-7 will be called f_ℓ', the

		T_1	T_2	T_3	T_4	T_5
R_1	d (mi)		0.471	0.487	0.1215	0.1425
	-20 LOG d		6.5	6.3	18.3	17
	-37		-37	-37	-37	-37
	SUM = M_c		-30.5	-30.7	-18.7	-20
R_2	d	0.471			0.35	0.329
	-20 LOG d	6.5			9.2	9.7
	-37	-37			-37	-37
	SUM = M_c	-30.5			-27.8	-27.3
R_3	d	0.97	1.1	1.1	0.98	0.98
	-20 LOG d	0.3	-0.8	-0.8	0.0	0.0
	-37	-37	-37	-37	-37	-37
	SUM = M_c	-36.7	-37.8	-37.8	-37	-37
R_4	d	0.97	1.1	1.1	0.98	0.98
	-20 LOG d	0.3	-0.8	-0.8	0.0	0.0
	-37	-37	-37	-37	-37	-37
	SUM = M_c	-36.7	-37.8	-37.8	-37	-37
R_5	d	0.14	0.33	0.25	0.02	
	-20 LOG d	17	9.7	12	34	
	-37	-37	-37	-37	-37	
	SUM = M_c	-20	-27.3	-25	-3	

Table 2-14. Distance Matrix for Computation of M_c.

		T_1	T_2	T_3	T_4	T_5
R_6	d	0.97	1.1	1.1	0.98	0.98
	-20 LOG d	0.3	-0.8	-0.8	0.0	0.0
	-37	-37	-37	-37	-37	-37
	SUM = M_c	-36.7	-37.8	-37.8	-37	-37
R_7	d	0.97	1.1	1.1	0.98	0.98
	-20 LOG d	0.3	-0.8	-0.8	0.0	0.0
	-37	-37	-37	-37	-37	-37
	SUM = M_c	-36.7	-37.8	-37.8	-37	-37
R	d					
	-20 LOG d					
	-37					
	SUM = M_c					
R	d					
	-20 LOG d					
	-37					
	SUM = M_c					
R	d					
	-20 LOG d					
	-37					
	SUM = M_c					

Table 2-14 (cont'd). Distance Matrix for Computation of M_c,

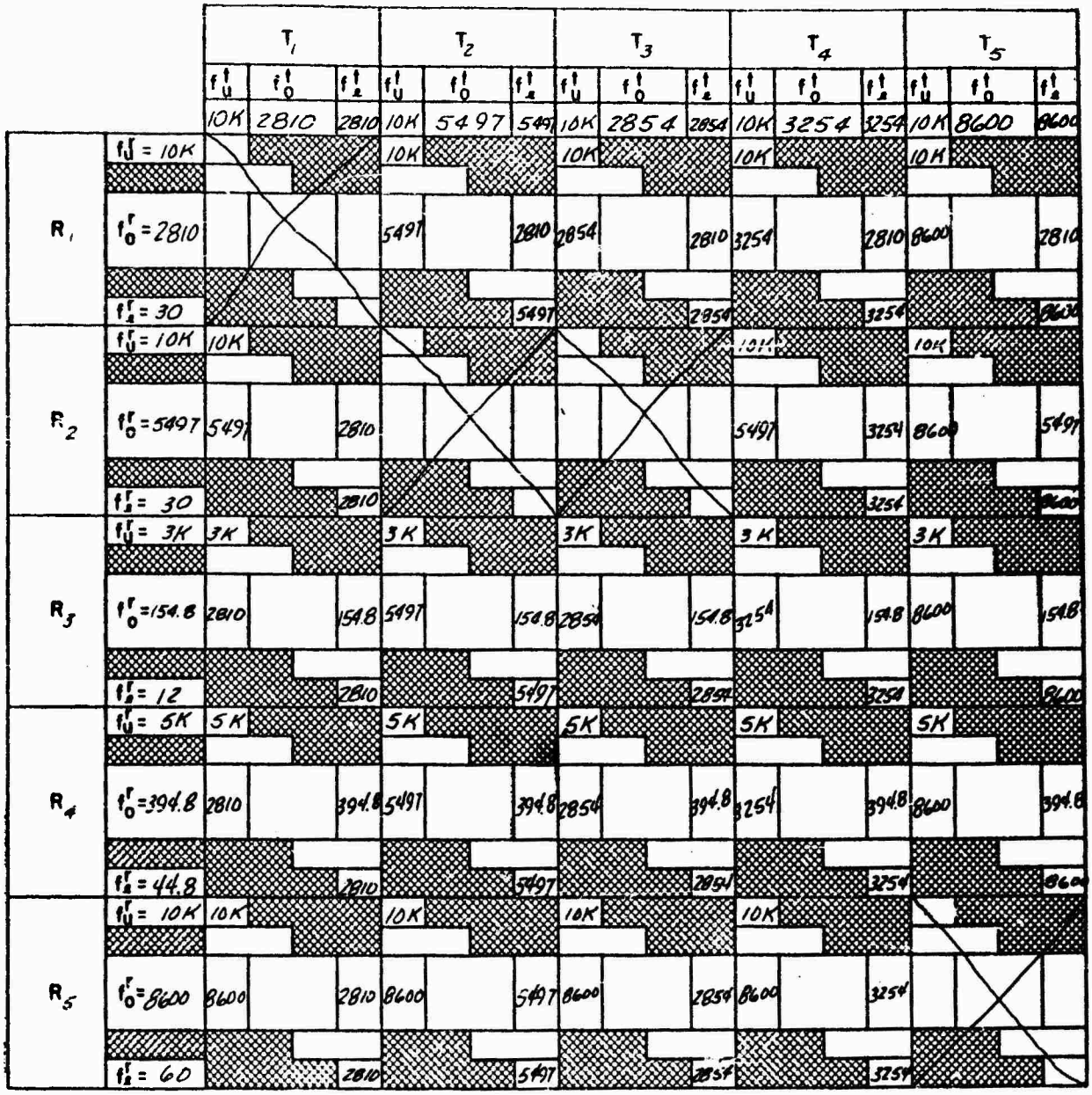

Table 2-15. Form for Interfering Frequency Range Computation.

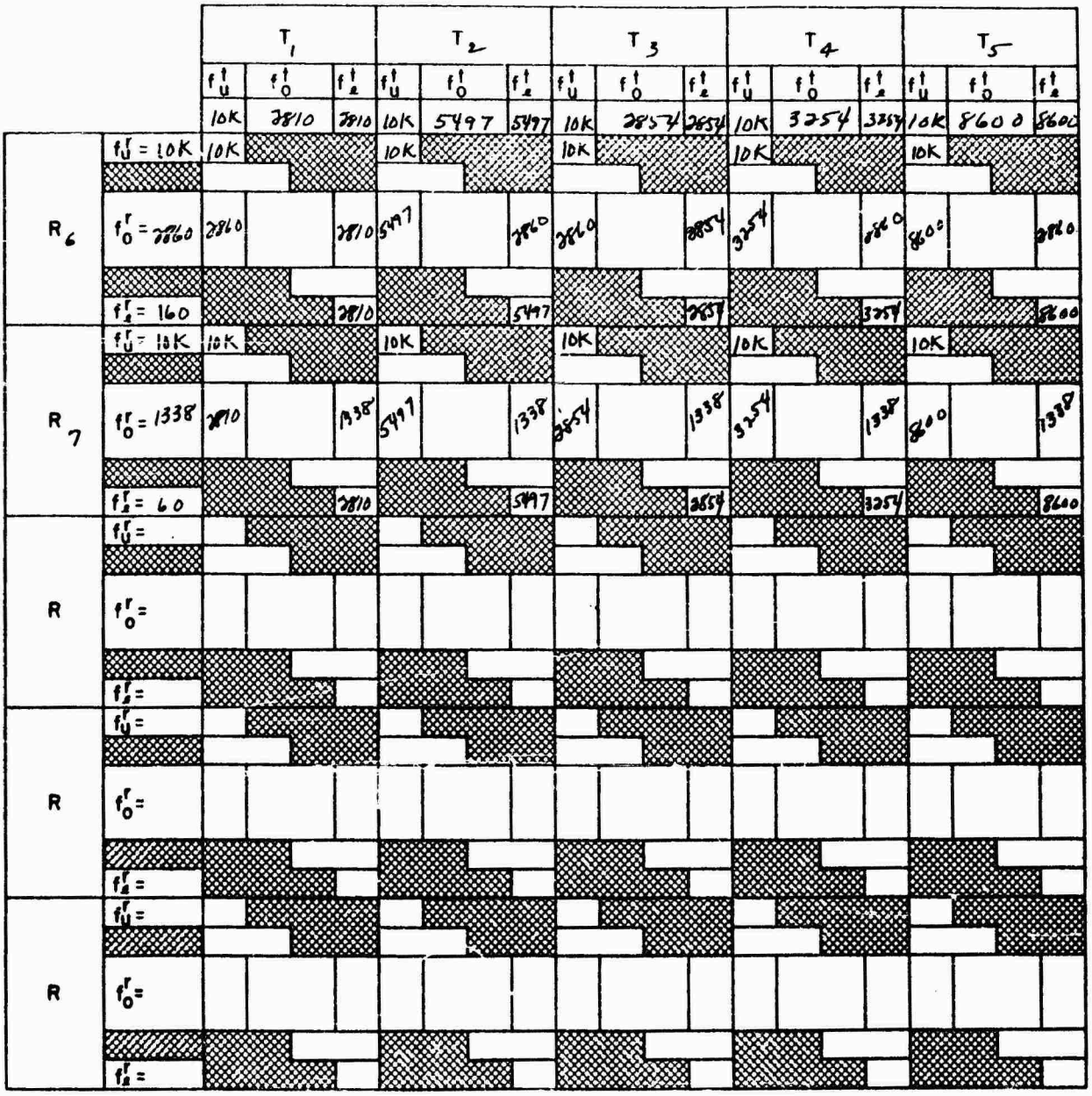

Table 2-15 (cont'd). Form for Interfering Frequency Range Computation.

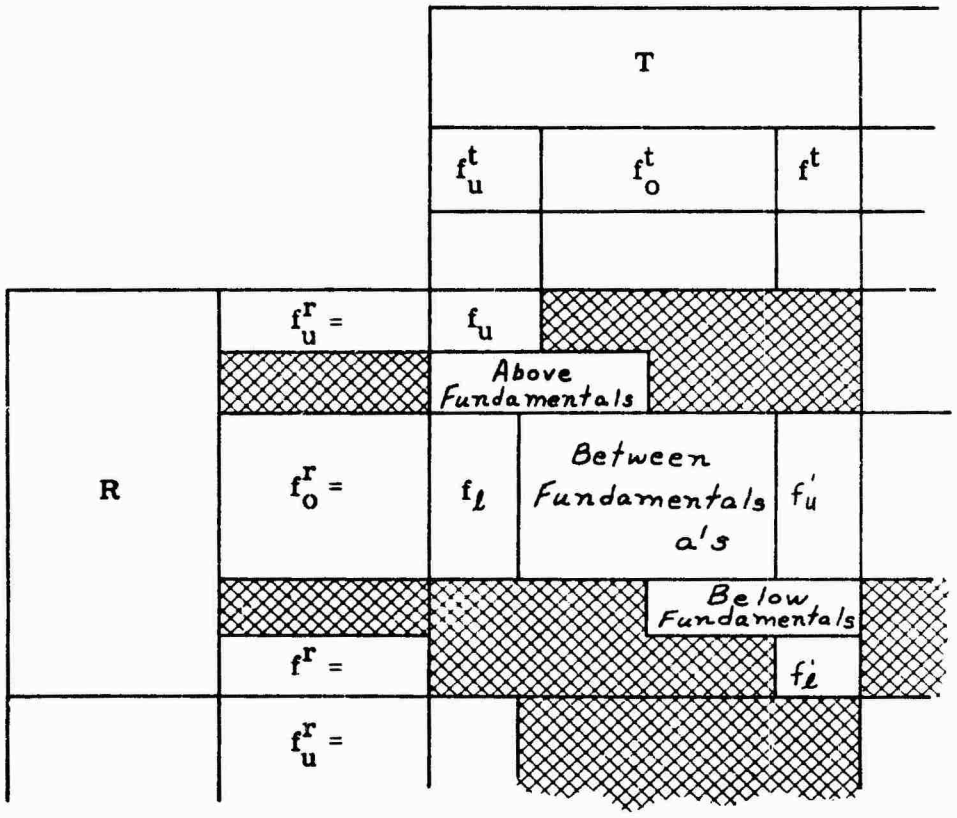

Figure 2-6. Sample Block from Table 2-15 showing the Names for each Square.

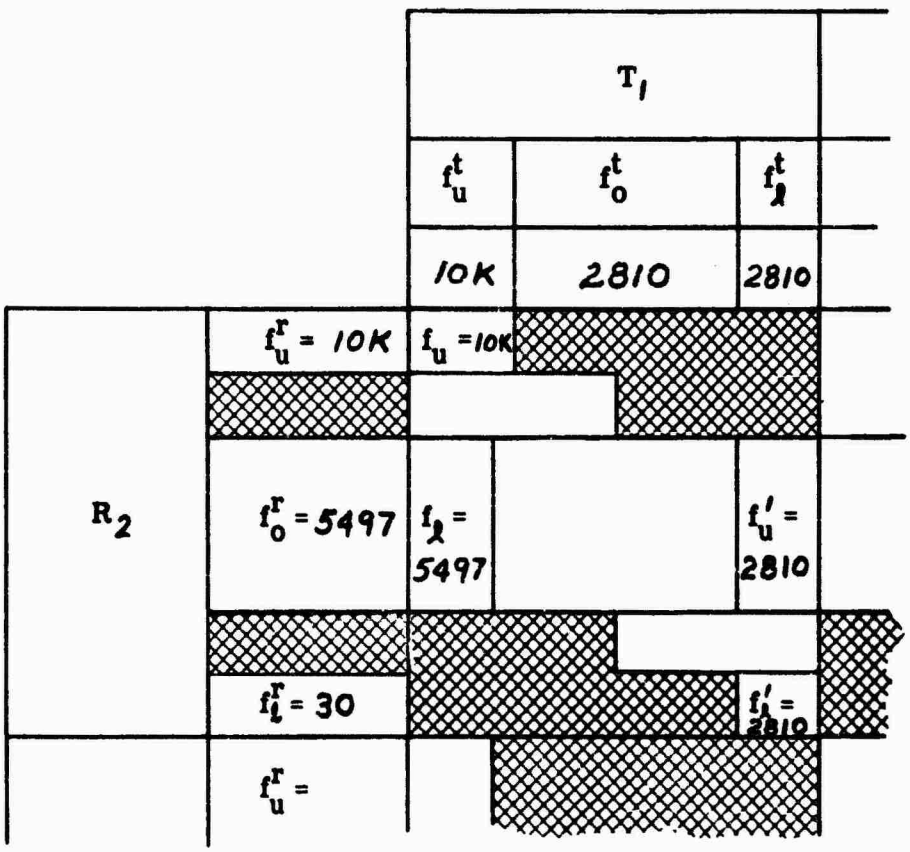

Figure 2-7. Sample Block from Table 2-15.

present lower frequency limit for the defined region below the transmitter and receiver fundamental frequencies.

4. Directly to the left of the intersection of each f_o^r row and f_o^t column is placed the higher value of f_o^r or f_o^t. This number as shown in Figure 2-7 will be called f_ℓ, the present lower frequency limit for the defined region above the transmitter and receiver fundamental frequencies; f_ℓ is also the present upper frequency limit for the region of possible interference between the transmitter and receiver fundamental frequencies.

5. Directly to the right of the intersection of each f_o^r row and f_o^t column is placed the lower value of f_o^r or f_o^t. This number as shown in Figure 2-7 will be called f_u', the present upper frequency limit for the region of possible interference below the transmitter and receiver fundamental frequencies; f_u' is also the present lower frequency limit for the defined region between the transmitter and receiver fundamental frequencies. So that the reader may easily follow the steps which are performed, Table 2-15 has been reproduced as Table 2-16 in which are entered the remaining steps of the frequency comparison process.

6. Compare f_ℓ' with f_u'. If $f_\ell' > f_u'$, then f_u' takes the value of f_ℓ' and the region below the receiver and transmitter fundamental frequencies is not defined. When this condition exists, the applicable space in Table 2-16 (designated "below fundamentals" in Figure 2-6 is crossed out.

7. Compare f_u to f_ℓ. If $f_u > f_\ell$, then f_ℓ takes the value of f_u and the region above the receiver and transmitter fundamental frequencies is not defined. When this condition exists, cross out

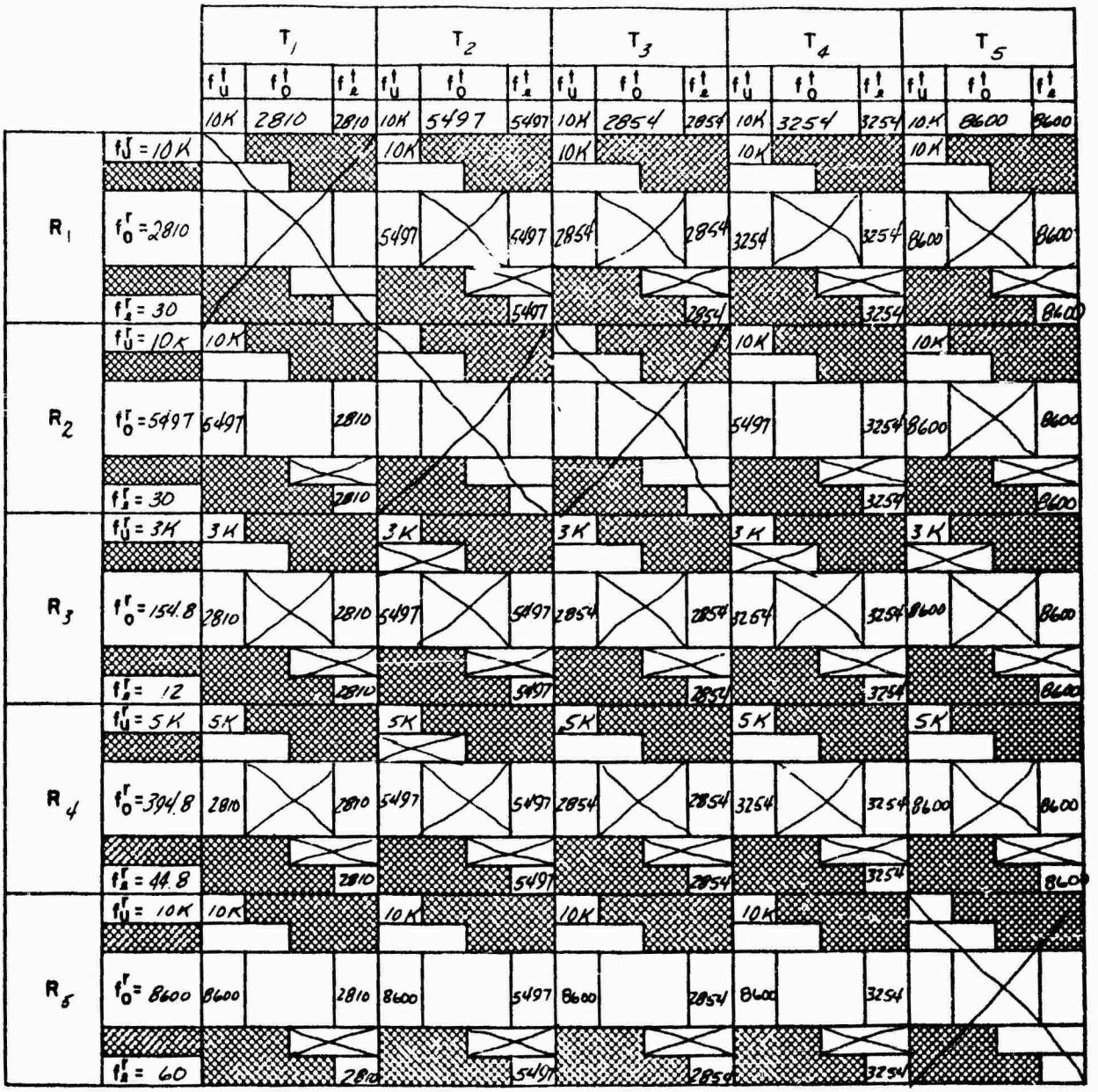

Table 2-16. Form for Interfering Frequency Range Computation.

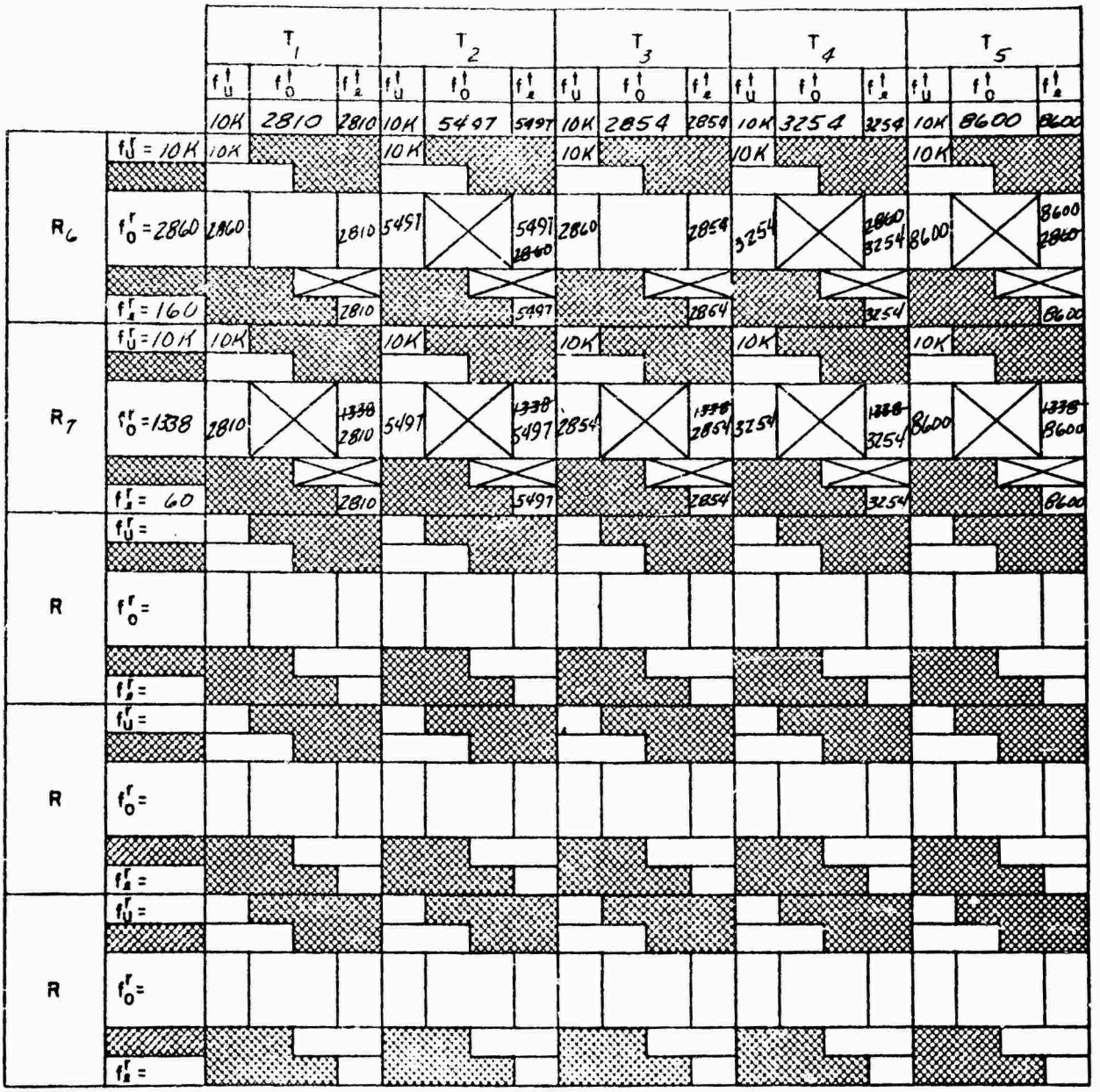

Table 2-16 (cont'd). Form for Interfering Frequency Range Computation.

the applicable space in Table 2-16 (designated "above fundamental" in Figure 2-6).

At this stage of the development of Table 2-16, each block contains three frequency ranges of interest - f_u to f_ℓ, f_ℓ to f'_u and f'_u to f'_ℓ - corresponding respectively to the region above, between and below the fundamental frequencies. For all regions where the upper bound is equal to the lower bound, the region is not defined and need not be considered further.

2.5.2.5 Computation of TFIL and RFIL

The fundamental output of the transmitter and the fundamental response of the receiver are the two most likely sources of interference in general and are treated as special cases. The transmitter fundamental interference level (TFIL) is defined as the interference margin at the fundamental frequency of the transmitter. The receiver fundamental interference level (RFIL) is defined as the interference margin at the fundamental frequency of the receiver. Tables 2-17 through 2-28 for the RFIL and TFIL computations respectively are filled in by the following steps:

1. Enter in Tables 2-17 through 2-28 the values of f_o^r from Table 2-5 and the values of f_o^t from Table 2-7.

2. RFIL cases need not be computed in the RFIL Tables 2-17 through 2-23 when the receiver fundamental frequency lies outside the frequency limits of definition for the transmitter function. The limits of definition for the transmitter function listed across the top of Table 2-16 and the receiver fundamental frequencies listed along the left margin of Table 2-16 may be used to check whether or not the receiver fundamental is within the frequency range of possible output for the transmitter. Those RFIL's which are determined by the above process as invalid are marked void on Tables 2-17 through 2-23. Similarly,

RFIL

R_1 $f_0^r = 2810$	T_1 $f_0^t = 2810$		T_2 $f_0^t = 5497$		T_3 $f_0^t = 2854$		T_4 $f_0^t = 3259$		T_5 $f_0^t = 8600$	
	$f_0^r > f_0^t$	$f_0^t > f_0^r$	~~$f_0^t > f_0^t$~~	$f_0^t > f_0^r$	~~$f_0^t > f_0^t$~~	$f_0^t > f_0^r$	~~$f_0^r > f_0^t$~~	$f_0^t > f_0^r$	~~$f_0^r > f_0^t$~~	$f_0^t > f_0^r$
M_t										
M_t'				123		119		125		124
M_c				-30.5		-30.7		-18.7		-20
N_t LOG f_0^r										
N_t' LOG f_0^r				0		0		0		0
N_c LOG f_0^r				-69		-69		-69		-69
$-S_0$				100		100		100		100
Y_0^r				39		39		39		39
TOTAL	VOID	VOID		162.5		158.3		176.3		174

Table 2-17. Form for Computing RFIL.

RFIL

R_2 $f_0^r = 5497$	T_1 $f_0^t = 2810$		T_2 $f_0^t = 5497$		T_3 $f_0^t = 2854$		T_4 $f_0^t = 3254$		T_5 $f_0^t = 8600$	
	$f_0^r > f_0^t$	$f_0^t > f_0^r$	$f_0^r > f_0^t$	$f_0^t > f_0^r$	$f_0^r > f_0^t$	$f_0^t > f_0^r$	$f_0^r > f_0^t$	$f_0^t > f_0^r$	$f_0^t > f_0^t$	$f_0^t > f_0^r$
M_t	114.5						174.3			
M_t'										124
M_c	-30.5						-27.8			-27.3
N_t LOG f_0^r	-37.4						-112.2			
N_t' LOG f_0^r										0
N_c LOG f_0^r	-74.8						-74.8			-74.8
$-S_0$	100						100			100
Y_0^r	33						33			33
TOTAL	104.8		VOID	VOID	VOID	VOID	92.5			154.9

Table 2-18. Form for Computing RFIL.

RFIL

R_3 $f_0^r = 154.8$	T_1 $f_0^t = 2810$		T_2 $f_0^t = 5497$		T_3 $f_0^t = 2854$		T_4 $f_0^t = 3254$		T_5 $f_0^t = 8600$	
	f_0^t ~~f_0^t~~	$f_0^t > f_0^r$	~~f_0^t~~ f_0^t	$f_0^t > f_0^r$	~~f_0^t~~ f_0^t	$f_0^t > f_0^r$	~~f_0^t~~ f_0^t	$f_0^t > f_0^r$	~~f_0^t~~ f_0^t	$f_0^t > f_0^r$
M_f										
M_f^i		136				119				
M_c		-36.7				-37.8				
N_f LOG f_c^r										
N_f^i LOG f_o^r		0				0				
N_c LOG f_o^r		-43.8				-43.8				
$-S_o$		95				95				
Y_o^r		2				2				
TOTAL		152.5	VOID	VOID		134.4	VOID	VOID	VOID	VOID

Table 2-19. Form for Computing RFIL.

RFIL

R_4 $f_0^r = 394.8$	T_1 $f_0^t = 2810$		T_2 $f_0^t = 5497$		T_3 $f_0^t = 2854$		T_4 $f_0^t = 3254$		T_5 $f_0^t = 8600$	
	~~$f_0^t > f_0^t$~~	$f_0^t > f_0^r$	$f_0^r > f_0^t$	$f_0^t > f_0^r$	~~$f_0^t > f_0^t$~~	$f_0^t > f_0^r$	~~$f_0^r > f_0^t$~~	$f_0^t > f_0^r$	$f_0^r > f_0^t$	$f_0^t > f_0^r$
M_t										
M_t'		136				119		125		
M_c		-36.7				-37.8		-37		
N_t LOG f_0^r										
N_t' LOG f_0^r		0				0		0		
N_c LOG f_0^r		-51.8				-51.8		-51.8		
$-S_0$		92				92		92		
Y_0^r		7				7		7		
TOTAL		146.5	VOID	VOID		128.4		135.2	VOID	VOID

Table 2-20. Form for Computing RFIL.

RFIL

R_5	T_1 $f_0^t = 2810$		T_2 $f_0^t = 5497$		T_3 $f_0^t = 2854$		T_4 $f_0^t = 3254$		T_5 $f_0^t = 8600$	
$f_0^r = 8600$	$f_0^r > f_0^t$	f_0^t ~~f_0^r~~	$f_0^r > f_0^t$	f_0^t ~~f_0^r~~	$f_0^r > f_0^t$	f_0^t ~~f_0^r~~	$f_0^r > f_0^t$	f_0^t ~~f_0^r~~	$f_0^r > f_0^t$	$f_0^t > f_0^r$
M_t	119.5		179.2		166.8		174.3			
M_t'										
M_c	-20		-27.3		-25		-3			
N_t LOG f_0^r	-39.3		-117.9		-117.9		-117.9			
N_t' LOG f_0^r										
N_c LOG f_0^r	-78.6		-78.6		-78.6		-78.6			
$-S_0$	100		100		100		100			
Y_0^r	40		40		40		40			
TOTAL	116.6		95.4		85.3		114.8		VOID	VOID

Table 2-21. Form for Computing RFIL.

RFIL

R_6 $f_0^r = 2860$	T_1 $f_0^t = 2810$		T_2 $f_0^t = 5497$		T_3 $f_0^t = 2854$		T_4 $f_0^t = 3254$		T_5 $f_0^t = 8600$	
	$f_0^r > f_0^t$	f_0^t ~~f_0^r~~	~~f_0^r~~ f_0^t	$f_0^t > f_0^r$	$f_0^r > f_0^t$	f_0^t ~~f_0^r~~	f_0^t ~~f_0^r~~	$f_0^t > f_0^r$	~~f_0^r~~ f_0^t	$f_0^t > f_0^r$
M_t	114.5				166.8					
M_t'				123				125		124
M_c	-36.7			-37.8	-37.8			-37		-37
N_t LOG f_0^r	-39.6				-103.8					
N_t' LOG f_0^r				0				0		0
N_c LOG f_0^r	-69.2			-69.2	-69.2			-69.2		-69.2
$-S_o$	95			95	95			95		95
Y_0^r	2			2	2			2		2
TOTAL	71			113	53			115.8		114.8

Table 2-22. Form for Computing RFIL.

RFIL

R_7 $f_0^r = 1338$	T_1 $f_0^t = 2810$		T_2 $f_0^t = 5497$		T_3 $f_0^t = 2854$		T_4 $f_0^t = 3254$		T_5 $f_0^t = 8600$	
	~~f_0^r f_0^t~~	$f_0^t > f_0^r$	~~f_0^r f_0^t~~	$f_0^t > f_0^r$	~~f_0^r f_0^t~~	$f_0^t > f_0^r$	~~f_0^r f_0^t~~	$f_0^t > f_0^r$	~~f_0^r f_0^t~~	$f_0^t > f_0^r$
M_t										
M_t'		136		123		119		125		129
M_c		-36.7		-37.8		-37.8		-37		-37
N_t LOG f_0^r										
N_t' LOG f_0^r		0		0		0		0		0
N_c LOG f_0^r		-62.6		-62.6		-62.6		-62.6		-62.6
$-S_0$		100		100		100		100		100
Y_0^r		32		32		32		32		32
TOTAL		168.7		154.6		150.6		157.4		156.4

Table 2-23. Form for Computing RFIL.

TFIL

T_1, f_o^t = 2810	R_1 f_o^r = 2810		R_2 f_o^r = 5497		R_3 f_o^r = 154.8		R_4 f_o^r = 394.8		R_5 f_o^r = 8600	
	$f_o^t > f_o^r$	$f_o^r > f_o^t$	$f_o^t = f_o^r$	$f_o^r > f_o^t$	$f_o^t > f_o^r$	$f_o^t = f_o^r$	$f_o^t > f_o^r$	$f_o^t = f_o^r$	$f_o^t = f_o^r$	$f_o^r > f_o^t$
M_r					138		55.2			
M_r'				-866						-907
M_c				-30.5	-36.7		-36.7			-20
N_r LOG f_o^t					-121		-24.1			
N_r' LOG f_o^t				831						831
N_c LOG f_o^t				-69	-69		-69			-69
P_o				97	97		97			97
Y_o^t				39	39		39			39
TOTAL	VOID	VOID		1.5	47.3		61.4			-29

Table 2-24. Form for Computing TFIL.

TFIL

T_1 f_o^t = 2810	R_6 f_o^r = 2860		R_7 f_o^r = 1338		R f_o^r =		R f_o^r =		R f_o^r =	
	~~$f_o^t > f_o^r$~~	$f_o^r > f_o^t$	$f_o^t > f_o^r$	~~$f_o^r > f_o^t$~~	$f_o^t > f_o^r$	$f_o^r > f_o^t$	$f_o^t > f_o^r$	$f_o^r > f_o^t$	$f_o^t > f_o^r$	$f_o^r > f_o^t$
M_r			72							
M_r'		57								
M_c		-36.7	-36.7							
N_r LOG f_o^t			0							
N_r' LOG f_o^t		0								
N_c LOG f_o^t		-69	-69							
P_o		97	97							
Y_o^t		39	39							
TOTAL		87.3	102.3							

Table 2-24 (cont'd). Form for Computing TFIL.

TFIL

T_2 f_o^t = 5497	R_1 f_o^r = 2810		R_2 f_o^r = 5497		R_3 f_o^r = 154.8		R_4 f_o^r = 394.8		R_5 f_o^r = 8600	
	$f_o^t > f_o^r$	~~$f_o^r > f_o^t$~~	$f_o^t > f_o^r$	$f_o^r > f_o^t$	$f_o^t > f_o^r$	$f_o^r > f_o^t$	$f_o^t > f_o^r$	$f_o^r > f_o^t$	~~$f_o^t > f_o^r$~~	$f_o^r > f_o^t$
M_r	79									
M_r'										
M_c	-30.5									-907
N_r LOG f_o^t	0									-27.3
N_r' LOG f_o^t										
N_c LOG f_o^t	-74.8									901
P_o	90									-74.8
Y_o^t	33									90
TOTAL	96.7		VOID	VOID	VOID	VOID	VOID	VOID		33
										14.9

Table 2-25. Form for Computing TFIL.

TFIL

T_2 f_o^t = 5497	R_6 f_o^r = 2860		R_7 f_o^r = 1338		R f_o^r =		R f_o^r =		R f_o^r =	
	$f_o^t > f_o^r$	~~$f_o^r > f_o^t$~~	$f_o^t > f_o^r$	~~$f_o^r > f_o^t$~~	$f_o^t > f_o^r$	$f_o^r > f_o^t$	$f_o^t > f_o^r$	$f_o^r > f_o^t$	$f_o^t > f_o^r$	$f_o^r > f_o^t$
M_r	57		72							
M_r'										
M_c	-37.8		-37.8							
N_r LOG f_o^t	0		0							
N_r' LOG f_o^t										
N_c LOG f_o^t	-74.8		-74.8							
P_o	90		90							
Y_o^t	33		33							
TOTAL	67.4		82.4							

Table 2-25 (cont'd). Form for Computing TFIL.

TFIL

T_s f_o^t = 2854	R_1 f_o^r = 2810		R_2 f_o^r = 5497		R_3 f_o^r = 154.8		R_4 f_o^r = 394.8		R_5 f_o^r = 8600	
	$f_o^t > f_o^r$	~~$f_o^r > f_o^t$~~	~~$f_o^t > f_o^r$~~	$f_o^r > f_o^t$	$f_o^t > f_o^r$	~~$f_o^r > f_o^t$~~	$f_o^t > f_o^r$	~~$f_o^r > f_o^t$~~	~~$f_o^t > f_o^r$~~	$f_o^r > f_o^t$
M_r	79				138		55.2			
M_r'										
M_c	-30.7				-37.8		-37.8			-907
N_r LOG f_o^t	0				-121		-24.2			-25
N_r' LOG f_o^t										
N_c LOG f_o^t	-69.2				-69.2		-69.2			833
P_o	84				84		84			-69.2
Y_o^t	35				35		35			84
TOTAL	98.1		VOID	VOID	29		43			35
										-24.2

Table 2-26. Form for Computing TFIL.

TFIL

T_3 f_o^t = 2854	R_6 f_o^r = 2860		R_7 f_o^r = 1338		R f_o^r =		R f_o^r =		R f_o^r =	
	~~$f_o^t > f_o^r$~~	$f_o^r > f_o^t$	$f_o^t > f_o^r$	~~$f_o^r > f_o^t$~~	$f_o^t > f_o^r$	$f_o^r > f_o^t$	$f_o^t > f_o^r$	$f_o^r > f_o^t$	$f_o^t > f_o^r$	$f_o^r > f_o^t$
M_r			72							
M_r'		57								
M_c		-37.8	-37.8							
N_r LOG f_o^t			0							
N_r' LOG f_o^t		0								
N_c LOG f_o^t		-69.2	-69.2							
P_o		84	84							
Y_o^t		35	35							
TOTAL		69	84							

Table 2-26 (cont'd). Form for Computing TFIL.

TFIL

T_4 $f_o^t = 3254$	R_1 $f_o^r = 2810$		R_2 $f_o^r = 5497$		R_3 $f_o^r = 154.8$		R_4 $f_o^r = 394.8$		R_5 $f_o^r = 8600$	
	$f_o^t > f_o^r$	$f_o^t < f_o^r$	$f_o^t > f_o^r$	$f_o^r > f_o^t$	$f_o^t > f_o^r$	$f_o^r > f_o^t$	$f_o^t > f_o^r$	$f_o^t < f_o^r$	$f_o^t > f_o^r$	$f_o^r > f_o^t$
M_r	79						55.2			
M_t^1										-907
M_c	-18.7						-37			-3
N_r LOG f_o^t	0						-24.6			
N_r^1 LOG f_o^t										846
N_c LOG f_o^t	-70.2						-70.2			-70.2
P_o	90						90			90
γ_o^t	35						35			35
TOTAL	115.1		VOID	VOID	VOID	VOID	48.9			-9.2

Table 2-27. Form for Computing TFIL.

TFIL

T_4 f_o^t = 3254	R_6 f_o^r = 2860		R_7 f_o^r = 1338		R f_o^r =		R f_o^r =		R f_o^r =	
	$f_o^t > f_o^r$	~~$f_o^r > f_o^t$~~	$f_o^t > f_o^r$	~~$f_o^r > f_o^t$~~	$f_o^t > f_o^r$	$f_o^r > f_o^t$	$f_o^t > f_o^r$	$f_o^r > f_o^t$	$f_o^t > f_o^r$	$f_o^r > f_o^t$
M_r	57		72							
M_r'										
M_c	-37		-37							
N_r LOG f_o^t	0		0							
N_r' LOG f_o^t										
N_c LOG f_o^t	-70.2		-70.2							
P_o	90		90							
Y_o^t	35		35							
TOTAL	74.8		89.8							

Table 2-27 (cont'd). Form for Computing TFIL.

TFIL

T_5 f_o^t = 8600	R_1 f_o^r = 2810		R_2 f_o^r = 5497		R_3 f_o^r = 154.8		R_4 f_o^r = 394.8		R_5 f_o^r = 8600	
	$f_o^t > f_o^r$	~~$f_o^r > f_o^t$~~	$f_o^t > f_o^r$	~~$f_o^r > f_o^t$~~	$f_o^t > f_o^r$	$f_o^r > f_o^t$	$f_o^t > f_o^r$	$f_o^r > f_o^t$	$f_o^t > f_o^r$	$f_o^r > f_o^t$
M_r	79		73							
M_r'										
M_c	-20		-27.3							
N_r LOG f_o^t	0		0							
N_r' LOG f_o^t										
N_c LOG f_o^t	-78.6		-78.6							
P_o	84		84							
Y_o^t	40		40							
TOTAL	104.4		91.1		VOID	VOID	VOID	VOID	VOID	VOID

Table 2-28. Form for Computing TFIL.

TFIL

T_5 f_o^t = 8600	R_6 f_o^r = 2860		R_7 f_o^r = 1338		R f_o^r =		R f_o^r =		R f_G^r =	
	$f_o > f_o^r$	~~f_o^t < f_o^r~~	$f_o^t > f_o^r$	~~f_o^t < f_o^r~~	$f_o^t > f_o^r$	$f_o^r > f_o^t$	$f_o^t > f_o^r$	$f_o^r > f_o^t$	$f_o^t > f_o^r$	$f_o^r > f_o^t$
M_r	57		72							
M_r'										
M_c	-37		-37							
N_r LOG f_o^t	0		0							
N_r' LOG f_o^t										
N_c LOG f_o^t	-78.6		-78.6							
P_o	84		84							
Y_o^t	40		40							
TOTAL	65.4		80.4							

Table 2-28 (cont'd). Form for Computing TFIL.

The TFIL cases need not be computed in the TFIL Tables 2-24 through 2-28 when the transmitter fundamental frequency lies outside the frequency limits of definition for the receiver function. The limits of definition for the receiver function listed along the left margin of Table 2-16 and the transmitter fundamental frequencies listed across the top of Table 2-16 may be used to check whether or not the transmitter fundamental is within the frequency range of possible receiver response. Those TFIL's which are determined by the above process as invalid are marked void on Tables 2-24 through 2-28.

3. Check for the condition in Tables 2-17 through 2-28 that $f_o^t > f_o^r$ and $f_c^r > f_o^t$, then note which statement is incorrect by crossing it out. Disregard all blocks in that column.

4. From Table 2-9 select the correct values of M_r and M'_r for each receiver and place them in the TFIL Tables 2-24 through 2-28.

5. From Table 2-11 select the correct values of M_t and M'_t for each transmitter and place them in the RFIL Tables 2-17 through 2-23.

6. From the receiver rows in Table 2-14 select the values of M_c and enter them in the correct location on the RFIL Tables 2-17 through 2-23.

7. From the transmitter columns in Table 2-14 select the values of M_c and enter them in the correct location on the TFIL Tables 2-24 through 2-28.

8. Enter the values of $N_t \log f_o^r$ (or $N'_t \log f_o^r$) and $N_c \log f_o^r$ in the RFIL Tables 2-17 through 2-23. N_t and N'_t may be obtained from Table

2-12; log f_o^r from Table 2-5; N_c is equal to -20.

9. Enter the value of N_r log f_o^t (or N_r' log $f^t{}_o$) and N_c log f_o^t in the TFIL Tables 2-24 through 2-28. N_r and N_r' may be obtained from Table 2-10, log f_o^t from Table 2-7; N_c is equal to -20.

10. For each receiver in Taole 2-5, enter the value of $-S_o$ and Y_o^r in every space for $-S_o$ and Y_o^r in the RFIL table corresponding to that receiver.

11. For each transmitter in Table 2-7 enter the value of P_o and Y_o^t in every space for P_o and Y_o^t in the TFIL table corresponding to that transmitter.

12. Add each column in the RFIL Tables 2-17 through 2-23. The receiver fundamental interference level in db is equal to the positive sum in each case. A negative sum indicates no interference.

13. Add each column in the TFIL Tables 2-24 through 2-28. The transmitter fundamental interference level in db is equal to the positive sum in each case. A negative sum indicates no interference.

2.5.2.6 Rapid Culling Answer

Next, all ranges of possible, interference are computed as a function of interference margin, P, given by equation 40.

$$P = \overline{N} \log f + \overline{M} \tag{40}$$

Table 2-29 is a tabulation of the frequency range f and corresponding $\overline{N}$ and $\overline{M}$ for the receiver-tramsitter pairs of the defined frequency regions given in Table 2-16. In Table 2-29 the column for $\overline{N}$ and $\overline{M}$ is filled in the following manner. Referring to Figure 2-5 select from Table 2-13 for the desired R and T combination values for N, N°, N', M, M° and M'. Add N_c = -20

to the corresponding N's and enter these in Table 2-29. Add the values for M_c, from Table 2-14 for the desired R and T combinations to the corresponding M's and enter these in Table 2-29. The interference margin, P, is then found by substituting the corresponding values for $\bar{N}$ and $\bar{M}$ in Equation 1. These results along with the corresponding RFIL's and TFIL's represent the output of the rapid culling step.

Table 2-29

TABULATION OF THE FREQUENCY RANGE, $\bar{N}$ AND $\bar{M}$ FOR RAPID CULL

T-R Combination	Above Fundamentals f(Mc)	$\bar{N}$	$\bar{M}$	Between Fundamentals f(Mc)	$\bar{N}$	$\bar{M}$
$T_1 - R_2$	5497-10,000	-30	157	2810-5497	211	-782
$T_1 - R_3$	2810-3000	-65	215.8			
$T_1 - R_4$	2810-5000	-37	133			
$T_1 - R_5$	8600-10,000	-30	157.5	2810-8600	211	-829.5
$T_1 - R_6$	2860-10,000	-30	134.8	2810-2860	-30	134.8
$T_1 - R_7$	2810-10,000	-30	149.8			
$T_2 - R_1$	5497-10,000	-50	227.7			
$T_2 - R_5$	8600-10,000	-50	231.9	5497-8600	191	-758.3
$T_2 - R_6$	5497-10,000	-50	198.4			
$T_2 - R_7$	5497-10,000	-50	223.4			
$T_3 - R_1$	2854-10,000	-50	215.1			
$T_3 - R_4$	2854-5000	-57	184.2			
$T_3 - R_5$	8600-10,000	-50	221.8	2854-8600	191	-765.2
$T_3 - R_6$	2860-10,000	-50	186	2854-2860	-50	186
$T_3 - R_7$	2854-10,000	-50	201			
$T_4 - R_1$	3254-10,000	-50	234.6			
$T_4 - R_2$	5497-10,000	-50	219.5	3254-5497	191	-719.5
$T_4 - R_4$	3254-5000	-57	192.5			
$T_4 - R_5$	8600-10,000	-50	251.3	3254-8600	191	-735.7
$T_4 - R_6$	3254-10,000	-50	194.3			
$T_4 - R_7$	3254-10,000	-50	209.3			
$T_5 - R_1$	8600-10,000	-50	244.9			
$T_5 - R_2$	8600-10,000	-50	231.6			
$T_5 - R_6$	8600-10,000	-50	205.9			
$T_5 - R_7$	8600-10,000	-50	220.9			

2.5.3 Final Cull for Sample Problem

As an example of the final culling step consider combinations $T_3 - R_1$. The range of possible interference lies between 2854 and 10,000 Mc. Table 2-30 is used to tabulate the solution to the equation

$$p = \frac{\left| \pm qnf_o^t - f_{if} \right|}{f_{\ell o}}$$

The value for the maximum n (n_{max}) is found by dividing the upper frequency limit (10,000 Mc) obtained from the rapid cull by the trasmitter fundamental frequency (2860 Mc) for the corresponding transmitter. For the combination $T_3 - R_1$, $n_{max} = 3$, which is the maximum number of harmonics of the transmitter fundamental to be considered for this case.

Table 2-30 is filled in the following manner.

1. Obtain $f_{if} = 30$ Mc from Table 2-5. Substitute the corresponding values for q, n, f_o^t and f_{if} in the expressions $\pm qnf_o^t$ and $\left| \pm qnf_o^t - f_{if} \right|$. Tabulate the values in the indicated columns.

2. Obtain $f_{\ell o} = 2897$ Mc fron Table 2-5. Then, the $p + \Delta p$ column is found by dividing the $\left| \pm qnf_o^t - f_{if} \right|$ column by $f_{\ell o}$. Enter these values in the indicated column.

3. Since p must be an integer, the $p + \Delta p$ column is rounded to the nearest integer and entered in the column marked p. The noninteger part, Δp, is entered in the Δp column.

4. The column Δf or $\Delta f/n$ is found by multiplying Δp by $f_{\ell o}$ and dividing by q. The value Δf is the frequency separation between the receiver spurious response and the corresponding harmonic of the transmitter. In this case T_3 is a radar transmitter and the frequency separation Δf is divided by n. Enter the values in the indicated

n 1 T_3-R_1 f_{0}^{t} = 2860 Mc f_{l_0} = 2897 Mc f_{l_f} = 30 Mc

q	$\pm qnf_0^t$	$\lvert \pm gnf_0^t - f_{l_f} \rvert$	p + Δp	p	Δp	Δf or Δf/n	Δf db	q Corr.	Frequency Cull db	Rapid Cull db	Total db	Prob. %
1	2860	2830	0.9768726	1	0.0231274	67.0	88	0	88	98	10	1.4
2	5720	5690	1.9641008	2	0.0358992	52.0	83	15	98	98		
3	8580	8550	2.9513289	3	0.0486711	47.0	81	20	101	98		
4	11440	11410	3.9385571	4	0.0614429	44.5	80	20	100	98		
-1	-2860	2890	0.9975837	1	0.0024163	7.0	50	0	50	158	108	100
-2	-5720	5750	1.9848118	2	0.0151882	22.0	67	15	82	98	16	4
-3	-8580	8610	2.9720400	3	0.0279600	27.0	71	20	91	98	7	0.7
-4	-11440	11470	3.9592682	4	0.0407318	29.5	72	20	92	98	6	0.6

n 2

q	$\pm qnf_0^t$	$\lvert \pm gnf_0^t - f_{l_f} \rvert$	p + Δp	p	Δp	Δf or Δf/n	Δf db	q Corr.	Frequency Cull db	Rapid Cull db	Total db	Prob. %
1	5720	5690	1.9641008	2	0.0358992	52.0	83	0	83	27		
2	11440	11410	3.9385571	4	0.0614429	44.5	80	15	95	27		
3	17160	17130	5.9130134	6	0.0869866	42.0	79	20	99	27		
4	22880	22850	7.8874697	8	0.1125303	40.8	78	20	98	27		
-1	-5720	5750	1.9848118	2	0.0151882	22.0	67	0	67	27		
-2	-11440	11470	3.9592682	4	0.0407318	29.5	72	15	87	27		
-3	-17160	17190	5.9337245	6	0.0662755	32.0	74	20	94	27		
-4	-22880	22910	7.9081808	8	0.0918192	33.2	75	20	95	27		

Table 2-30. Frequency Cull.

n 3 T_3-R_1 f_{o}^{t} = 2860 Mc f_{l_o} = 2897 Mc f_{l_f} = 30 Mc

q	$\pm qnf_o^t$	$\lvert \pm gnf_o^t - f_{l_f} \rvert$	p + Δp	p	Δp	Δf or Δf/n	Δf db	q Corr.	Frequency Cull db	Rapid Cull db	Total db	Prob. %
1	8580	8550	2.9513289	3	0.0486711	47.0	81	0	81	19		
2	17160	17130	5.9130134	6	0.0869866	42.0	79	15	94	19		
3	25740	25710	8.8746979	9	0.1253021	40.3	78	20	98	19		
4	34320	34290	11.8363823	12	0.1636177	39.5	78	20	98	19		
-1	-8580	8610	2.9720400	3	0.0279600	27.0	71	0	71	19		
-2	-17160	17190	5.9337245	6	0.0662755	32.0	74	15	89	19		
-3	-25740	25770	8.8954089	9	0.1045911	33.7	75	20	95	19		
-4	-34320	34350	11.8570934	12	0.1429066	34.5	75	20	95	19		

n ___

q	$\pm qnf_o^t$	$\lvert \pm gnf_o^t - f_{l_f} \rvert$	p + Δp	p	Δp	Δf or Δf/n	Δf db	q Corr.	Frequency Cull db	Rapid Cull db	Total db	Prob. %
1								0				
2								15				
3								20				
4								20				
-1								0				
-2								15				
-3								20				
-4								20				

Table 2-30. (cont'd). Frequency Cull.

column.

5. Next, the Δf db column is obtained by selecting from the composite bandwidth curve for $T_3 - R_1$ (Figure 2-8) the db for the corresponding Δf/n.

6. The q correction is a constant chosen for the receiver spurious responses when q>1.

7. Add the Δf db and the corresponding q correction db to obtain the Frequency Cull db column. Tabulate the values in the indicated column.

8. From Table 2-26 select the correct value of TFIL and enter this value in the Rapid Cull db column under n = 1, for all the p- q responses except the p = 1, q = -1 response. The p = 1, q = -1 response corresponds to the fundamental frequency of the receiver, and the following equation is used to determine the rapid cull db:

$$TFIL = RFIL = P_o - S_o + Y_o^t + Y_o^r - 20 \log d - 20 \log f_o^t - 37 \qquad (41)$$

The values of the terms on the right-hand side of Equation 41 can be obtained from Tables 2-5, 2-7 and 2-14. The TFIL = RFIL = 84 + 100 + 35 + 39 + 613 - 69.2 - 37 = 158. Enter the TFIL = RFIL = 158 in the Rapid Cull db column for the p = 1, q = -1 response.

9. From Table 2-29 obtain the corresponding $\bar{N}$ and $\bar{M}$ for $T_3 - R_1$, and substitute these values in Equation 40 to obtain the rapid cull db for the frequency corresponding to an n of 2. Tabulate this rapid cull db in the Rapid Cull db column under n = 2.

10. Using the equation discussed in (9) above, obtain the rapid cull db for the frequency corresponding

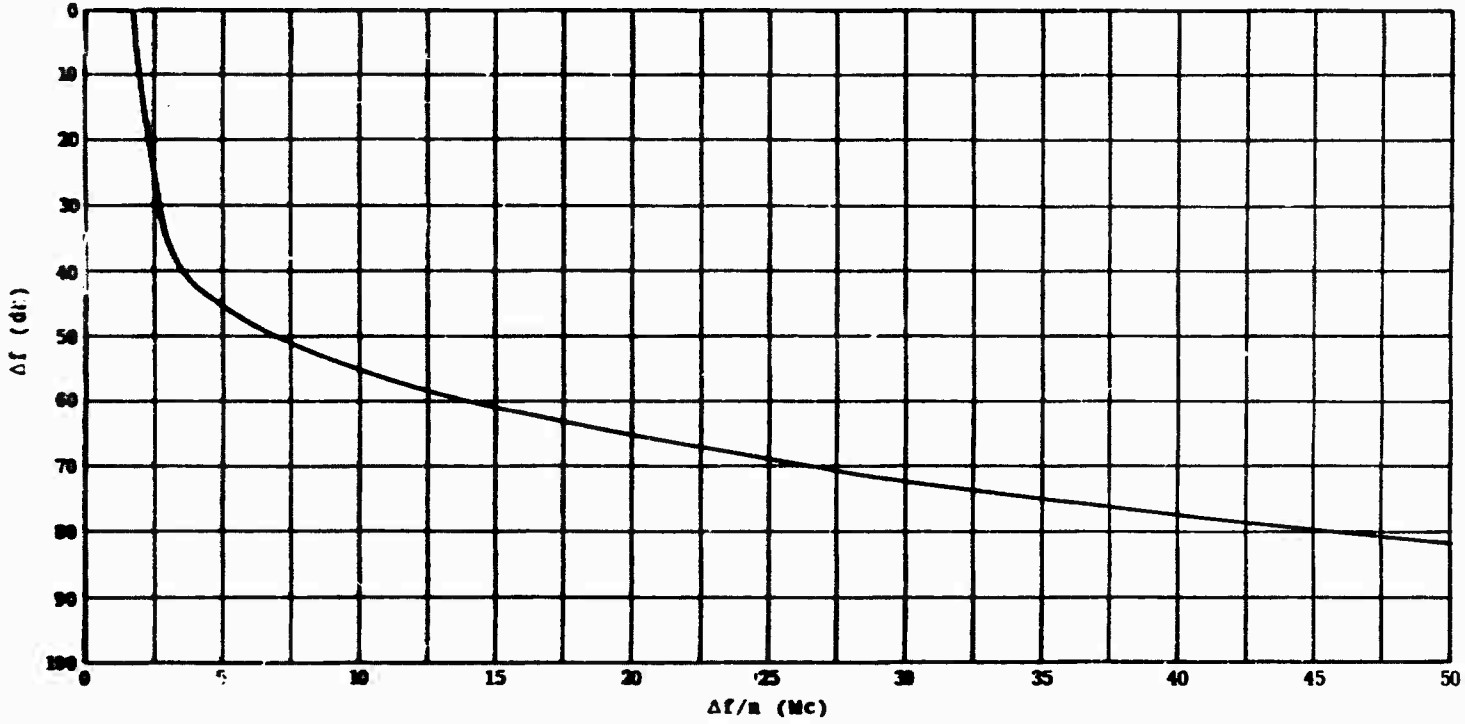

Figure 2-8. Frequency Cull Bandwidth Correction Factor for T_3-R_1.

to an n of 3. Tabulate this rapid cull db in the Rapid Cull db Column under n = 3.

11. The interference margin (Total db) column is obtained by subtracting the frequency cull db from the corresponding rapid cull db.

12. The probability of interference for each emission that could possibly interfere is found by using the appropriate curve from Figure 2-4 and the interference margin (Total db) given in Table 2-30. The probability of interference is tabulated in Table 2-30.

2.5.4 Validation

The sample prediction just presented represents an actual equipment configuration which exists at the Air Force Test Facility in Verona, New York. Table 2-31 presents a comparison between the predicted probabilities of interference and the actual occurrence of interference. Actual nomenclatures of the equipments are omitted to avoid security classifications. In those cases where the transmitter and receiver are co-located or are part of the same equipment, neither measurements nor predictions were made. The probability of interference is a direct measure of the liklihood that interference occurs. A probability of 100 infers that interference is certain to occur and a probability of zero infers that interference is certain to never occur. Any intermediate probability indicates the relative likelihood of interference under such wide uncertainties as variations in propagation conditions, equipment tuning, component aging, etc.

In addition to performing interference measurements, the personnel of the Verona Facility were requested to measure the three predominant environmental components contributed by each equipment. Table 2-32 presents these measured environmental components along with the predicted levels which were used. Again, equipment nomenclatures are omitted to avoid security classification. Since the transmitter power output, antenna gain and propagation functions are all defined in a statistical fashion, the comparison in Table 2-32

Table 2-31

INTERFERENCE PREDICTION

Transmitter-Receiver Combination	Measured Interference	Predicted Probability of Interference in Percent
$T_1 - R_1$	Same Equipment	-
$T_1 - R_2$	No	0.6
$T_1 - R_3$	No	0
$T_1 - R_4$	No	1.0
$T_1 - R_5$	No Data	-
$T_1 - R_6$	Yes	88.0
$T_1 - R_7$	No	25.5
$T_2 - R_1$	No	0
$T_2 - R_2$	Same Equipment	-
$T_2 - R_3$	No	0
$T_2 - R_4$	No	0
$T_2 - R_5$	No	0
$T_2 - R_6$	No	0
$T_2 - R_7$	No	0
$T_3 - R_1$	Yes	100
$T_3 - R_2$	Co-located	-
$T_3 - R_3$	No	0
$T_3 - R_4$	No	0
$T_3 - R_5$	Yes	62.0
$T_3 - R_6$	Yes	100
$T_3 - R_7$	No	56
$T_4 - R_1$	No Data	-
$T_4 - R_2$	No Data	-
$T_4 - R_3$	No	0
$T_4 - R_4$	No	0
$T_4 - R_5$	No Data	-
$T_4 - R_6$	Co-located	-
$T_4 - R_7$	No	2.5
$T_5 - R_1$	No	28.0
$T_5 - R_2$	No	8.0
$T_5 - R_3$	No	0

Table 2-31 (cont'd)

INTERFERENCE PREDICTION

Transmitter-Receiver Combination	Measured Interference	Predicted Probability of Interference in Percent
$T_5 - R_4$	No	0
$T_5 - R_5$	Same Equipment	-
$T_5 - R_6$	No	0
$T_5 - R_7$	No	0

cannot be direct. Several pertinent details of the predicted statistical level are presented in Table 2-32 for comparison with the measured value. The first is the 95.5 percent level which according to the prediction is almost never exceeded (i.e., only exceeded 4.5 percent of the time). The second is the 4.5 percent level which according to prediction is exceeded 95.5 percent of the time. There is a range of values between these levels into which 91 percent of the measured values should fall.

Since there was a total of thirty-five measured outputs, it is expected that either three or four of these observed values will be outside of the predicted range. From Table 2-32 it can be seen that, as expected, there are four measurements which are not included within the specified range.

Another factor presented in Table 2-32 is the predicted probability that the level which was actually observed is exceeded. This factor is a measure of the position of the measurement within the predicted statistical range of possible values.

A low probability that the measurement is exceeded indicates that the measurement fell near the predicted upper bound. A high probability that the measurement is exceeded indicates that the measurement fell near the predicted lower bound. A probability near 50 percent indicates that the measurement fell near the predicted median. In every case, the measured values fell somewhere between the predicted upper and lower bounds, i.e., the predicted probability was was never zero or 100. Also, the measured values were well distributed over the predicted range indicating that the spread of the predicted statistic was proper. If all environmental components were measured, we

Table 2-32

COMPARISON OF MEASURED AND PREDICTED TRANSMITTER OUTPUTS

Xmtr	Emission	Frequency (Mc)	Distance (ft)	Pred. Max. Power (95.5%)	Measured Power (dbm)	Pred. Min. Power (4.5%)	Pred. Probability That Measured is Exceeded (%)
T_1	Fundamental	2812.21	2489	36	-22	-5	99.9
	Spurious	3075	2489	-16	-40	-96	24.5
	Spurious	3200	2489	-17	-65	-97	77.5
T_1	Fundamental	2808.94	5107	29	1	-12	72
	Spurious	5558.4	5107	-45	-65	-125	17.7
	Second Harmonic	5616.2	5107	-36	-54	-128	17
	Third Harmonic	8400	5107	-41	-67	-120	28
T_2	Fundamental	5490	1737	21	-13	-20	86
	Spurious	5860	1737	-31	-68	-111	54
T_2	Fundamental	5461	2489	18	-20	-23	92
	Spurious	5895	2489	-34	-76	-114	65.5
T_2	Fundamental	5494.95	5790	10	4	-31	11
	Spurious	7758	5790	-55	-72	-135	13.5
	Spurious	7809	5790	-55	-75	-135	17.7
	Spurious	8575	5790	-59	-63	-139	3
T_3	Fundamental	2859.86	1332	25	-26	-16	99.3
	Spurious	3571	1332	-32	-80	-112	78
T_3	Fundamental	2859.86	2576	19	-26	-22	97.5
	Spurious	3571	2576	-41	-80	-121	59

Table 2-32 (cont'd)

COMPARISON OF MEASURED AND PREDICTED TRANSMITTER OUTPUTS

Xmtr	Emission	Frequency (Mc)	Distance (ft)	Pred. Max. Power (95.5%)	Measured Power (dbm)	Pred. Min. Power (4.5%)	Pred. Probability That Measured is Exceeded (%)
T_3	Fundamental	2859.86	5829	12	-13	-29	63
	Spurious	3568	5829	-48	-77	-128	35
T_4	Fundamental	3254	1848	27	23	-14	8.5
T_4	Fundamental	3254	2337	25	19.5	-16	10.5
T_4	Fundamental	3254	5187	18	14.5	-23	8
	Spurious	4622	5187	-47	-59	-127	8
	Spurious	4842	5187	-50	-67	-130	13.5
T_5	Fundamental	8598.5	1737	18	-30	-23	98.7
T_5	Fundamental	8598.5	2448	15	-8	-26	57
	Spurious	9151	2448	-37	-57	-117	18
	Spurious	9780	2448	-40	-55	-120	11
T_5	Fundamental	8601.9	5190	8	-5	-33	26
	Spurious	8781	5190	-43	-66	-123	23
	Spurious	9079	5190	-44	-60	-124	12
	Spurious	9639	5190	-47	-52	-127	3.5
	Spurious	9669	5190	-47	-54	-127	4.5

expect to see the probability, that each measurement was exceeded, distributed equally above and below 50 percent. However, only the three highest outputs from each equipment were measured, ignoring many lower, but still possibly significant output levels. Hence, there should be significantly more low probabilities that each measurement was exceeded than high probabilities. Out of thirty-five measurements noted in Table 2-32, 21 were below 50 percent and 14 were above 50 percent. Table 2-32 provides excellent validation for the transmitter, antenna and propagation statistics which are used.

Section 3

TRANSMITTERS

3.1 INTRODUCTION

High-power radar transmitters have presented a major problem in the development of mathematical models to describe transmitter output spectra. The harmonic outputs of these transmitters can be presented in a manner similar to other transmitters and therefore do no present any special problems. However, this representation is not always sufficient to completely describe the output. For example, in addition to the fundamental and harmonic outputs, there may be other discrete spurious outputs of considerable amplitude that must be included in a mathematical model of these transmitters. Nonharmonically related spurious outputs are almost always present in transmitters that use magnetrons and are sometimes present in transmitters that use other types of final power tubes. The problem in specifying these outputs is that they are not precisely defined in either amplitude or frequency. Thus, although their amplitude may be described statistically in a manner similar to the harmonically related outputs, (i.e., in terms of the probability that a particular level will be equaled or exceeded), a second statistic may be required to describe the probability of an output occurring within any given frequency range. In addition to the above mentioned discrete outputs, measurements have indicated that high-power radar transmitters also produce an output which resembles noise. This "noise" exists at all frequencies and exhibits random amplitude variations about some mean value. However, because of the relatively low-power level associated with this noise, it is not as important as the higher amplitude discrete outputs.

During the past quarter, an extensive study was conducted to establish methods for considering magnetron nonharmonic outputs in the interference analysis process. The results of this study are presented in this report.

3.2 Theoretical Discussion of Magnetrons[1,2]

In order to provide an understanding of the magnetron spurious output generating mechanism and of the associated analysis problems, some of the more pertinent factors that must be considered will be discussed.

Basically, a magnetron consists of a cathode, an anode, the electron interaction space, and the resonant system. The resonant system, which usually consists of a number of coupled cavities surrounding a relatively large cylindrical cathode, is of primary interest to the interference analyst since the frequency of both the desired and undesired outputs are determined by these resonators. Three commonly used types of resonant systems are shown in Figure 3-1. Both capacitive and inductive coupling exist between the individual cavities and although the relative magnitude of the two types of coupling depends on the structural parameters, capacitive coupling usually dominates.

Analysis of a system such as the one shown in Figure 3-1 shows that for N coupled resonant circuits there are N fundamental modes of resonance which are in general different from each other and from the resonant frequency of the individual uncoupled resonators. The zero mode cannot be excited readily, so that practically, there will be N-1 modes of resonance. In addition, if the resonant system is completely symmetrical, there will be only $\frac{N}{2}$ principal modes. The reason for the reduction in the number of modes of resonance is that $\frac{N}{2} - 1$ of the modes of a symmetrical system are degenerate or "doublet" modes each having two identical resonance frequencies. In an actual magnetron, asymmetries usually exist so that each doublet mode breaks up into two separate modes having slightly different frequencies. One mode, the $\frac{N}{\pi}$ or Π mode, is a nondegenerate mode. Because of the nondegenerate characteristic of the Π mode, magnetrons are usually designed for operation in this mode.

---

1. Collins, Microwave Magnetrons, Mass. Inst. Tech., Cambridge, Mass., Rad. Lab. Ser. Vol. 6, McGraw-Hill Book Co., Inc., New York, N.Y., 1948.
2. H.J. Reich, P. F. Ordung, H. L. Krauss, and J. G. Skaluik, Microwave Theory and Techniques, D. Van Nostrand Co., Inc., New York, N.Y., 1953.

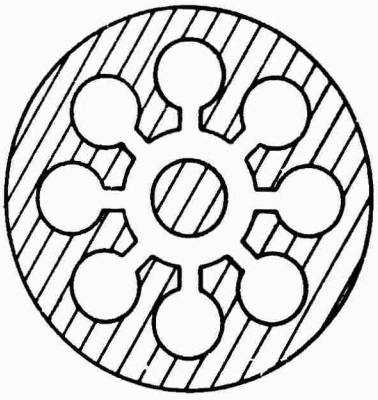

a. Hole and Slot

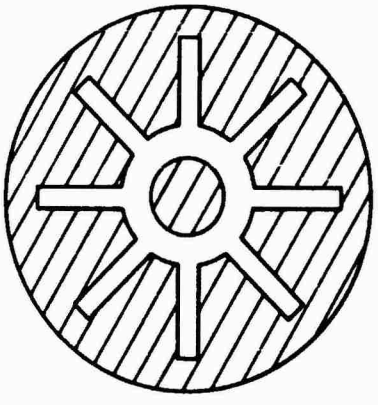

b. Slot

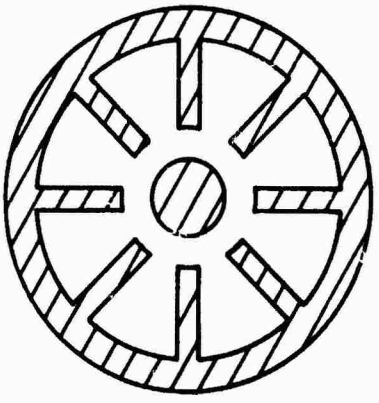

c. Vane

Figure 3-1. Typical Magnetron Cavity Configurations.

In general, frequencies of the various modes differ, but the frequency separation between modes is not as great as is desirable. One method that proved effective in increasing the separation between the Π mode and the nearest spurious mode is strapping. However, straps become difficult to implement at frequencies higher than 10 kMc due to small spacings. Mode separation as a function of strapping is shown in Figure 3-2 for an eight oscillator 10 cm magnetron. For this magnetron, coupling between cavities was such that the spurious modes occur at a frequency above the Π mode. The rising-sun resonant system, Figure 3-3, is characterized by alternately large and small resonators and produces good mode separation at high frequencies.

In interference analysis, it is necessary to determine the mode spectrum of the magnetron. The frequency at which spurious modes occur is a function of a number of parameters associated with the resonant circuit. One factor that is very important in determining the frequencies at which spurious modes will occur is the coupling between resonators. For example, in a magnetron containing a symmetrical cavity such as those shown in Figure 3-2, the principal spurious modes will occur at frequencies above the fundamental if inductive coupling predominates and below the fundamental if capacitive coupling predominates. Typical mode spectra for 3 kMc magnetrons are shown in Figure 3-4a for inductive coupling and Figure 3-4b for capacitive coupling. From the figure, it can be seen that for the hole and slot resonant system, the Π mode lies at either the upper or lower extreme of the mode spectrum. The mode spectrum associated with a rising-sun resonant system is considerably different from the mode spectrum of the hole and slot system. Although the desired operating mode in both systems is the Π mode, this mode lies between groups of modes in the rising-sun system. A typical spectrum for a rising-sun magnetron is shown in Figure 3-4c.

Now that some important characteristics of magnetron principal spurious modes have been discussed qualitatively it is desirable to obtain quantitative expressions that permit the computation of the approximate frequencies at which outputs can be expected.

There are two approaches that may be used to derive an expression for calculating the frequencies of the principal spurious

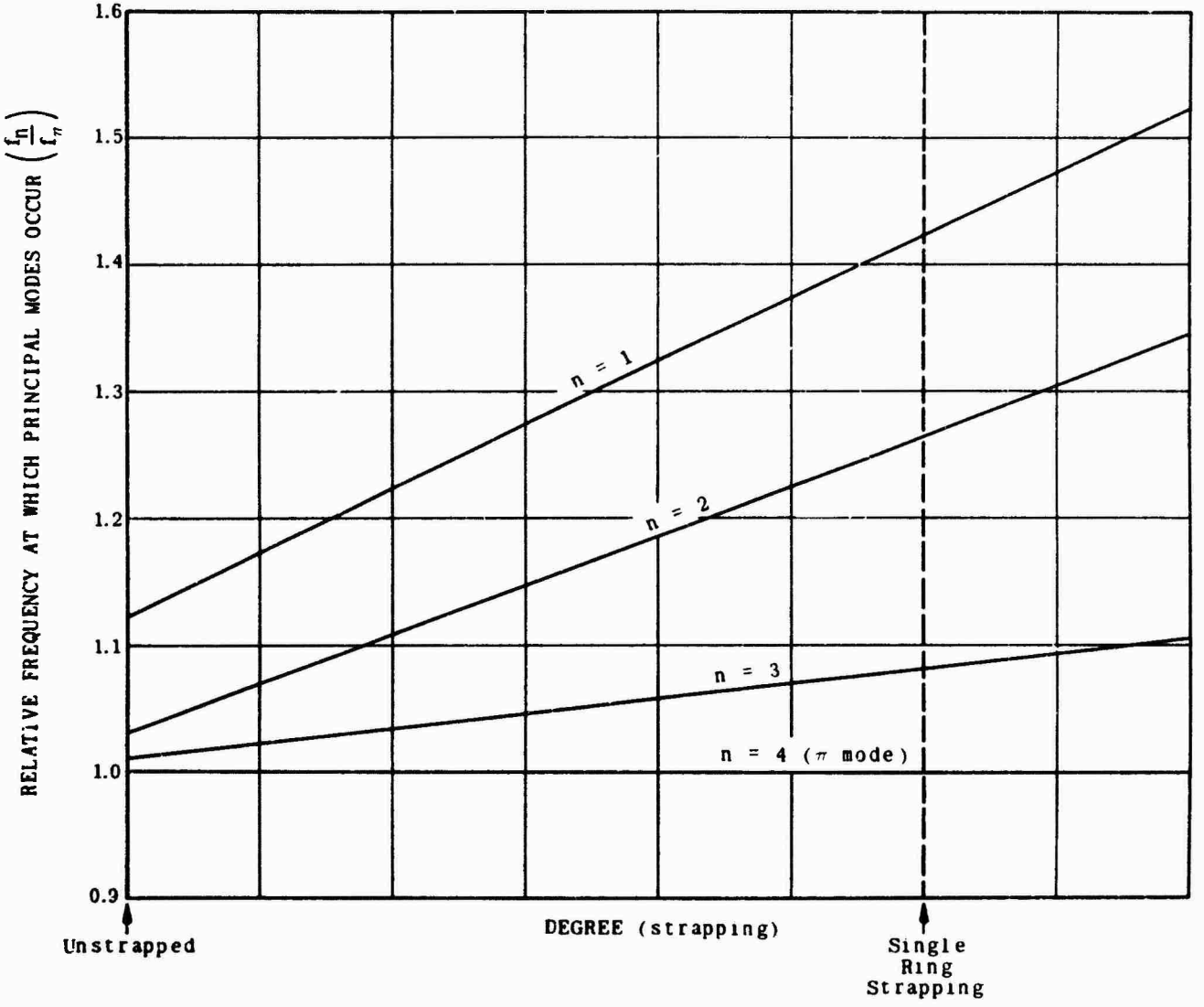

Figure 3-2. Effect of Strapping on Principal Modes.

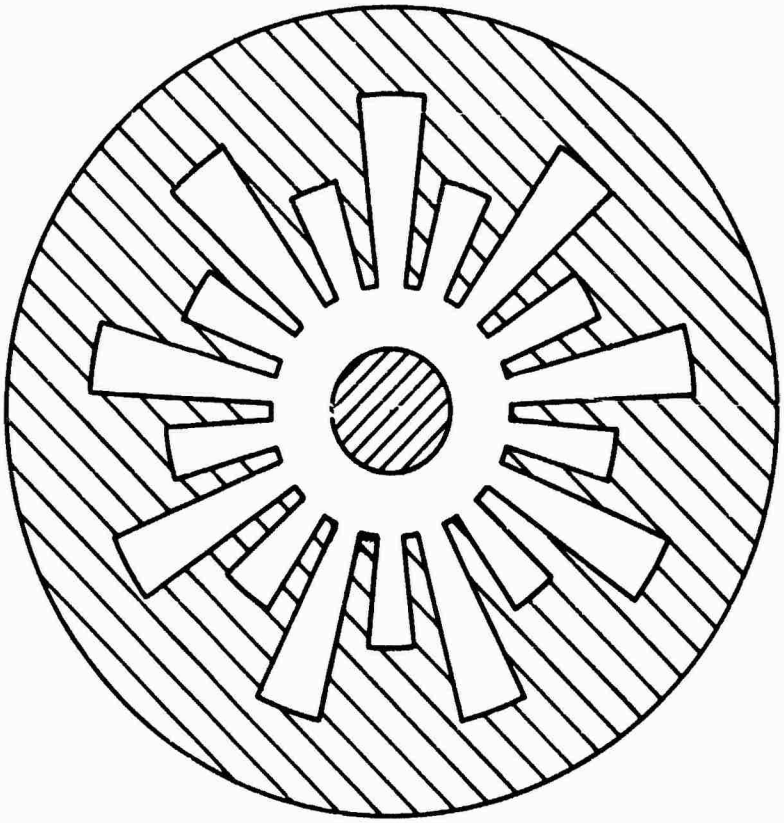

Figure 3-3. Rising-Sun Cavity Configuration.

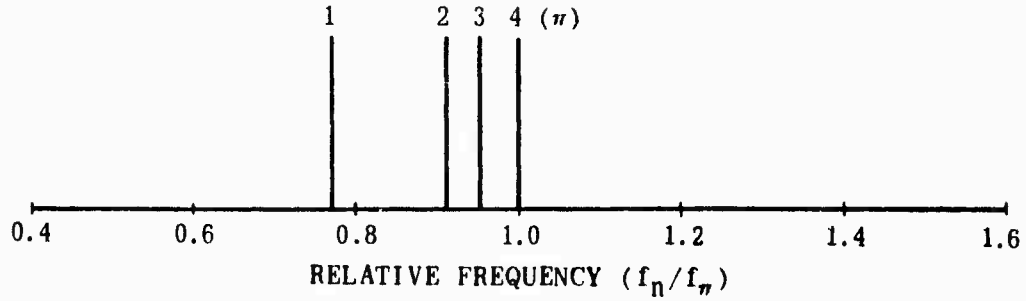

a. Eight Cavity Hole and Slot Magnetron (Capacitive Coupling)

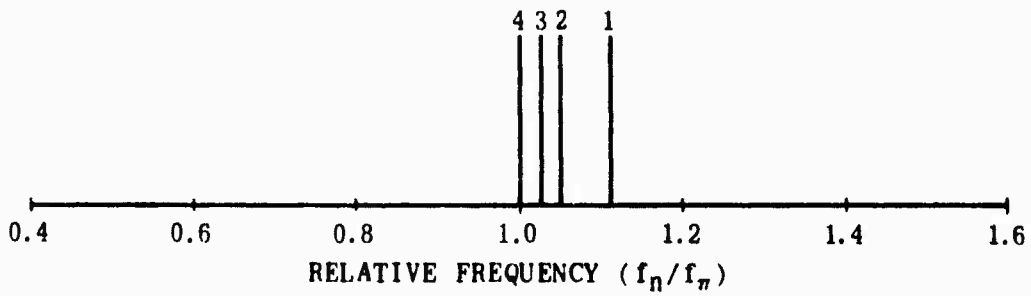

b. Eight Cavity Hole and Slot Magnetron (Inductive Coupling)

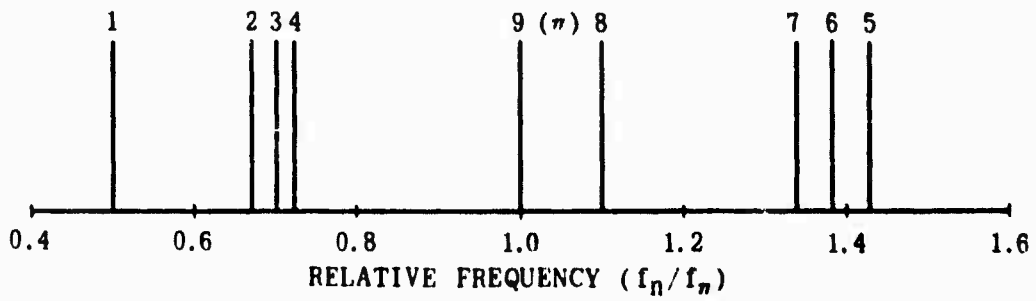

c. 18 Cavity Rising-Sun Resonant System

Figure 3-4. Mode Spectra for Typical Magnetrons.

modes of operation. These are circuit theory and field theory. Both of these methods have certain advantages. With the network approach, it is necessary to represent the resonant system by an equivalent circuit. Any network that is selected is only an approximate representation of the true system, but the circuit theory approach has the advantage of simplicity and does demonstrate some important concepts. On the other hand, although a vigorous application of field theory would provide more accurate results, solutions can ordinarily be found for only the simplest geometries. Even in these cases, it is necessary to make restrictive assumptions concerning the distribution of charge, current, and fields.

The equivalent network shown in Figure 3-5 can be used to determine the resonant frequencies of principal spurious modes for basic resonant systems of the type shown in the first figure. Of course, it is emphasized that there are several assumptions that must be made if this circuit is to be used to represent the resonant system. These assumptions are given below:

1. It is assumed that there are no resistive losses (i.e., the walls of the cavity are made of perfectly conducting material).

2. It is assumed that the inductive and capacitive effects between anode segments are negligible.

3. It is assumed that all of the side resonators are identical (i.e., the system is symmetrical).

The second assumption presented above is probably the most restrictive of the three, since it limits the analysis to those magnetrons in which the predominate coupling between resonators is capacitive. The conditions specified by the assumption are most nearly met when the anode circumference is small compared with the wavelength and the distance between the cathode and the anode is small compared with the width of the anode segments. With the above assumptions, the frequencies at which resonances will occur are given by

$$f = f_o \sqrt{1 + \frac{\frac{1}{P}}{2\left(1 - \cos \frac{2\pi n}{N}\right)}} \qquad (1)$$

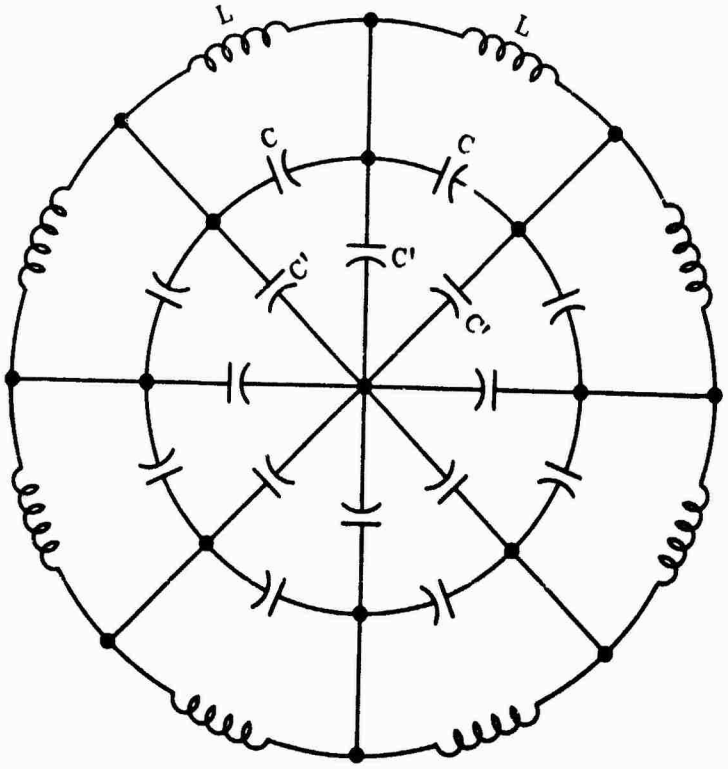

Figure 3-5. Magnetron Equivalent Circuit.

where

$$f_o = \frac{1}{\sqrt{LC}}$$

$$p = \frac{C'}{C}$$

n = mode number

N = total number of cavities

Examination of this expression shows that a different resonant frequency is obtained for each value of n in the range of n = 0 to $\frac{N}{2}$ $\left[\text{or } \frac{N-1}{2} \text{ if N is odd}\right]$. For higher values of n, the frequencies begin to repeat.

Although application of circuit theory provides a good qualitative understanding of the order and separation of magnetron spurious modes, quantitative agreement depends upon the validity of the equivalent circuit and the particular way in which the parameters p and f_o are evaluated. If the frequencies of the n = 1 and the π modes are available, then p and f_o can be determined. When p and f_o are determined by this method, the frequencies of the intermediate modes may be given with reasonable accuracy. Regardless of the manner in which p and f_o are determined, there will probably not be perfect agreement between the predicted and observed results. These variations are produced by slight variations from symmetry in the resonant system and by other microscopic factors that cannot be specified exactly in a practical analysis. Instead, it will be necessary to use statistical methods to describe the probability that a spurious output will occur within a given frequency range.

The previous discussion has been confined to the principal spurious modes of operation in a magnetron. Actually there may be a number of additional secondary modes of operation corresponding to values of n > N. Also, because of the nonlinearity of magnetron operation, there may be other spurious outputs that result from mixing of the principal modes. Although, it is theoretically possible to compute the frequencies of the more important mixing products, no method has yet been established for determining the coupling factor for a particular mixing product. Examination of

measured data has indicated that only a fraction of the possible mixing products are coupled efficiently to the output. In fact, in cases where waveguide is used in the output circuit, all of those spurious outputs that occur at frequencies below the waveguide cutoff frequency will not be radiated. In this case, even principal spurious modes that occur below the cutoff frequency will not appear in the output. Until some practical method (which may not exist) is devised to specify which products will appear at the output, it will be necessary to resort to statistical methods to specify the probability of an output occurring within a given frequency range.

To illustrate the large number of possible mixing products that may be present in a magnetron output spectra, an eight cavity hole and slot type of output cavity was considered. This output configuration will have, in addition to the fundamental output, six other principal modes of operation. Thus, there are a total of seven principal spurious outputs that can mix together to form higher order mixing products. For the particular cavity configuration being considered, there will be 84 second order mixing products and 231 third order mixing products that must be considered. Of course, some of these products will occur at frequencies which are either too low or too high to be coupled efficiently to the output. However, there will still be a large number of frequencies at which significant outputs may possibly occur. From examination of measured data, it is obvious that only a small percentage of the mixing products experience efficient coupling. Also, there is apparently a serial number to serial number difference in those mixing products that are coupled to the output. As a result, it should be obvious that it is not practical to specify exactly which outputs will appear.

Although it is not practical to predict the frequencies at which outputs actually appear, it may be possible to identify the measured spurious outputs of a magnetron as either a principal mode or as a particular mixing product. As an example, consider the measured outputs of the eight cavity hole and slot magnetron which are presented in Table 3-1. The first requirement in identifying the spurious outputs is to identify the six principal spurious modes. Those principal modes should occur in pairs that are fairly

Table 3-1

MEASURED SPURIOUS OUTPUTS

Frequency of Observed Output (Mc)	Harmonic Number	Output Level (Db Below f_o)	Identification of Principal Modes
1654	0.58	85	
1702	0.60	89	
1784	0.63	89	
1838	0.65	89	
1899	0.67	90	
2154	0.76	91	
2259	0.80	95	
2311	0.82	90	
2363	0.83	86	
2415	0.85	79	
2473	0.87	71	
2830	1.00	0	f_o
3001	1.06	50	f_1
3105	1.10	49	f_2
3233	1.15	69	
3299	1.16	68	
3346	1.18	71	
3372	1.19	69	
3419	1.21	76	
3477	1.23	80	
3716	1.31	79	
3751	1.33	73	f_3
3797	1.34	77	f_4
3855	1.38	83	
4202	1.49	86	f_5
4295	1.52	82	f_6
8390	2.96	84	

closely spaced in frequency and should have relatively high amplitudes. Examination of data shows there are six such outputs and these have been identified as f_1, f_2, f_3, f_4, f_5, and f_6. If these six outputs are actually the principal spurious modes of oscillation and if the other spurious outputs result from mixing between either these outputs or these outputs and the fundamental (f_o) then it is possible to identify the other outputs as a particular mixing product. Table 3-2 shows the frequencies of the observed outputs, the frequencies of the nearest computed outputs, and the identification of the computed outputs. Most of the computed frequencies compare very favorably with observed output frequencies. Since the observed frequencies of the principal outputs are accurate to within $\pm$ 10 Mc, second order outputs must compare to within $\pm$ 20 Mc, and third order outputs must compare to within $\pm$ 30 Mc. All of the computed and predicted frequencies compare within the required limits.

For the example considered, it was apparently possible to identify all of the spurious outputs. However, this does not imply that such identification is always possible or that the mixing products that will appear in the output can be specified without a prior knowledge of the output frequencies.

3.3 Magnetron Output Statistics

In an attempt to increase the understanding of radar transmitter output spectra, a number of measurements were subjected to a statistical analysis. Results of this analysis are discussed and particular emphasis is given to the development of a statistical method for specifying the nonharmonically related spurious outputs.

The output spectra of a typical radar transmitter that utilizes a magnetron final power tube is shown in Figure 3-6. The discrete outputs which occur at seemingly unrelated frequencies between the harmonics can be seen in the figure. In addition to these discrete outputs, the broadband noise-like output is also evident. The first question that must be answered is: How does one distinguish between the discrete spurious outputs and the higher levels of the random amplitude variations in the noise? Examination of Figure 3-6 indicates that there is no readily apparent "point of division" between the discrete outputs and the noise. In spite

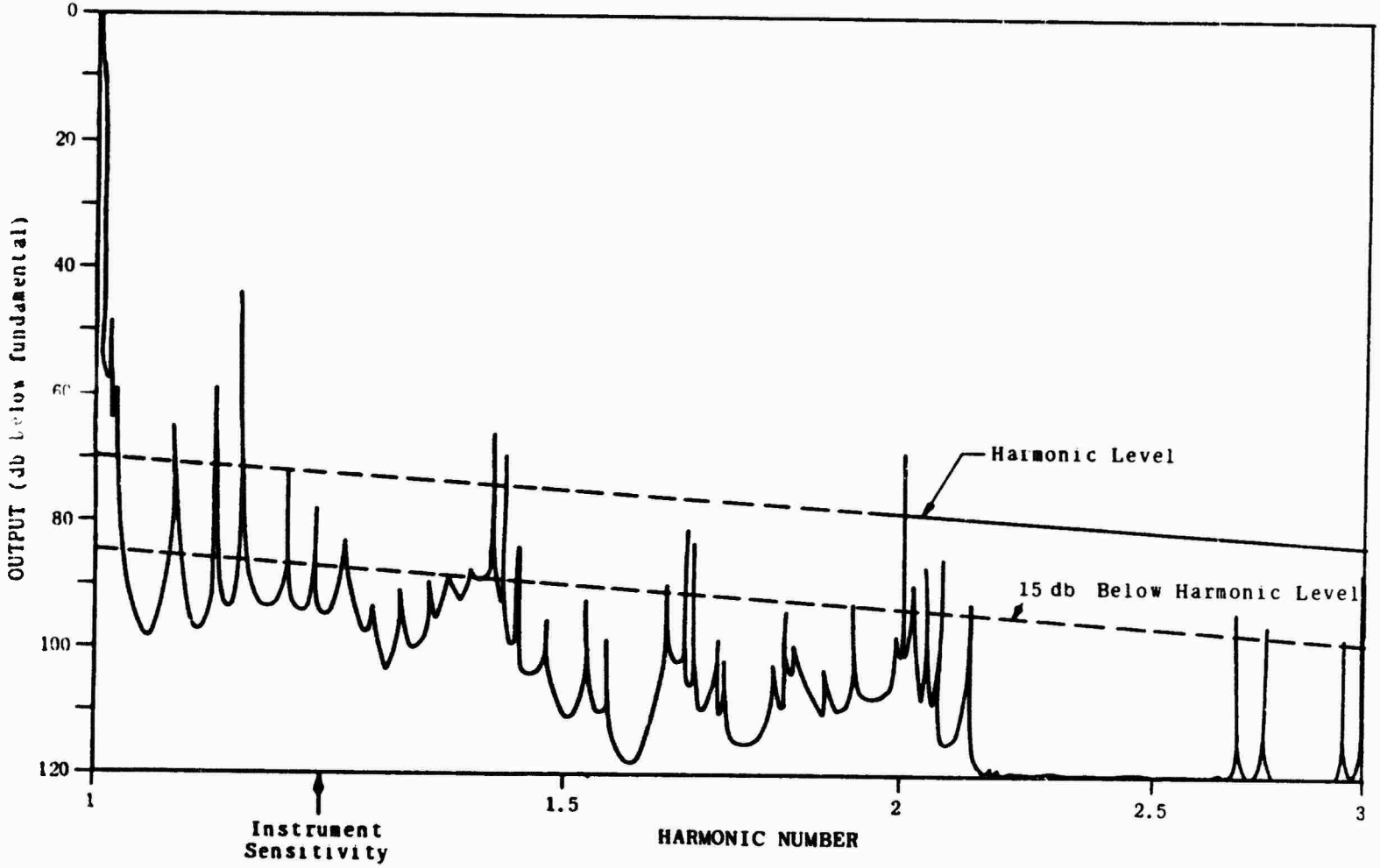

Figure 3-6. Typical Magnetron Output Spectra.

Table 3-2

SPURIOUS OUTPUT IDENTIFICATION

Frequency of Observed Output (Mc)	Frequency of Nearest Computed Output (Mc)	Identification
1654	1629	$f_o + f_1 - f_5$
1702	1707	$2f_1 - f_6$
1784	1800	$2f_1 - f_5$
1838	1811	$f_1 + f_2 - f_6$
1899	1904	$f_1 + f_2 - f_5$
2154	2138	$f_o + f_2 - f_4$
2259	2251	$2f_1 - f_3$
2311	2309	$f_1 + f_2 - f_4$
2363	2355	$f_1 + f_2 - f_3$
2415	2413	$2f_2 - f_4$
2473	2459	$2f_2 - f_3$
2830	2830	f_o
3001	3001	f_1
3105	3105	f_2
3233	3235	$f_o + f_5 - f_4$
3299	3299	$2f_4 - f_6$
3346	3346	$f_3 + f_4 - f_5$
3372	3374	$f_o + f_6 - f_3$
3419	3406	$f_1 + f_5 - f_4$
3477	3476	$f_o + f_3 - f_2$
3716	3705	$2f_3 - f_4$
3751	3751	f_3
3797	3797	f_4
3855	3855	$f_2 + f_3 - f_1$
4202	4202	f_5
4295	4295	f_6
8390	8404	$2f_5$

of the lack of an obvious "point of division" some definite criteria must be established for classifying outputs as discrete or noise. This criteria should be such that the most significant spurious outputs are identified as discrete outputs. For example, any outputs that are above the harmonic level would definitely be considered as discrete outputs. On the other hand, those outputs that are classified as noise should have a relatively low amplitude.

From the figure it can be seen that if only those outputs that are above the harmonic level are considered as discrete, then a number of relatively high amplitude outputs will be excluded from the analysis. Therefore, it is felt that a lower level must be used to separate the discrete outputs from the noise. A second level (15 db below the harmonic level) is shown in Figure 3-6. This level appears to be a much more suitable dividing line, and therefore will be used as the criteria for distinguishing between discrete outputs and noise. There are several other very significant characteristics that are evident in the figure and should be mentioned before continuing the analysis further. First, there is no readily apparent relationship between the frequencies at which the spurious outputs occur. Secondly, the amplitude of the outputs exhibit a decreasing trend with increasing frequency. Finally, although the frequency scale in the figure is compressed to the extent that the sidebands around each output are not to scale, it should be pointed out that there is a bandwidth associated with each of the spurious outputs.

A criterion has been established for distinguishing between discrete spurious outputs and noise. This criterion was applied to measured data for several different radar transmitters so that the discrete outputs (i.e., those outputs that are above the arbitrary line) could be isolated and subjected to a detailed statistical analysis. Results of an analysis of nineteen sets of measurements on four different radars (AN/FPS-36, AN/MPQ-10, AN/MPQ-35, and T-33)* will be presented. This data were used to generate statistics to describe both the amplitude and frequency distribution of the spurious outputs for these radars.

* These measurements were made at the USAEPG, Ft. Hauchuca, Arizona

Now that some of the problems associated with predicting the frequencies at which spurious outputs occur have been discussed, the output distribution as a function of frequency will be examined. It has been stated that it may not be practical to specify the precise frequencies at which outputs occur, and therefore, statistics must be used to describe the probability of an output occurring as a function of the separation from a given frequency f. Of course, it is necessary to realize that the statistics will probably be a function of the frequency relative to the fundamental frequency. Because of this fact, and because of the necessity for a common reference, all frequencies were normalized to the transmitter fundamental frequency (f_o^t). Also, due to the possible dependence of the statistical distributions on frequency, caution must be used in developing the statistics. Several different distributions may be required to describe the statistic for the entire frequency range over which spurious outputs occur. Each individual relation will specify the statistics for a frequency interval over which the distribution remains essentially constant.

Figures 3-7, 3-8, and 3-9 show those frequencies, above the fundamental, at which outputs occur for all of the magnetrons for which data were available. Although it is recognized that spurious outputs can also occur at frequencies below the fundamental, these will not generally appear in the output if waveguide is used. Examination of the figures reveals that with the exception of transmitter number three, the density of the outputs decreases considerably for frequencies greater than 1.50 or 1.75 of the fundamental frequency. One other factor that is evident in the figures is that the number of spurious outputs and the frequencies at which they occur vary considerably from serial number to serial number for a particular nomenclature transmitter. Thus, precise prediction of the frequencies at which spurious outputs will occur is not practical. Since more measurements were available for transmitter number four than for the other transmitters, it will be used to illustrate the methods of analysis.

In deriving the statistics to describe the output distribution for the transmitters, it was assumed that the statistics remained essentially constant over each interval of 0.25 f_o^t. Separate statistics were derived to describe the probability of an output occurring within a separation of $\frac{\Delta f}{f_o^t}$ for each interval of 0.25 f_o^t. The resultant sta-

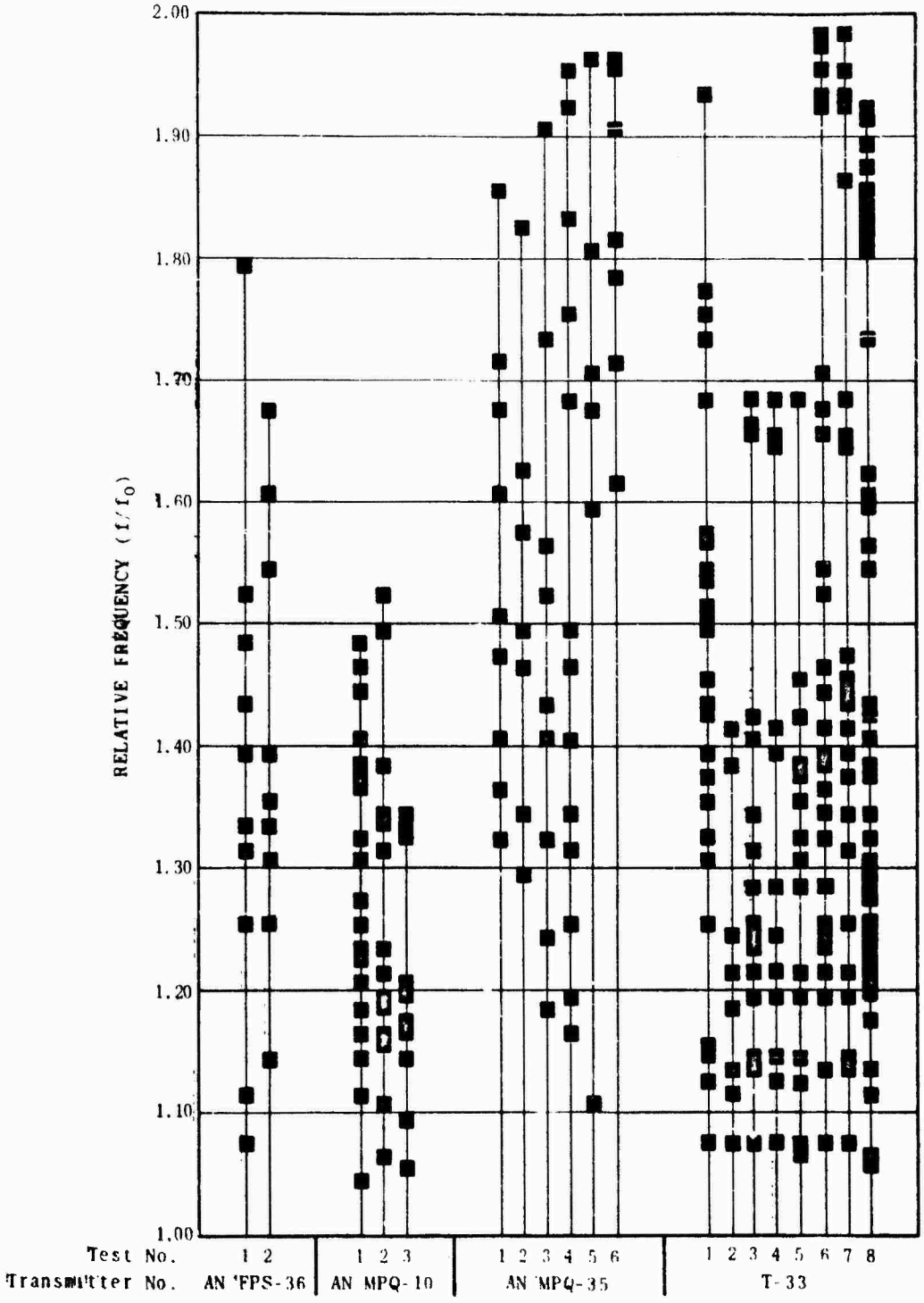

Figure 3-7. Frequency Distribution of Spurious Outputs ($1 < f/f_o < 2$)

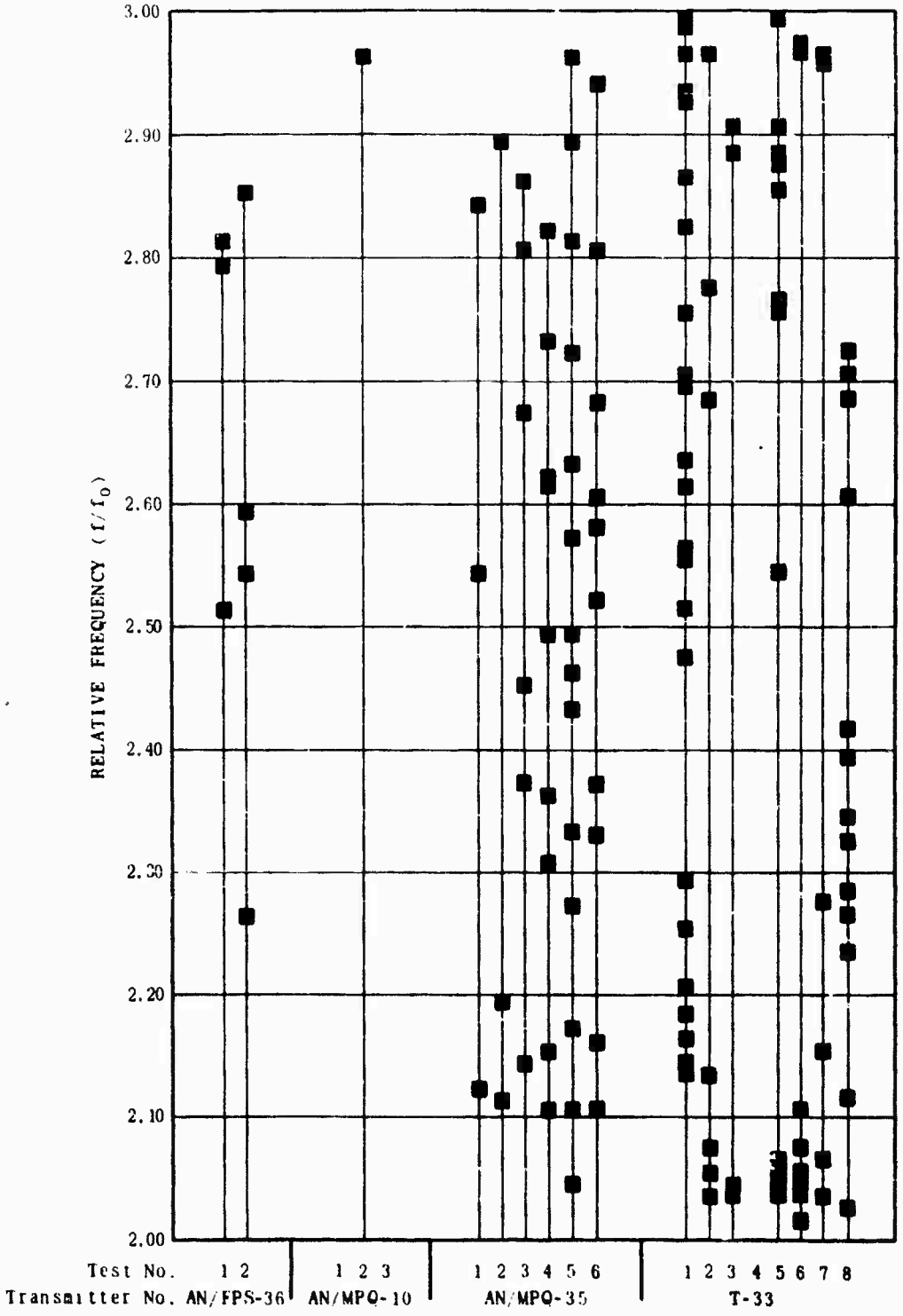

Figure 3-8. Frequency Distribution of Spurious Outputs ($2 < f/f_o < 3$).

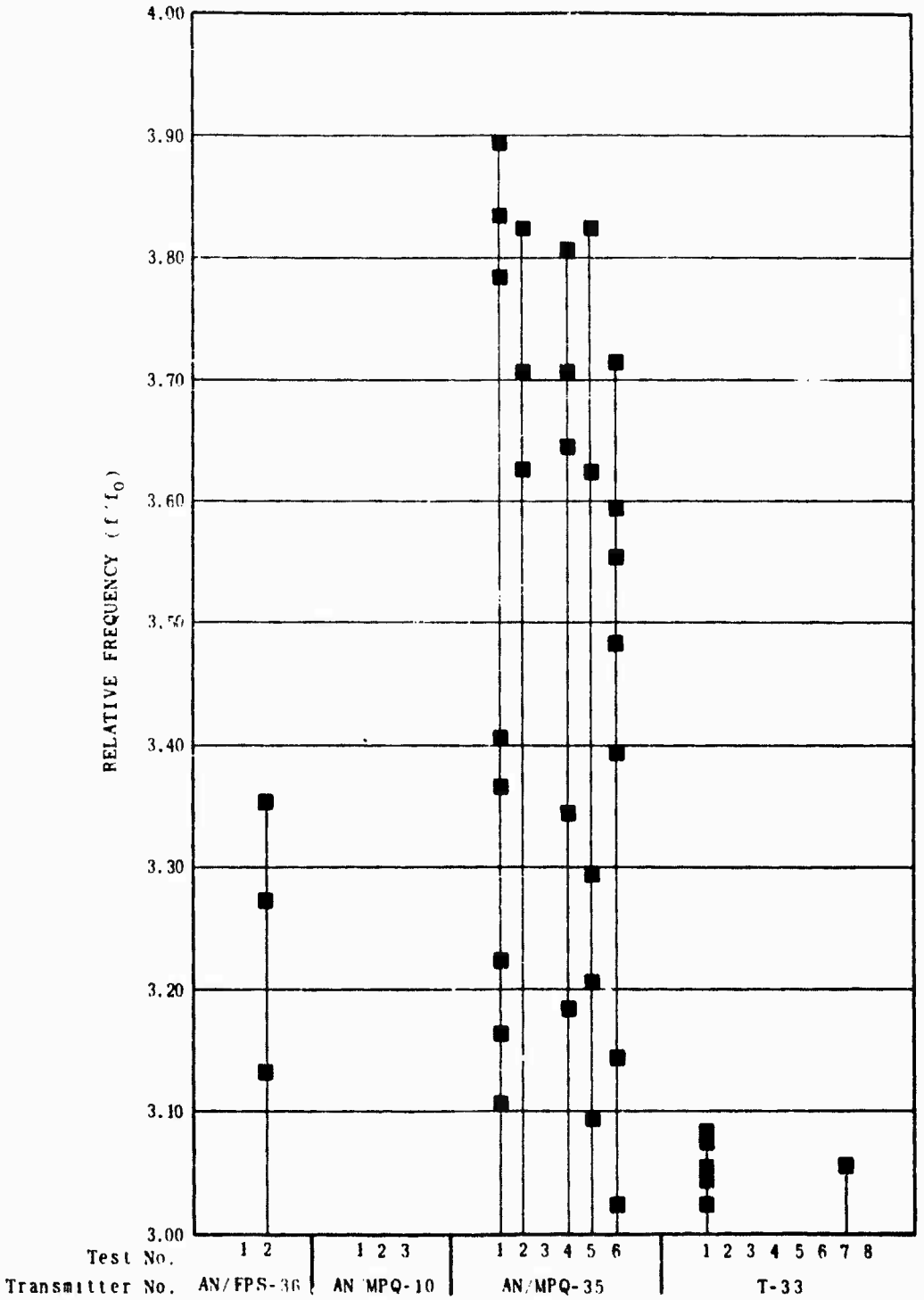

Figure 3-9. Frequency Distribution of Spurious Outputs ($3 < f/f_o < 4$).

tistical distributions are shown in Figure 3-10 for separations of $\frac{\Delta f}{f_o^t}$ of up to 0.25. Although the curves were derived for larger values of $\frac{\Delta f}{f_o^t}$, it is not felt that it is worthwhile considering any spurious outputs that are separated by more than 0.25 f_o^t from a receiver spurious response. From Figure 3-10, it can be seen that for this transmitter, there are two distinct classes into which the individual statistical distributions can be grouped. The first class would cover the frequency interval from 1.00 f_o^t to 1.75 f_o^t, whereas the second class would cover the remaining portion of the frequency range over which response outputs were observed. Resultant statistics for these two classes are shown in Figure 3-11.

Similar distributions were derived for the other three transmitters and the resultant curves are shown in Figures 3-12, 3-13 and 3-14.

Figures 3-11 through 3-14 describe the probability that an output will occur as a function of the separation from a given frequency. The lower portion of these curves is of primary interest since it describes the probability that an output will occur at a small separation from a given receiver response. As the separation from a receiver response increases, the probability that a spurious output will cause interference is reduced because of the selectivity of the receiver. In addition, since the amplitudes of the spurious outputs are expected to be lower for frequencies significantly removed from the fundamental, the most important distributions are those that describe the probability that an output will occur at a small separation ($\frac{\Delta f}{f_o^t} < 0.05$) from a given frequency which is relatively close to the fundamental (i.e., $\frac{f}{f_o^t} < 1.50$). Figure 3-15 shows those portions of the curves which are of primary interest plotted on an expanded scale. This figure demonstrates that for the area of primary interest, there is not a significant difference between the statistical distributions for the various transmitters. The dashed curve should provide a reasonable approximation for all of the distributions.

A similar set of curves is shown in Figure 3-16 for frequencies greater than 1.50 f_o^t. In this case, more significant differences do exist between the distributions for the various transmitters. However, it is emphasized that for those frequencies above 1.50 f_o^t there is less probability of a spurious output occurring within a given separation of

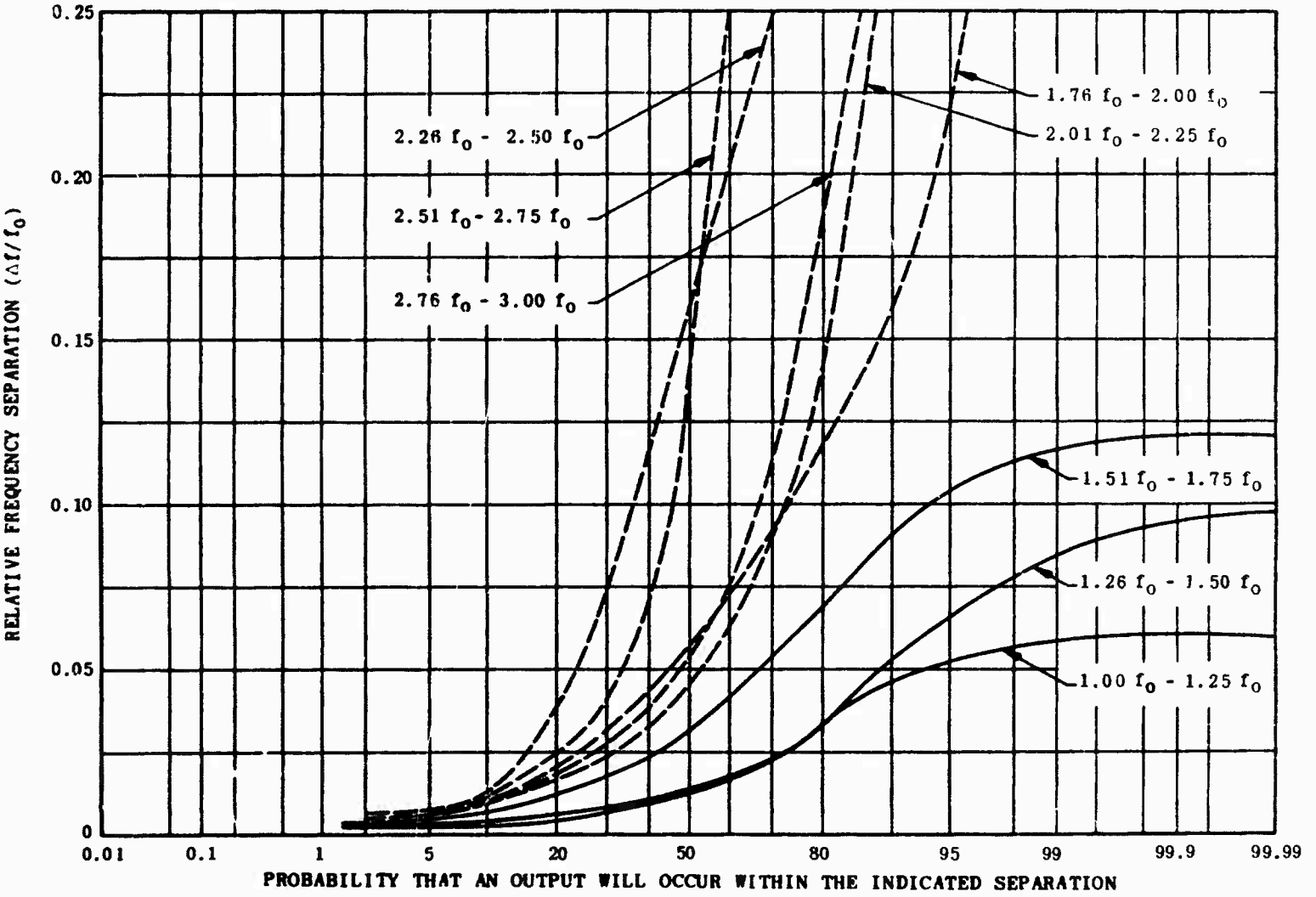

Figure 3-10. Preliminary Magnetron Output Statistics for T-33.

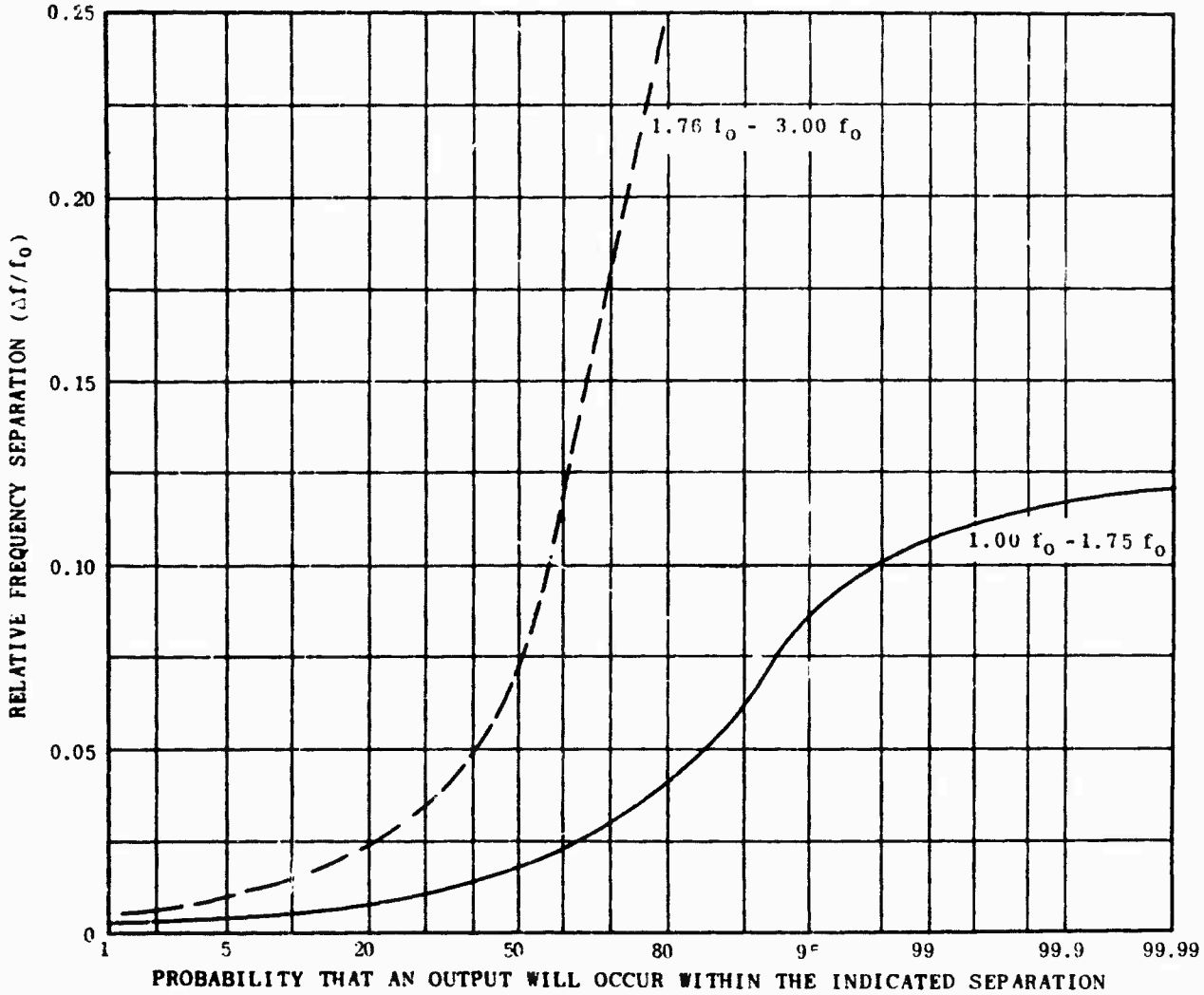

Figure 3-11. Magnetron Output Statistics for T-33.

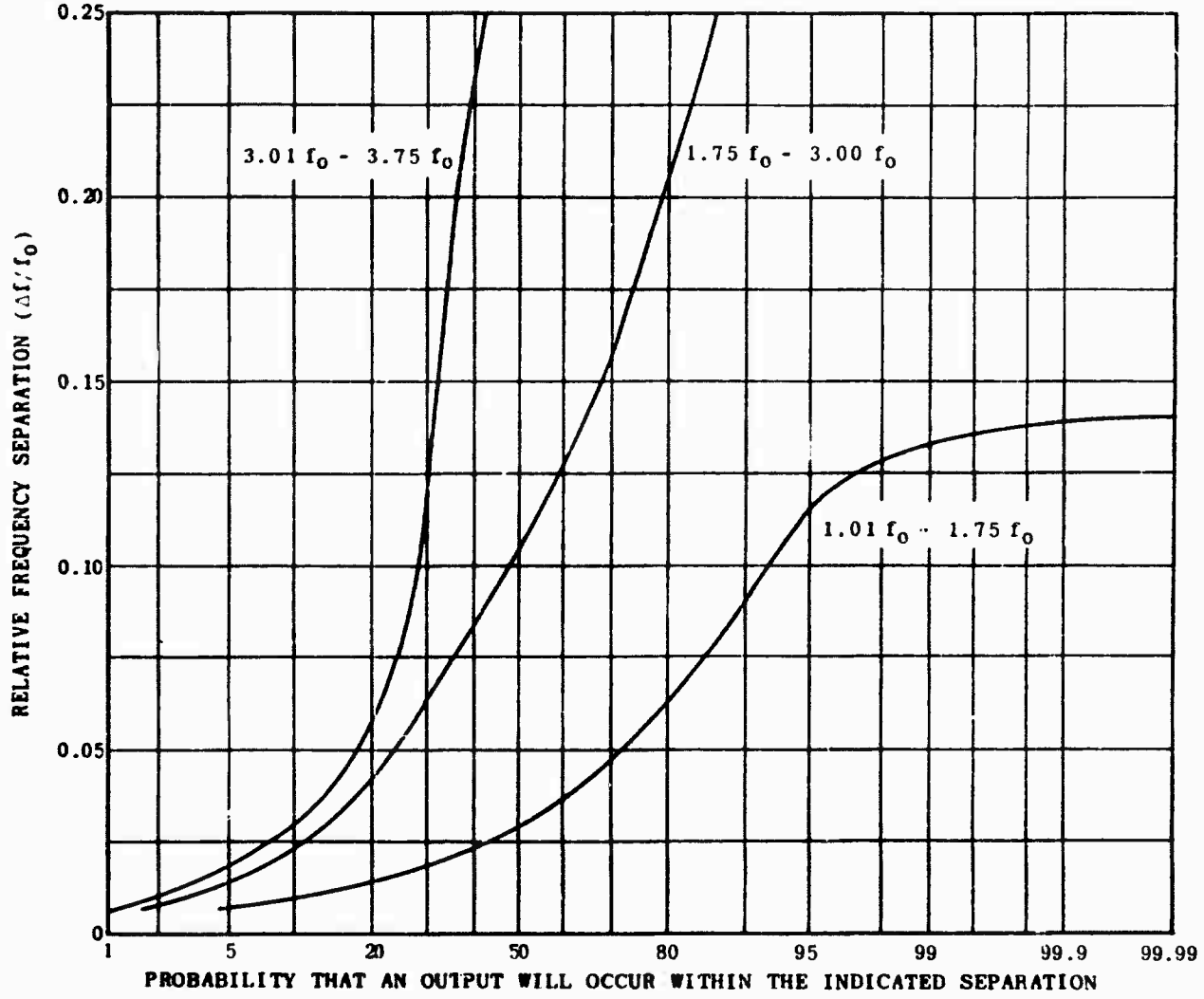

Figure 3-12. Magnetron Output Statistics for AN/FPS-36.

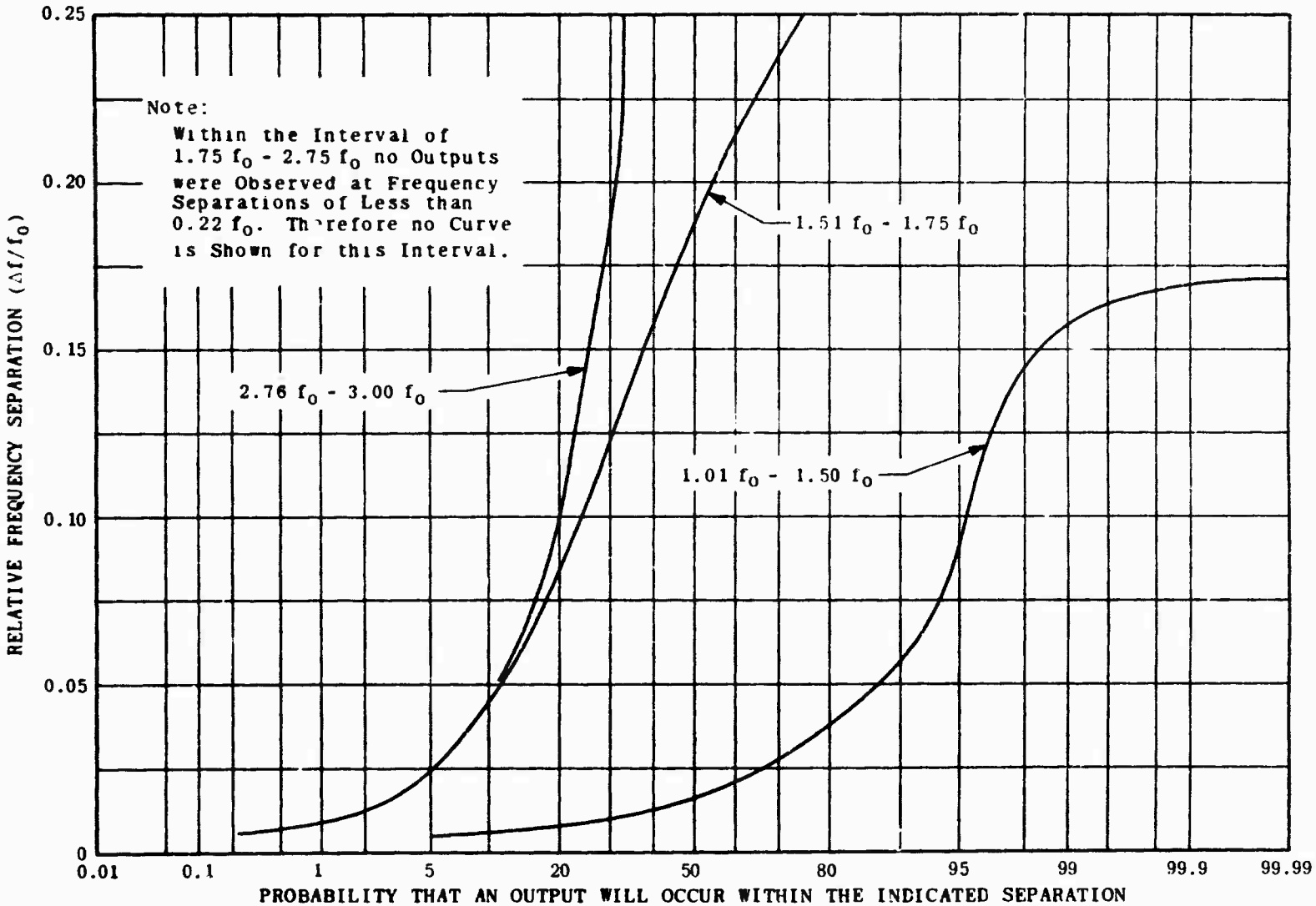

Figure 3-13. Magnetron Output Statistics for AN/MPQ-10.

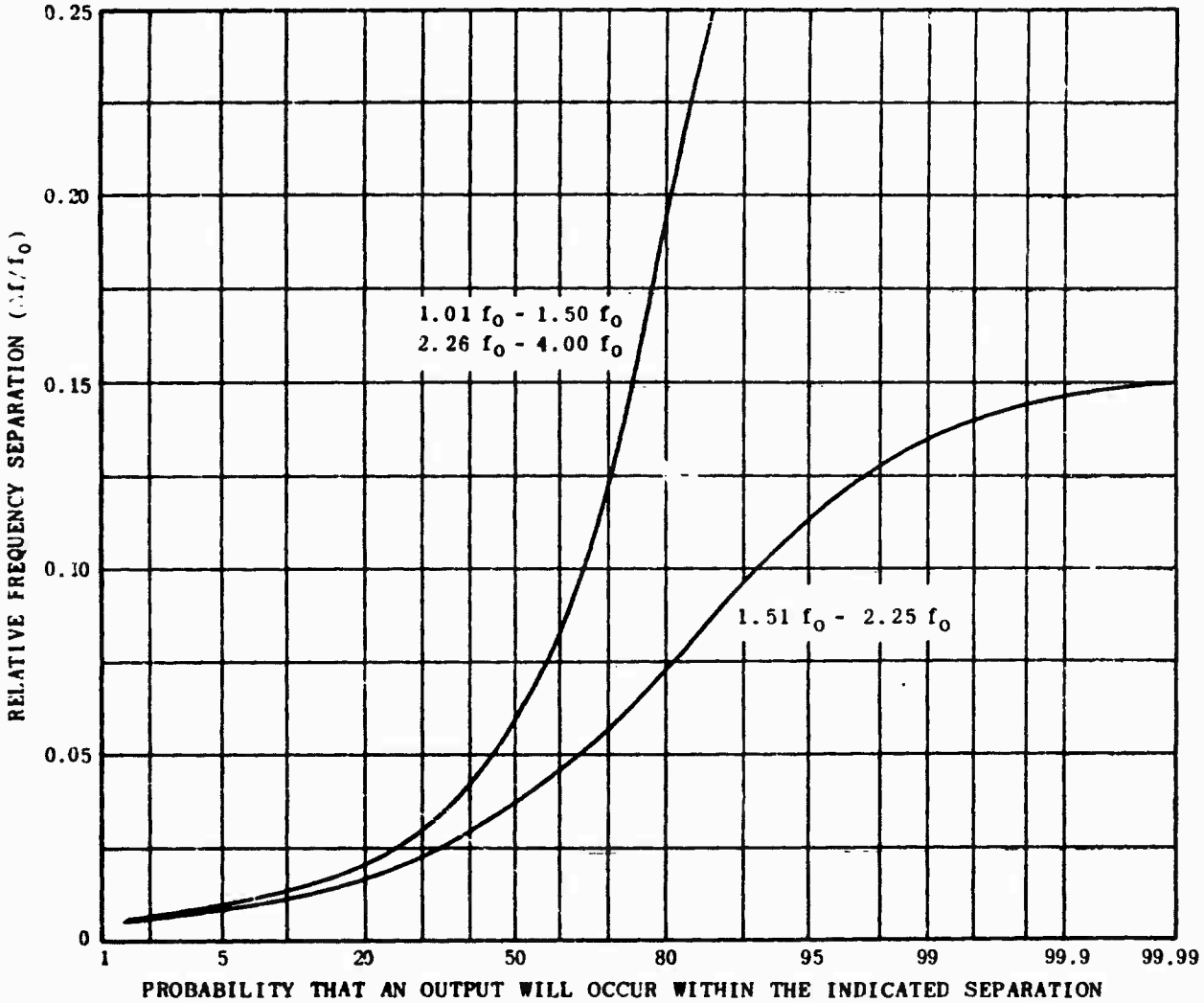

Figure 3-14. Magnetron Output Statistics for AN/MPQ-35.

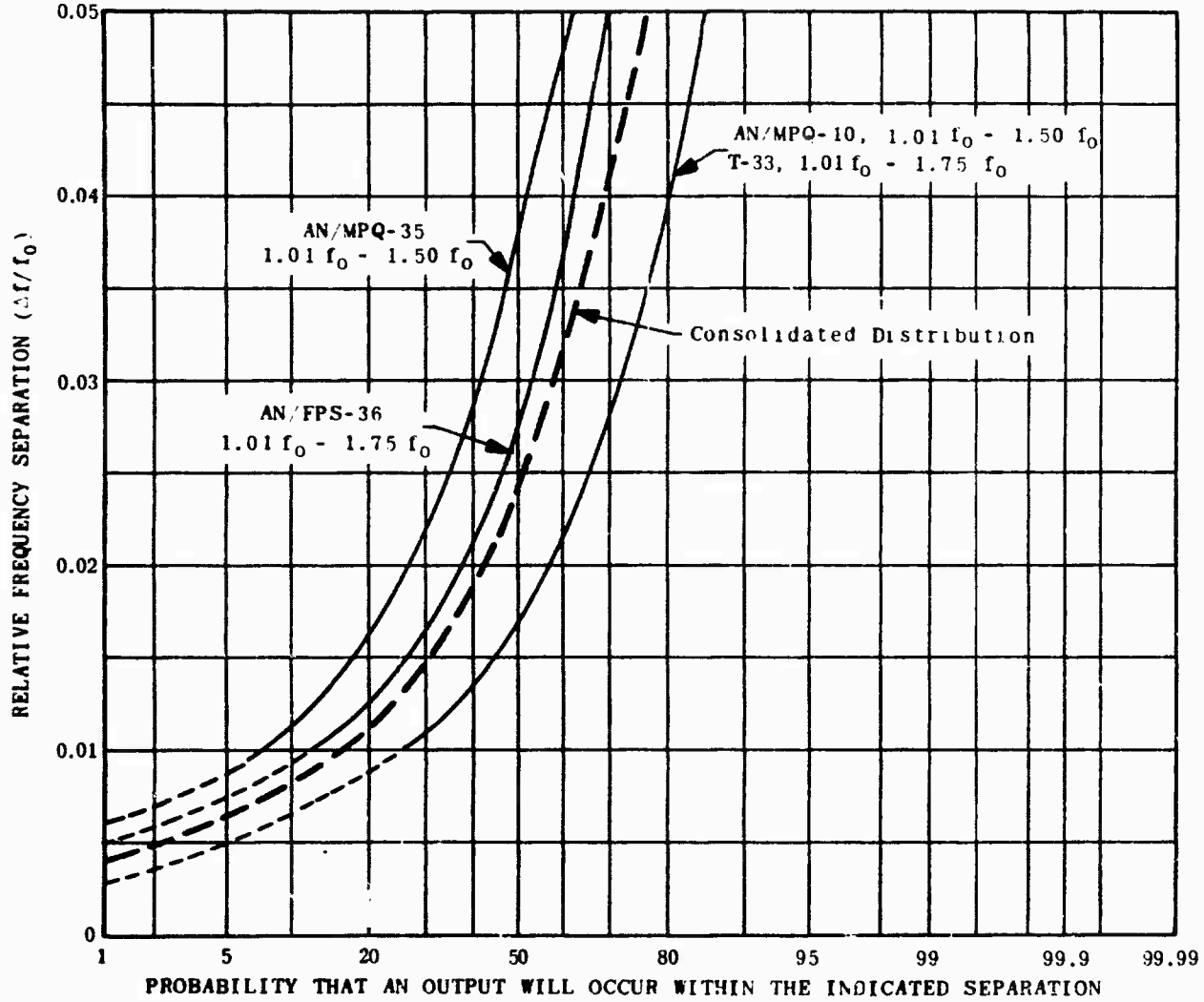

Figure 3-15. Summary of Magnetron Output Statistics.

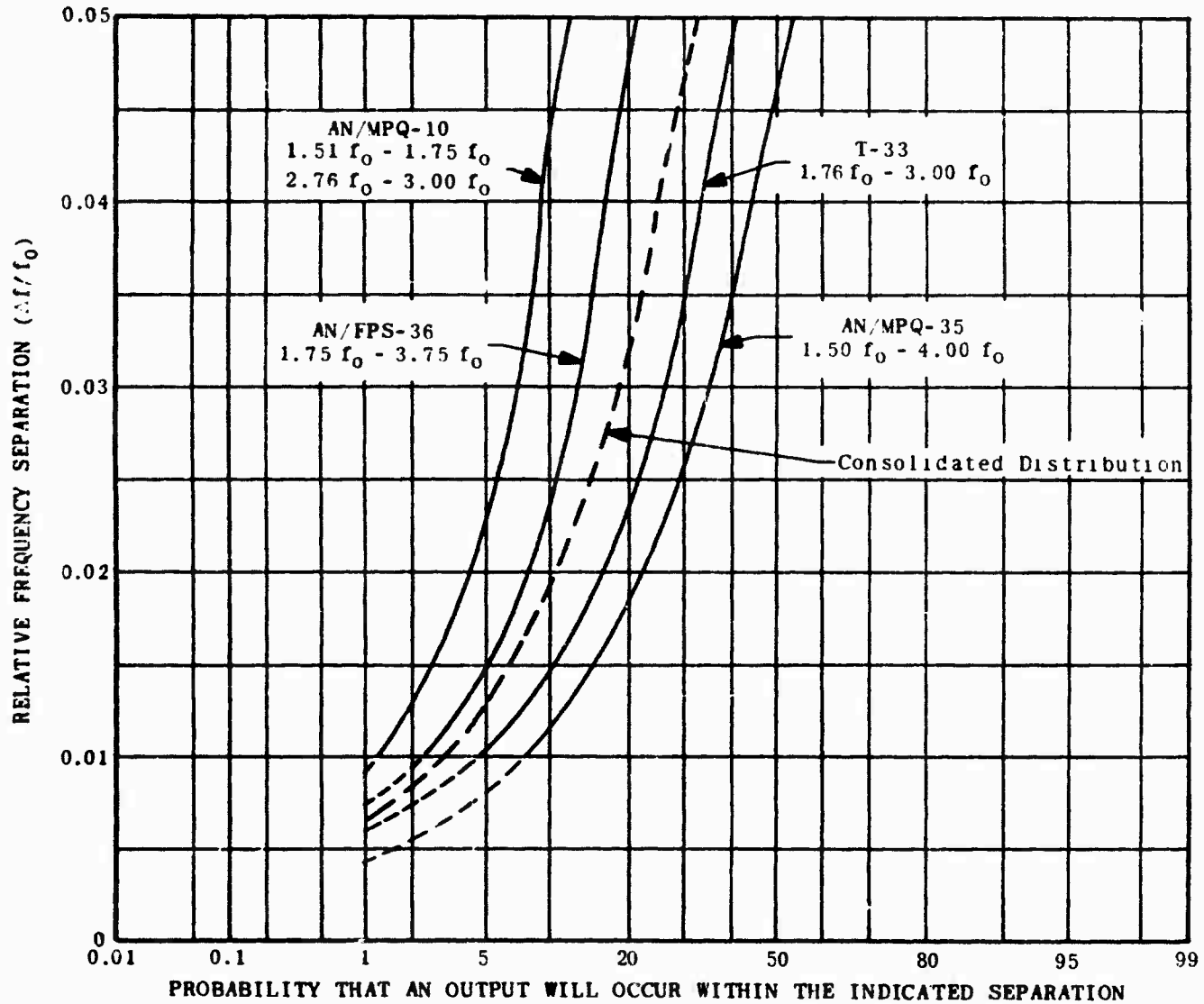

Figure 3-16. Summary of Magnetron Output Statistics.

specific frequency, and the average amplitude of the outputs will be lower than those that occur closer to the fundamental. Thus, for practical purposes, the distributions shown in Figure 3-15 might be represented by a single distribution.

The amplitudes of the nonharmonically related spurious outputs exhibit characteristics similar to those observed for the harmonic outputs. The methods that were developed to represent the harmonic outputs have worked very well in the analysis process. Therefore, these methods will be investigated to determine their applicability to the nonharmonic spurious outputs. It has been shown that the statistical average of the transmitter harmonic output level (y) can be expressed by

$$y = a + b \log N \tag{2}$$

where a and b are constants that must be evaluated in the analysis and N is the harmonic number. If a similar relationship is used to describe the amplitude of the mean spurious output level, then at a frequency, f, the level might be approximated by

$$y = a_s + b_s \log \frac{f}{f_o^t} \tag{3}$$

where f_o^t is the transmitter tuned frequency.

The logarithmic function presented above provides a realistic description of the amplitude of the harmonic outputs and it appears probable that it may also provide a reasonable approximation of the amplitude of nonharmonically related spurious outputs. The results of performing least squares fit to the spurious outputs for the four transmitters considered is shown in Table 3-3.

Table 3-3

TRANSMITTER DESCRIPTIVE CONSTANTS

Nomenclature	Intercept	Slope	Standard Deviation
AN/FPS-36	50	68	6
AN/MPQ-10	50	200	7
AN/MPQ-35	70	25	8
T-33	67	80	10

With transmitter harmonic outputs, it was observed that compared to other statistical variations that are known to exist, there was not in general a significant variation in the statistical averages for different tuned frequencies or for different serial number equipments of a particular nomenclature. The same observation has been made for nonharmonic outputs. The variation in average output level produced by changing the fundamental frequency is shown in Figure 3-17a. Figure 3-17b illustrates the variation in the average output level for three different serial numbers.

As mentioned in the preceding discussion, there is in addition to the discrete outputs a noise-like output which exists at all frequencies and exhibits a random amplitude variation about some mean value. This noise will be represented by a relationship of the form given by Eq. 3. For the transmitters analyzed, the noise was characterized by an intercept of 100 and a slope of 30.

Statistical distributions that describe the amplitude and frequency distribution of the transmitter nonharmonic spurious outputs have been presented. One other factor that is essential in the prediction process is the bandwidth that is associated with each of these outputs. In general, the sidebands associated with spurious outputs exhibit a similarity with the modulation spectrum around the fundamental and harmonic outputs. Therefore, it will be assumed that the sidebands of the spurious outputs can be represented by the function that was derived for the immediately preceding harmonic output. That is, the sidebands of all spurious outputs that occur between the fundamental and the second harmonic will be represented by the function that was derived for the modulation envelope around the fundamental output. Similarly, the sidebands of outputs

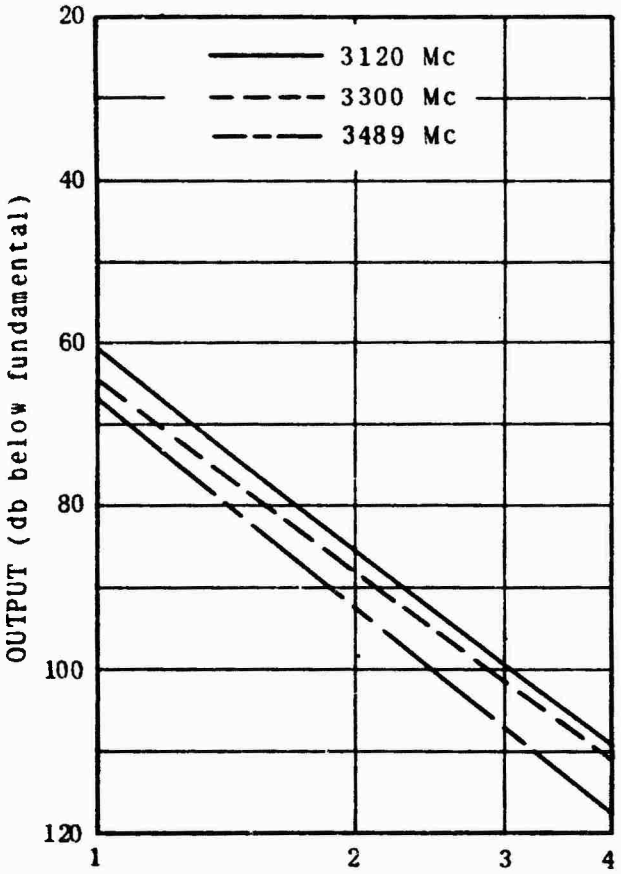

a. Effects of Frequency

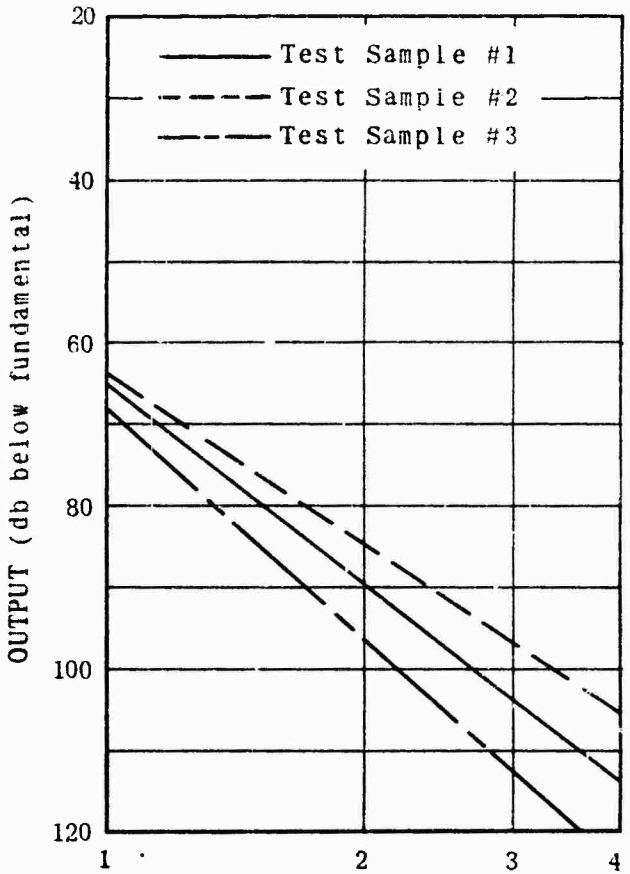

b. Effects of Serial Number

Figure 3-17. Effects of Frequency and Serial Number on Non-Harmonic Output Levels.

occurring between the second and third harmonic will be represented by the function that describes the envelope associated with the second harmonic.

3.4 SUMMARY

The analysis presented in this report provides a basis for the mathematical model required to describe the nonharmonic spurious outputs of magnetron transmitters. As a result of this analysis, it appears that the exact frequencies at which spurious outputs occur cannot be adequately determined by a practical prediction method. Instead, the frequency distribution of the outputs must be described statistically. If the physical characteristics of the resonant system are known, it is possible to predict the number of principal spurious outputs and the approximate frequencies at which they will occur.. Also, it is possible to compute the frequencies at which higher level modulation products might occur. However, at the present time, no methods have been developed for determining which modulation products will be coupled to the output. From analysis of measurements, it appears that there will be set-to-set variations in the frequencies at which products are coupled efficiently.

Measurements on several radar transmitters were subjected to a statistical analysis. Distributions were derived to describe the probability of an output occurring as a function of the separation from a given frequency. The measurements that have been analyzed indicate that at least two separate statistics will be required to describe the frequency distribution of the output of a given transmitter. The first distribution will cover the interval from the fundamental frequency to approximately 1.50 or 1.75 times the fundamental frequency. The second distribution will cover the remaining interval over which spurious outputs were observed. Although differences were observed between the magnetron output statistics for different nomenclature transmitters, they were not significant for the most important portion of the distributions; (i.e., at small separations from a given frequency). Thus, it might be possible to derive a general set of distributions that will provide an adequate description of the spurious output

statistics of any magnetron for small separations from a given frequency.

It is emphasized that the analysis presented is not conclusive. The observations that were made represent an initial step in the development of an analysis procedure for magnetron transmitters. Extension of this analysis to other transmitters will provide either justification for the development of a general set of statistics or a basis for classifying magnetron transmitters for further analysis.

Section 4

RECEIVERS

4.1 THEORETICAL DISCUSSION

4.1.1 Introduction

The main goal of the receiver section is to develop a programmable analysis technique with which all outputs of any particular receiver may be determined for any electromagnetic environment. This will require supplementation of techniques illustrated in previous reports under Air Force Contract No. RADC-TDR-61-312, the organizations of these techniques in a logical and practical manner, and finally the programming of the analysis for a digital computer.

The following pages present the analysis technique as it has been developed thus far. It is, however, subject to addition, or change, as the program progresses.

In order to determine the effect of the electromagnetic environment on a receiving system, it is necessary to determine:

1. The level of the desired signal at the output of the receiver
2. The level of the combined interfering signals at the receiver output
3. The characteristics of the resulting interference and its effect on the desired signal intelligence.

The method of approach to the problem of determining the interference effect is to first determine the amount of interfering signal energy in the passband of the receiver, and then the efficiency with which the type of interference is demodulated by the particular type of detection process. An interfering signal can enter the passband if:

1. It is at or near the receiver-tuned frequency
2. It is related in frequency with another signal in the environment such that a low order intermodulation product between any two is at or near the receiver-tuned frequency
3. A portion of the frequency spectrum of the signal is common to the passband of a particular receiver spurious response.

Sections 4.1.2 through 4.1.4 of this report deal with updating developed analysis techniques to provide the capability of picking out the interfering signals due to their frequency relationships and determining the amount of interfering power produced in a receiver passband.

Section 4.1.5 discusses how the interference contributed by several signals and intermodulation processes are added together to determine the total effect. Once this has been done, it is necessary to determine how the detection system processes the interference. A discussion of this is given in Section 4.1.6.

Since the electromagnetic environment is the result of various transmitter outputs which are known statistically, it is necessary to carry the statistical process through the various stages of the receiver and to specify the total interference or the output signal-to-noise ratio as a statistic. The output statistic will be a function of the statistical properties of the receiver parameters as well as a function of the input functions. Applicable statistical methods are discussed and methods presented for accomplishing this are given in Section 4.1.7.

The organization of Section 4.2 is such that each part deals with an individual problem of the over-all receiver analysis. In some cases, a finalized solution to a particular part of the problem is not complete. Where necessary, the particular problems requiring further effort are noted.

4.1.2 Intermodulation Products

The output of a nonlinear device, which can be characterized by a single valued transfer characteristic, can be expressed as:

$$i_p = \sum_{r=0}^{\infty} a_r e_{in}^r \qquad (1)$$

where

i_p = the output plate current of the nonlinear device

a_r = the power series coefficient of the rth term

e_{in} = input voltage to the device

Considering the input to the nonlinear device to be a sum of individual frequency components, the output signal will contain all individual frequencies which are the sums and differences of all possible

integer multiples of the input frequencies. These are termed the intermodulation products. The amplitude of each of these products is determined by contributions from the various terms of the power series. Considering the input to a device to be A cos $\omega_1 t$ + B cos $\omega_2 t$ + ..., a general output signal of the device is

$$K(m_1, m_2, \ldots) \cos \left[m_1 (\omega_1 t) \pm m_2 (\omega_2 t) \pm \ldots \right] \tag{2}$$

where

$K(m_1, m_2 \ldots)$ = the amplitude of the intermodulation product

m_1, m_2 = non-negative integers which represent the signal multiples

In order to determine the amplitude $K(m_1, m_2 \ldots)$ of any particular intermodulation product, it is necessary to insert

$$e_{in} = A \cos \omega_1 t + B \cos \omega_2 t + \ldots \tag{3}$$

into Equation 1, expand Equation 1 and then collect similar frequency terms. When Equation 3 is inserted into Equation 1, the nth term of the power series (1) is

$$a_n (A \cos \omega_1 t + B \cos \omega_2 t + \ldots)^n \tag{4}$$

with the aid of algebraic manipulation, Equation 4 can be rewritten as

$$\sum \frac{a_n n!\, A^{\alpha} B^{\beta} \ldots \cos \left[(\alpha - 2n_\alpha)\, \omega_1 \pm (\beta - 2n_\beta)\, \omega_2 \pm \ldots \right] t}{2^{(n-1)} (\alpha - n_\alpha)!\, (\beta - n_\beta)! \ldots n_\alpha!\, n_\beta!} \tag{5}$$

where α, β, ..., n_α, n_β, ..., are positive integers or zero. The summation which determines only the nth term of Equation 1 is taken over all possible sets of values for α, β, ..., n_α, n_β, ... such that $(\alpha + \beta + \ldots)$ equals n and $2n_\alpha \leq \alpha$, $2n_\beta \leq \beta$ ... .

Expression 5 may be used to compute the amplitude of any particular intermodulation product $K(m_1, m_2, \ldots)$.

The intermodulation products resulting from only two input signals are usually the highest in magnitude by several degrees. In general, when considering two signals, A cos $\omega_1 t$ and B cos $\omega_2 t$, we will refer to a particular intermodulation product as (p,q). The (p,q) intermodulation product is that product of order p + q which is at an angular frequency of $(p\omega_1 \pm q\omega_2)$.

To compute the magnitude of the (p,q) product we must add up the contributions from each term in Equation 1. Expression 5 gives us the general term and thus for each possible n (i.e., 0, 1, 2, ...) we choose those permissible values of α, β, n_α and n_β for which

$$\alpha - 2n_\alpha = p$$

$$\beta - 2n_\beta = q$$

These values for α, β, n_α and n_β contribute to K(p,q) which is the amplitude of the (p,q) intermodulation product. All other values may be ignored in considering a particular (p,q) since they contribute to other intermodulation products.

Table 4-1 shows the values of α, β, n_α, n_β and n which must be considered for any general intermodulation product, (p,q) which arises from the interaction of two signals.

The above discussion applies to narrowband signals. If one or more of the signals are broadband, the problem is much more complex. Consider, as an example, the case of one broadband signal, B, and one narrowband signal, A. The broadband signal amplitude may be represented as $B(\omega)$, a voltage distribution in frequency. It is possible to consider the total intermodulation product as the result of each point of the voltage distribution intermodulating with the narrowband frequency and producing a point of the voltage distribution of the intermodulation product. This being the case, the voltage distribution is translated in frequency to form the intermodulation product. It is, however, not in general a linear superposition. This is true since the minimum value of β is equal to q (the harmonic number associated with $B(\omega)$), and this is the term which is the most significant in determining the amplitude of the intermodulation product. With this assumption, it is possible to relate the voltage spectrum of the intermodulation product to the voltage spectrum of the input signal.

To determine the effect of intermodulation on the receiver, it is necessary to know the power density spectrum of the product. This is given by the relation

$$P_{D2}(\omega_\alpha) = \left(\frac{B_1(\omega)}{B_2(\omega_\alpha)}\right)^2 P_{D1}(\omega) \qquad (6)$$

Table 4-1

GENERAL INTERMODULATION CONTRIBUTION CHART

n	α	β	n_α	n_β
p + q	p	q	0	0
p + q + 2	p	p + 2	0	1
	p + 2	q	1	0
p + q + 4	p	q + 4	0	2
	p + 2	q + 2	1	1
	p + 4	q	2	0
p + q + 6	p	q + 6	0	3
	p + 2	q + 4	1	2
	p + 4	q + 2	2	1
	p + 6	q	3	0
p + q + 8	p	q + 8	0	4
	p + 2	q + 6	1	3
	p + 4	q + 4	2	2
	p + 6	q + 2	3	1
	p + 8	q	4	0
p + q + i	p	q + i	0	i/2
	p + 2	q + i - 2	1	i/2-1
	.	.	.	.
	.	.	.	.
	.	.	.	.
	p + i	q	i/2	0

where

$B_1(\omega)$ = the voltage spectrum of the input signal

$B_2(\omega_\alpha)$ = the resulting voltage spectrum of the intermodulation product

$P_{D1}(\omega)$ = power density distribution of the broadband input signal

$P_{D2}(\omega_\alpha)$ = power density distribution of the intermodulation product

ω_α = that frequency in the intermodulation product distribution which resulted from the ω frequency in the broadband signal

An illustration showing the voltage and power density distribution is given in Figure 4-1. In this case, the broadband signal has a sawtooth voltage distribution in frequency. The resulting shape of P_{D1}, P_{D2}, and $A_2(\omega)$ are as shown for a case in which $\alpha = 2$.

4.1.3 Frequency Relations

A possible cause of interference is that any two signals of the electromagnetic environment may produce an intermodulation frequency in the first nonlinear stage of a receiver which falls in the passband of the receiver. A thorough analysis, therefore, must take this into account by comparing in the frequency domain each signal with every other signal to determine which of these signals are so related in frequency as to cause interference in this manner.

Considering two signals within the environment, S_1 and S_2, whose energy is contained in the frequency bands $(f_1 \pm \Delta f_1)$ and $(f_2 \pm \Delta f_2)$ their resultant intermodulation product frequency band is given as

$$(f_{ip} \pm \Delta f_{ip}) = a(f_1 \pm \Delta f_1) \pm b(f_2 \pm \Delta f_2) \qquad (7)$$

where

a = harmonic number of S_1 associated with the intermodulation product

b = harmonic number of S_2 associated with the intermodulation product

A possible way of determining if any two signals are of the correct frequencies to cause interference is to pick one signal (S_1) and determine the frequency band in which energy is capable of intermodulating with S_1 and entering the passband. Considering the receiver passband to be determined by f_{min} and f_{max}, the frequency ranges of possible inter-

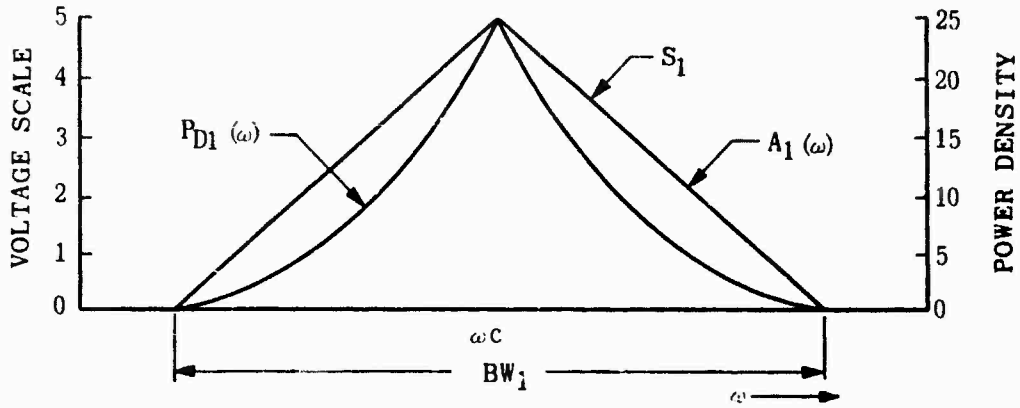

a. Voltage and Power Density Distribution of a Broadband Signal.

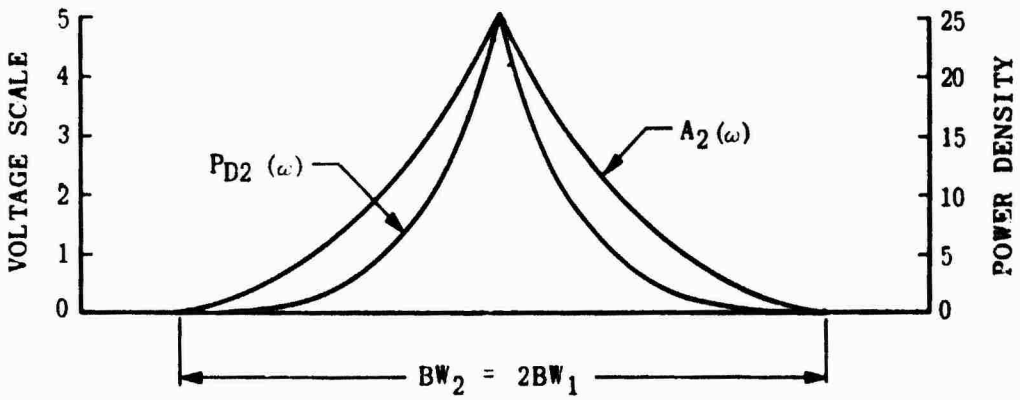

b. Voltage and Power Density Distribution of the Intermodulation Product.

Figure 4-1. Intermodulation Product Characteristics Resulting from a Broadband Signal.

ference normalized to the receiver bandpass can be determined from Table 4-2.

Table 4-2

INTERMODULATION FREQUENCY RELATIONSHIPS

Sign	Restriction	Low Frequency Component	High Frequency Component
+	$f_1 < f_{min}$	$\frac{f_{2L}}{f_{min}} = \frac{1}{b} - \frac{a}{b}\frac{(f_1 + \Delta f_1)}{f_{min}}$	$\frac{f_{2H}}{f_{max}} = \frac{1}{b} - \frac{a}{b}\frac{(f_1 - \Delta f_1)}{f_{max}}$
-	$bf_2 > af_1$	$\frac{f_{2L}}{f_{min}} = \frac{1}{b} + \frac{a}{b}\frac{(f_1 - \Delta f_1)}{f_{min}}$	$\frac{f_{2H}}{f_{max}} = \frac{1}{b} + \frac{a}{b}\frac{(f_1 + \Delta f_1)}{f_{max}}$
-	$af_1 > bf_2$	$\frac{f_{2L}}{f_{min}} = \frac{a}{b}\frac{(f_1 + \Delta f_1)}{f_{min}} - \frac{1}{b}$	$\frac{f_{2H}}{f_{max}} = \frac{a}{b}\frac{(f_1 + \Delta f_1)}{f_{max}} - \frac{1}{b}$

An illustration of these relations is given in Figure 4-2, where it is assumed the receiver bandpass is small compared to the interfering signal bandwidths

$$f_{min} = f_{max} = f_0$$

The following relation shows the bandwidth of the intermodulation product in terms of the constituent signals.

$$BW_{ip} = aBW_1 + bBW_2 \tag{8}$$

Another type of intermodulation product which can cause interference is spurious response in which the local oscillator beats with the undesired signal to form products in the IF passband. The frequencies at which interfering signals can cause spurious responses are well defined by the spurious frequency relation

$$f_s = \frac{|pf_{LO} \pm f_{if}|}{q} \tag{9}$$

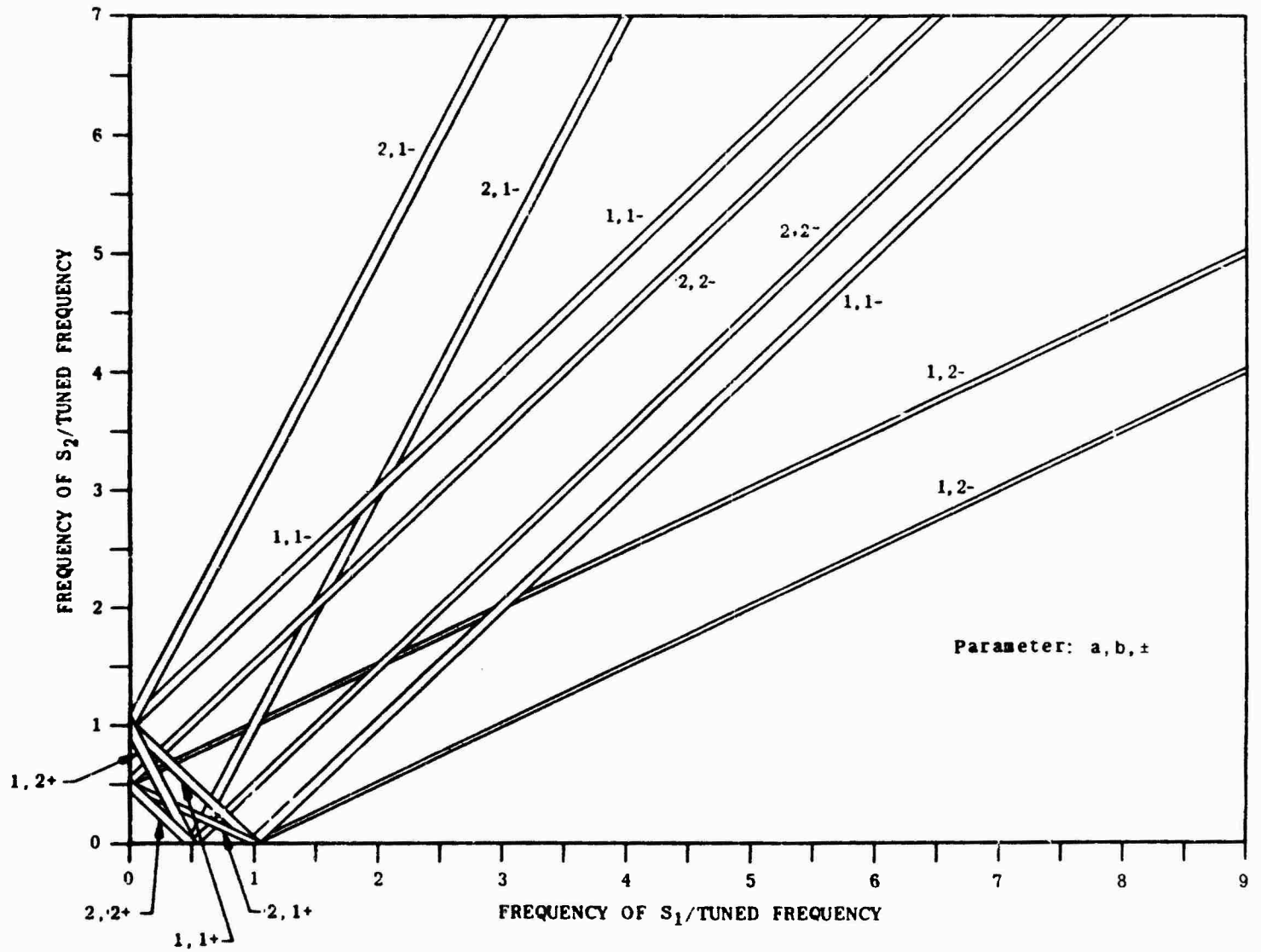

Figure 4-2. Frequency Ranges of Possible Intermodulation Between Two Signals.

where

$$K = \frac{P(\omega)}{\left|V(\omega)\right|^2}$$

ω_1, ω_2 = upper and lower frequency limits over which the power is summed

The primary concern with any interfering signal is what amount of the interfering signal is present at the final receiver detection process. It is necessary to consider this fact in determining the limits of integration (ω_1, ω_2). In the particular stage of interest (that stage at which the interference enters the passband) the frequency selectivity may not be very sharp so that the tendency is to extend the limits ω_1 and ω_2. However, the following stages may be extremely sharp and reduce the energy integrated from the extremities of the frequency range. This is usually the case in the stage of interest. Therefore, reasonable values of ω_1 and ω_2 are the effective bandwidth limits of the receiver from that point on. It must be emphasized that judgment must be used in determining ω_1 and ω_2.

If the limits can be justified to be the bandwidth of the receiver, a good approximation is to assume $S(\omega)$ is a constant (C_S) over this region so that the passband power becomes

$$P = KC_S^2 \int_{\omega_1}^{\omega_1 + BW} \left|V(\omega)\right|^2 \, d\omega \qquad (11)$$

Due to complex modulation processes, the above integral is often difficult if not impossible to obtain analytically; however, the voltage distribution, $V(\omega)$, is usually known. It is, therefore, possible to perform the integration numerically. A numerical integration procedure which can be used and which gives accurate results is Simpson's rule.

Figure 4-3a shows a typical relation between an interfering product and the stage selectivity function. Figure 4-3b shows the resulting power density distribution which is essentially the function to be integrated. In order to apply Simpson's rule to integrate this function, it is necessary to divide the integration interval into an even number of subintervals (n) each of width h. The function is evaluated at the ends of these subintervals to give P_0, P_1, P_2 ... P_n.

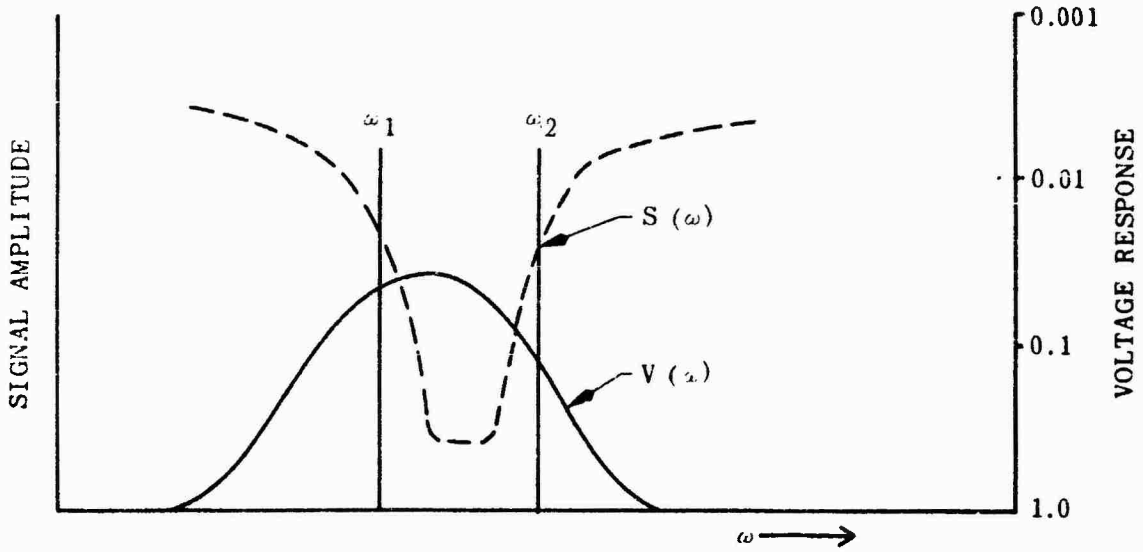

a. Typical Signal Spectrum and Filter Response

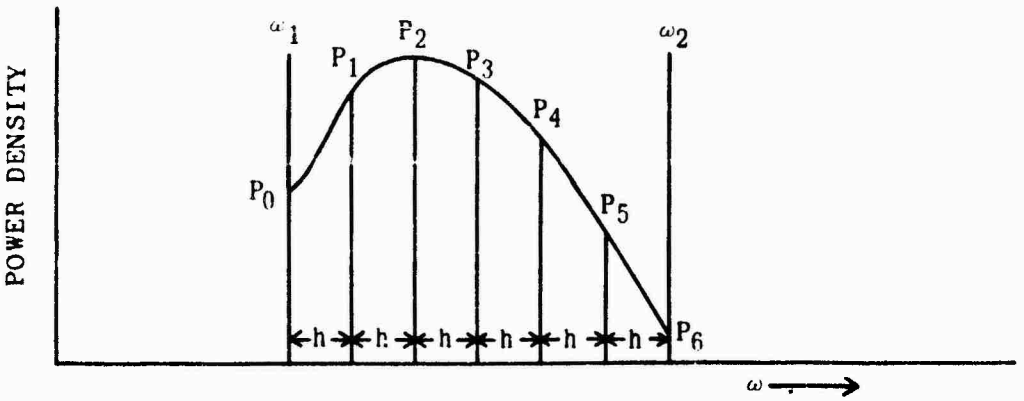

b. Resulting Power Distribution at the Following Receiver Stage

Figure 4-3. Resulting Energy Distribution and Integration Process of a Typical Interference Product.

The value of the integral is then

$$\int_{\omega_1}^{\omega_2} P(\omega)\, d\omega = \frac{(\omega_2 - \omega_1)}{3n} \sum_{i=0}^{n} C_i P_i \qquad (12)$$

where

$$C_i = 1,4,2, \ldots 2,4,1$$

for

$$i = 0,1,2, \ldots n-2, n-1, n$$

This method approximates the function with second order curves and does not consider higher order components. The manner in which the various parameters are related to the actual function is illustrated in Figure 4-3b.

4.1.5 Addition of Interfering Effects

In order to determine the total effect of the interfering signals it is practical to combine signals which have similar characteristics into a single representation. This is, of course, due to the fact that it is easier to evaluate the effect of a single signal than many.

In order to find an easier form of representation, it is necessary to classify each interference component into a particular category. Since it is impossible to completely specify an interference component and the minute effects of the receiver on each component, the following general classes of signals will be used to categorize the components:

1. Noise
2. Unmodulated CW
3. CW - AM
4. CW - FM
5. Pulse

In classifying signals, a decision must be made as to whether the interference component maintains, to a noticeable degree, the particular modulation characteristics associated with it. If a portion of a 10 Mc pulse enters a 1 Mc passband receiver, not enough of the signal will be present in the receiver to reconstruct the pulse. A signal of

this nature must be classified as noise, since it is highly impractical to attempt to reconstruct the time function from the little that is known about the frequency distributions.

In general, any signal which does not sufficiently enter the receiver passband, or is the result of a complex modulation process, will be classified as noise. Also, a fairly good approximation to the overall components is an equivalent noise representation. However, signal characteristics will be maintained, if possible, since various types of signals respond differently to particular detection processes. The components to be considered as noise can be combined simply if it is assumed that each has a Gaussian amplitude distribution in time. If this is the case, each component may be characterized by the following probability distribution.

$$P(x) = \frac{e^{-x^2/2\sigma^2}}{\sqrt{2\pi\sigma^2}} \tag{13}$$

where

x = the instantaneous amplitude value of the noise waveform

σ = the standard deviation of the distributions which is the RMS value of the waveform

If each of the noise components has a similar distribution, the RMS values of each may be combined by the relation

$$\sigma_T = \sqrt{\sum_{i=0}^{n} \sigma_i^2} \tag{14}$$

where

σ_T = RMS value of the waveform of all the components

σ_i = RMS value of the waveform of the ith component

The distribution of the total waveform is then

$$P(x) = \frac{e^{-x^2/2\sigma_T^2}}{\sqrt{2\pi\sigma_T^2}} \tag{15}$$

It will also be assumed that the total noise is uniformly distributed over the receiver bandwidth, or that its frequency distribution will be similar to the shape of the receiver bandpass. Equation 14 is a valid relation for combining the RMS values of any uncorrelated signals, not necessarily noise. The RMS value of the total interference can, therefore, be determined, but the resulting waveform will not, in general, have the characteristics of noise. Combination of the interfering signals in this manner is an approximation since the effect of the actual interfering signal may not be the same as noise.

In summary, the interference components will be categorized and all components in a particular class will be combined by Equation 14. σ_T will then represent all components in the particular category and will have associated with it the general characteristics of the particular category.

4.1.6 Detector Response to Signal and Interference

In order to fully evaluate the effect of the interference components on the intelligibility of the desired signal, it is necessary to determine the signal and interference components in the frequency band in which the intelligence is derived, and to evaluate the intelligibility in terms of the signal and interfering component characteristics.

The detection process converts the signal from either the IF or RF to audio or video. It consists of signal processing circuitry which is designed with respect to the desired signal modulation characteristics the object of which is to enhance the signal and suppress interference, and a nonlinear device which accomplishes the frequency conversion. The analysis of the nonlinear portion of the detector process is more complicated than that of the mixer. In the mixer, the signal and noise in the RF passband beats with a single local oscillator frequency and, as a result, is linearly translated in frequency to the IF. In the detector, however, the frequency shift is accomplished by each frequency component of the signal and noise beating with every other component of the signal and noise to produce the audio output. Because of this, the audio signal consists of signal cross signal (s×s), noise cross noise (n×n), and signal cross noise (s×n) intermodulation components. The (s×s) components constitute the desired signal, while both the (s×n) and (n×n) components constitute interference. It can be seen that due to the (s×n) components, the amount of interference in the

output is a function of the desired signal. It can also be shown that, for small signal-to-noise ratios, the (nxn) components predominate over the (sxn) components in the output, and for large signal-to-noise ratios, the (sxn) components are largest.

Most detectors can be classified as either halfwave linear or halfwave square law, Figure 4-4. Detector operation for the purpose of interference analysis can be specified as the signal-to-noise ratio of the output in terms of the signal-to-noise ratio of the input, and it is possible to do this for certain detector configurations with certain applied approximations. However, a universal representation of the desired form is unavailable.

Considering the nonlinear stage as the portion of the receiver which detects envelope amplitude variations, as shown in Figure 4-4, it can be represented by a nonlinear device and low-pass filter. The effect of the nonlinear element, as far as detection is concerned, is to produce beat frequency components in the vicinity of the low-pass filter between individual IF components. The beat frequency associated with the particular intermodulation component resulting from any two individual IF components is the difference of the frequencies of the components.

A quantity which will prove useful in the analysis of the detector is the amount of energy resulting from the (sxn) or (nxn) components which is in the detector bandpass in terms of the total energy resulting from (nxn) or (sxn) components. A quantity of this nature, which will be called a bandwidth noise factor, can be approximately determined with the aid of Figure 4-5. For purposes of analysis, the noise distribution in the IF pass band can be considered a uniform distribution with equally spaced components, as shown in Figure 4-5a. If each noise component, as illustrated, beats with every other noise component in the band and an amount of energy associated with each (nxn) component is placed in its respective position in the audio frequency spectrum, the shape of the energy spectrum of all components will be as shown in Figure 4-5b. The ratio of the energy in BW_D (the detector bandwidth) to the total energy is

$$k_{nn} = \frac{BW_D}{BW}\left(2 - \frac{BW_D}{BW}\right) \qquad (16)$$

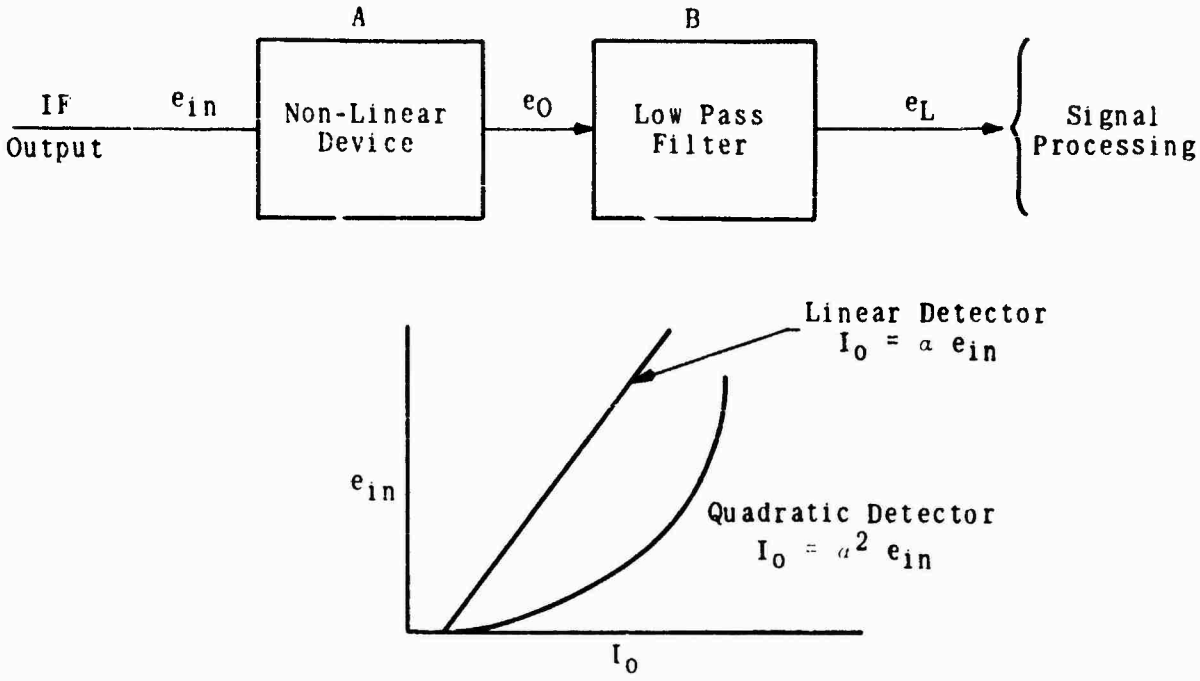

a. Voltage Characteristic of Non-Linear Device.

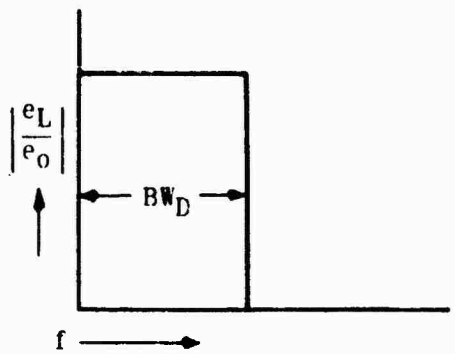

b. Frequency Characteristic of Ideal Low Pass Filter.

Figure 4-4. Functional Representation of a Typical Detector.

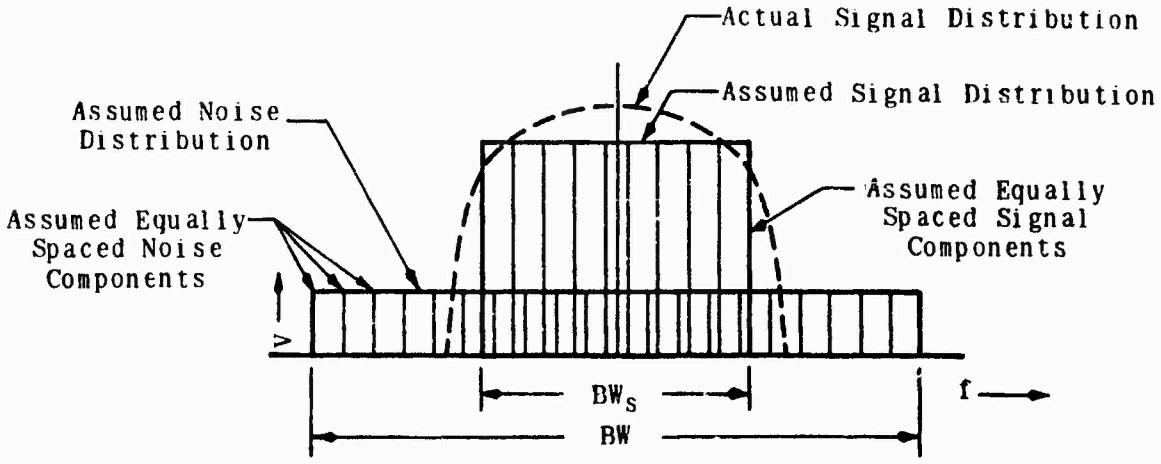

a. IF Signal and Noise Distribution

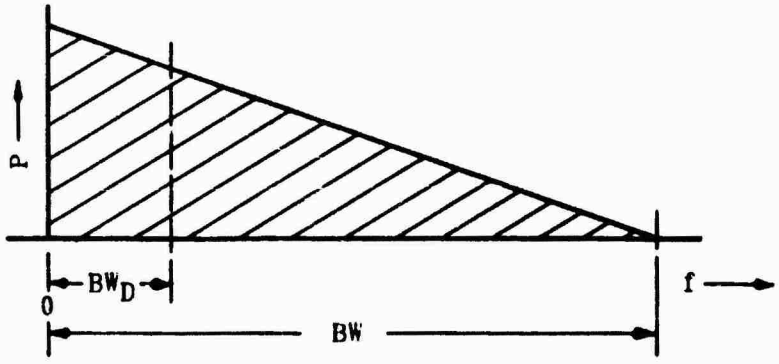

b. Energy Distribution of the (nxn) Components

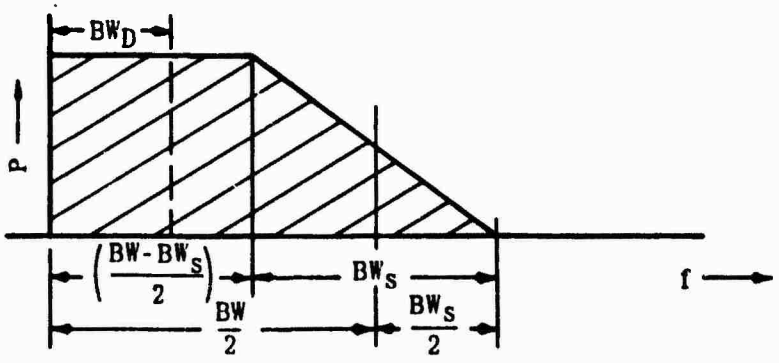

c. Energy Distribution of the (sxn) Components

Figure 4-5. (nxn) and (sxn) Low Frequency Noise Distributions Resulting from an Approximate IF Signal and Noise Distribution.

where

k_{nn} = bandwidth noise factor for (n×n) components

BW = predetector bandwidth

BW_D = postdetector bandwidth

In order to determine the bandwidth noise factor for the (s×n) components, an approximation must be made to the signal distribution. As shown in Figure 4-5a, the signal will be considered as an equivalent rectangular distribution with equally spaced components. If a process similar to that carried out for the (n×n) cases is now applied, each component of the approximate signal distribution can be visualized as beating with every component of the noise distribution. The energy of the (s×n) process will be distributed in frequency as shown in Figure 4-5c. The noise bandwidth factor can then be determined from the geometry of the distribution, and is

$$k_{sn} = \frac{1}{BW}\left\{\frac{BW}{2} + \left(\frac{BW}{2} - BW_D\right)^2 \frac{BW_s}{2}\left(BW_s - BW - BW_D - 1\right)\right\} \qquad (17)$$

where

k_{sn} = noise bandwidth factor for the (s×n) components

BW_D = approximated signal bandwidth

For the case of a quadratic detector (Figure 4-4), an analysis has been made[1] which gives the output signal-to-noise power ratio in terms of the input signal-to-noise power ratio, where the output signal is the demodulated waveform. However, the output noise is given as the total from the (n×n) and (s×n) components. By using the bandwidth noise factors which have been developed, the relation can be modified to give

$$\lambda_m = \frac{2\lambda_o^2 a^2}{\frac{k_g k_{nn}}{k} + 2\lambda_o k_{sn}} \qquad (18)$$

1. R.H. DeLano, "Signal-to-Noise Ratios of Linear Detectors,", Proc IRE, vol 37, pp 1120-1126; October 1949.

where

λ_o = input signal-to-noise power ratio

a = modulation index of the wave

k = $f_r T$, the duty cycle of the pulse if pulse is modulated. k = 1 for continuous wave

f_r = pulse repetition frequency

T = pulse length

k_g = $f_r t_g$, takes into account that the pulses may be surrounded by a gate of length t_g

λ_m = output signal-to-noise ratio of the demodulated component

Equation 18 enables the determination of output signal-to-noise ratio from a quadratic detector for any AM signal which appears at its input. Equation 18 is plotted on Figure 4-6 for the case $k = k_g = k_{sn} = k_{nn} = 1$. This corresponds to $BW_s = BW = BW_D$, and a continuous signal. Linear detectors (Figure 4-4) are not as convenient to analyze. An analysis method can be developed separately for pulses and continuous AM signals. For linear or envelope detectors, Equation 40 of footnote reference 1 can be modified with the aid of the bandwidth noise factors to give

$$\lambda_L = \frac{4\left[{}_1F_1\left(-\frac{1}{2};\ 1;\ -\lambda_o\right) - 1\right]^2}{\left[\left(\frac{k_g}{k} - 1\right) + {}_1F_1^2\left(\frac{1}{2};\ 1;\ -\lambda_o\right)\right] k_{nn} + 2\lambda_o\ {}_1F_1^2\left(\frac{1}{2};\ 2;\ -\lambda_o\right) k_{sn}} \qquad (19)$$

where

λ_L = output signal-to-noise ratio of the detected pulse-to-noise ratio

${}_1F_1(\alpha;\beta;\gamma)$ = confluent hypergeometric function of α, β, γ

An analysis of linear detectors for AM modulated continuous waves is presented in footnote reference 2. The analysis is broken into

---

2. David Middleton, "Rectification of a Sinusoidally Modulated Carrier in the Presence of Noise," Proc IRE, vol 36, pp 1467-1477; December 1948.

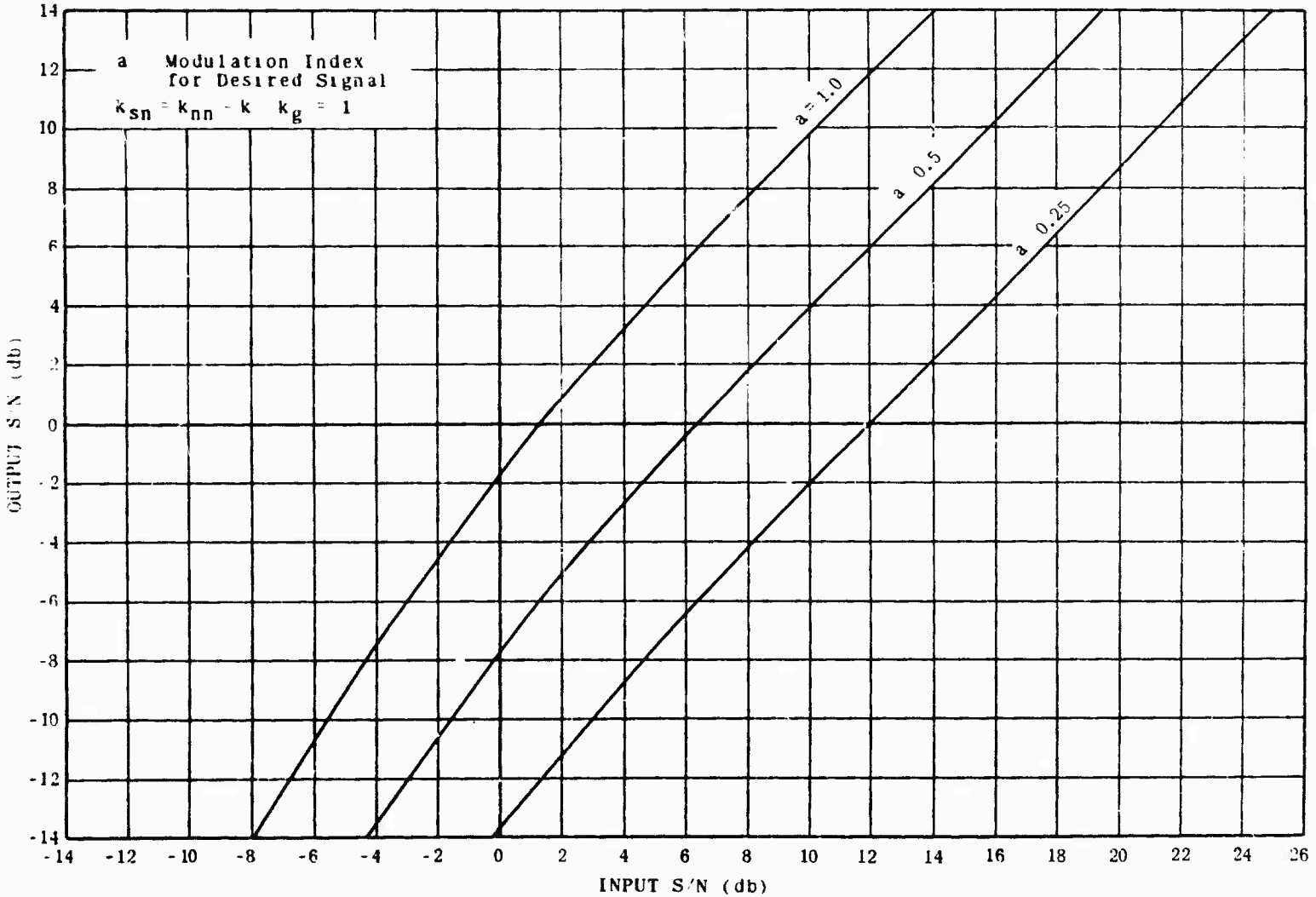

Figure 4-6. Output Signal to Noise Power Ratio Versus Input Signal to Noise Power Ratio for a Square L_{aw} Detector.

two sections; the first is for small λ_o and the second is for large λ_o. For small λ_o, where $\lambda_o(1 + a)^2 \leq 4$, λ_m is found to be a function of the shape of the IF passband. Classifying the shape of the IF passband as either "optical" (single tuned), rectangular, or Gaussian, the functional relation between input and output λ is shown on Figure 4-7. The parameter of the curves is modulation index, and the ordinate (λ_m) is in terms of a scaling factor $(\pi BW/BW_D)^{1/2}$ In order to determine λ_m, the ordinant is multiplied by the scale factor. As used in the scale factor, BW and BW_D are the three db bandwidths of the IF stage and detector, respectively. For larger λ_o, an approximate relation for λ_m is given as

$$\lambda_m = \frac{a\lambda_o^{\frac{1}{2}}}{\sqrt{2}} \left(\frac{\pi BW}{BW_D \Gamma^{(1)}} \right) \tag{20}$$

where

$\Gamma^{(1)}$ = $\pi/2$; π; 1 for rectangular, Gaussian, and optical IF passbands in that order

4.1.7 Probability Aspect

It has been determined that the statistical nature of a transmitter output is defined by the following probability distribution

$$P(v) = \frac{1}{2\pi\sigma} \exp \left((m_\gamma - v)/2\sigma^2 \right) \tag{21}$$

where

v = transmitter output voltage measured in db

m_γ = median value of the distribution, and the mean value on the logarithmic plot

σ = standard deviation of the logarithmic plot

The development of Equation 21, as it applies to transmitter output signals, is shown in a previous report.[3] It is easily seen that Equation 21 is a normal distribution in the logarithm of the variable v. However, in order to process the distribution through the receiver, it is necessary that the distribution be expressed in terms of a linear

3. Interference Analysis Study, Jansky & Bailey, Washington, D. C., Final Report, RADC-TDR-61-312, Contract No. AF 30(602)-1934; January 1962.

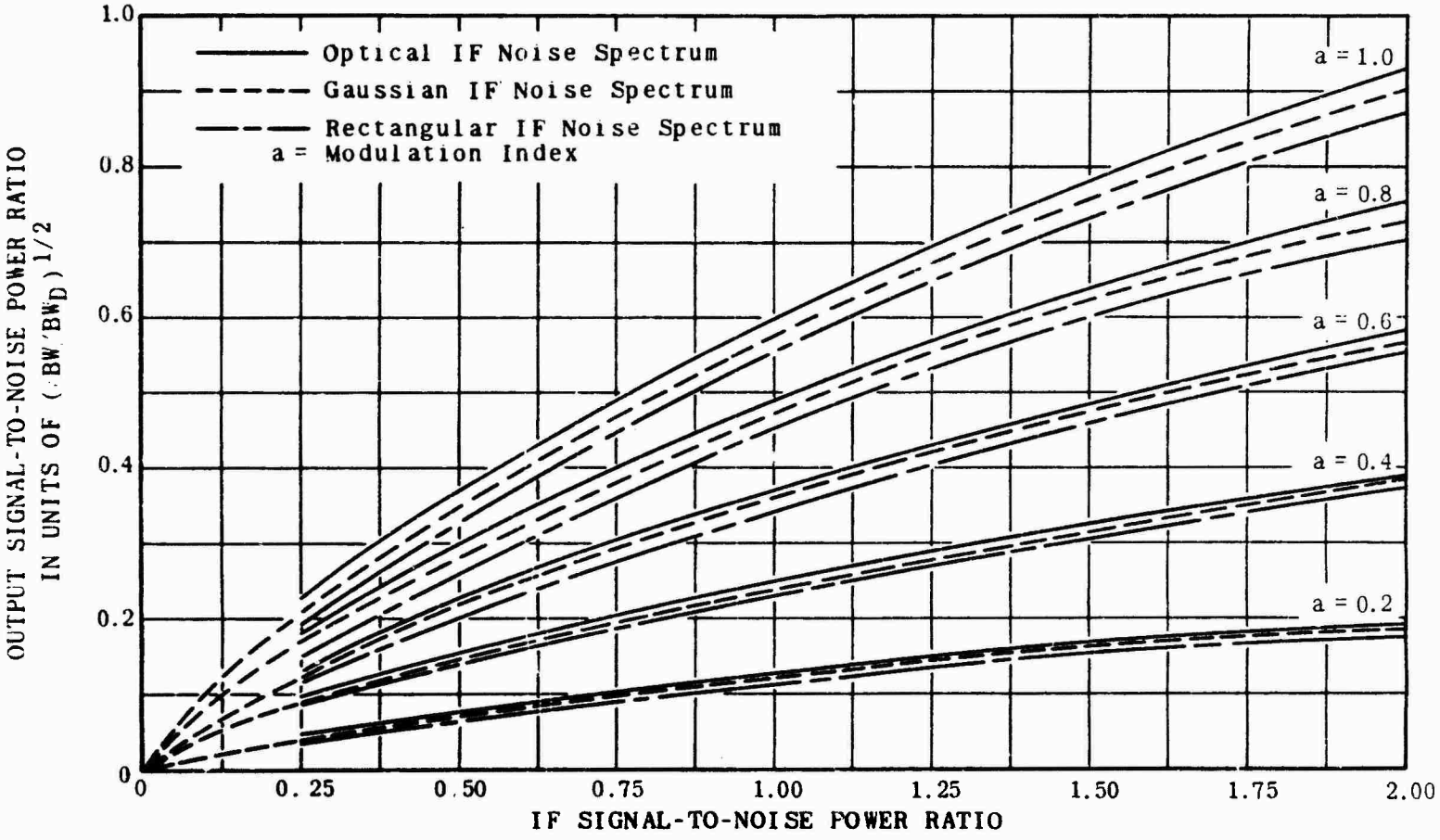

Figure 4-7. RMS Signal-to-Noise Ratio After Rectification by a Linear Detector.

scale in the variable. This distribution will not be normal. A proper distribution in a linear scale can be generated by assuming the variable, v, goes through a transform given by the relation $v = 20 \log_{10} y$, where y will be the transmitter output in appropriate linear units (volts, milliwatts, etc.). Taking Equation 21 through the transform relation, the resulting expression is

$$P(y) = \frac{B}{y} \exp\left(-A(\log_{10} y - \log_{10} m_y)\right) \qquad (22)$$

where

$$A = 200/\sigma^2$$

$$B = 20 \log_{10} e/\sqrt{2\pi}\sigma$$

$$m_y = \frac{1}{20} \text{ antilog}_{10} m_\gamma$$

The new distribution is not normal, but the median value, m_y, corresponds to the median value, m_γ, of the logarithmic distribution. A very important quantity of the new distribution is its mean value, and it will have to be determined from the new distribution since the mean values of the two distributions do not correspond through the transform relation $v = 20 \log_{10} y$.

The mean value of a distribution is given by the relation

$$\bar{y} = \int_{-\infty}^{\infty} y\, P(y)\, dy$$

In Equation 22, the probability function is only defined for positive values of the variable, and the mean value is given by

$$\bar{y} = \int_{0}^{\infty} B \exp\left(-A(\log_{10} y - \log_{10} m_y)\right) dy$$

This integral will be determined by numerical integration and tables given for it for various values of m_y and σ. Once the mean has been determined, the variance can be determined from the relation

$$\mu_y = \int_{0}^{\infty} (y - \bar{y}) \frac{B}{y} \exp\left(-A(\log_{10} y - \log_{10} m_y)\right) dy$$

from which the standard deviation is given as $\sigma_y = \mu_y^{\frac{1}{2}}$. This being the distributional form associated with each transmitter output, a transformation process of particular importance is $x = k\, y^n$. Since this

gives the relationship between an intermodulation product and one of the intermodulating signals, transforming the distribution given in Equation 22 by $x = k\ y^n$ gives the following probability distribution for x:

$$P(x) = \frac{B}{n}\, x^{\left(\frac{n-2}{n}\right)} \exp\left(-A/n^2 \left(\log_{10} x - n \log_{10} \frac{\bar{y}}{c}\right)^2\right)$$

where

$$c = \left(\frac{1}{k}\right)^{\frac{1}{n}}$$

Further work is necessary for the case in which the product in the pass band results from two statistically defined functions, such as in the case of intermodulation between two environmental signals. Once this has been done, it will be possible with the relations given to statistically define all signals in the IF pass band.

In the receiver analysis technique, after all components in the IF pass band are determined, components with similar characteristics are then added together to determine the net effect. Therefore, it becomes necessary to determine the statistical nature of the resultant. It is a difficult process to add several distributions, and further work is needed along these lines.

4.2 SAMPLE ANALYSES FOR RF PORTION OF RADAR RECEIVERS

4.2.1 Introduction

The analysis of the RF section of microwave receivers is for the purpose of providing engineering data for use in radio frequency interference prediction. Specific operational radars were chosen as samples, and the analysis is based on components used in these operational "work-horse" radars. The sample radar analyses are straightforward approaches to determine characteristics of components and over-all susceptibility to radio interference.

4.2.1.1 RF Receiver Section

The function of the RF receiver section of any radar is to convert input signal intelligence into a form that can be handled by a normal low-frequency receiver for eventual display.

To accomplish this purpose, the RF section need consist of a signal converter and a signal oscillator. Echo signals and oscillator signals are fed into the mixer unit simultaneously and are "mixed" in such a manner that sum and difference frequencies are generated. Any nonlinear element will produce sum and difference frequencies, under these circumstances, and could be a frequency converter. The oscillator must be a stable source of signals different in frequency from the echo signal.

As the art progressed it was considered important to use the same antenna system for the radar transmitter and receiver. Hence, precautions were necessary to protect the frequency converter from the high power of the transmitter output. In some cases, the echo signal was too weak and a method of amplification had to be inserted. Situations existed where it was imperative to make the RF section more frequency-sensitive, thus filtering devices were inserted. Obtaining a stable source of signal generation required the use of sophisticated devices and complementing circuitry. Coaxial cable or waveguide was needed to direct signals from one component to another. These items made the RF section a sophisticated part of the over-all system.

4.2.1.2 Functional Block Diagrams

A functional block diagram will be presented for each of the sample radars. These diagrams provide the complete signal path for echo and oscillator signals, and each component in the diagram must be assessed separately as to its influence on the final output. The diagrams were obtained in conference with supervisory engineers and technicians responsible for maintaining and operating the radars.

Not all of the components are standard. In numerous cases, components were designed and produced specifically for one radar set.

4.2.1.3 Sample Radar Analyses

It has proven difficult to obtain component characteristics outside their operating frequencies. However it is evident that, for our purposes we must consider component characteristics over the entire military microwave range. Thus, we are interested in component behavior from the lower microwave frequencies up to approximately 12 GCS, i.e., the range listed in MIL-STD-449A.

Where possible, we have obtained selectivity characteristics of components over their operating range. In addition, we have predicted a selectivity over the entire military microwave range and have explained the reasoning for the construction of these selectivity curves.

4.2.1.4 Experimental Verification

There has been no experimental verification of any predicted characteristics. It appears that with sufficient experimentation on commercial components it would be possible to construct selectivity characteristics for families of components and to use these characteristics to provide a reasonably accurate susceptibility prediction on any RF receiver section containing such components.

It should be noted that the approach taken is a phenomenological one and that no rigorous explanation was attempted or even contemplated. If spectrum signature measurements reasonably confirm the predicted susceptibility characteristics, then we would

strongly advise the undertaking of a program of experimental component investigation.

4.2.2 Fundamental Relationships

As in many technical fields, basic radar work centers around a fundamental relationship. This relationship is known as the radar equation and is

$$P_R = P_T \cdot \frac{G}{4\pi R^2} \cdot \sigma \cdot \frac{A}{4\pi R^2}$$

where

P_R is the power of the receiver echo signal
P_T is the power of the transmitted pulse
G is the gain of the transmitting antenna
R is the distance of the target from the antenna
σ is the scattering cross section characterizing the target
A is the absorbing cross section (effective area) of the receiving antenna.

Examination of this basic relationship emphasizes that the most effective radar has the highest possible transmitting power, the most sensitive receiver, and the largest antennas for transmission and reception.[4]

Using an unclassified radar, AN/TPS-1D, as an illustration, we find that its range is 300 yards to 160 nautical miles, the antenna area is approximately 60 square feet, its output power is 0.5×10^6 watts peak, the IF bandwidth is 1×10^6 cps and its antenna gain is approximately 1000.[5] Thus, for a target cross section of 1000 square feet (a WW II medium bomber)[6] we find that the power of the received echo signal ranges from approximately 0.3 watts at minimum target distance to approximately $10^{-12.8}$ watts

4. Smullen & Montgomery. Microwave Duplexers, MIT Radiation Laboratory Series Volume 14, McGraw-Hill Book Company, Inc., 1948.
5. Military Technical Order Applicable to Specific Radar.
6. Smullen & Montgomery, op. cit. p. 150.

at maximum target distance. We would, therefore, suspect that the radar receiver was designed to cover the echo signal power range from 0.3 watts maximum to $10^{-12.8}$ watts minimum.

It has been generally recognized that the heterodyne receiver has one of the lowest noise figures and has been universally used where weak signals are encountered.[7] Ginzton[8] has presented a means of calculating a minimum detectable signal by the following relationship

$$P_m = k\ T\ \Delta f\ NF \qquad (23)$$

For an ideal circuit that has no sources of noise except temperature fluctuations, the noise power is k T ΔF.[9] The Boltzman Constant

$$k = R_o/N_o = 1.38 \times 10^{-23}\ \text{watts}/^oK$$

relates energy per particle per degree Kelvin. T is the Kelvin temperature and is taken at room temperature to provide a standard. Δf is simply the bandwidth of the receiver which normally implies the IF bandwidth of a heterodyne or first IF bandwidth of a superheterodyne receiver. NF is an arbitrary quantity used by Ginzton[10] to define other noise in crystal rectifiers. In the crystal rectifiers encountered in this research, NF is less than 20.

We emphasize that the P_{min} yielded by the above relationship becomes not the minimum detectable signal per se, rather, it is the noise power of the crystal rectifier, which greatly influences the receiver noise when the receiver contains no RF amplifier. If

---

7. Lawson & Uhlenbeck, Thresholds Signals, MIT Radiation Laboratory Series, Vol. 24, McGraw-Hill Book Co., Inc., 1957.
8. Ginzton, Edward L., Microwave Measurements, McGraw-Hill Book Co., Inc., 1957.
9. Smullen & Montgomery, op. cit., p. 150.
10. Ginzton, Edward, L., op. cit., p. 151.

the receiver contains an RF amplifier, the over-all noise figure of the receiver is determined almost entirely by the noise figure of the RF amplifier itself.[11] In effect, the quantity we have identified as P_{min} is the noise power of the frequency converter. Therefore, to be detected, a signal amplitude must be above this noise power.

Using equation 23, we have calculated the theoretical minimum detectable signal (MDS) of the AN/TPS-1D to be approximately $10^{-13.5}$ watts. A comparison of the theoretical MDS with the minimum echo signal of $10^{-12.8}$ watts illustrates an allowable attenuation of 7 db from the antenna to the crystal rectifier in the mixer. Such an allowance is reasonable because the appt ent attenuation at operating frequency is closer to 3 db than to 7 db in the radars examined. In the other direction, we find that the burn-out level (single pulse) of the AN/TPS-1D crystal rectifier (1N21B) is 2.5 watts.

There has been much work and little general agreement as to the discrete definition and cause of crystal burn-out. Three factors must be considered: (1) T, pulse time (2) W, pulse energy and (3) P, pulse power. It has been conceded that pulse energy is a determining factor in crystal burn-out, and manufacturers rate their product in ergs for burn-out tests in meeting military specifications. However, experimental tests on large numbers of crystal rectifiers have provided no clear evidence for a discrete cause of crystal burn-out.[12]

Since we are considering only a single, discrete echo signal, it is convenient for us to consider burn-out as occurring when a single pulse is of sufficient level to cause deterioration of the crystal. We, therefore, define crystal burn-out as occurring when any deterioration in the performance of a crystal is observed. In some cases, crystals deteriorate slowly, inothers rapidly.[13]

Thus, a burn-out limit in the present context means the

---

11. Lawson & Uhlenbeck, op. cit., p.151.
12. Torrey & Whitmer, Crystal Rectifiers, MIT Radiation Series, Vol. 15, McGraw-Hill Book Co., Inc., 1957.
13. Ibid.

level of a single pulse which will cause deterioration of the crystal.

4.2.3 Basic Components

Aside from general receiver characteristics, it is necessary to look closely at the specific RF section components of (1) waveguide (2) duplexer of T-R device (3) mixer unit (4) local oscillator unit.

4.2.3.1 Waveguide

The sample radars use coaxial cable and rigid rectangular waveguide exclusively. The important considerations of coaxial cable are that it acts as a low-pass filter and will have an upper cut-off limit determined by geometry and composition. The important consideration of rectangular waveguide is that it is a high-pass filter with a lower cut-off limit determined by its geometry.

4.2.3.2 Duplexer or T-R Device[14]

A radar duplexer is little more than the microwave equivalent of a fast-time, double-pole, double-throw, low-loss switch. The duplexer may contain any or all of the following components: an anti-transmit-receive (ATR) tube, a pre-transmit-receive (pre T-R) tube, a transmit-receive (T-R) tube. The pre T-R and T-R tubes have a primary purpose of disconnecting the receiver from the system. The ATR tube has a primary purpose of disconnecting the transmitter from the system.

The duplexer tubes should (1) operate nonlinearly when a gas discharge is passing through the tube and (2) linearly when exposed to the low power levels of an echo signal. A super-strong echo signal could conceivably cause the T-R tube to "fire". However, such an echo signal would be of a level to cause crystal burn-out.

Design procedure of the duplexer tubes has been largely empirical. The need for such a device was great and satisfactory solutions were the objectives rather than an understanding of the phenomena involved. A continuingly important consideration in

14. Smullen & Montgomery, op. cit., p. 150.

the design of these and other microwave tubes is the ease with which they can be manufactured. Hence, fundamental theory is lacking except in the areas investigated, to facilitate production and to meet specifications.

Fixed tuned tubes can be characterized by a curve of the resonant wavelengths versus the tube geometry.[15] A tunable T-R tube is normally used with a separate cavity and experiences a higher leakage power for a given insertion loss or a higher insertion loss for a given leakage power. This amounts to approximately 1.5 db. It is noted that once a tube and cavity are selected the couplings can be adjusted for the desired insertion loss in the desired manner.

The desired insertion loss can be obtained through equal coupling, input matching, output matching, etc. Even though variations are common, a properly designed and maintained set will not be "lossy" in our context. For the purposes of this analysis, an over-all loss of 3-5 db is considered as not too extreme. However, in the equivalent design problem we would be talking of fractional db losses.

For instance, in design work, a loss of 0.1 db at operating frequencies is considered bordering on excess. For our purposes a 0.1 db loss would be considered negligible.

A complicated tuning procedure involving the components of the RF section can result in a 10-40 db sensitivity decrease. This fact was prominent in the promotion of T-R improvement.

Decrease in receiver sensitivity due to poor tuning has been a prime consideration in our construction of a tunable T-R characteristic. In previous wartime studies,[16] it was found that the receiver sensitivities were 6-12 db down from optimum due merely to poor T-R tuning. Also, it was observed that a cavity tuned to a frequency would indicate as little as 6 db attenuation to a signal at twice that frequency. Further, it was noted that harmonic

15. Ibid.

16. Ibid.

transmission conditions differed from tuned-frequency transmissions by as much as 10 db.

It should also be pointed out that T-R tubes are designed to protect the mixer during transmission and not as RF filters. The fact that the tubes act as a filter at low power is merely a bonus.

4.2.3.3 Mixer Unit

The mixer unit is the component which actually accomplishes frequency conversion. In fact, crystal mixer and converter are used interchangeably when discussing the mixer unit. In our approach to the analysis problem, it has been apparent that the mixer unit is the most selective of the RF components and is perhaps the central consideration of the RF section analysis.

The mixer unit itself consists of a crystal holder, a crystal rectifier (or balanced crystal rectifiers), an input, local oscillator output positions and perhaps a dc return path. Narrow-band mixers normally used in radar sets are designed to operate at a single frequency and can be fixed tuned for optimum performance at the frequency of the particular radar.[17]

Since the prime element of the mixer is a crystal rectifier, it is necessary to examine closely the characteristics of the common crystal rectifier. Figure 4-8 is a diagram of a metal-semiconductor contact that is the critical area of any common crystal rectifier. Figure 4-9 is the equivalent circuit of the metal-semiconductor contact and serves to illustrate the filter qualities of a crystal rectifier. Resistance R represents the nonlinear action of the potential barrier and C the capacitance at contact. Resistance r represents the bulk resistance of the semi-conductor considering the spreading nature of the current from the whisker contact.[18]

The critical nature of the contact between the metal "cat's

17. Carlson, Eric, A Broadband Microstrip Crystal Mixer With Integral D.C. Return, IRE Trans, on MTT, Vol. MTT-3, No. 2, March, 1955.

18. Ginzton, Edward L., op. cit., p. 151.

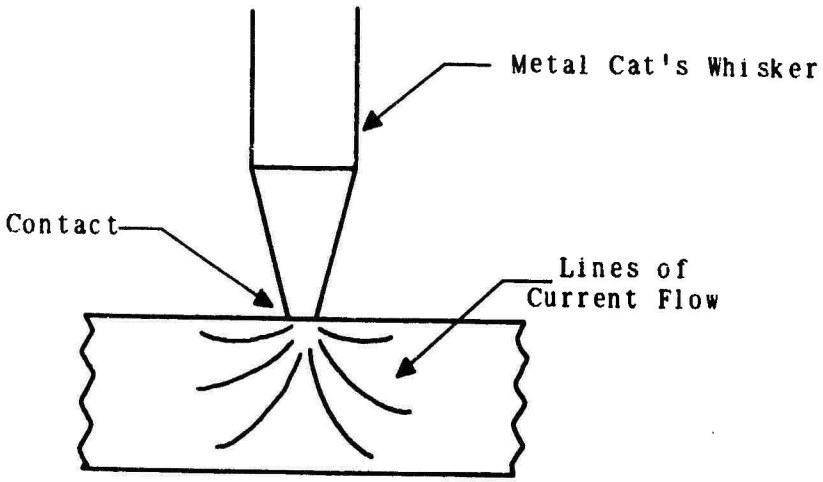

Figure 4-8. Metal-Semiconductor Contact.

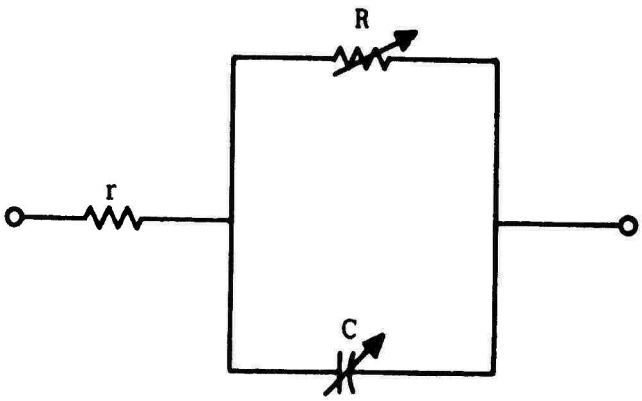

Figure 4-9. Equivalent Circuit.

whisker" and the semi-conductor is an important feature of the device, but the characteristics of the device depend upon the nature of the semi-conductor itself. The work functions of the whisker and the semi-conductor are generally different, creating a potential barrier to the flow of electrons. This barrier varies with the applied potential but effectively prevents electron flow at low potential. As the semi-conductor potential is increased, electron flow is enhanced, permitting current in one direction but not in the other.

A static characteristic of a crystal rectifier used as a frequency converter is shown in Figure 4-10. From this characteristic, it appears that the I-F output of the crystal rectifier is a gain over the echo signal input. This is actually misleading since the "gain" of a crystal rectifier used in the radars examined is normally minus (5-10 db). From the static characteristic, it is apparent that operation in the linear portion of the curve is desirable. This can be accomplished by fixing the local oscillator power level at a point to allow 5 ma of rectified current in this particular case. Then, the linear operation will be assured if the local oscillator signal is large in comparison to the input echo signal.

Manufacturers do not make available characteristics of their products outside the advertised operating range. In practice, this information is not needed by component designers, and the manufacturers have not fully investigated the effects of their mixers across a wide frequency range. We have based a selectivity characteristic on the selectivity of a crystal filter and will use this characteristic throughout the analysis. Such a construction is at best approximate but offers a base otherwise obtainable only through experimental investigation. Figure 4-11 is the constructed curve of frequency versus attenuation for a crystal mixer at its fundamental and multiple-fundamental frequency points. As frequency increases, attenuation approaches a constant level. The dotted line represents the envelope of predicted response points outside the operating frequency range. Figure 4-12 is similar to Figure 4-11 except that it is approximately 20 db "better" as a characteristic of a pair of matched crystal rectifiers used as a mixer. The 20 db "improvement" is used because that is the relationship between single

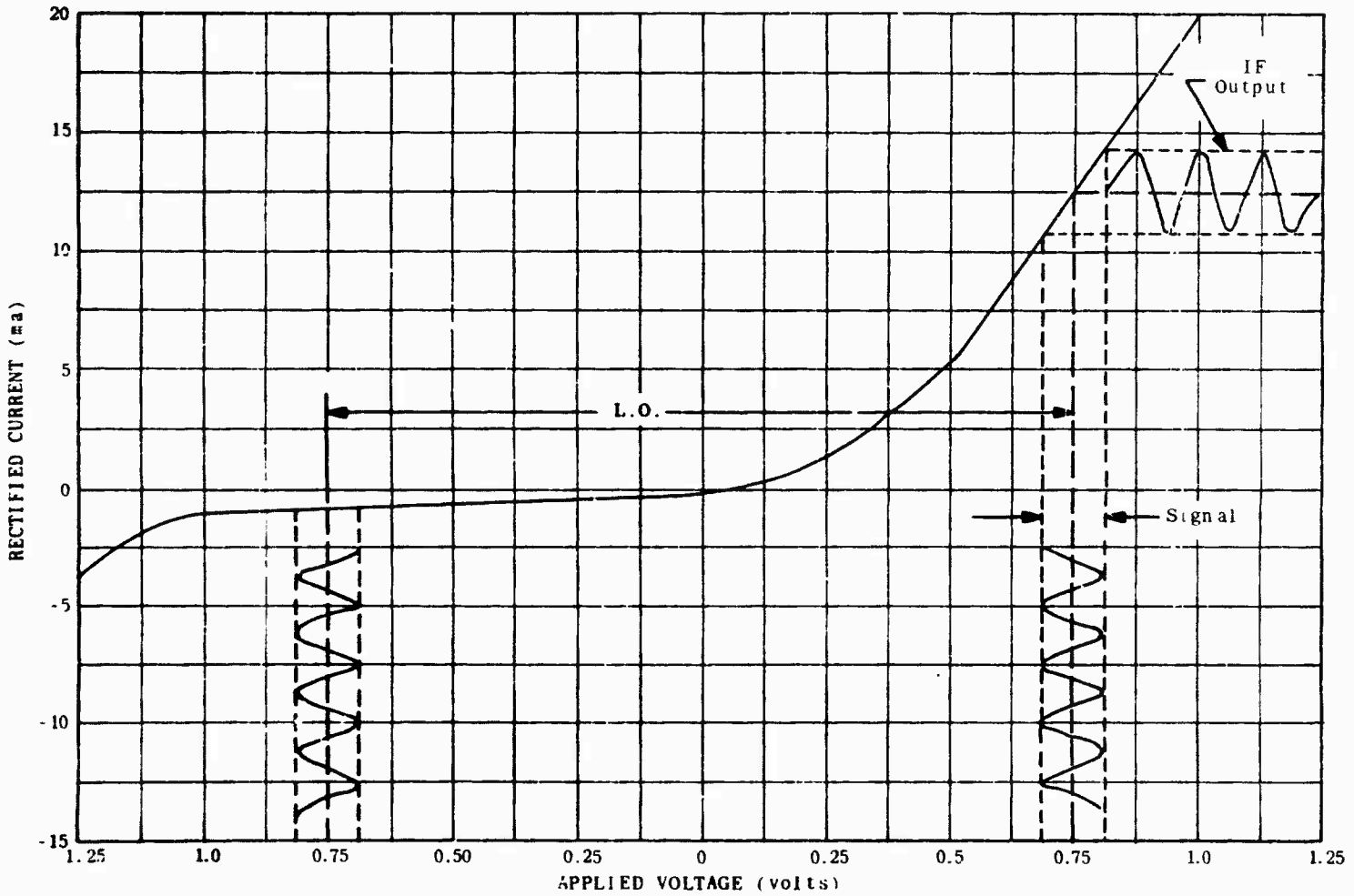

Figure 4-10. Static Characteristic of Crystal Rectifier Used as Converter.

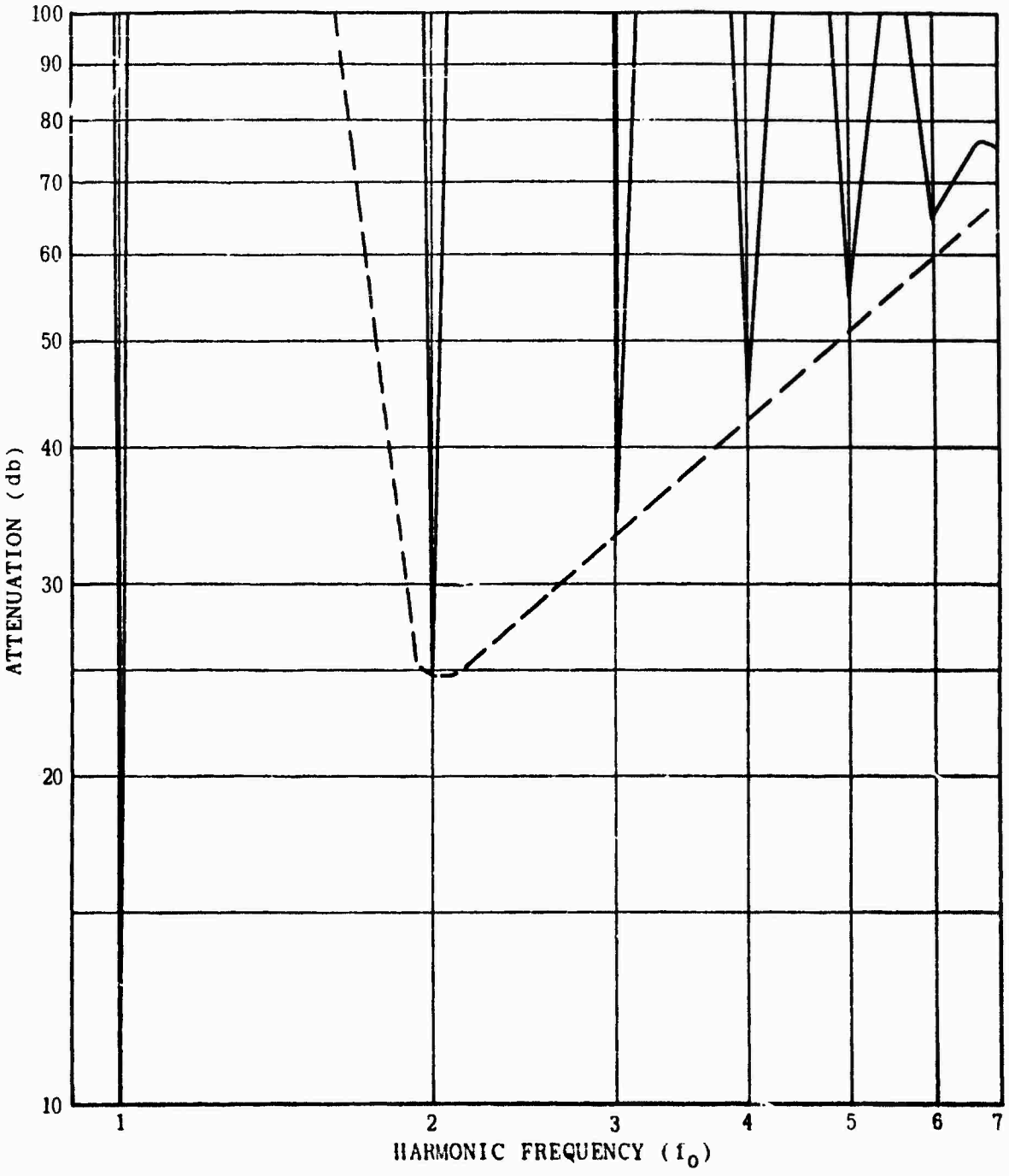

Figure 4-11. Constructed Single Crystal Rectifier Mixer Characteristic.

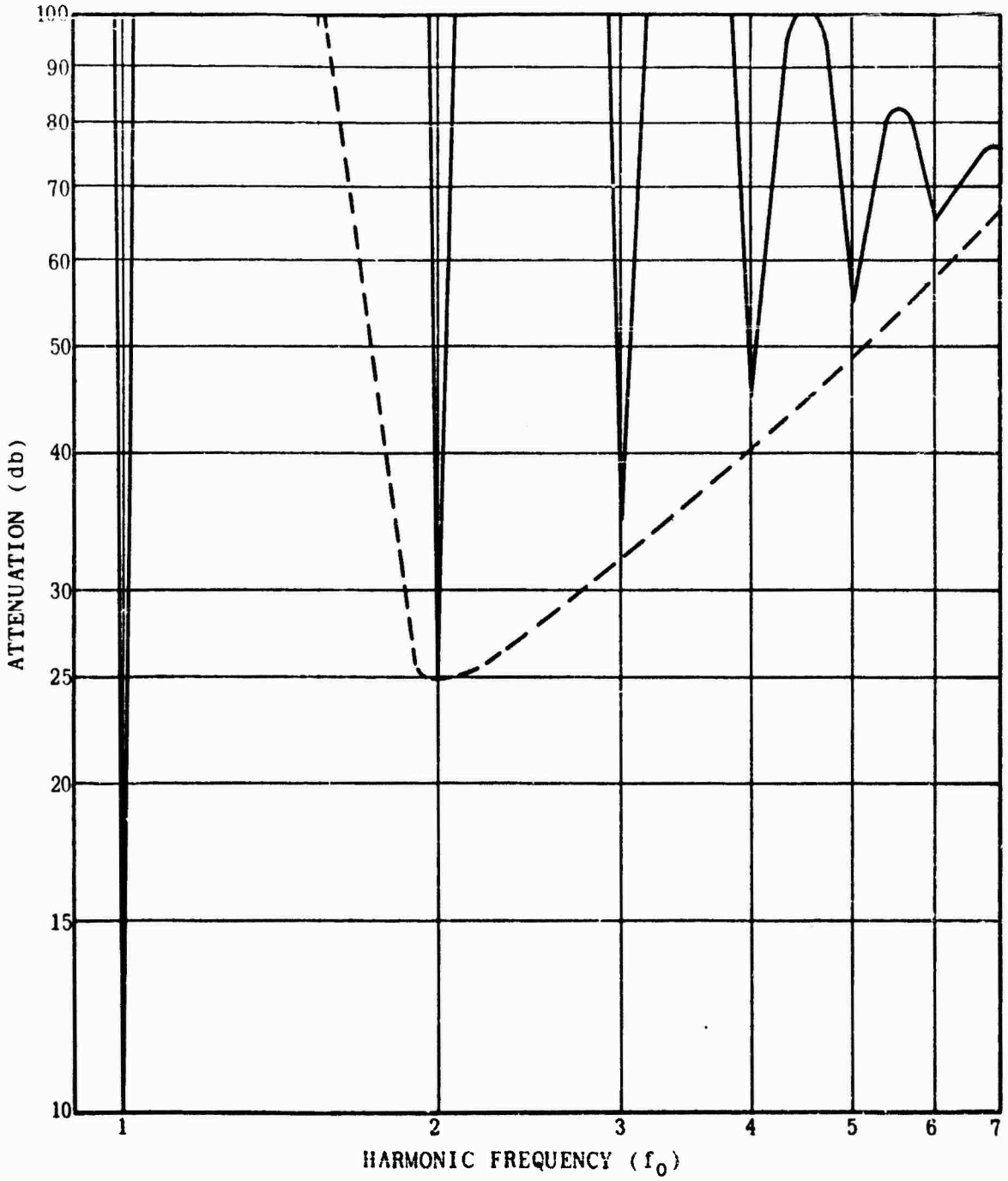

Figure 4-12. Constructed Matched Crystal Rectifier Mixer Characteristic.

and matched electron tube mixers.[19]

4.2.3.4 Local Oscillator Unit

The function of the local oscillator unit is to supply signals to the mixer unit at a frequency different from the echo signal frequency by the amount of the desired intermediate frequency. The amplitude (according to our established convention) must also exceed the amplitude of the echo signal by a factor of 10. The desired output from the local oscillator unit is a stable signal of low noise and large amplitude in comparison with the echo signal.

Local oscillator noise can be suppressed in a straightforward manner by placing a tuned RF filter between the mixer and the local oscillator. If the filter is tuned to the local oscillator frequency and has a bandwidth smaller than the I-F itself, the local oscillator noise sidebands will not be transmitted through the filter to the mixer. The resonant property of an oscillator cavity constitutes such an RF filter. Therefore, oscillator noise is reduced to a negligible amount.

Obtaining a stable signal has been the objective of much of the work in local oscillator design. It has been found that local oscillator stability has been sufficient for operational radars, although advanced radar sets are using more sohpisticated local oscillator sources.

4.2.4 Sample Radar I

The block diagram of the sample radar is shown in Figure 4-13. The block diagram is functional and includes the complete signal path from antenna connector to mixer output. Antenna characteristics are not considered in this analysis.

The heart of the receiver RF section is the signal mixer and its complementary components. The mixer contains a standard 1N28 crystal rectifier. The I-F preamplifier is coupled directly to the mixer. Local oscillator signals are generated by a standard cavity containing a 6BL6 tube (the characteristics of this unit are

19. Georgia Institute of Technology Engineering Experiment Station, Atlanta, Georgia, A Summary of Work on AF 30(602-2366), June, 1962.

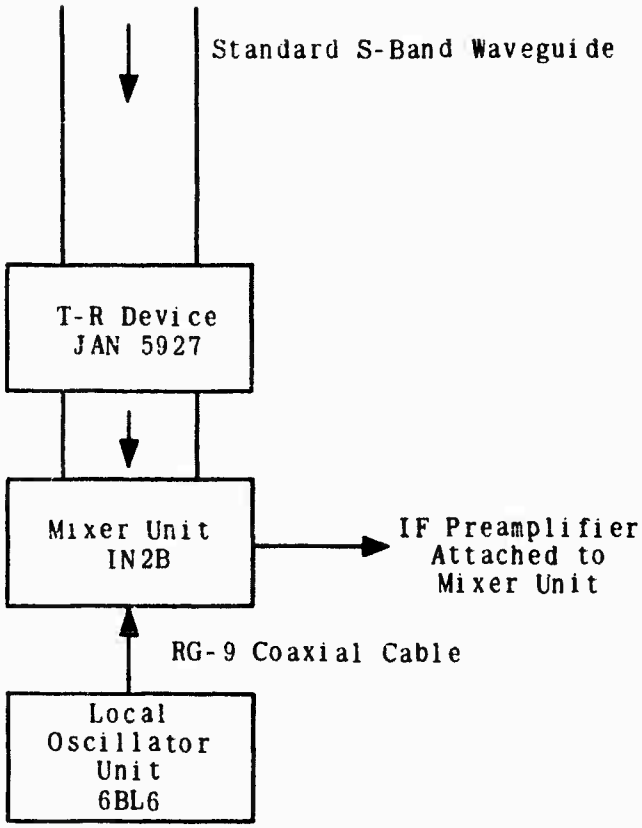

Operating Frequency: 3100-3500 Mc

Figure 4-13. Sample Radar I.

similar to those of a 5836 klystron) and are passed into the mixer unit via standard RG-9 coaxial cable. Echo signals are passed from the receiver antenna connector to a T-R device containing a JAN 5927 T-R tube via standard S-Band waveguide and thence to the mixer.

4.2.4.1 Determining Echo Signal Frequency

It can be assumed that signals of any frequency are present at the receiver antenna connector. For any practical approach, frequency limits must be established - even if the limits are arbitrary. Hence a limit of 12.0 GCS will be used as the upper range of common military transmitters.[20] The establishment of a lower range is not such a nebulous one because waveguide is itself a high-pass filter. Hence, the cutoff frequency of the waveguide will establish the lower limit.

4.2.4.1.1 Computation of Lower Frequency Limit

Standard S-band waveguide has inner dimensions of 1.340 inches by 2.840 inches. Using standard nomenclature as established in Section 4.2.1, a = 2.840 inches and b = 1.340 inches. Therefore, the cutoff wavelength λ becomes

$$\lambda_o = \frac{2}{\sqrt{\left(\frac{m}{a}\right)^2 + \left(\frac{n}{b}\right)^2}} = \frac{2}{\sqrt{\left(\frac{m}{2.840}\right)^2 + \left(\frac{n}{1.340}\right)^2}}$$

Again, using standard nomenclature as established in the Introduction, frequency modes will be designated as $TE_{m,n}$ or $TM_{m,n}$. Since the lowest order mode which will propagate in standard S-band waveguide is the $TE_{1,0}$ mode, the cutoff wavelength can now be calculated.

$$\lambda_o = \frac{2}{\sqrt{\left(\frac{1}{2.840}\right)^2 + \left(\frac{0}{1.340}\right)^2}} = 5.68 \text{ inches}$$

λ_o = 5.68 inches or 14.41 cm.

The cutoff frequency is calculated as follows.

20. MIL-STD-449A, Measurement of Military Standard Radio Frequency Spectrum Characteristics, 24 October 1961.

$$f_o = \frac{c}{\lambda_o} = \frac{3 \times 10^{10} \text{ cm/sec}}{14.41 \text{ cm}} = 2.080 \times 10^9 / \text{ sec.}$$

$$f_o = 2\ 080 \text{ GCS}$$

Therefore, a frequency below 2.080 GCS will not propagate in Standard S-Band waveguide and hence, a lower limit is established.

4.2.4.1.2 Determination of T-R Device Pass Band

The operating frequency of a JAN 5927 T-R tube is 3.100 - 3.500 GCS. It is a bandpass broadband fixed tuned tube with a peak power of 750 kw.[21]

Bandpass characteristics of three T-R tubes similar to the 5927 are shown in Figures 4-14, 4-15, 4-16. Bandpass frequencies are normally taken from the characteristic curve as the frequency range below a VSWR of 1.5. It is noted that a VSWR of 1.5 is normalized to be approximately 0.2 db. A VSWR of 1.2 is normalized to be approximately 0.035 db.[22] Thus, the bandpass of a fixed tuned bandpass T-R tube is the frequency range where insertion loss is below 0.2 db. A bandpass characteristic, therefore, is practically useless in this analysis. A selectivity characteristic over a wide frequency range must be constructed.

A bandpass characteristic for the 5927 has been constructed and is shown in Figure 4-17. Figure 4-18 is a constructed selectivity characteristic based on the following reasoning: (1) Insertion loss of a fixed tuned bandpass T-R tube is a maximum of 0.2 db over its designed passband operating frequency. For our purpose this loss appears negligible, hence a base is established which extends over the passband, (2) At frequencies outside its bandpass, the T-R tube would have an insertion loss of 10 db or higher. Thus

21. Specification Sheet, Tube Type MST-21/5927 S-Band T-R Metcom, Inc., Salem, Mass.

22. Saad, T.S., et al., The Microwave Engineer's Handbook, Horizon House, Microwave, Inc., 1961.

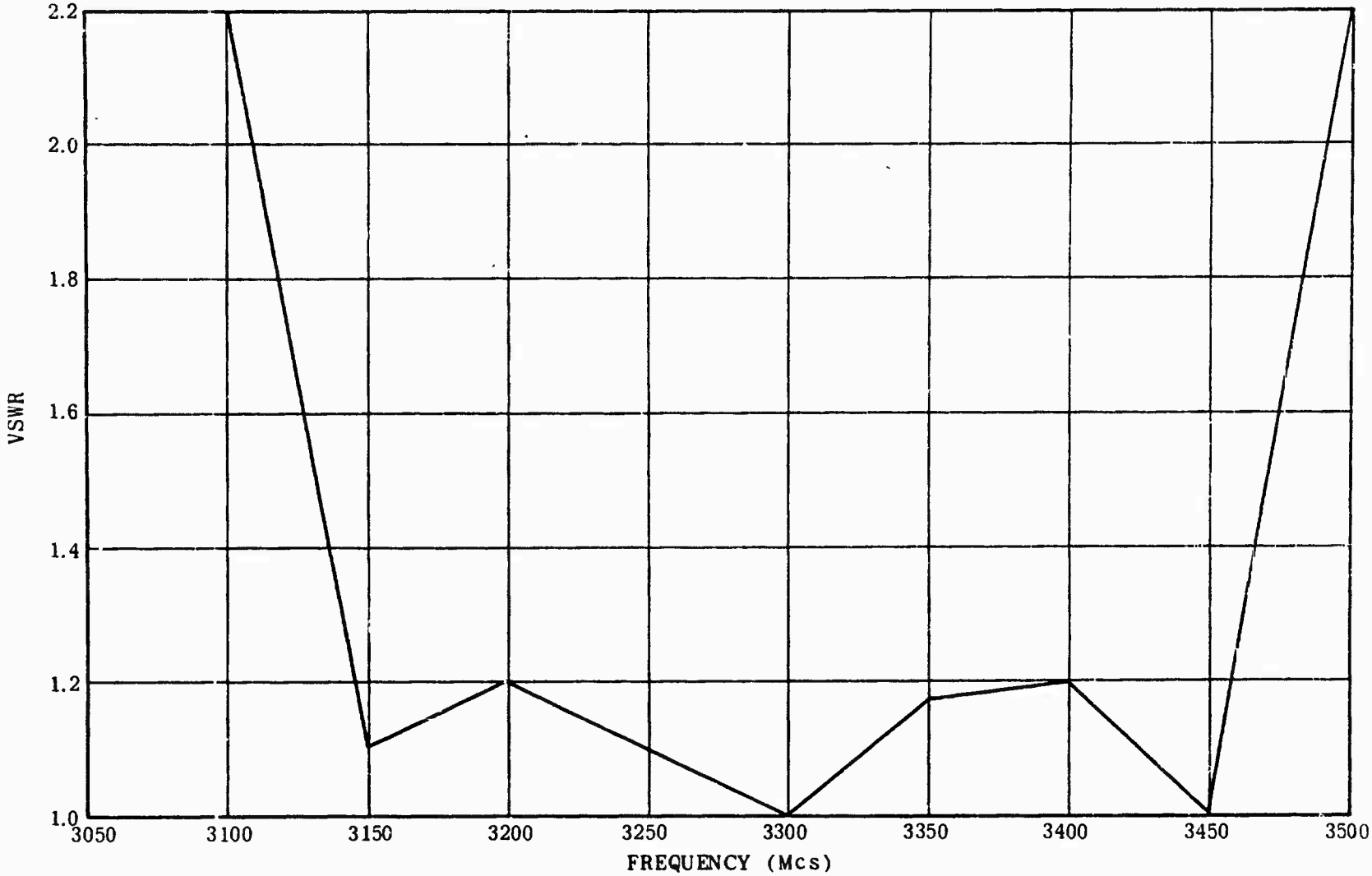

Figure 4-14. PS3S Bandpass Characteristic.

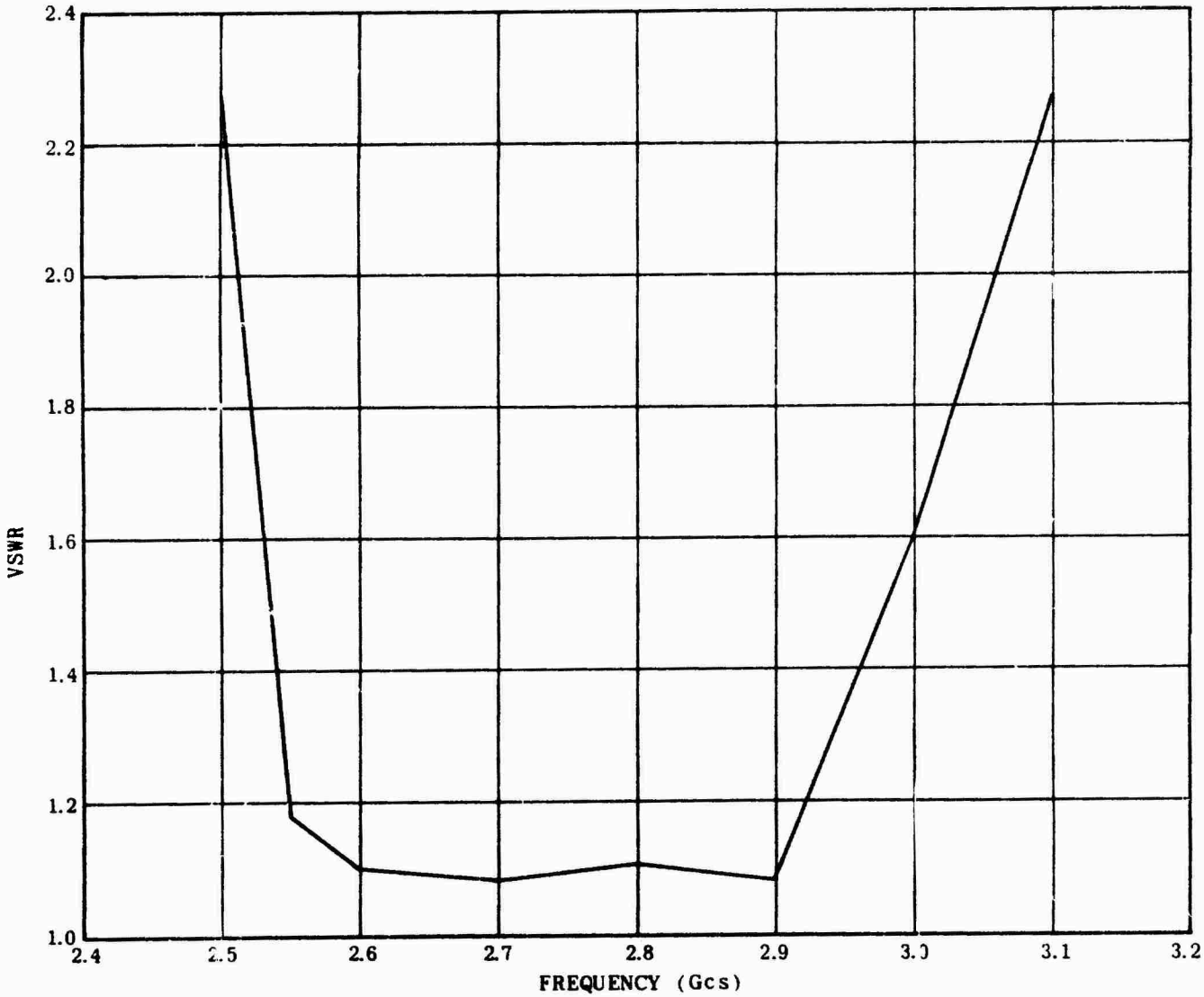

Figure 4-15. 1B58 Bandpass Characteristic.

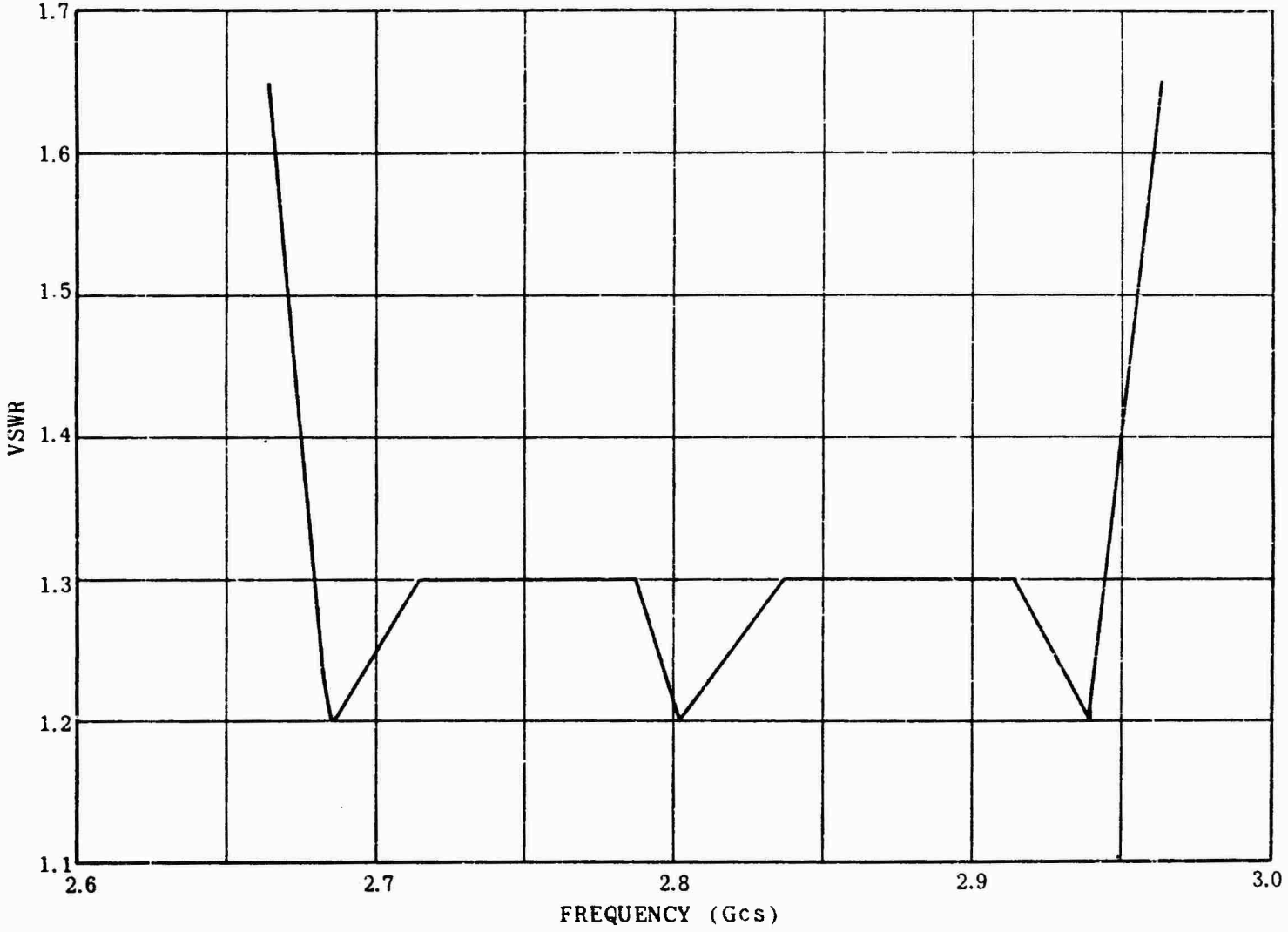

Figure 4-16. IB58A Bandpass Characteristic.

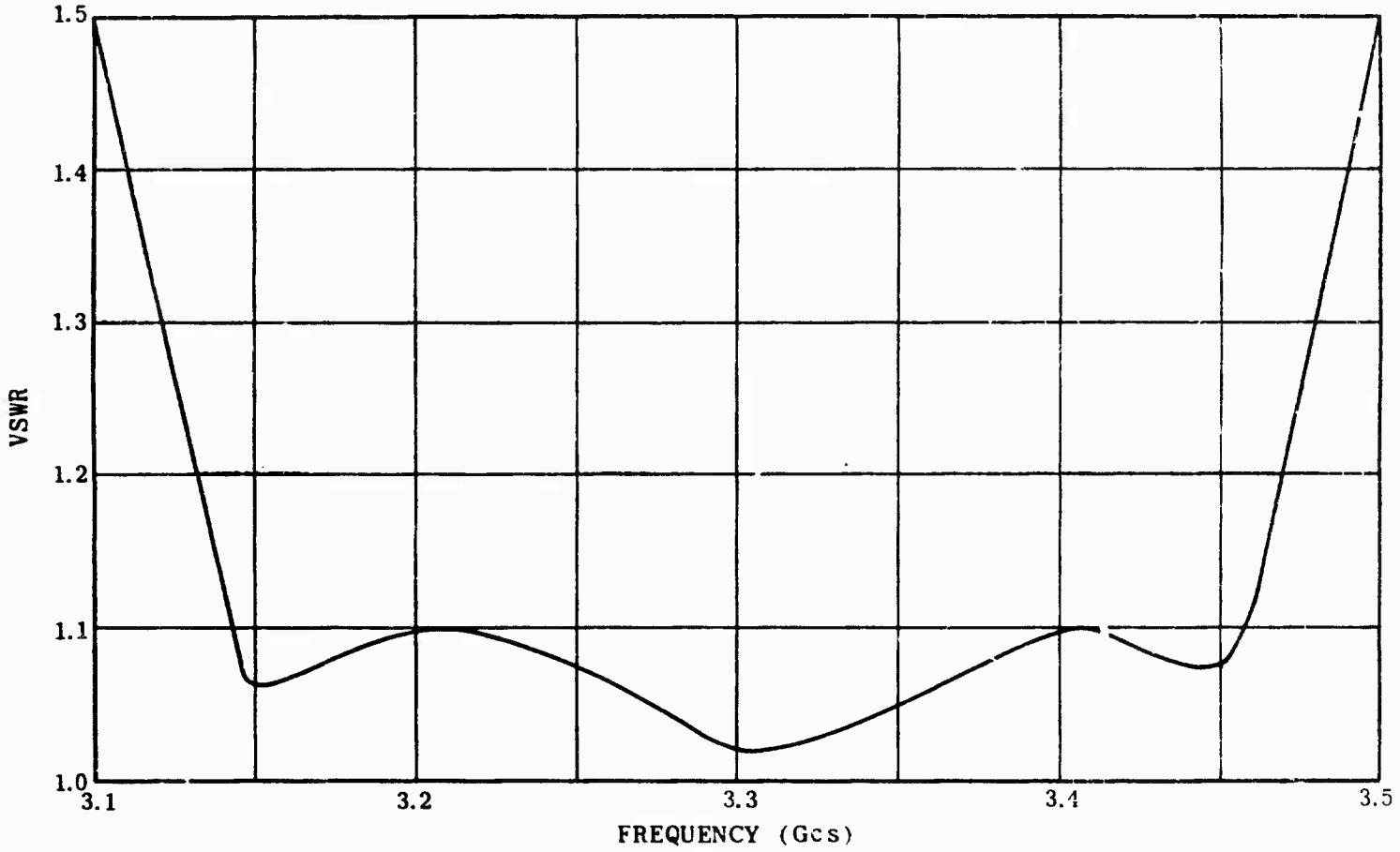

Figure 4-17. 5927 Bandpass Characteristic.

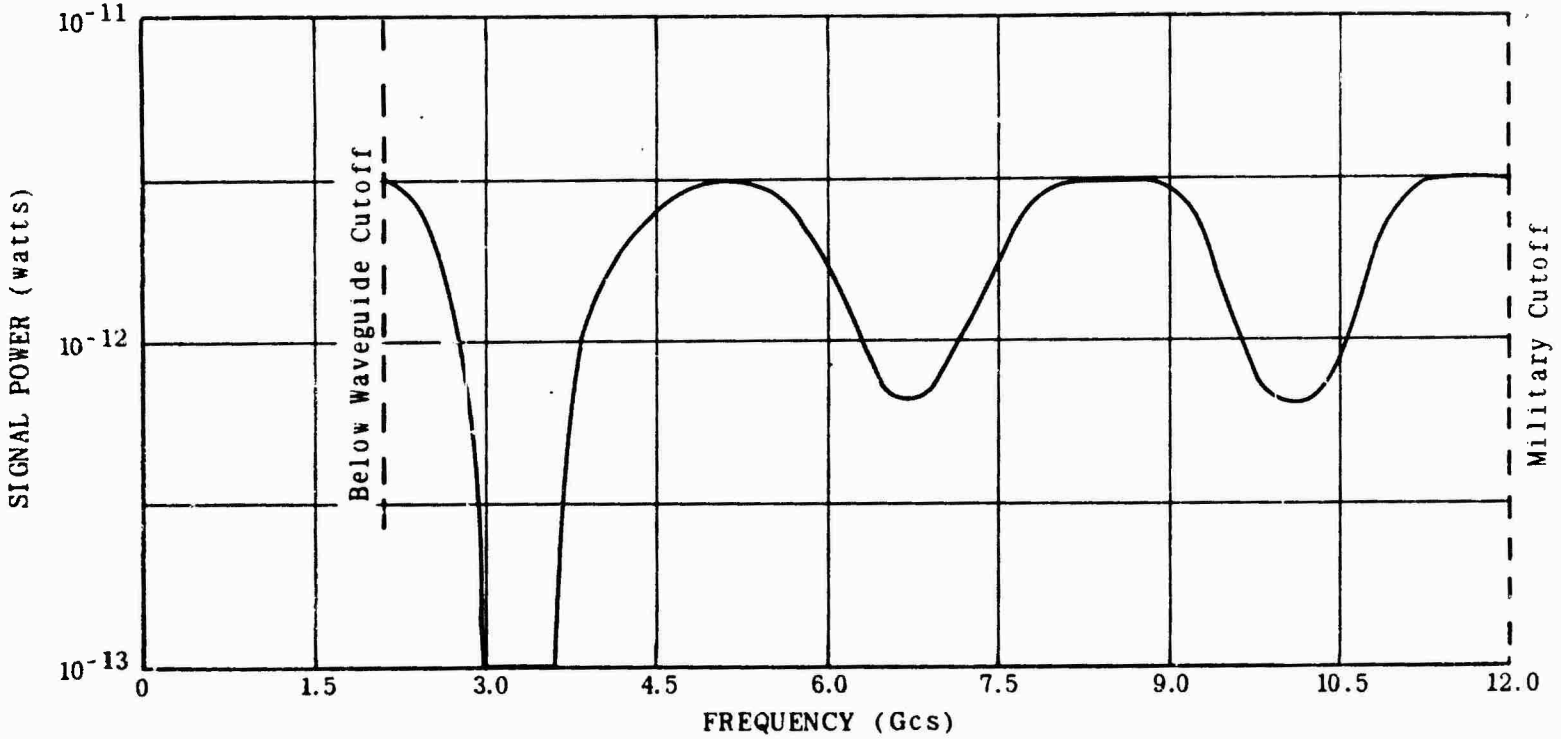

Figure 4-18. 5927 Selectivity Characteristic.

an attenuation level outside the pass band is established; (3) "Windows" would certainly be present for specific frequency ranges outside the bandpass. Insertion loss for these frequency ranges is probably 5 db or higher, thus, another level is established; (4) The "windows" would most likely occur at frequency ranges where wavelengths are multiples of bandpass wavelengths. Thus, discrete frequency ranges are identified.

From the constructed selectivity curve, it is apparent that the optimum selectivity occurs at the bandpass (operating) frequencies.

4.2.4.1.3 Establishing Optimum Range of Signal Frequencies

From the selectivity curve of Figure 4-18, it is apparent that the optimum range of signal frequencies exceeds the designed operating frequency range of the tube. In fact, the optimum range of signal frequencies approximately covers the 1000 Mcs domain which extends from 2800 Mcs to 3800 Mcs. Insertion loss rapidly increases on either side of these frequencies until a "window" is apparent. Signal frequency is thus established as in the range of 2800 Mcs to 3800 Mcs. Echo signal frequency for Sample Radar I is between 3100 and 3500 Mcs. Any signal 300 Mcs on either end of this range would be considered in the optimum frequency range of the 5927 T-R tube.

4.2.4.2 Consideration of Echo Signals at Mixer

Having established an optimum signal frequency range of 2800-3800 Mcs at the T-R tube, we now consider the effect of system components on the signal as it proceeds from the antenna connector to the mixer unit.

Waveguide affects a signal only by attenuation. Spurious signals do not originate in waveguide, hence no additional frequencies are present due to the waveguide itself. Signal frequency at the T-R device input remains 2800 Mcs to 3800 Mcs.

The T-R tube consists of a resonant gas-filled cavity. Spurious emissions are generated in such a device and should be considered as a problem in their own right. In this analysis however, we are forced to consider spurious generation on a relative basis,

and the fact is that in comparison with other spurious signal generators, the T-R device is negligible. The considered result, then is a signal frequency of 2800 Mcs to 3800 Mcs at the T-R device output.

Signal frequency at the mixer unit input is thus established, by assumptions that are arbirary, as being 2800 Mcs to 3800 Mcs. In short, any discrete signal frequency in this optimum range is important.

4.2.4.3 Local Oscillator Considerations

The local oscillator is connected to the signal mixer by a short run of RG-9 standard coaxial cable. This feature is important because coaxial cable characteristics are such that at high frequencies, the cable effectively attenuates signals (coaxial cables are low-pass devices). The RG-9 coaxial cable characteristic has been constructed in Figure 4-19. As the characteristic illustrates, RG-9 coaxial cable offers such a high resistance to frequencies above 22,000 Mcs that it becomes a block to those frequencies. Thus, the RG-9 coaxial cable is a low-pass device with frequency cutoff of approximately 22 GCS.

4.2.4.3.1 Local Oscillator Requirements

As explained in Section 4.2.1, the signal level from the local oscillator unit must be on the order of 10^1 greater than the echo signal level if the mixer output level is to be proportional to the echo signal input level. Unless this rule is followed, the mixer output signal level would have no fundamental linear relation to the echo signal level. Hence, the optimum usefulness of the mixer would not be experienced.

The local oscillator is a standard cavity containing a 6BL6. The frequency range of this unit is 1600-5500 Mcs at a power output of 75 mw.[23] Since we normally speak of an echo signal power range of 10^{-3}-10^{-13} watts, the power level of the local oscillator signal must have a maximum output on the order of 10^{-2} watts. The 6BL6 output of 7.5×10^{-2} watts, thus meets this basic criterion. As a general rule, echo signal strength will be

23. Saad, T.S., op. cit., p. 164

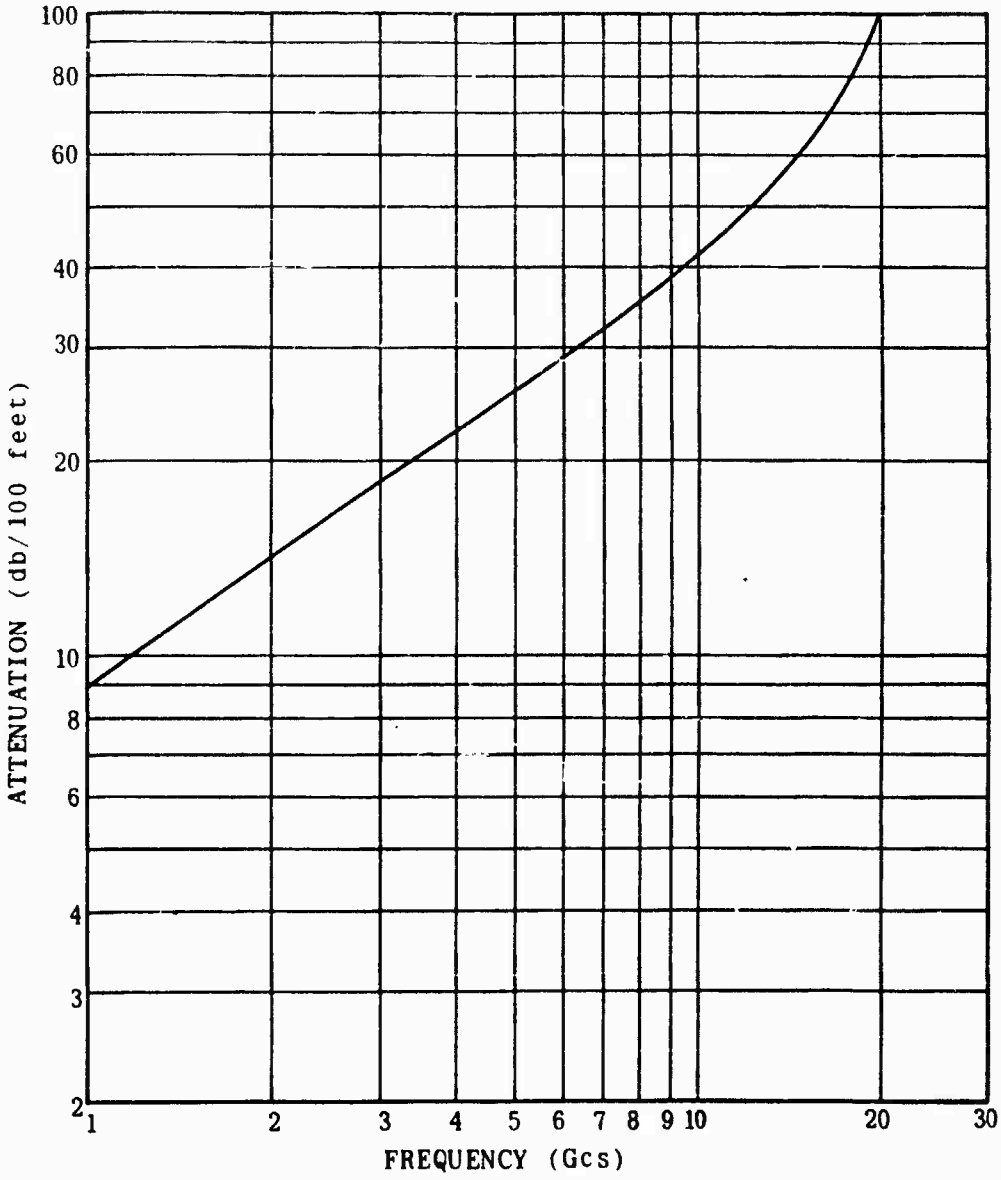

Figure 4-19. RG-9 Characteristic.

on the order of 10^{-6} watts or less.

The frequency of the local oscillator signal must differ from the echo signal frequency by the I-F frequency of the receiver. Since the operating range of this sample radar is 3100-3500 Mcs, the local oscillator must be capable of generating signals from 3070-3530 Mcs. However, the oscillator is tunable over the range of 1600-5500 Mcs, a region which encompasses the operating frequency range.

Thus, the 6BL6 local oscillator meets the basic signal power and frequency range requirements.

4.2.4.3.2 Consideration of Local Oscillator Harmonics

In all respects, the local oscillator must be treated as a signal transmitter, that is harmonics of the fundamental signal will be generated along with the fundamental signal. All signals will be passed to the output of the oscillator unit. The frequency ranges of the fundamental signal and harmonics are listed below:

Fundamental:	3070-3530 Mcs
2nd Harmonic:	6140-7060 Mcs
3rd Harmonic:	9210-10,590 Mcs
4th Harmonic:	12,280-14,120 Mcs
5th Harmonic:	15,350-17,650 Mcs
6th Harmonic:	18,420-21,180 Mcs

From a frequency consideration, we can eliminate frequencies above the 6th harmonic because those frequencies will be blocked by the RG-9 coaxial cable.

Signal amplitudes are also important at this point. A bar chart of relative amplitudes of the fundamental and harmonics is shown in Figure 4-20. According to the figure, the sixth harmonic would be down 60 db in amplitude. More specifically, the 6th harmonic from a 6BL6 oscillator would be 75×10^{-9} watts in signal strength. Thus, the 6th harmonic would "mix" with an echo signal on the order of 10^{-8} watts without adversely affecting the linear mixer output. Since the frequency range of the local oscillator 6th harmonic is 18,420-21, 180 Mcs, one would normally expect the echo signal to be less than 10^{-8} watts. That is an echo

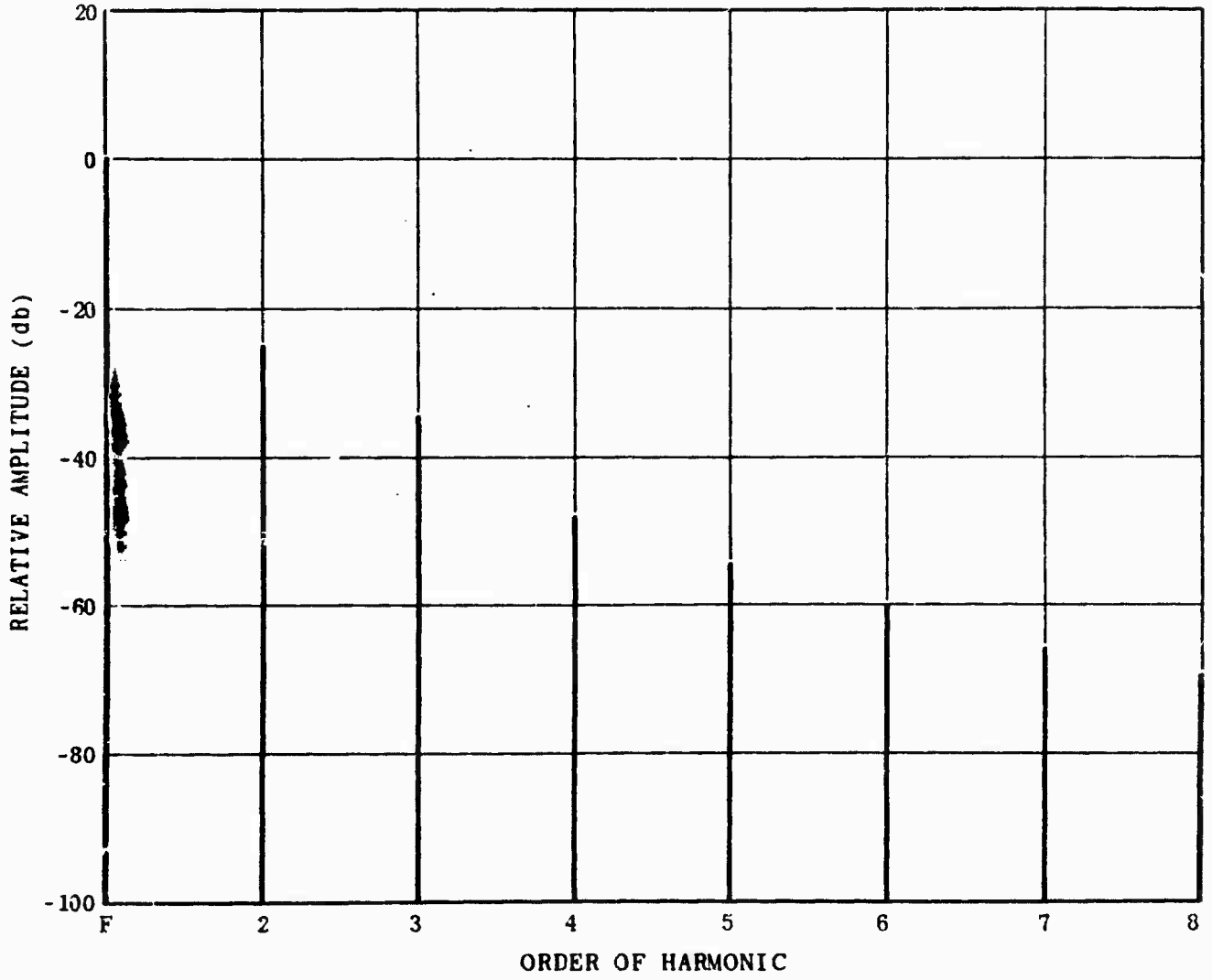

Figure 4-20. Harmonic Amplitude Relationship.

signal at such a frequency would be a harmonic of the fundamental frequency of some transmitter systems. Local oscillator harmonics can be considered relevant without degrading the presumption of "linear" mixer action.

The harmonic amplitude levels of the 6BL6 are taken to be:

Fundamental: 75×10^{-3} watts
2nd Harmonic: $75 \times 10^{-5.5}$ watts
3rd Harmonic: $75 \times 10^{-6.5}$ watts
4th Harmonic: $75 \times 10^{-7.8}$ watts
5th Harmonic: $75 \times 10^{-8.5}$ watts
6th Harmonic: 75×10^{-9} watts

These signal levels, at the specific harmonic frequencies, are assumed sufficient to allow the mixer output signal to retain its linear characteristic.

4.2.4.4 Mixer Unit Capabilities

Parameters and capabilities of mixers are generally discussed in Section 4.2.1. Specific capabilities and limitations will be considered in this section.

4.2.4.4.1 Computation of Minimum Detectable Signal

In determining the minimum detectable signal of any crystal rectifier certain assumptions must be made. Standard assumptions are (1) room temperature (2) I-F noise level of 5 db.[24] These assumptions have become standard because they are reasonable and generally approximate the minimum detectable signal. P_{min} is determined by

$$P_{min} = kT \Delta f NF^{25}$$

24. Ginzton, Edward L., op. cit., p. 151
25. Ibid.

where

k is the Boltzmann Constant 1.38×10^{-23} watts/^{o}K

T is the Kelvin Temperature

Δf is the I-F bandwidth

NF is the Noise Figure of the crystal rectifier

For the 1N28 crystal rectifier

$$P_{min} = (1.38 \times 10^{-23} \text{ watts}/^{o}\text{K})\ (313^{o}\text{K})(1 \times 10^{6}/\text{cps})(20.9)$$

$$P_{min} = 90.5 \times 10^{-15} \text{ watts}$$

The I-F bandwidth was taken as 1 Mc. An I-F bandwidth of 2 Mcs would double P_{min} but would not change its order of magnitude. Thus, P_{min} is 9.05×10^{-14} watts or approximately $10^{-13.1}$ watts. Any signal with amplitude less than $10^{-13.1}$ watts would not be detected by the crystal rectifier in the mixer unit.

4.2.4.4.2 Transfer Characteristics

There are two transfer characteristics to consider: (1) the signal amplitude transfer characteristic and (2) the signal frequency transfer characteristic.

4.2.4.4.2.1 Signal Amplitude Characteristic

A standard mixer characteristic is shown in Figure 4-10. As long as the linear characteristic of the mixer is valid, the output signal amplitude is proportional to the input signal amplitude. The proportionality factor is G, the gain of the mixer. As could be expected, G is the reciprocal of L, the conversion loss of the mixer.

Maximum conversion efficiency of the 1N28 crystal rectifier is 7 db, and its gain G is $10^{-0.7}$. The relationships mentioned are:

$$P_{I-F} = GP_{S}$$

where

P_s is the echo signal power

P_{I-F} is the I-F signal power

$G = \frac{1}{L}$ is the gain of the crystal rectifier, where L is the conversion loss of the crystal rectifier.

The computed efficiency characteristic of the 1N28 crystal rectifier is shown in Figure 4-21.

4.2.4.4.2.2 Signal Frequency Characteristic

Frequency conversion from a high frequency to some lower frequency is accomplished by beating the higher frequency with a local oscillator frequency in a nonlinear element. The nonlinear element generates, among other outputs, a frequency equal to the difference between the high frequency and local oscillator frequency. If the high frequency is an amplitude-modulated wave, the mixer output will consist of a carrier at the intermediate frequency plus sidebands which produced the original modulation of the high frequency. If the high frequency isan I-F echo signal, the mixer output is a signal at the intermediate frequency.

In addition to the difference frequency, any nonlinear element will generate harmonics of both the high frequency and local oscillator inputs. These harmonics will then "mix" to produce intermediate frequency outputs. However, the amplitude of such signals may be so small that they are not detectable.

In this context, the 1N28 crystal rectifier is simply a nonlinear element.

4.2.4.5 Mixer Unit Selectivity

Attempting a broad range selectivity prediction is somewhat of a nebulous undertaking. For obvious reasons, manufacturers establish the optimum ranges of their products through testing and then advertise their products as operating in the optimum range. Therefore, no broad range selectivity information is available on units in operational receivers.

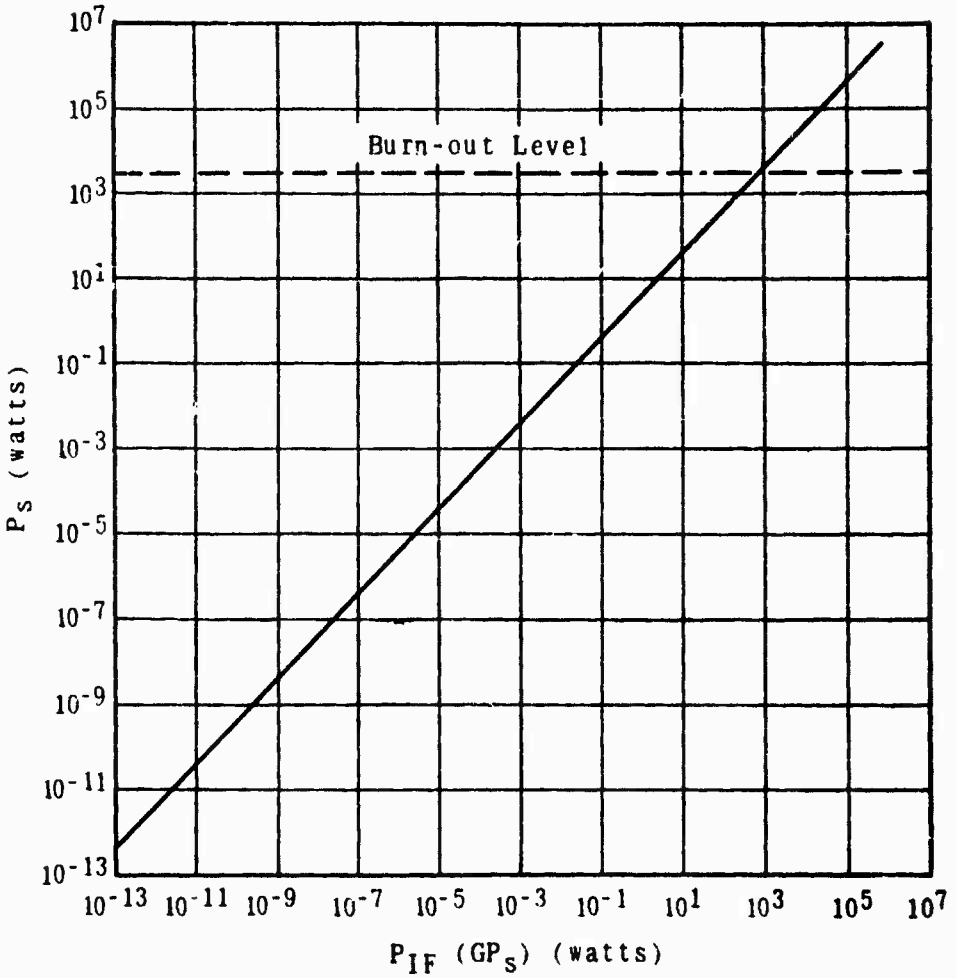

Figure 4-21. IN28 Signal Amplitude Characteristic.

Following our discussion in Section 4.2.1 and using a crystal filter characteristic as a base, a selectivity curve for a crystal rectifier has been constructed in Figure 4-22. The band-pass area of the characteristic is pronounced and the optimum operating frequency band signal level for frequencies between 2850 and 3600 Mcs lies below 10^{-6} watts. This optimum band is more restricted than any other component selectivity characteristic. Hence, the mixer unit (containing the I-F strip) is the most highly selective unit in the R-F portion of the receiver.

That portion of the curve outside the optimum operating passband was constructed as an estimate. The square curves represent predicted estimates of the maximum and minimum susceptibility levels. The rounded curve represents the most probable susceptibility. No susceptibility prediction was made in the narrow regions of nonlinearity or reverse linearity. A valid prediction in this area would require experimental investigation outside the scope of this analysis. "Windows" in the characteristic were constructed at harmonic response bands. The windows are present because local oscillator harmonics might be present which would "mix" with signals at these frequencies to produce a valid I-F frequency output.

4.2.4.6 Susceptibility Curve-Sample Radar I

Based on the selectivity characteristic of the T-R device and the mixer unit, a susceptibility curve has been constructed for Sample Radar I. This curve, shown in Figure 4-23 was constructed without consideration of the nonlinear and reverse linear regions of the mixer unit. The saturation line of this radar was determined by the crystal rectifier burn-out level plus a 5 db loss in the RF section, i.e., a signal pulse entering the RF section at the level indicated would cause degradation of the crystal rectifier.

4.2.5 Sample Radar II

The block diagram of Sample Radar II is shown in Figure 4-24. The block diagram is functional and includes the complete signal path from antenna connector to the mixer output. Antenna characteristics are not considered in this analysis.

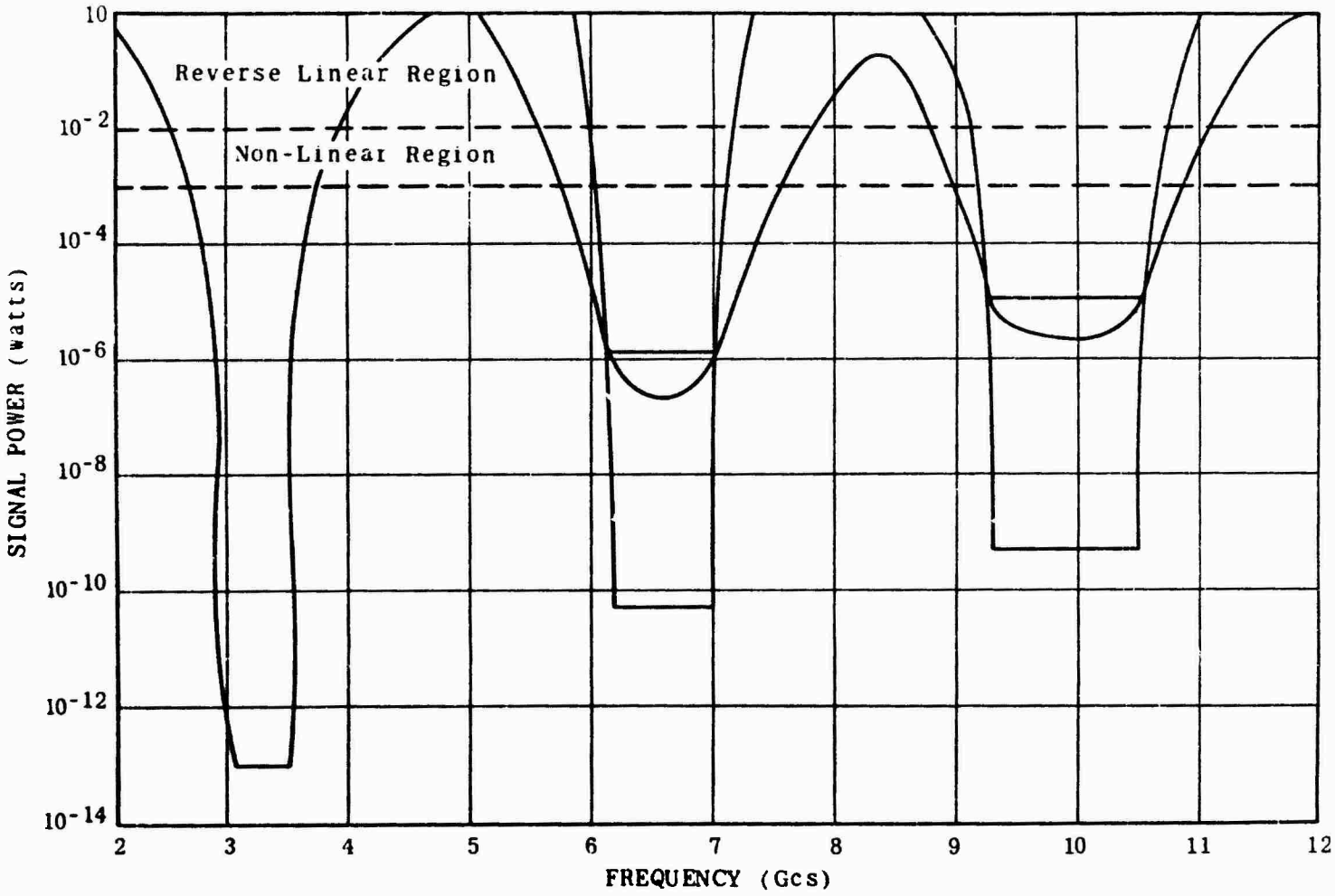

Figure 4-22. Mixer Selectivity Characteristic.

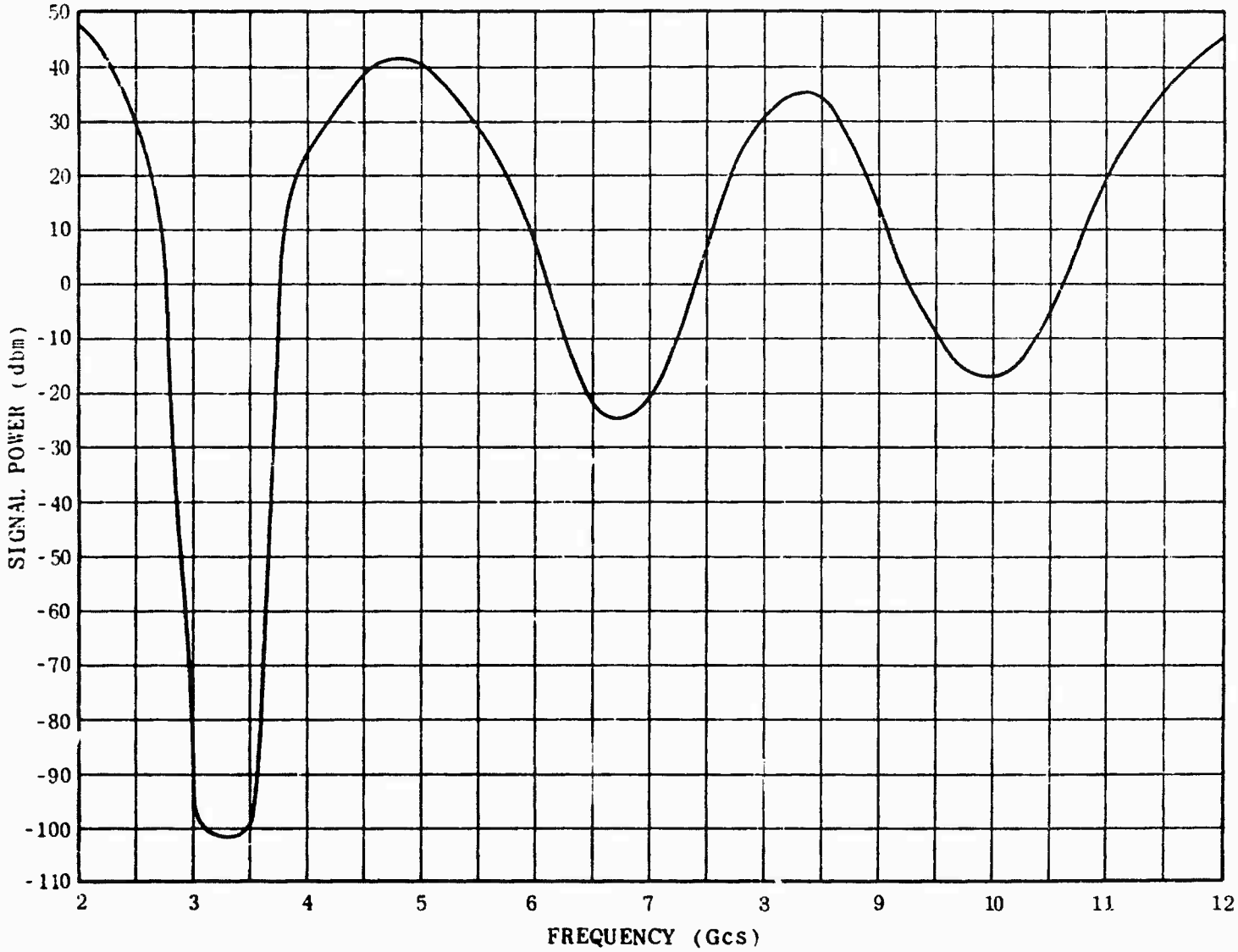

Figure 4-23. Susceptibility Curve-Sample Radar 1.

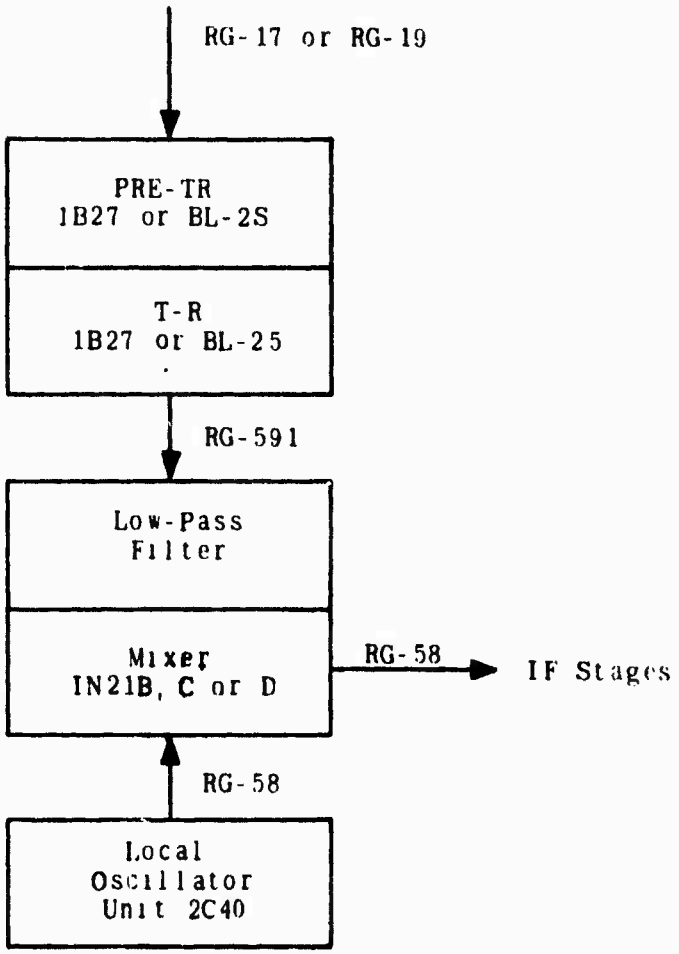

Operating Frequency: 1220-1350 Mc

Figure 4-24. Sample Radar II.

The mixer units contain either a 1N21B, 1N21C, or 1N21D crystal rectifier. Local oscillator signals are generated by a 2C40 tube in a double cavity and are passed to the mixer via RG-58 coaxial cable. The echo signal is passed from the antenna connector via RG-17 or RG-19 coaxial cable to a Pre-TR cavity containing either a 1B27 or a BL-25 tube. The signal is then passed to the T-R cavity containing either a 1B27 or a BL-25 tube and then via RG-591 coaxial cable to a low-pass filter assembly and onto the mixer.

4.2.5.1 Determining Echo Signal Frequency

We must assume the presence of signals of all frequencies at the antenna connector. A lower frequency limit cannot be established at this time as it was with other sample radars because the input of this radar is via coaxial cable rather than waveguide. Moreover, the exactness of the cable in use is in doubt because either of two cables are used. Figure 4-25 is the attenuation characteristic of RG-17 coaxial cable and Figure 4-26 is the attenuation characteristic of RG-19 coaxial cable. From these constructed characteristics, it can be seen that both cables offer high attenuation to frequencies above 10 GCS. The upper limit of these cables is probably on the order of 15 to 18 GCS. At these frequencies attenuation would be great enough to effectively block signals. The cutoff limit of the cable is above the limit we have established as the upper limit for common transmitters. Thus, this latter limit will again be used.

4.2.5.1.1 Determination of Lower Frequency Limit

A lower frequency cutoff limit based on input waveguide cannot be computed for this radar receiver. A practical lower limit will be established later and will be based on the characteristics of the components past the T-R device in the signal path.

4.2.5.1.2 Determination of a T-R Pass Band

The T-R pass band will actually be a combination of two T-R pass bands since duplicate cavities serve as the Pre-TR and the T-R. In operating practice either a 1B27 or a BL-25 tube is used, depending upon the availability of the tubes. Hence, we must consider a combination of two BL-25's, two 1B27's or one of each.

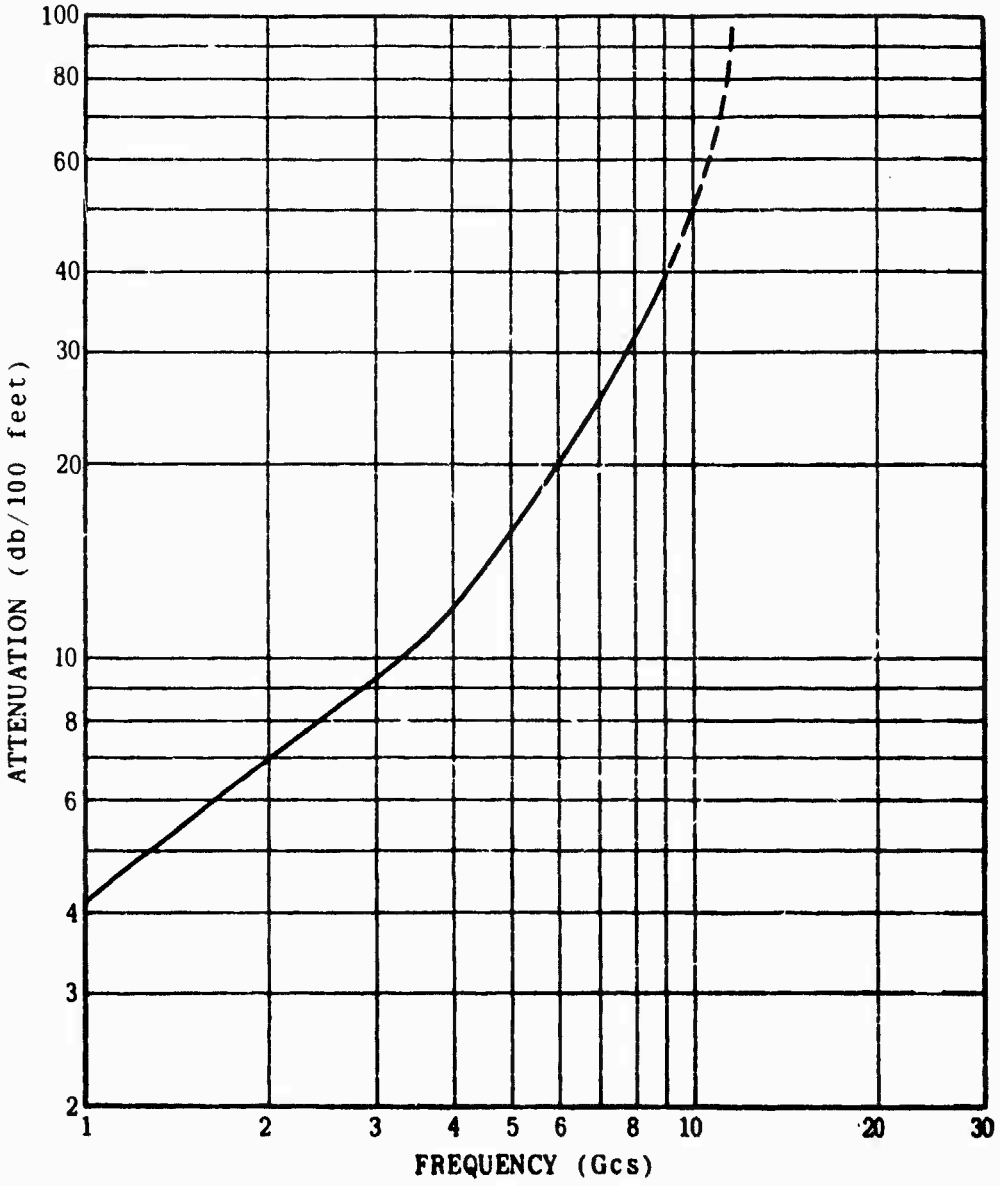

Figure 4-25. RG-17 Characteristic.

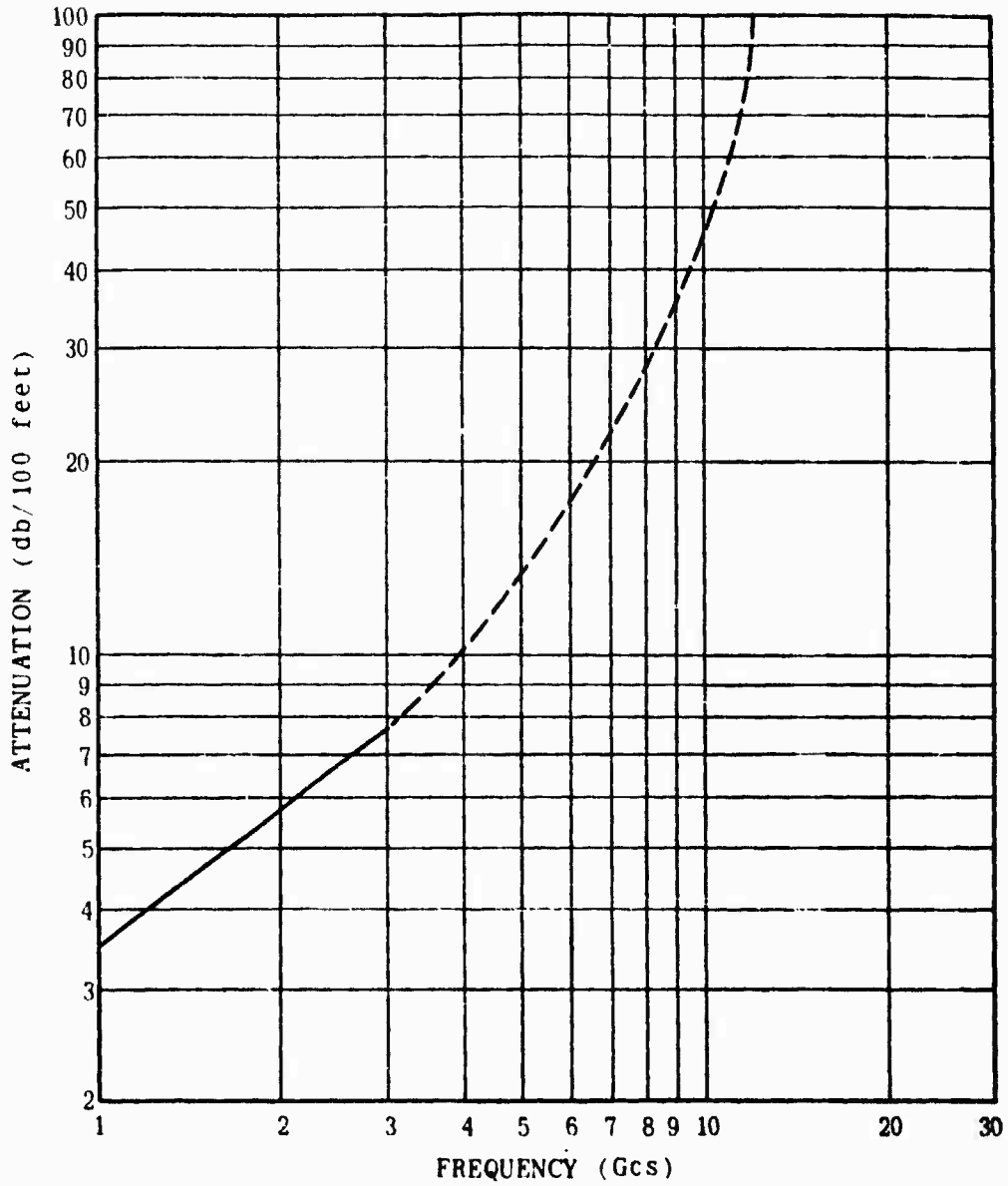

Figure 4-26. RG-18 Characteristic.

The relative response curve of a BL-25 tube mounted in a standard cavity is shown in Figure 4-27. The relative response of a T-R device is published as a function of the half-power frequencies. For our purposes, such a response curve is useless because we need to know selectivity over a wide frequency range and at considerably lower power levels.

The BL-25 is a bandpass tube tunable over the range of 1.215-1.355 Mcs.[26] This tuning range is just slightly greater than the operating frequency range of Sample Radar II. An inert T-R tube is not an effective filtering device,[27] however, it will offer greater excitation to frequencies at or near its tuned frequency and will pass such frequencies with negligible insertion loss. Losses incurred by signals at frequencies away from this tuned frequency can be predicted to be on the order of 20-30 db except at "window" frequencies.

Figure 4-28 is a constructed selectivity characteristic of the BL-25 tube mounted in a standard cavity. The curve was constructed on the following reasoning. (1) insertion loss of this tube over its tuning range is negligible (2) at frequencies outside this tuning range, the tube, acting as a filter, will probably cause insertion losses on the order of 20-30 db (3) the tube, acting as a filter, would have passband "windows" at multiple wavelengths of the tunable frequency. Also, insertion losses at these windows would probably be on the order of 10 db.

The published response curve of the 1B27 tube is in the same category as the response curve for the BL-25. The curve is drawn over such a limited range that it is useless for our purposes. The 1B27 tube is a bandpass device tunable from just under 2600 Mcs to just over 3000 Mcs.[28] The tuning range of this tube is outside the operating frequency of the radar. This fact, however, illustrates the caliber of the tube as a filter. If the tube acted as an

26. Specification Sheet, Type 6322 (BL-25) Tunable TR Tube, Separate Cavity Type, Bomac Laboratories, Inc., Beverly, Mass.

27. Smullen & Montgomery, op. cit., p. 150.

28. Specification Sheet, Type 1B27 Tunable TR Tube, Separate Cavity Type, Bomac Laboratories, Inc., Beverly, Mass.

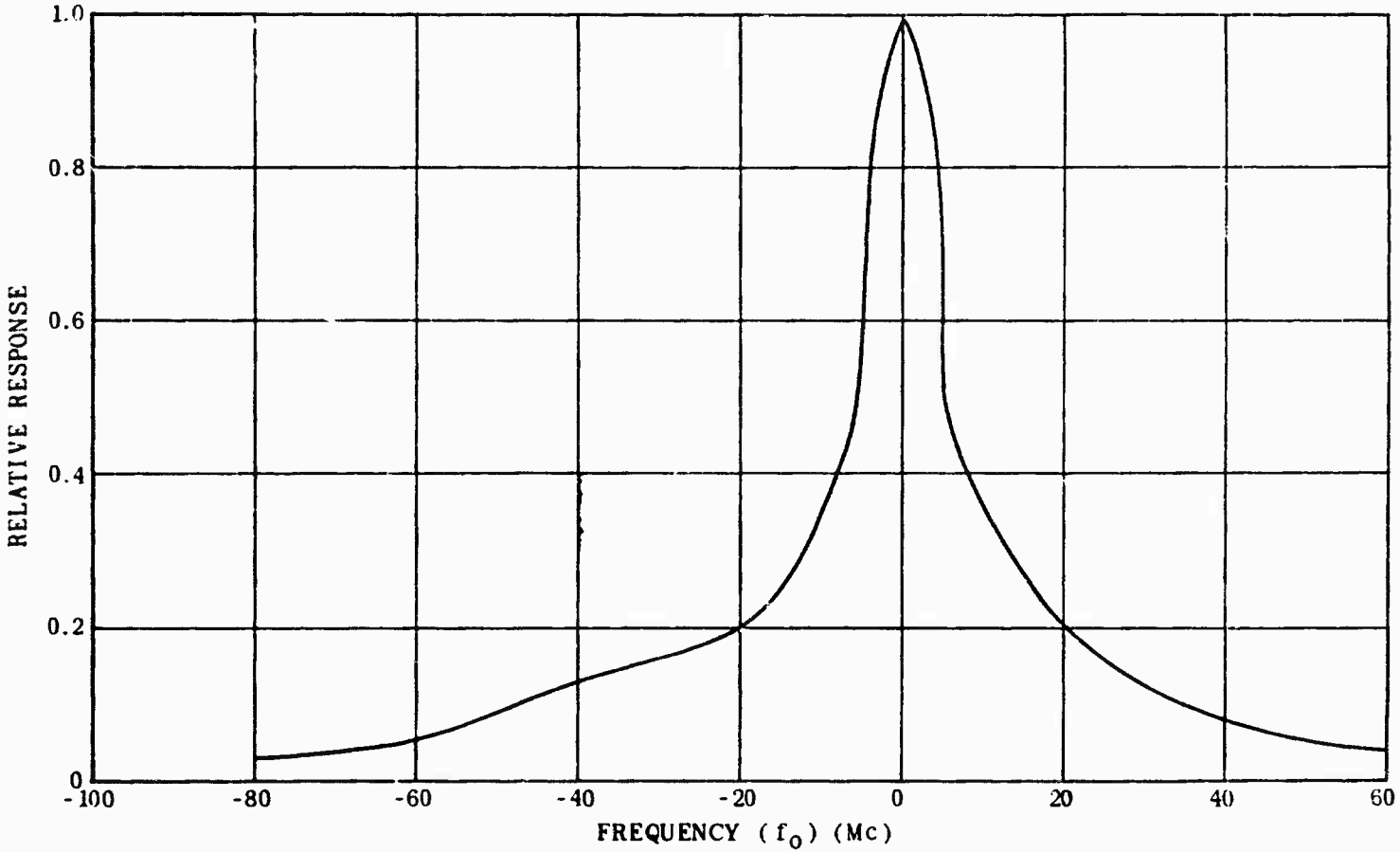

Figure 4-27. BL-25 Relative Response Curve.

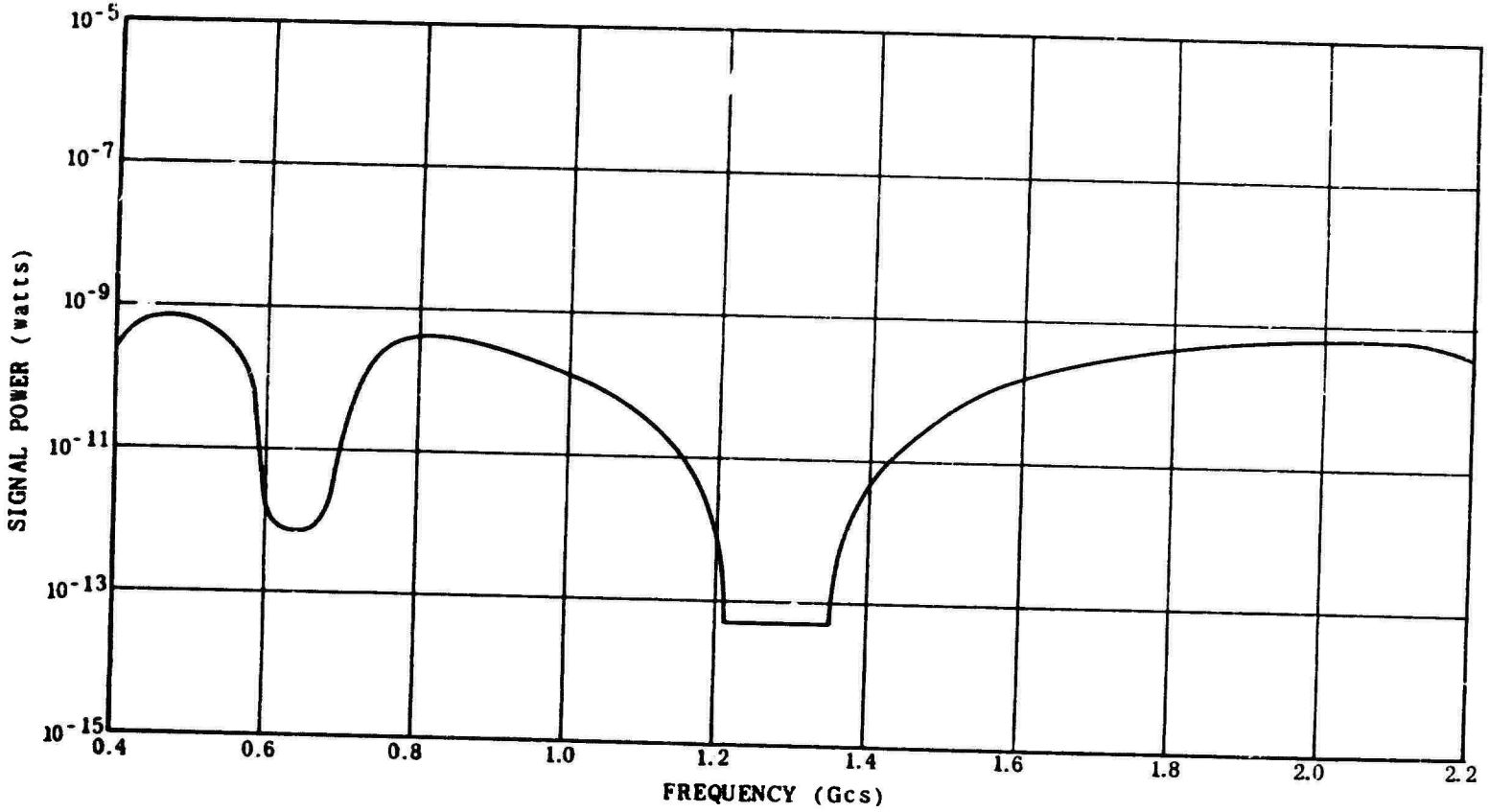

Figure 4-28. BL-25 Selectivity Curve.

effective filter it could not be used in this radar. Of course, the primary purpose of the T-R tube is to protect the crystal rectifier from transmitted signals. Hence, this tube would protect the crystal rectifier to a degree even though it was inert.

A selectivity characteristic of a tunable bandpass filter has been constructed in Figure 4-29. This filter is designed for use in S-band and is used in association with S-band waveguide. The selectivity of the 1B27 tube would probably be less effective - especially outside the tuning range. A selectivity characteristic of the 1B27 has been constructed and is presented in Figure 4-30. The following reasoning was used in constructing the curve: (1) insertion loss in the tuning range is negligible (2) at frequencies outside the tuning range the tube, acting as a filter, would probably cause attenuation on the order of 15 db to incoming signals (3) the tube would have "windows" at multiple wavelengths of the tuned frequency (4) insertion loss at these "window" frequencies increases in both directions from the tunable frequency and would be a minimum of approximately 5 db.

Using these constructed curves for each of the possible T-R tubes, we can determine the pass band of the T-R device. A T-R device containing double cavity mounted BL-25's would have a characteristic as shown in Figure 4-31, one with double cavity 1B27's, as in Figure 4-32 and one with a double cavity containing one BL-25 and one 1B27, as in Figure 4-33. Thus for a double BL-25 device, we would set an optimum pass band within the operating frequency of the radar at 1150-1330 Mcs, for a double 1B27, at 800-1700 Mcs and for a combination, at 1100-1400 Mcs. It is emphasized that in the three pass bands, signal strength would be different in each case. This fact serves to illustrate the different characteristics of the device.

4.2.5.1.3 Examination of RG-591 Coaxial Cable

There is no standard RG-591 coaxial cable or rigid coaxial waveguide. Information in the sample radar parts list, however, lists this component as being rigid waveguide with inner dimensions of 3/4" x 5-5/16" x 3-1/6". Standard RG-58 coaxial cable

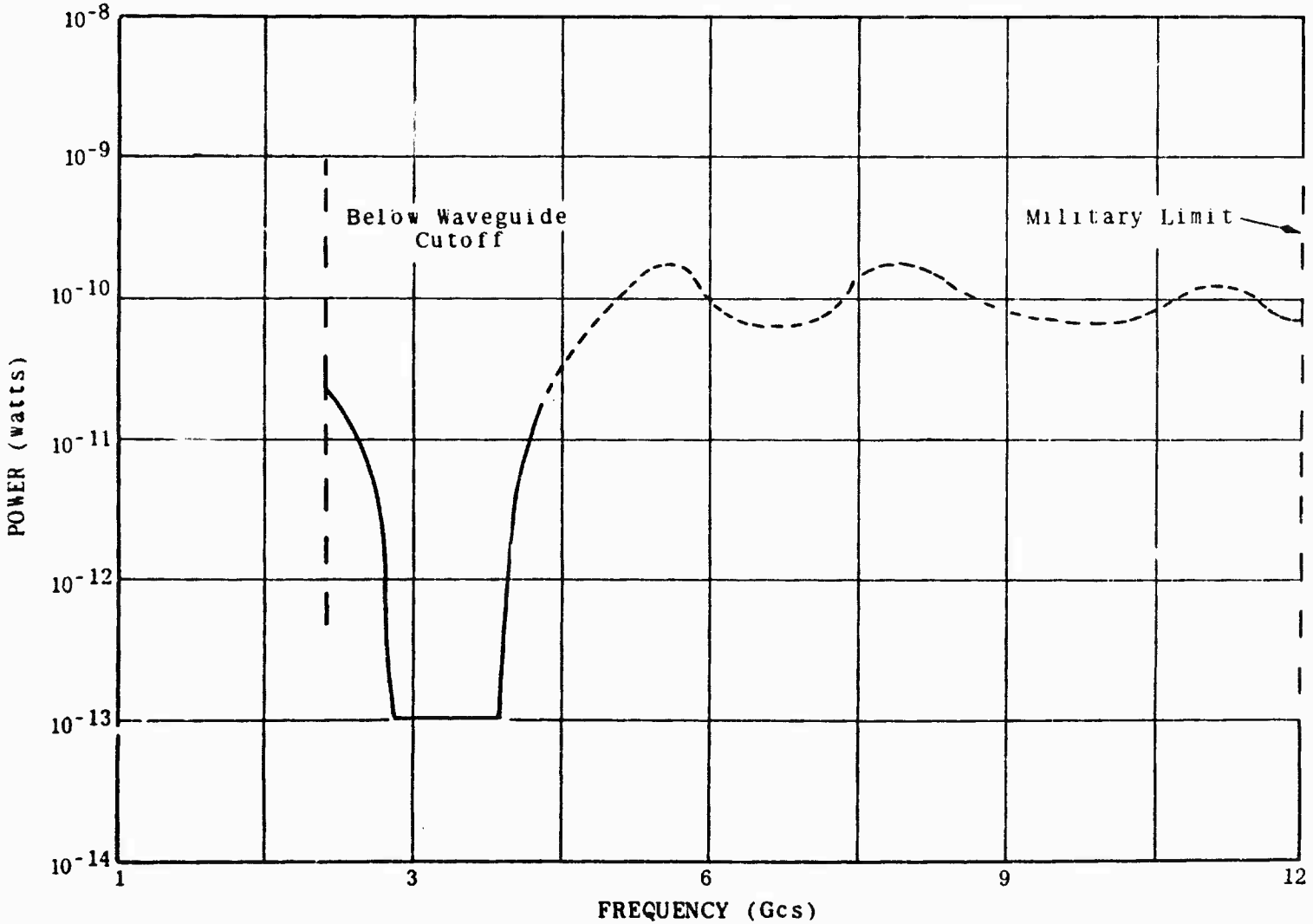

Figure 4-29. Filter Selectivity Characteristic.

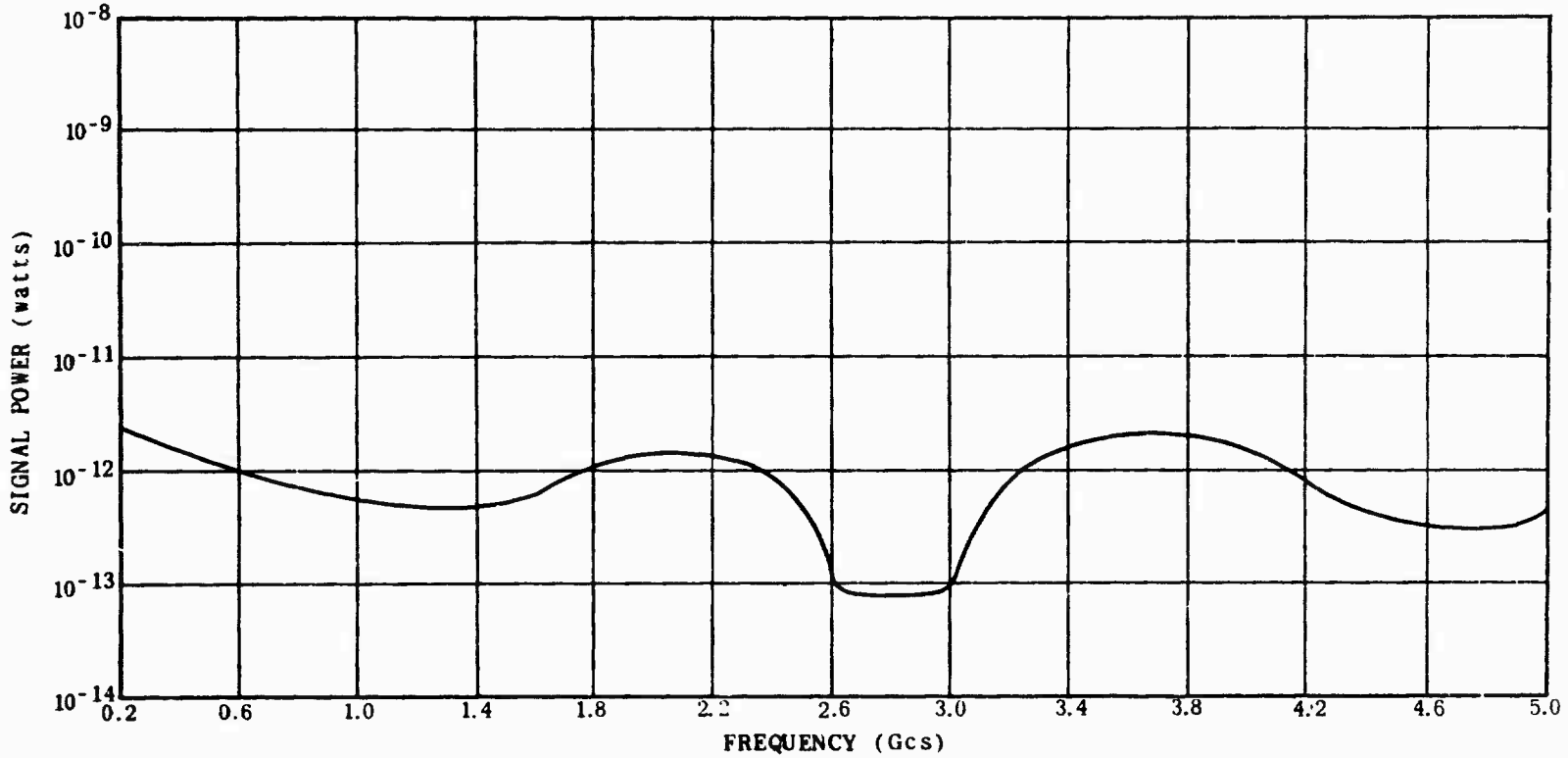

Figure 4-30. 1B27 Selectivity Characteristic.

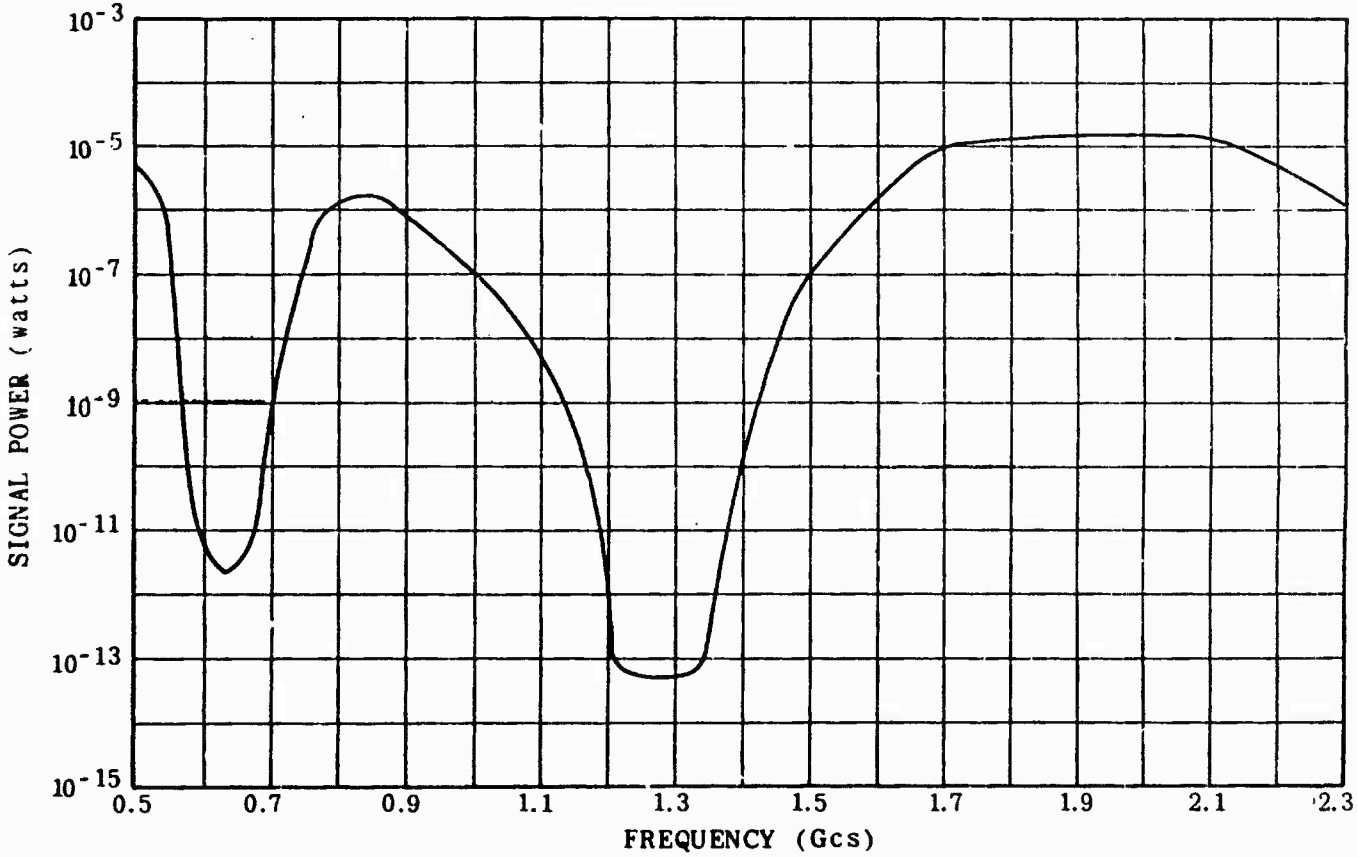

Figure 4-31. Double BL-25 T-R Device.

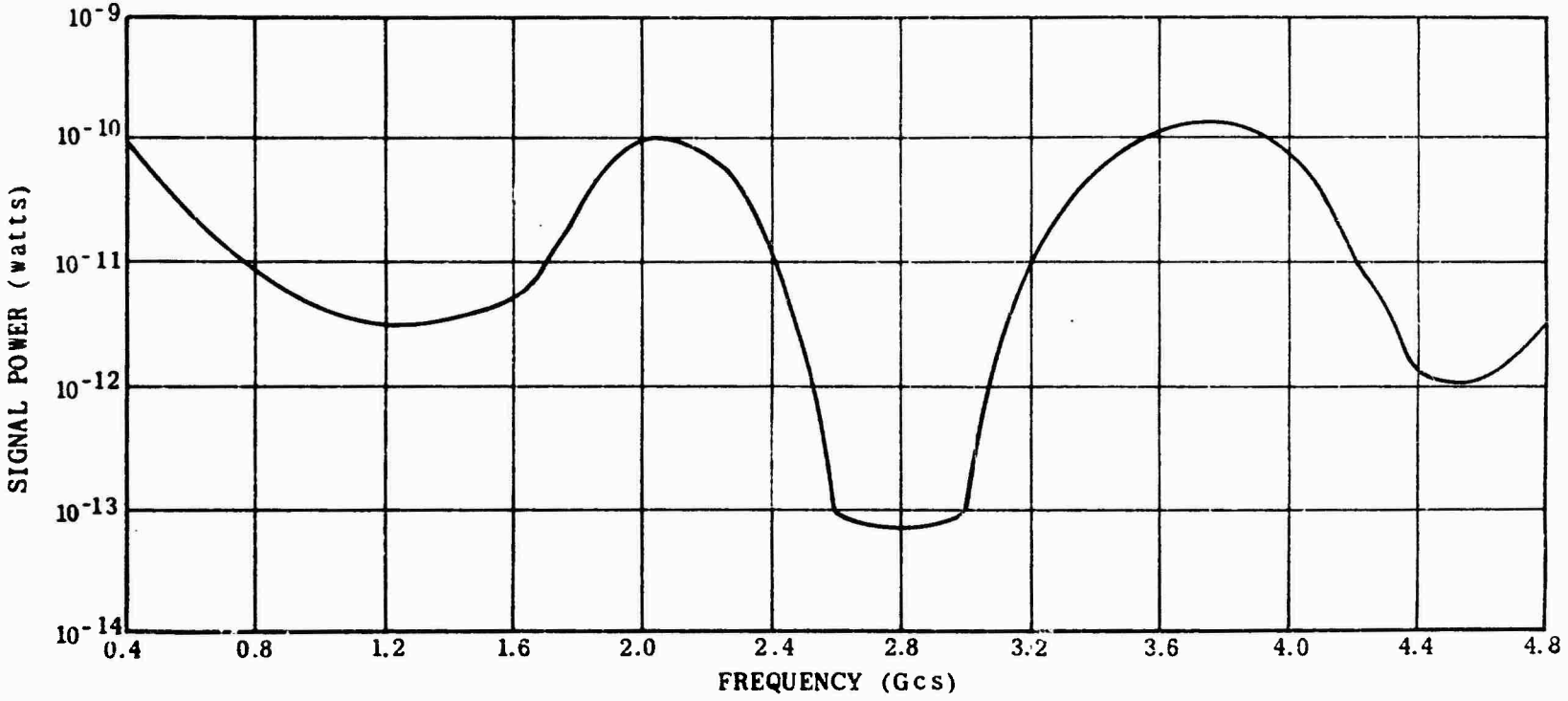

Figure 4-32. Double 1B27 T-R Device.

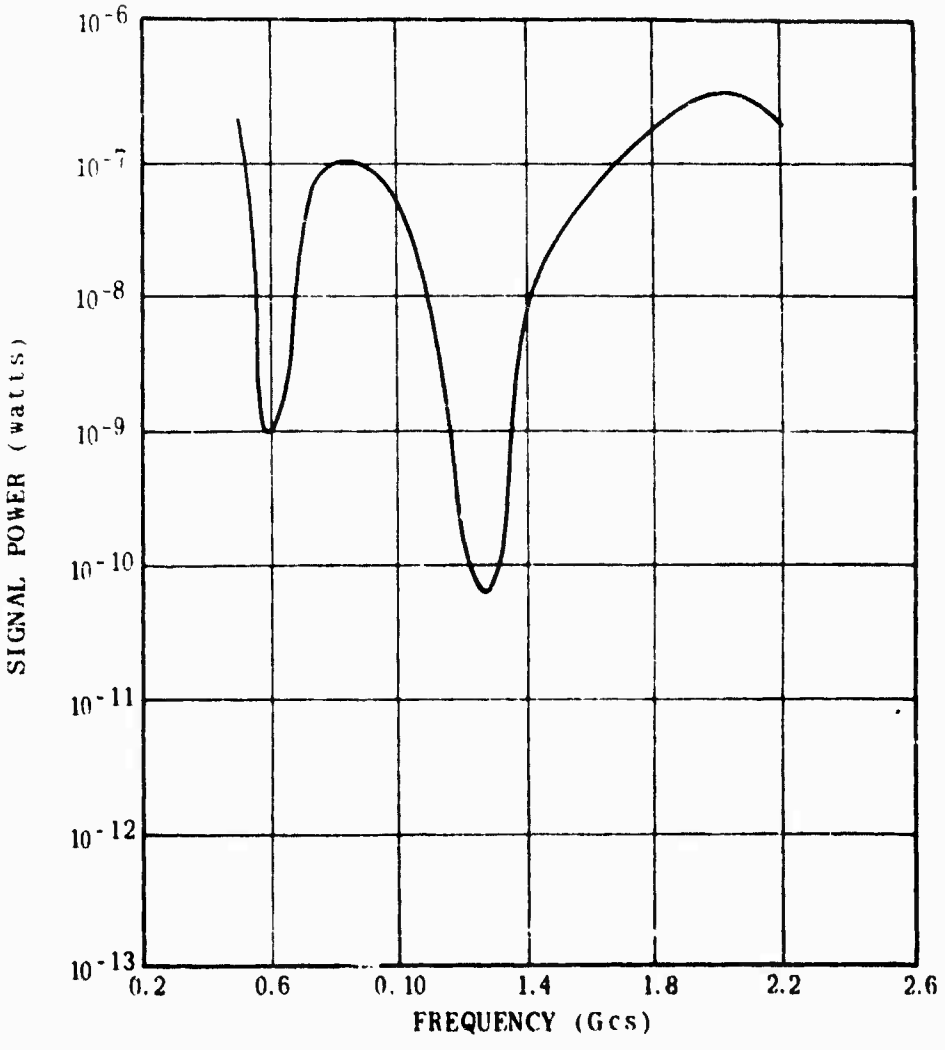

Figure 4-33. Combination BL-25/1B27 T-R Device.

is listed as connecting this rigid waveguide to the harmonic attenuator (low-pass filter) device. It could be that the entire unit from the T-R output to the harmonic attenuator was designated RG-591. For our purposes, however, we must look at the separate sections.

The rigid waveguide is effectively a short section of rectangular waveguide with dimensions a = 5-5/16" and b = 3-1/6". A lower cutoff frequency can be established for this component because waves below the cutoff frequency would not propagate in this section of waveguide. The calculation is

$$\lambda_o = \frac{2}{\sqrt{\left(\frac{a}{m}\right)^2 + \left(\frac{b}{n}\right)^2}} = 10.65 \text{ inches or } 27.1 \text{ cm}$$

$$f_o = \frac{C}{\lambda_o} = \frac{3 \times 10^{10} \text{cm/sec}}{27.1} = 1108 \text{ Mcs}$$

Thus we can conclude that any frequency below 1108 Mcs will not propagate past this section of rigid waveguide. Therefore, a lower frequency limit for the receiver has not been established.

4.2.5.1.4 Examination of Harmonic Attenuator

The harmonic attenuator[29] consists of a section of S-band waveguide mounted perpendicular to the signal path. The purpose in using such a component is to protect the crystal rectifier from transmitter harmonics that are not blocked by the T-R device.

A piece of unshielded cable runs through the S-band waveguide, the theory being that the operating frequency will not propagate in the waveguide and hence negligible insertion loss will occur at the operating frequency. At higher frequencies (above 2.080 GCS, see Section 4.2.4.1.1) signals will propagate in the waveguide, causing signal attenuation. The designers claim a minimum of 20 db loss at second and third harmonic frequencies with higher losses at higher frequencies. It is noted that this attenuation is approximately that caused by the inert T-R device for frequencies outside the bandpass (excluding "windows"). See curve in Figure 4-34.

29. Military Technical Order applicable to Specific Radar.

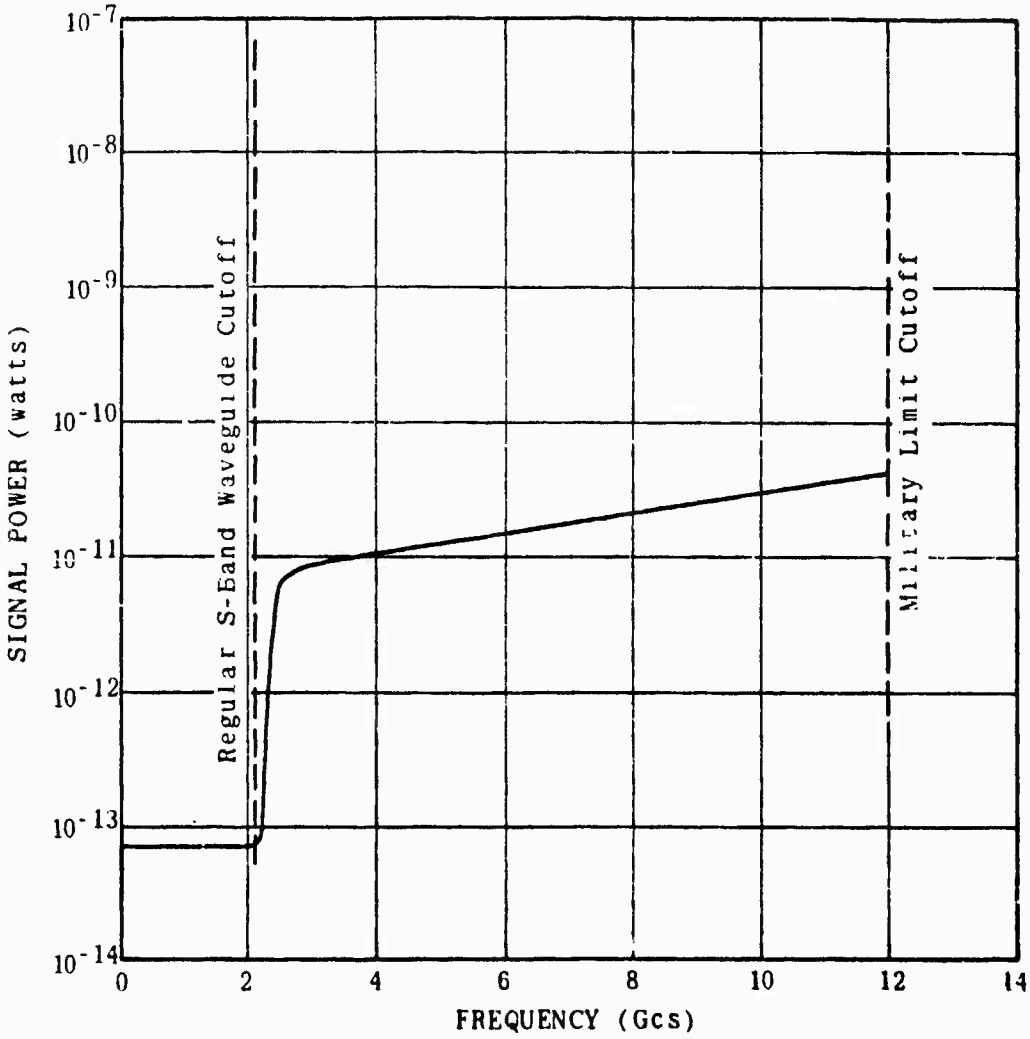

Figure 4-34. Harmonic Amplitude Characteristic.

Metal discs are placed at each end of the S-band waveguide to absorb propagated signals.

At this point, we can construct a selectivity curve from the lower frequency limit to the upper frequency limit. The curve is presented in Figure 4-35. In constructing the curve, the following assumptions were made in addition to those already made: (1) a twenty-five foot length of RG-19 coaxial cable from antenna connector to T-R device (2) a T-R device containing a BL-25 in the Pre-TR and a BL-25 in the T-R (3) RG-58 coaxial cable with negligible attenuation loss from the output of the rigid waveguide to the input of the harmonic attenuator (4) negligible insertion losses in the harmonic attenuator at the tuned frequency.

4.2.5.1.5 Establishing Optimum Range of Signal Frequencies

From the pre-mixer selectivity characteristic of Figure 4-35, it is apparent that the optimum signal frequency range is from the rigid waveguide cutoff at 1108 Mcs to approximately 1500 Mcs. The operating frequency range of the radar, 1220-1350 Mcs, is approximately centered in the optimum signal frequency band. Thus, we must consider any frequency from 1108 Mcs to 1500 Mcs as being in the optimum frequency range of the radar pre-mixer RF section.

4.2.5.2 Consideration of Echo Signals at Mixer

The pre-mixer selectivity curve of Figure 4-35 has been constructed from component selectivity curves. We must assume that signals can be passed to the mixer unit over the frequency range from 1.108 GCS to 12.0 GCS.

4.2.5.3 Local Oscillator Consideration

The local oscillator is connected to the mixer unit by RG-58 coaxial cable. The attenuation versus frequency curve for RG-58 is shown in Figure 4-36. At frequencies above 10 GCS, RG-58 offers such a high attenuation that it effectively blocks those frequencies. We can consider RG-58 as a low-pass device with a 10 GCS cutoff.

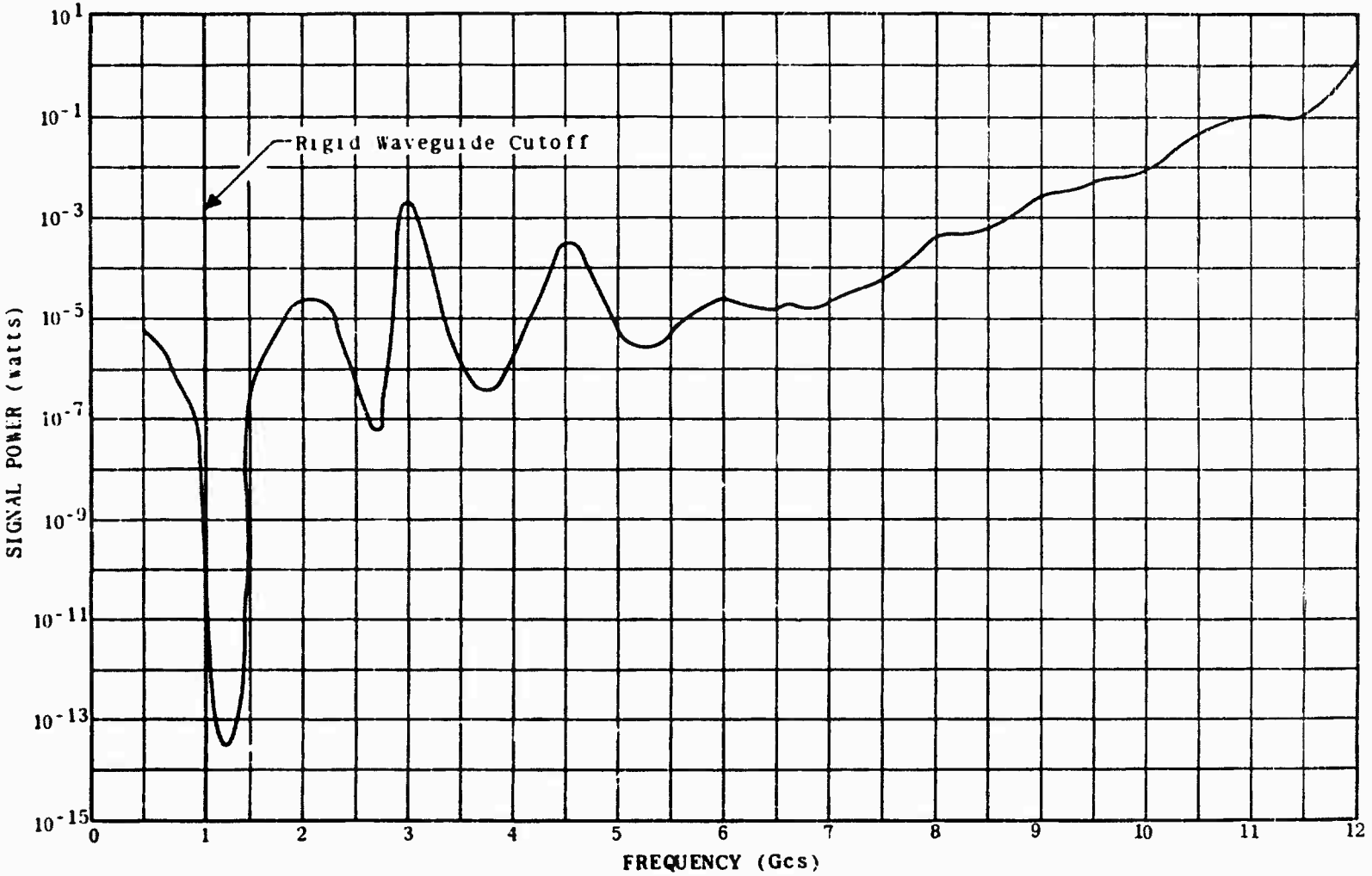

Figure 4-35. Sample Radar II-Pre-Mixer Selectivity Characteristic.

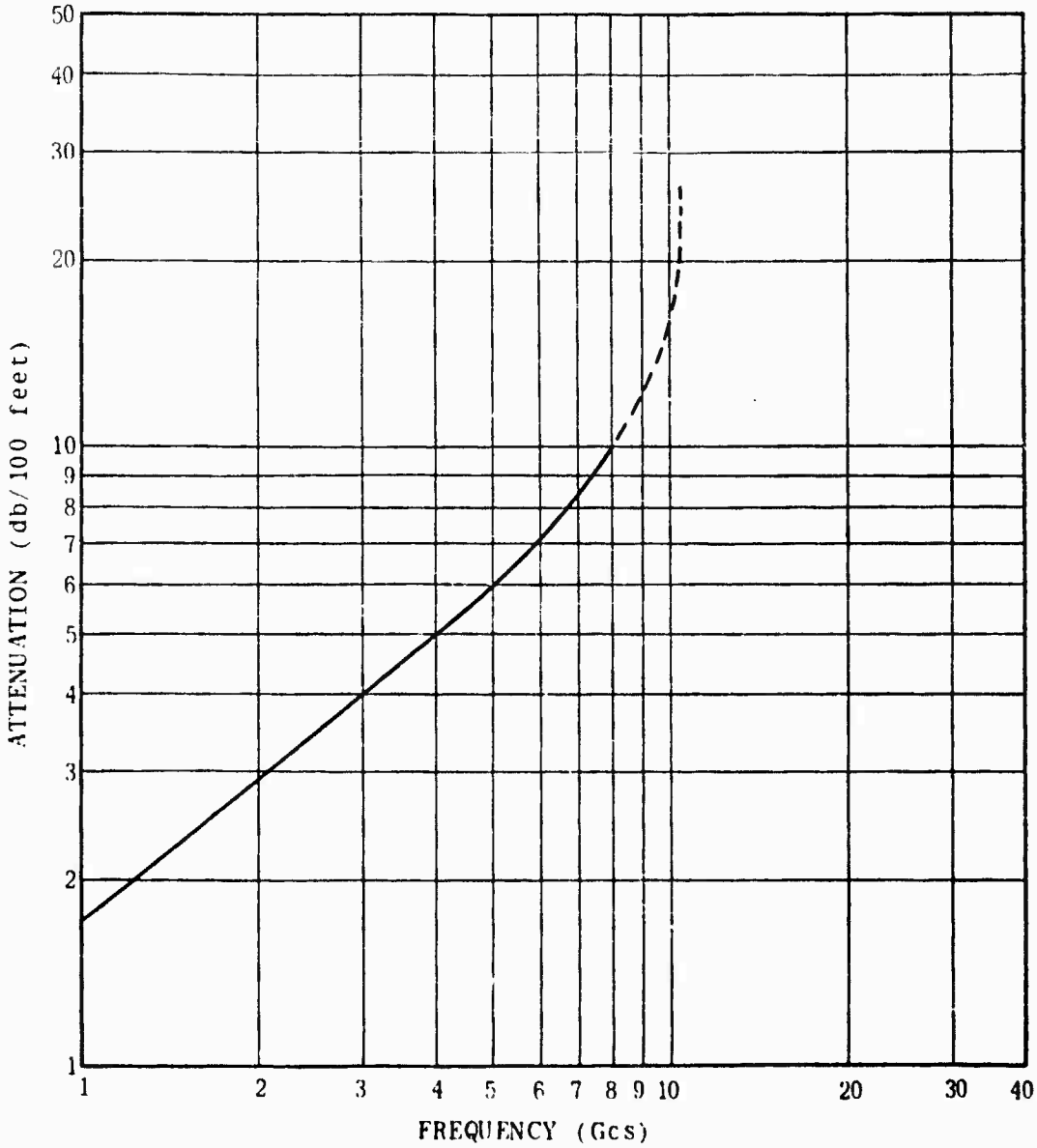

Figure 4-36. RG-58 Characteristic.

4.2.5.3.1 Local Oscillator Requirements

To avoid getting into the nonlinear region, the local oscillator output should be approximately 10^1 greater than the received echo signal. Since the burn-out limit for the 1N21B crystal is 2.5 watts pulse power,[30] it is apparent that a local oscillator signal above 25 watts would meet this requirement. The maximum output of a light-house tube at L-band frequencies is approximately 25-50 watts.[31] This output thus assures us of continuous operation in the linear mixer region.

The frequency of the local oscillator must differ from the operating frequency of the radar by the IF frequency. In this sample radar, the IF frequency is 60 Mcs and the operating frequency range is 1220-1350 Mcs. The local oscillator must be capable of generating signals from 1160-1410 Mcs. We find that the 2C40 light-house tube is capable of generating signals from a low microwave frequency to S-band depending on the cavity.[32] Thus, the oscillator will generate the desired frequencies.

4.2.5.3.2 Consideration of Local Oscillator Harmonics

The local oscillator is a signal transmitter, therefore harmonics of the fundamental signal will be transmitted along with the fundamental signal. However, we have already determined that signals above 10 GCS will be blocked by the RG-58 coaxial cable.

The frequency ranges of the local oscillator and harmonics are:

Fundamental:	1160-1410 Mcs
2nd Harmonic:	2320-2820 Mcs
3rd Harmonic:	3480-4230 Mcs
4th Harmonic:	4640-5640 Mcs
5th Harmonic:	5800-7050 Mcs
6th Harmonic:	6960-8460 Mcs

30. Torrey & Whitmer, op. cit., p. 152.

31. Reich, Ordung, Krauss, Skalnik, Microwave Theory and Technique, P. Van Nostrand Company, Inc., 1953.

32. Ibid.

7th Harmonic: 8120-9870 Mcs
8th Harmonic: 9280-11,280 Mcs
9th Harmonic: 10,440-12,690 Mcs

From a frequency consideration, we can eliminate any generation above the 8th harmonic because such a frequency would not be passed by the RG-58 coaxial cable.

Signal amplitude remains an important consideration. The bar chart in Figure 4-20 exhibits relative amplitudes of harmonics. Thus, we would have the 8th harmonic approximately 70 db down from the fundamental. The absolute magnitude of this harmonic would be approximately 10^{-6} watts. Such a signal would "mix" with an echo signal, at the proper frequency, of 10^{-7} watts amplitude without degrading the linear characteristic of the mixer. Therefore, from an amplitude consideration, all harmonics passed by the RG-58 coaxial cable must be considered as valid inputs to the mixer unit.

4.2.5.4 Mixer Unit Capabilities

The mixer unit contains either a 1N21B, 1N21C or 1N21D crystal rectifier depending upon availability of parts. In our considerations we will use the characteristics of the 1N21B crystal rectifier.

4.2.5.4.1 Computation of Minimum Detectable Signal

In making this computation we assume room temperature and an IF noise level of 5 db. These assumptions are standard.

The minimum detectable signal, P_{min}, is expressed

$$P_{min} = k\,T\,\Delta f\,\,NF$$

For the 1N21B crystal

$$P_{min} = (1.38 \times 10^{-23} \text{ watts}/^{\circ}K)\ (313^{\circ}K)\ (1 \times 10^{6} \text{ cps})\ (18.63)$$

$$P_{min} = 80.5 \times 10^{-15} \text{ watts}$$

Thus, the minimum detectable signal is 8.05×10^{-14} watts or approximately $10^{-13.2}$ watts. Any signal of amplitude less than $10^{-13.2}$ watts would not be detected by the 1N21B crystal rectifier.

4.2.5.4.2 Mixer Transfer Characteristics

The maximum conversion efficiency of a 1N21B crystal rectifier is -6.5 db.[33] The gain G of the crystal is $10^{-0.65}$ or approximately $10^{-0.7}$ db. This conversion efficiency compares favorably with that of the 1N28 crystal rectifier of Sample Radar I. The amplitude transfer characteristic of the 1N21B compares with that of the 1N28 shown in Figure 4-21 except that the burn-out limit for the 1N21B crystal rectifier is 2.5 watts pulse power.[34]

4.2.5.4.3 Mixer Selectivity

As mentioned earlier, the construction of a selectivity characteristic for the mixer unit is a nebulous undertaking. Manufacturers simple do not provide characteristics for their products outside the recommended operating range. The constructed selectivity curve for the 1N21B crystal rectifier is presented in Figure 4-37. In constructing the curve, the same general assumptions were made as discussed previously.

4.2.5.5 Susceptibility Curve - Sample Radar II

An over-all susceptibility curve has been drawn in Figure 4-38. This curve is based on the constructed selectivity characteristics of all components through the mixer. No consideration was made of mixing phenomena. Therefore, this curve is not yet the completed susceptibility curve of the radar receiver RF section. A sample analysis of the mixing phenomena is given in Section 4.2 of this report. Methods for analyzing the nonlinear performance of the mixer have been presented in detail in previous reports.[35]

33. Ginzton, Edward L., op. cit. p. 151.

34. Torrey & Whitmer, op. cit., p. 152.

35. Interference Analysis Study, Jansky & Bailey, Washington, D.C. Final Report, RADC-TDR-61-312, Contract No. AF 30(602)-1934; January, 1962.

Interference Prediction Study, Jansky & Bailey, Washington, D.C. First Quarterly Report, Contract No. AF30(602)-2665, August, 1962.

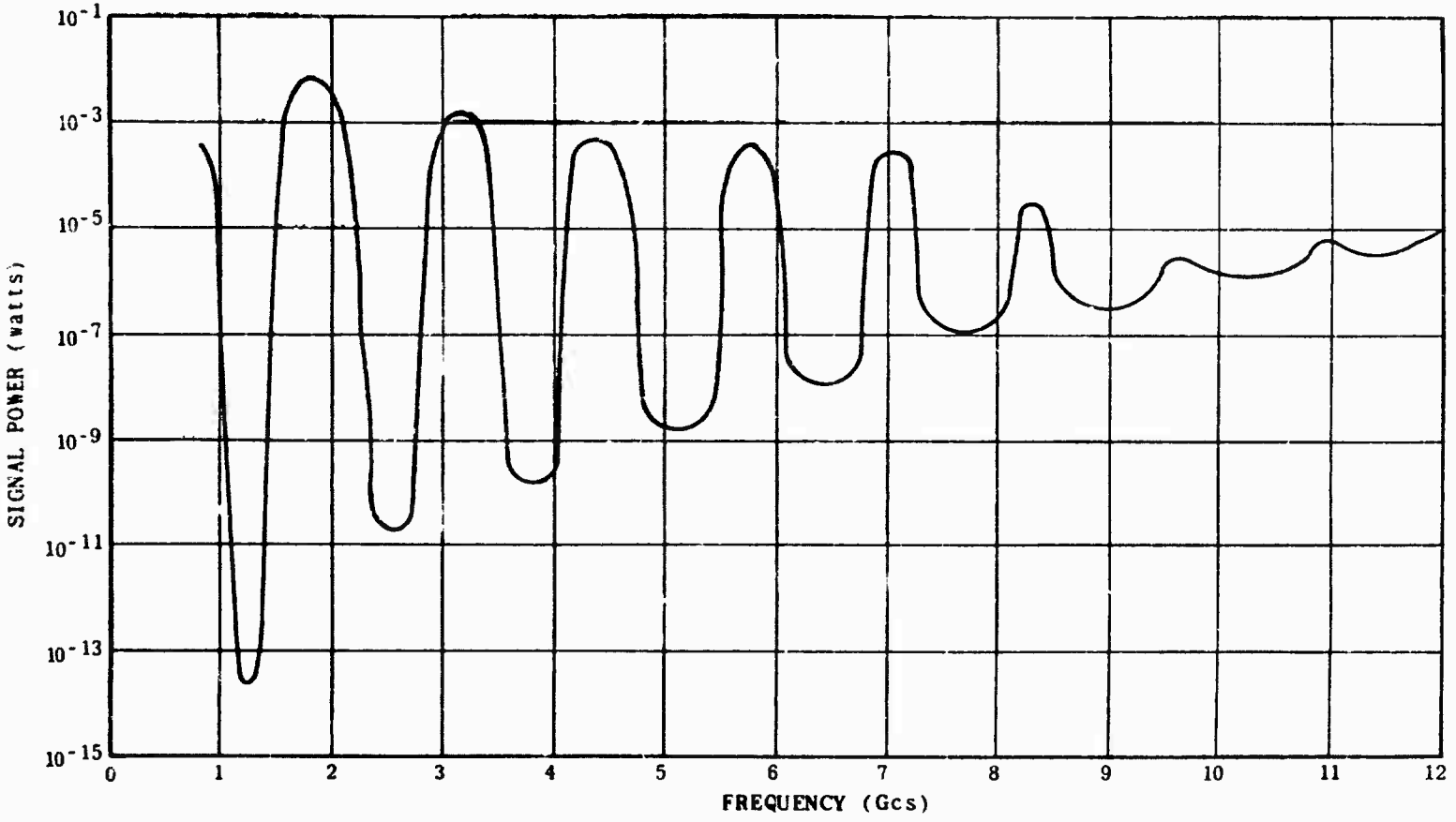

Figure 4-37. Mixer Selectivity Characteristic.

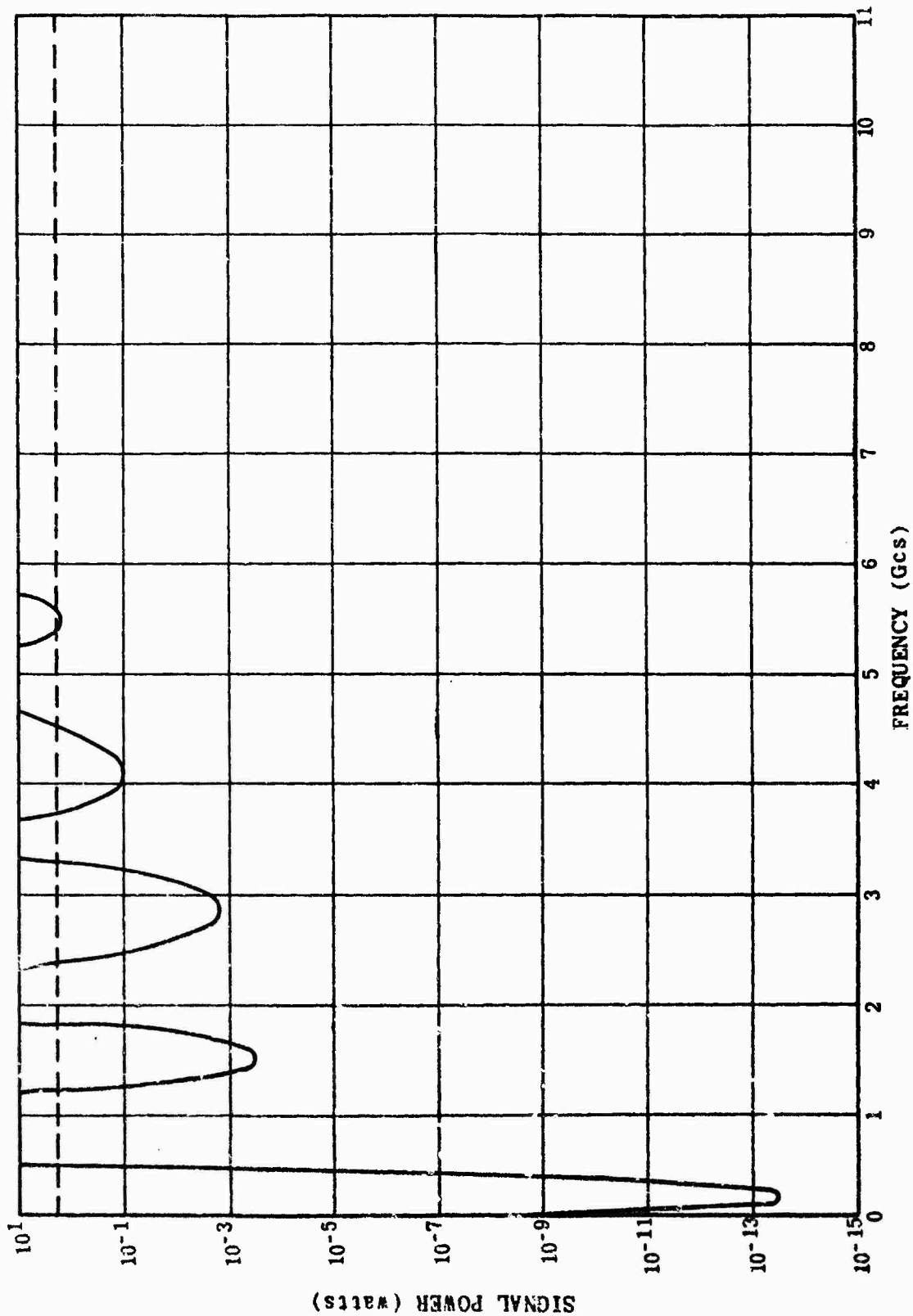

Figure 4-38. Susceptibility Curve - Sample Radar II.

4.2.6 Sample Radar III

The block diagram of sample radar III is shown in Figure 4-39. The block diagram is functional and includes complete signal path from antenna connector to mixer output. Antenna characteristics are not considered in this analysis.

A 1N21E crystal is used in the mixer. The mixer is connected to the I-F stages via a piece of coaxial cable with a critical electrical length. Local oscillator signals are generated by a 2C40 light-house tube mounted in a cavity. The signals are passed through a section of RG-9 coaxial cable to two buffer stages (cavities containing 2C39 tubes) and onto the mixer via RG-55 coaxial cable.

The echo signal is passed from the antenna connector via standard L-Band Waveguide to an ATR device (a BL-612 tube). From this point, the signal goes immediately to a Pre-TR device (a BL-612 tube), then directly to the T-R cavity containing a BL-25 tube and finally on to the mixer.

4.2.6.1 Determining Echo Signal Frequency

It is assumed that signals of all frequencies are present at the antenna connector. We have previously limited the frequency range by establishing 12.0 GCS as the upper limit of common military transmitters[36] and have designated the lower frequency limit as the waveguide cutoff frequency. The cutoff frequency for standard L-Band waveguide is 908 Mcs.

4.2.6.1.1 Determination of T-R Pass Band

For all practical purposes we can consider the T-R device as consisting of three sections: (1) ATR (2) Pre-TR (3) T-R. Hence, for the T-R pass band, we must establish a selectivity characteristic for each of the BL-612's and the BL-25.

The Bl-612 has a VSWR of 1.5 over its operating frequency[37] pass band. A 1.5 VSWR is normalized to be 0.2 db.[38] This pass band

36. MIL-STD-449A, op. cit., p. 163.

37. Specification Sheet, Type 7152/BL-612 Pre-TR Tube, L-Band, Bomac Laboratories, Inc., Beverly, Mass.

38. Saad, T.S., op. cit., p. 164.

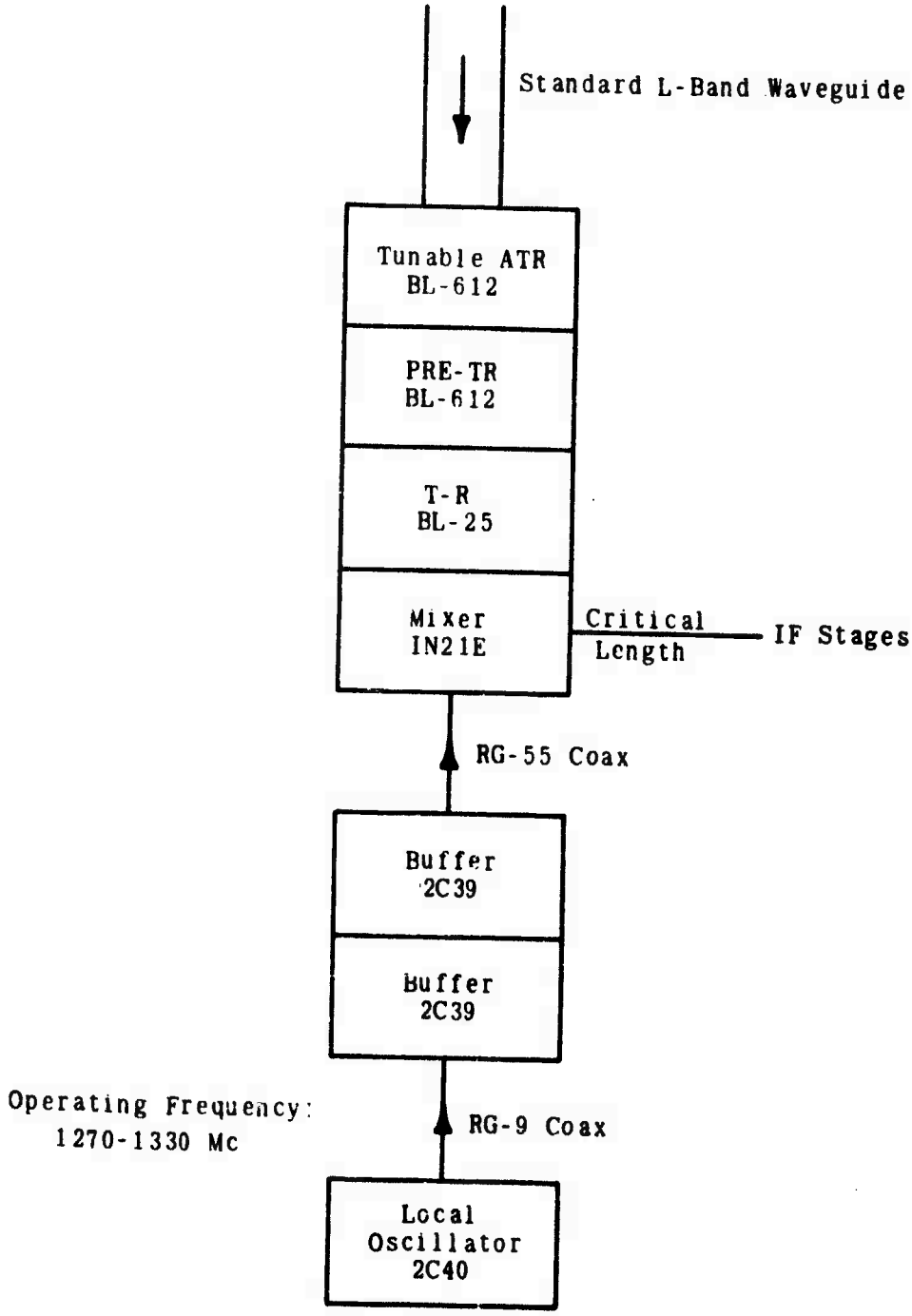

Figure 4-39. Sample Radar III.

characteristic is helpful only in establishing the fact that the energy loss at the operating frequency is negligible for our purposes.

4.2.6.1.1.1 The BL-612 Selectivity Characteristic

An estimate of the filtering effectiveness of the BL-612 would be an attenuation of 0.2 db at the operating frequency, 10 db at other frequencies and less at "window" frequencies when the signal wavelength is a multiple of the operating frequency wavelength. A selectivity curve using those considerations is shown in Figure 4-40. The effect gives rise to only a slight selectivity. However, with two BL-612's in tandem, the total effect is greater than shown for the single tube.

4.2.6.1.1.2 The BL-25 Selectivity Characteristic

A selectivity curve for a BL-25 tube mounted in a standard cavity was shown in Figure 4-28. The BL-25 is a more selective device because it is tunable over its operating range. This feature allows more effective filtering.

4.2.6.1.1.3 The Combination Selectivity Characteristic

By using the curves constructed for the BL-612 tubes and the BL-25 tube, it is now possible to graph a combination of the three tubes and hence provide a constructed characteristic for the complete T-R device. The constructed curve is shown in Figure 4-41.

4.2.6.1.2 Establishing Optimum Echo Signal Band

From Figure 4.41 we can say that the optimum echo signal pass band is 1000-2000 Mcs. Signals in this range would be passed into the mixer unit and must be considered as optimum. The fundamental signal range would thus be 1000-2000 Mcs.

4.2.6.2 Consideration of Echo Signals at Mixer

The curve in Figure 4-41 is actually the pre-mixer selectivity curve sample radar III. In summation, we must consider echo signals from 908 Mcs to 12,000 Mcs to be present at the mixer. These frequencies would respond to the RF hardware as illustrated in the pre-mixer selectivity curve.

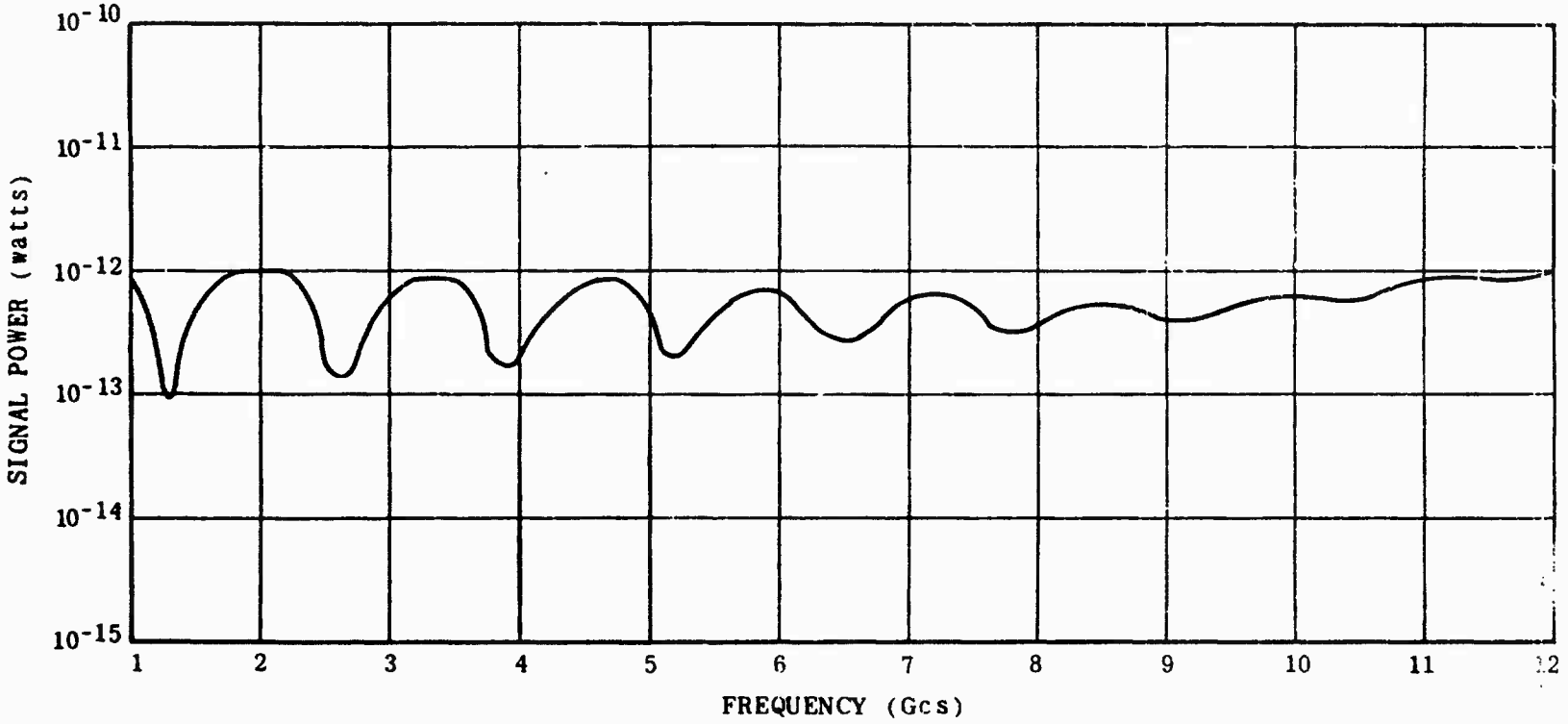

Figure 4-40. BL-612 Selectivity Characteristic.

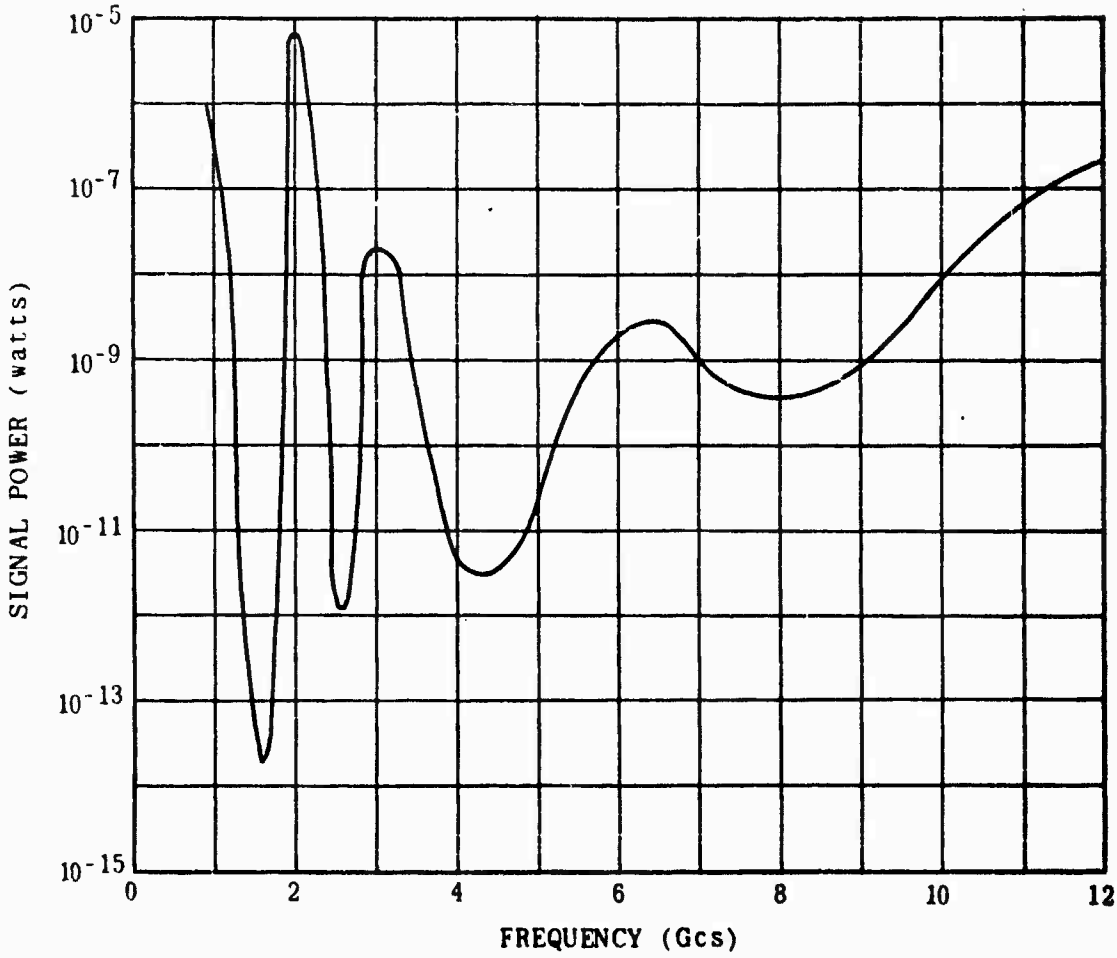

Figure 4-41. T-R Selectivity Characteristic.

4.2.6.3 Local Oscillator Considerations

The local oscillator is connected to the buffer stages by a short run of RG-9 coaxial cable. The frequency versus attenuation characteristic of RG-9 is shown in Figure 4-19. RG-9 offers effective attenuation to signals above 22,000 Mcs and can be considered as a low-pass device with an upper cutoff limit of 22 GCS.

4.2.6.3.1 Local Oscillator Requirements

To avoid mixer operation in the nonlinear region, the local oscillator input of the mixer must be 10^1 greater than the echo signal. There is no power problem with this local oscillator unit because three oscillator tubes comprise the unit. An estimate of the power output of this local oscillator unit would be approximately 100 watts, see Section 4.2.5.3.1.

4.2.6.3.2 Consideration of Local Oscillator Harmonics

The input to the mixer unit from the local oscillator is via RG-55 coaxial cable. The characteristic of this cable is shown in Figure 4-42. RG-55 appears to have a practical upper cutoff of 12-15 GCS. Above these frequencies the cable offers such attenuation properties that signals are effectively blocked.

Since the operating range of the radar is 1270 - 1330 Mcs and the I-F frequency is 30 Mcs, the local oscillator will be tunable from 1240 - 1370 Mcs. The frequency ranges of the local oscillator fundamental and harmonics are:

Fundamental:	1240 -1370 Mcs
2nd Harmonic:	2480 - 2740 Mcs
3rd Harmonic:	3720 - 4110 Mcs
4th Harmonic:	4960 - 5480 Mcs
5th Harmonic:	6200 - 6850 Mcs
6th Harmonic:	7440 - 8220 Mcs
7th Harmonic:	8680 - 9590 Mcs
8th Harmonic:	9920 - 10,960 Mcs
9th Harmonic:	11,160 - 12,330 Mcs
10th Harmonic:	12,400 - 13,700 Mcs

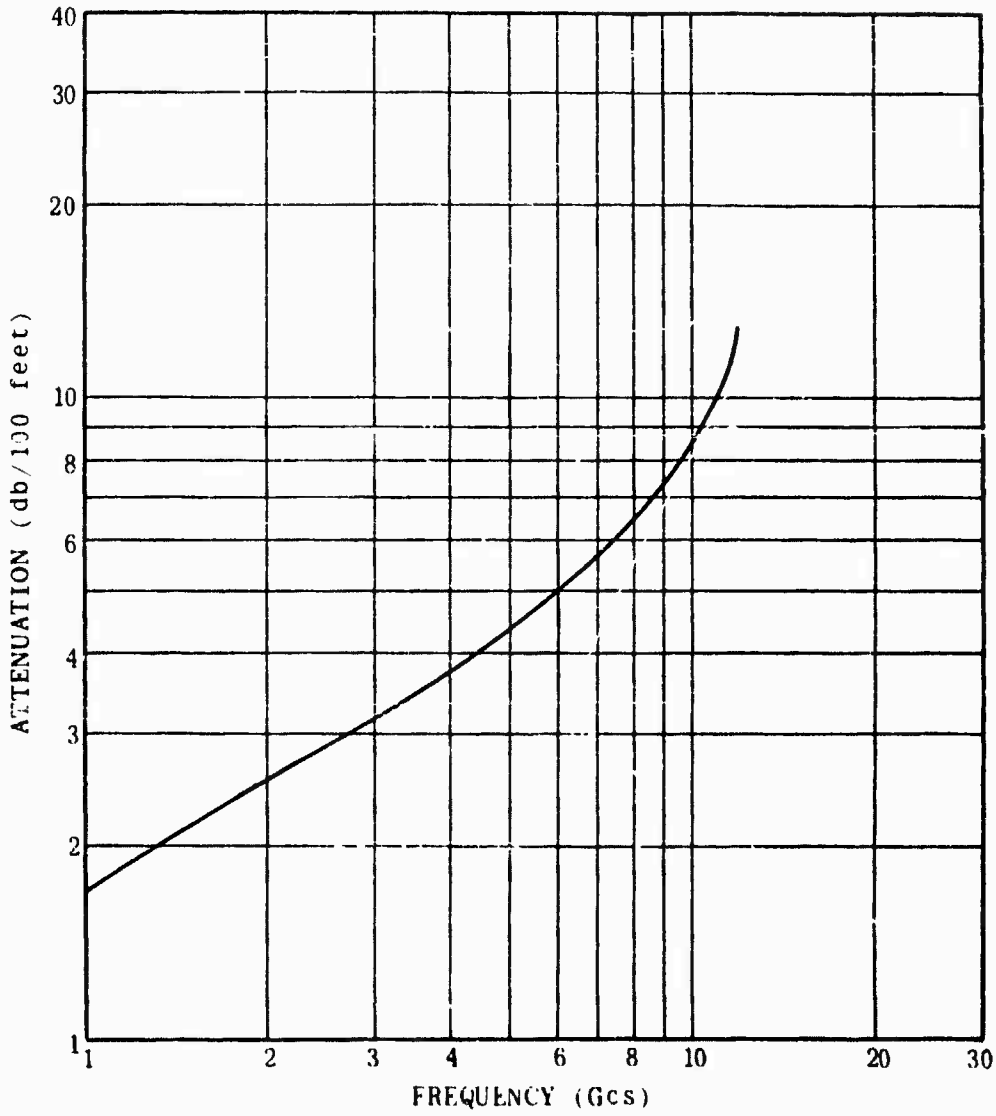

Figure 4-42. RG-55 Characteristic.

From a frequency point of view, we can eliminate any frequency above the 9th harmonic because the RG-55 coaxial cable would effectively block these higher frequencies.

Signal amplitudes would have relative relationships as shown in Figure 4-20. Even the 9th harmonic would be of sufficient amplitude to "mix" with echo signals without degradation of the mixer's linear characteristic.

4.2.6.4 Mixer Unit Capabilities

The mixer unit contains a 1N21E crystal rectifier. This crystal rectifier is an improved version in the 1N21 series and has similar characteristics except that the conversion loss is less, the burn-out limit is higher, the noise figure is lower, and the conversion efficiency is better. The improvements increase the sensitivity of the crystal rectifier and improve its over-all capability.

4.2.6.4.1 Computation of Minimum Detectable Signal

Assuming room temperature and an I-F noise level of 5 db, we can compute the minimum detectable signal, P_{min} by

$$P_{min} = k\ T\ \Delta f\ NF$$

$$P_{min} = (1.38 \times 10^{-23} \text{watts}/^{o}\text{K})(315^{o}\text{K})(1 \times 10^{6} \text{cps})(14)$$

$$= 60.5 \times 10^{-15} \text{ watts}$$

Thus, the minimum detectable signal is 6.05×10^{-14} watts or approximately $10^{-13.4}$ watts. Any signal of amplitude less than $10^{-13.4}$ watts would not be detected by the mixer unit.

4.2.6.4.2 Mixer Transfer Characteristic

The maximum conversion efficiency of the 1N21E crystal rectifier is -4.0 db. The gain, G, of the crystal is $10^{-0.4}$. The amplitude transfer characteristic compares with previous sample radars except the transfer loss in this case is 4.0 db where it was

7.0 db in previous radars. The burn-out limit of the crystal is approximately 2 watts.

4.2.6.4.3 Mixer Selectivity

The mixer selectivity characteristic is constructed on the same basis as that for previous sample radars. The characteristic is based on that of a crystal filter and is generalized over the applicable frequency range. The curve is shown in Figure 4-43.

4.2.6.5 Susceptibility Curve-Sample Radar III

An over-all susceptibility curve has been constructed in Figure 4-44. This curve is based on the selectivity characteristics of all components including the mixer unit. Since no consideration was made of the mixing phenomena, this curve is not the completed susceptibility characteristic of the RF receiver. Methods for analyzing the nonlinear performance of the mixer have been presented in detail in previous reports.[39]

39. Interference Analysis Study, Jansky & Bailey, op. cit., p. 202. Interference Prediction Study, Jansky & Bailey, op. cit., p. 202.

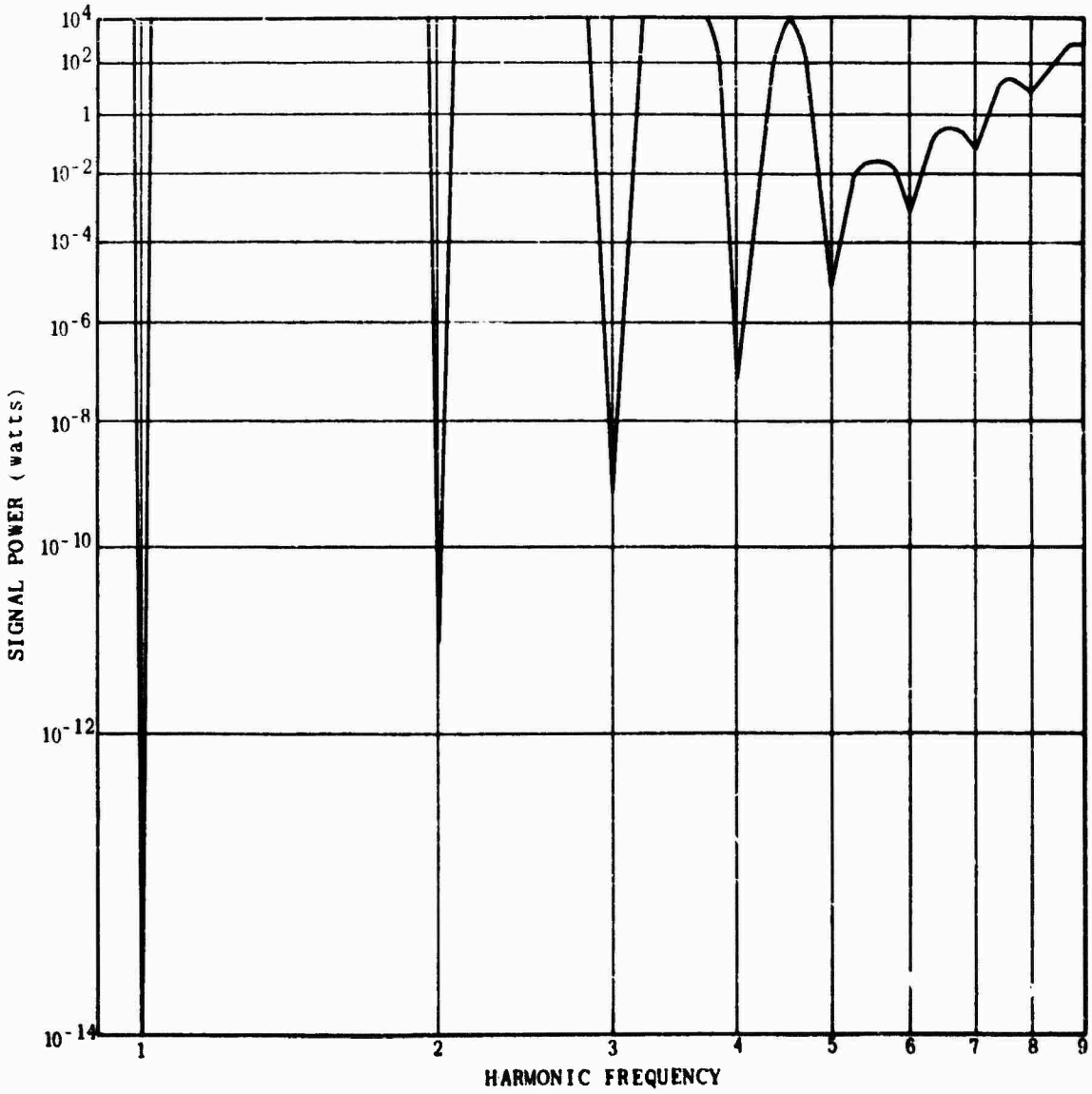

Figure 4-43. Mixer Selectivity Curve-Sample Radar III.

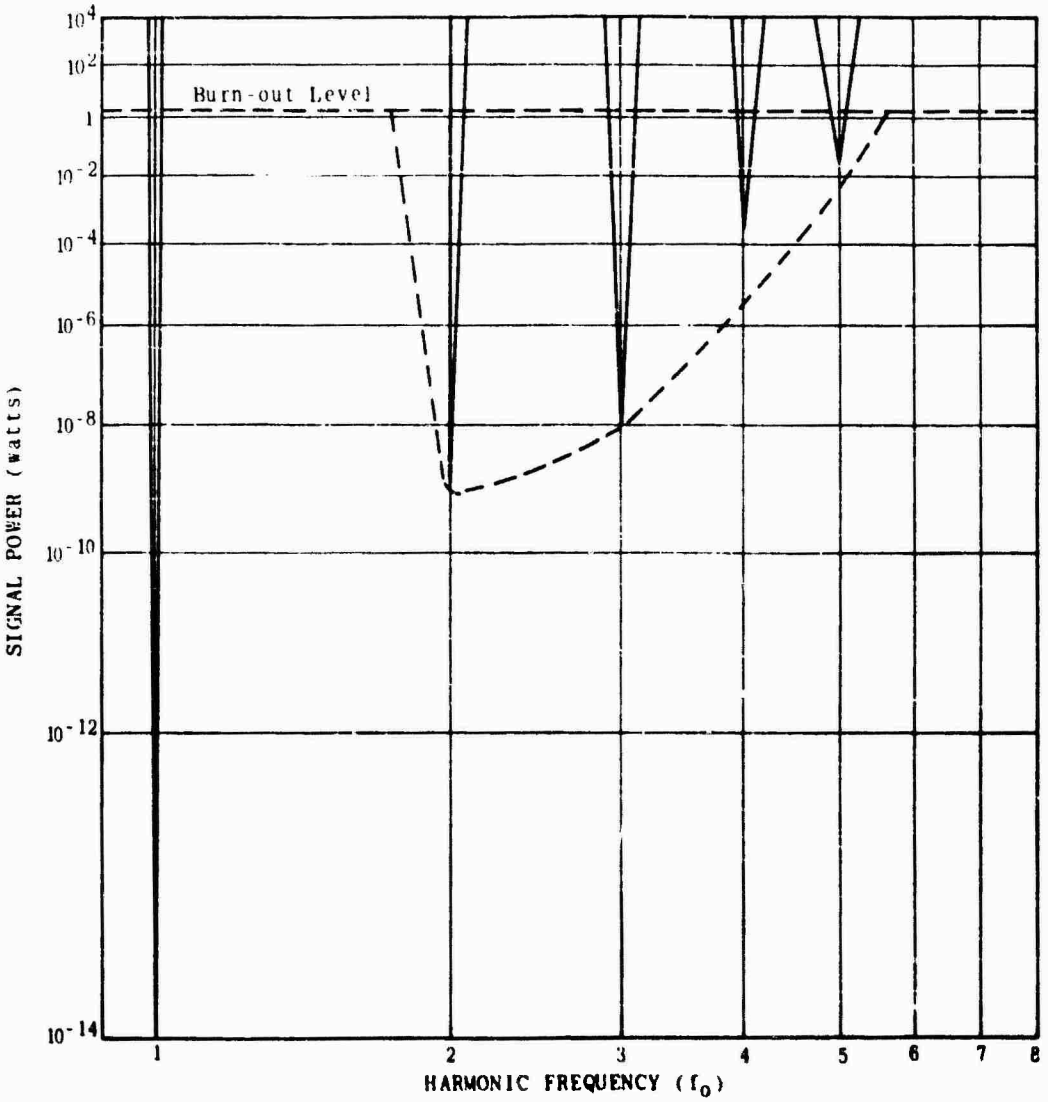

Figure 4-44 Susceptibility Curve-Sample Radar III

Section 5

ANTENNAS

5.1 Pattern Distribution Functions

A great deal of effort has been spent during the last quarter in statistical analysis of currently available measured antenna patterns. The statistical reduction of measured data is aimed toward conversion of raw data into useable forms to verify antenna theories which have been developed and are now under development as well as providing direct input material for certain antenna classes.

As an example of the data which has been obtained, a complete pattern distribution function analysis for the AN/FPS-36 radar antenna will be presented. The AN/FPS-36 antenna is a horn-fed reflector. The reflector is a parabolic section with a horizontal dimension of 40 feet and a vertical dimension of approximately 6 feet. Thirty-six individual antenna patterns were analyzed for the AN/FPS-36. Antenna patterns at each of the first six harmonic output frequencies of the transmitter were available for both horizontal and vertical polarization. These 12 antenna patterns were taken for each of three serial numbers.[1] Figure 5-1 is a summary of the pattern distribution functions which were computed from the measured data taken on one of the serial number equipments. The data of Figure 5-1 show the PDF's for horizontal polarization at the first six harmonic outputs of the transmitter.

From the large number of calculations which have been made it becomes apparent that the data follows a normal distribution for large aperture, high-gain antennas if the main beam region of the antenna pattern is excluded from the function. In practice some significant deviations from normality are usually noted near the low level (i.e., high probability) tail of the function. Any measurement is limited by the over-all sensitivity of the measuring

---

1. Spectrum Signature Data of Radar Set AN/FPS-36, Serial No. 215, Serial No. 69 and Serial No. 1240, U.S. Army Electronic Proving Ground, Fort Huachuca, Arizona, Contract DA 36-039-SC-80424, May and June, 1962, Three Volumes

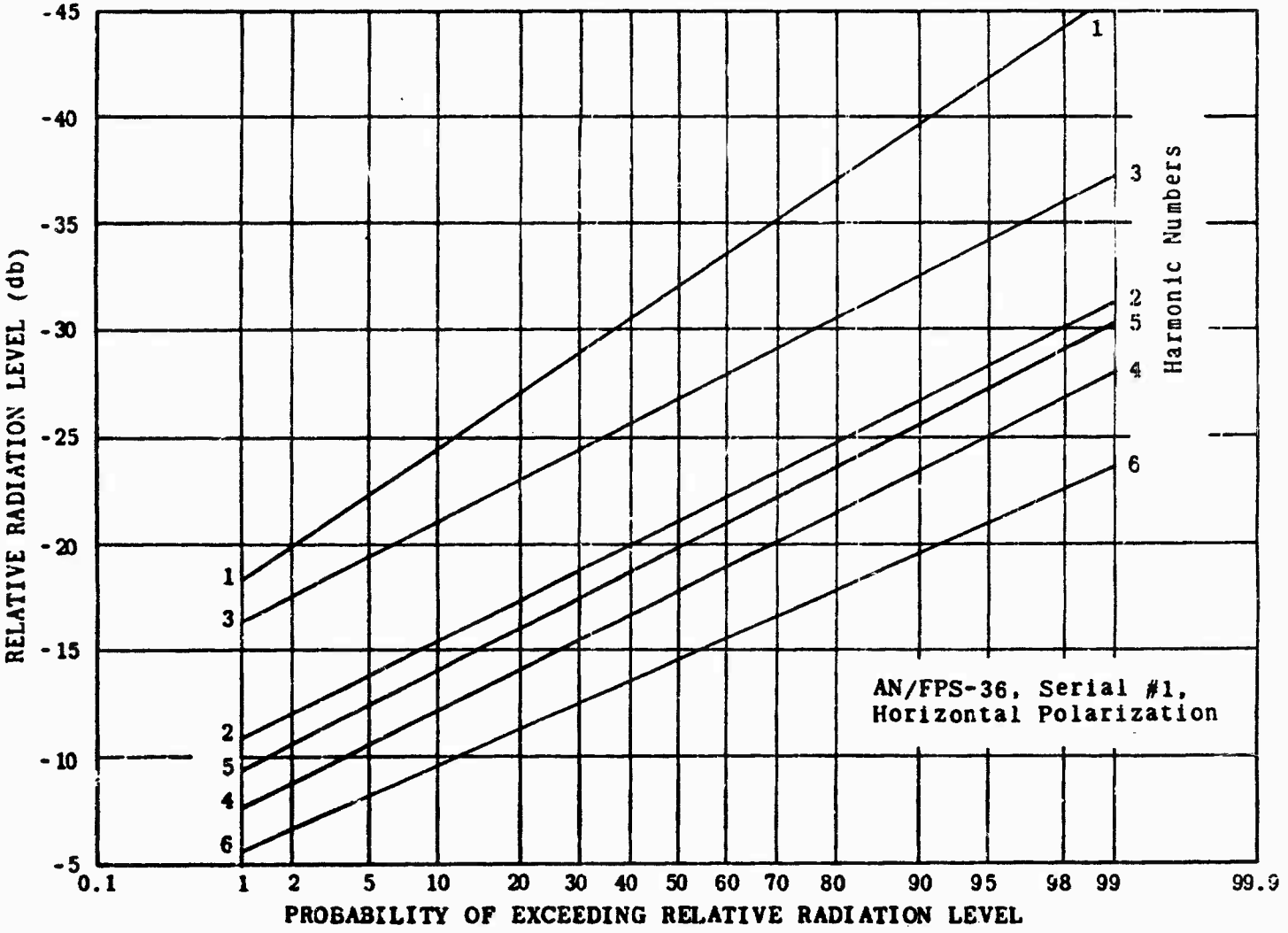

Figure 5-1 Pattern Distribution Functions

system or the ambient noise level. As the lower limit of the measuring ability is approached the distribution of measured values therefore tend to level off unnaturally. If the extreme lower end of the data is excluded from analysis, a normal distribution results.

The pattern distribution functions shown on Figure 5-1 appear to tend toward a definite family of curves. In general, the radiation levels relative to the main lobe appear to increase with increasing harmonic number, with the even harmonics displaced slightly toward the higher radiation levels.

Figures 5-2 and 5-3 contain the pattern distribution functions which were calculated from a set of measured data for a second and third serial number of the same equipment. The PDF's shown on Figures 5-2 and 5-3 are for horizontal polarization and tend toward the same family relationships indicated by Figure 5-1.

Figures 5-4, 5-5 and 5-6 present similar results for vertical polarization. A family relationship similar to that for horizontal polarization seems to be suggested although in the case of vertical polarization the pattern distribution functions exhibit more irregularity.

In order to examine the variations which exist in the same measurements made on differently serial numbered equipments, the data shown on Figures 5-1 through 5-6 have been replotted on Figures 5-7 through 5-12. Figure 5-7 summarizes the pattern distribution functions derived from measured data for the first harmonic. Figure 5-7 shows that for the first harmonic the curves associated with horizontal polarization group themselves separately from those for vertical polarization. Figure 5-7 also shows that there are small differences between the same measurements on differently serial numbered equipments. As Figures 5-8 through 5-12 show, these differences tend to increase as harmonic number increases. Data from two serial numbers of radar set AN/MPQ-10 were examined to determine the effect of elevation angle on the pattern distribution functions. Elevation angles of 6°, 24°, 55°, 70°, and 87° were used at the fundamental, second and third harmonic frequencies. As can be determined from Figures 5-13 through 5-18, a change in elevation angle produces an insignificant effect on the pattern distribution function for horizontal polarization.

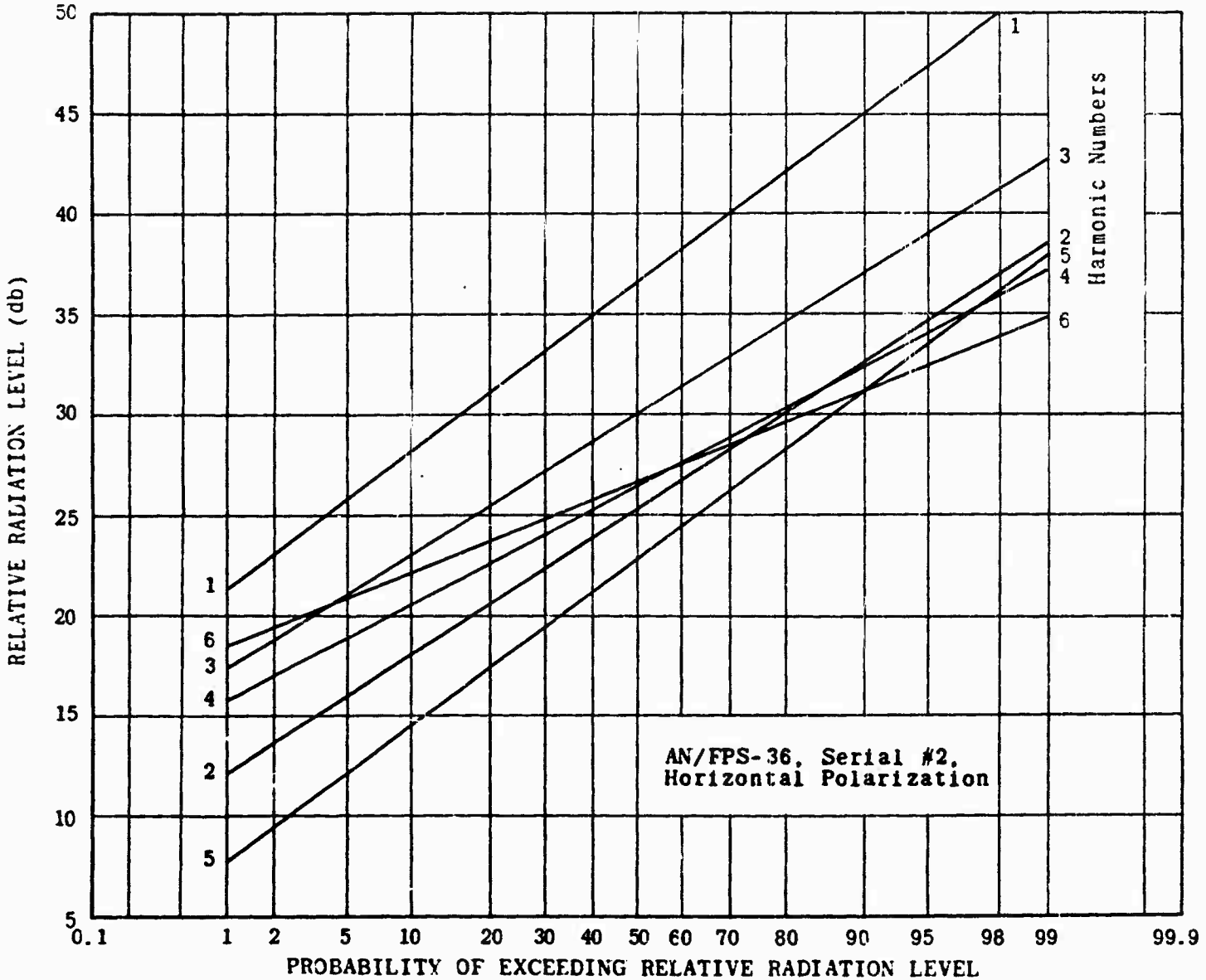

Figure 5-2. Pattern Distribution Functions.

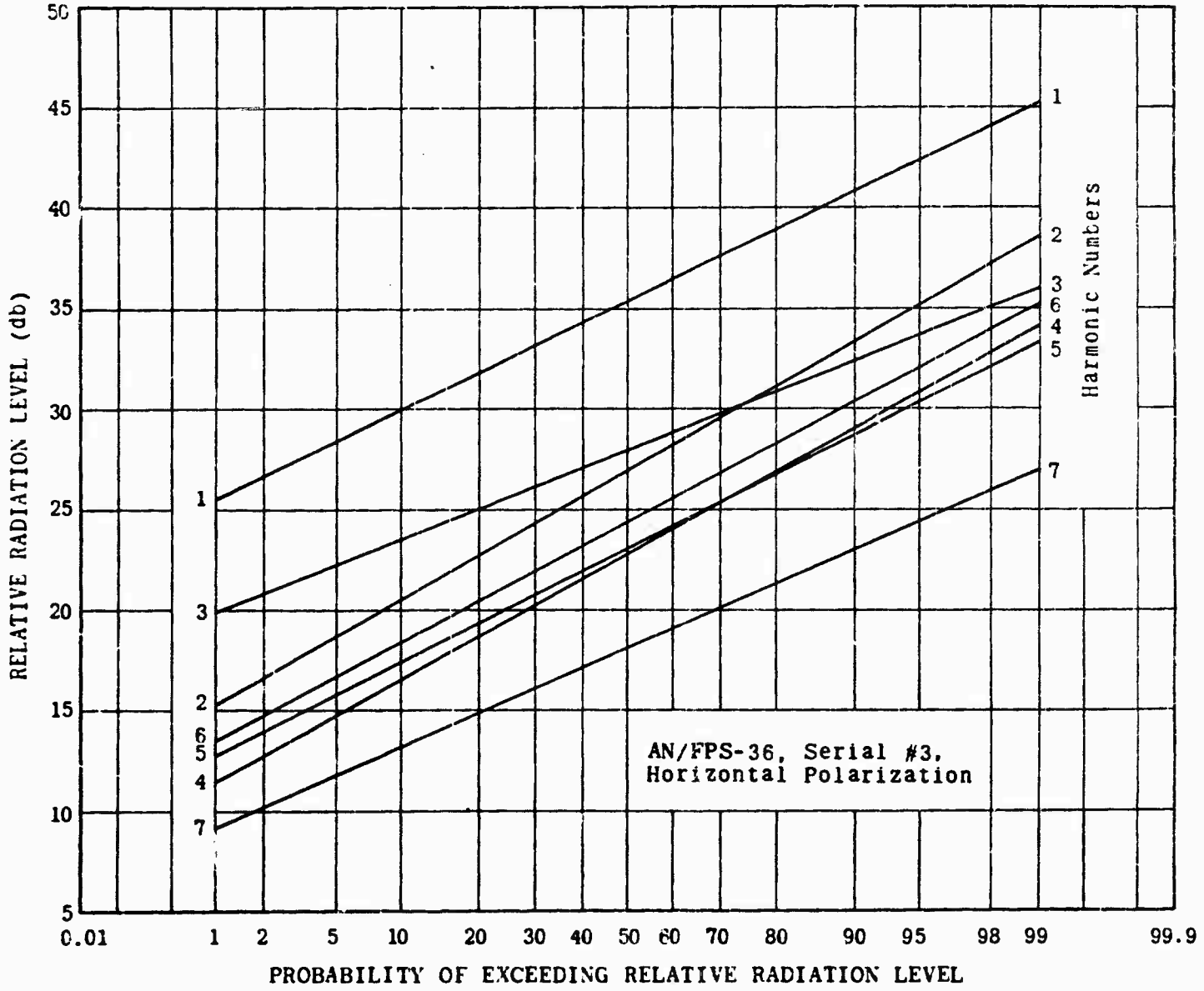

Figure 5-3. Pattern Distribution Functions.

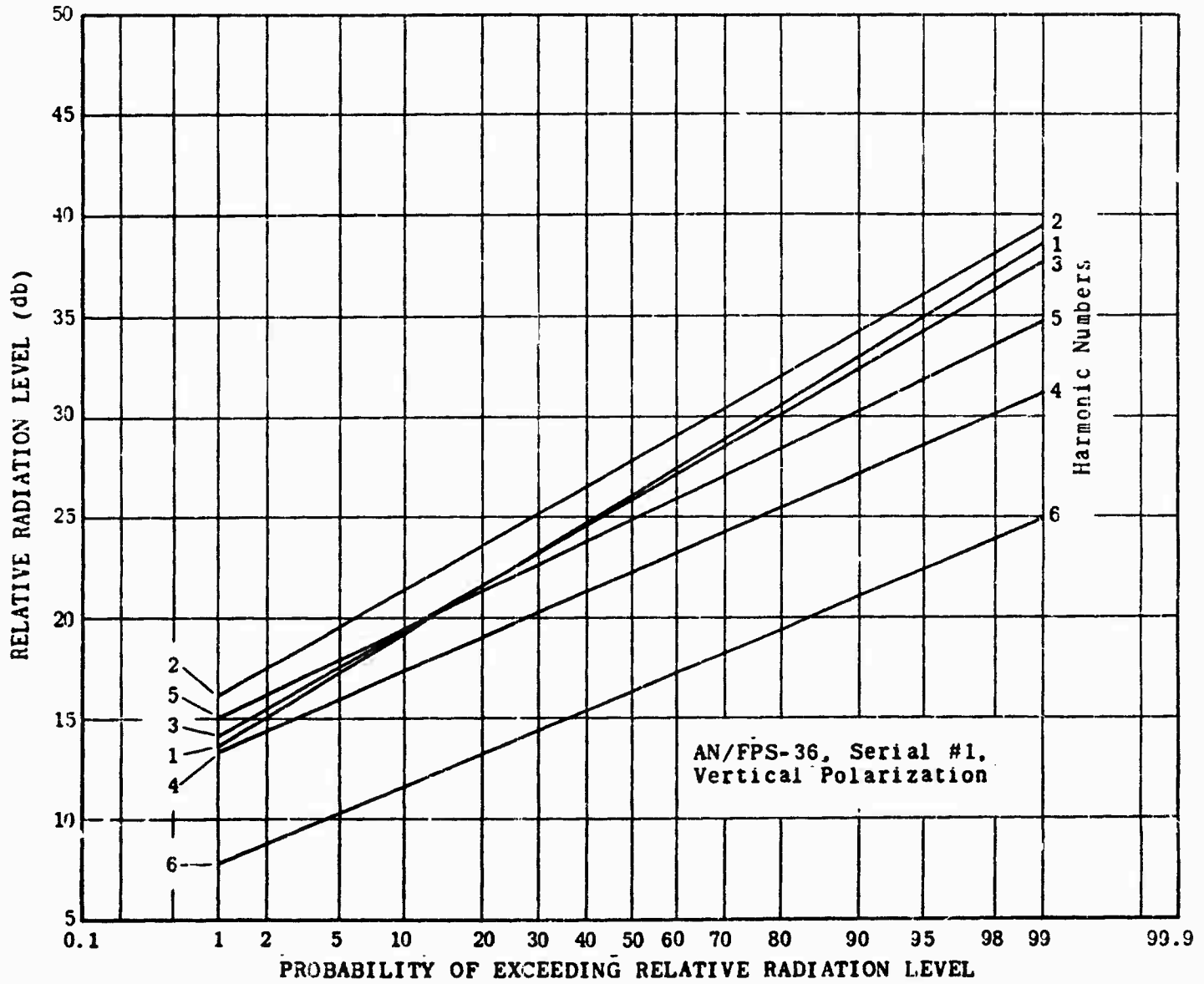

Figure 5-4. Pattern Distribution Functions.

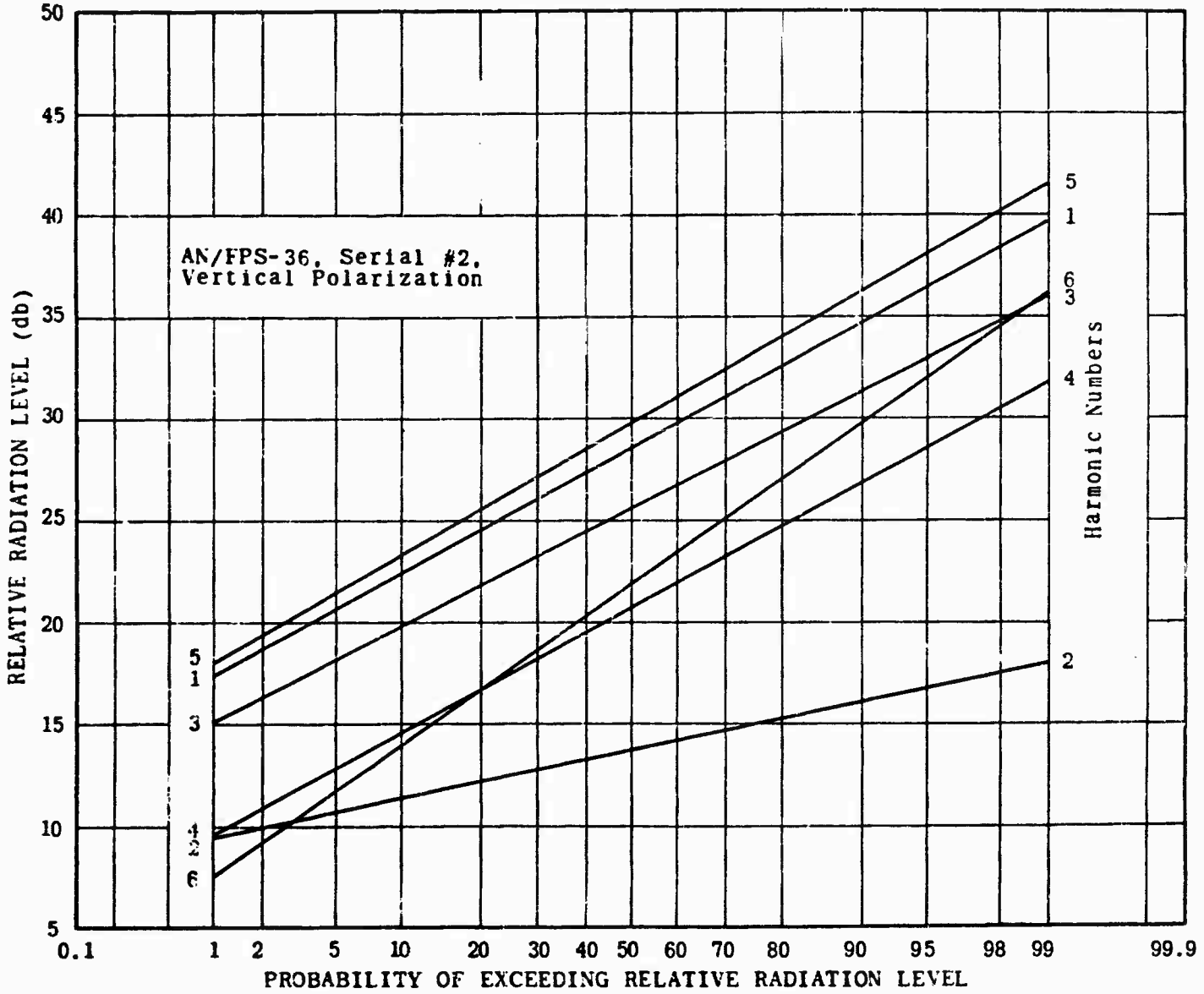

Figure 5-5. Pattern Distribution Functions.

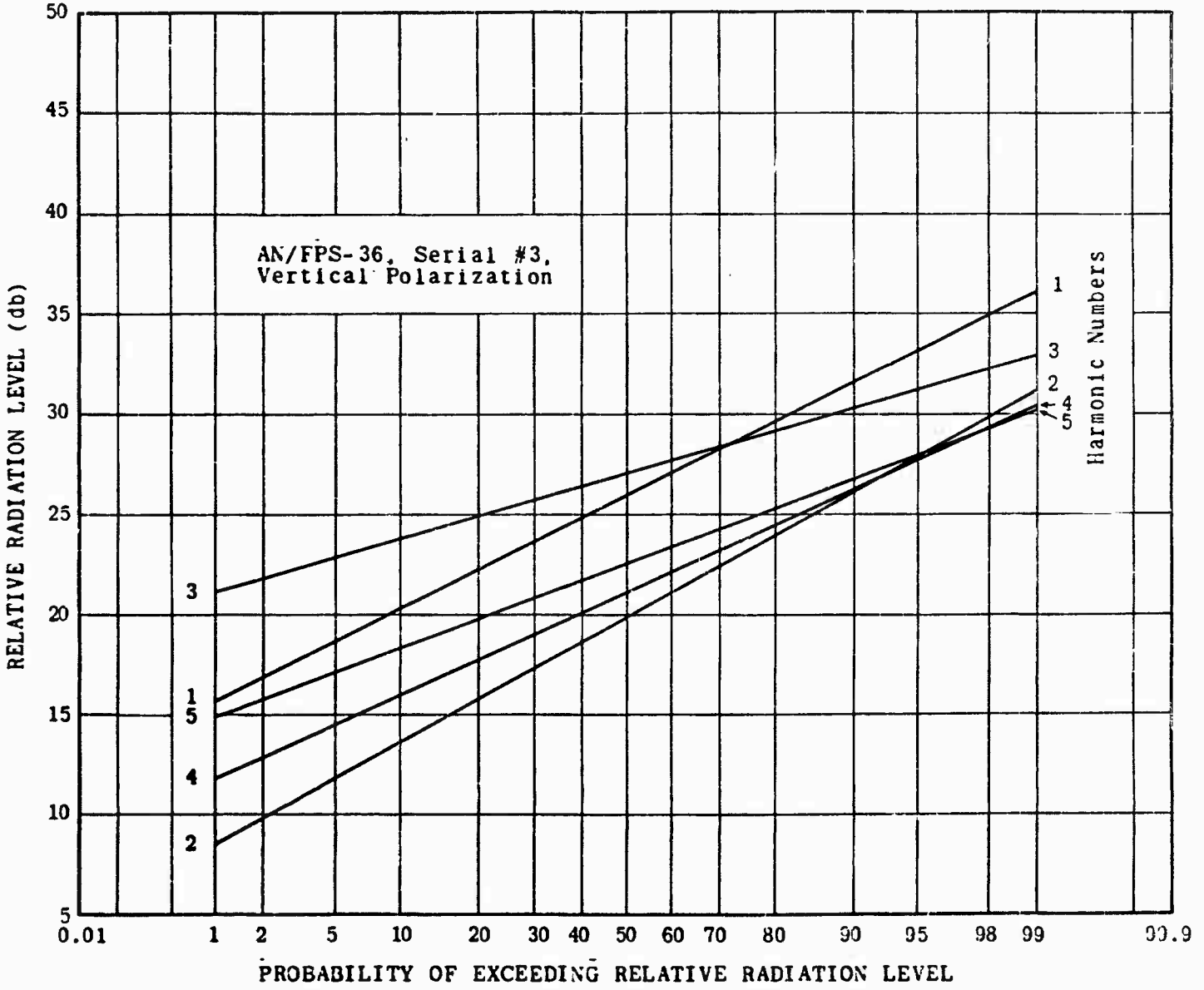

Figure 5-6. Pattern Distribution Functions.

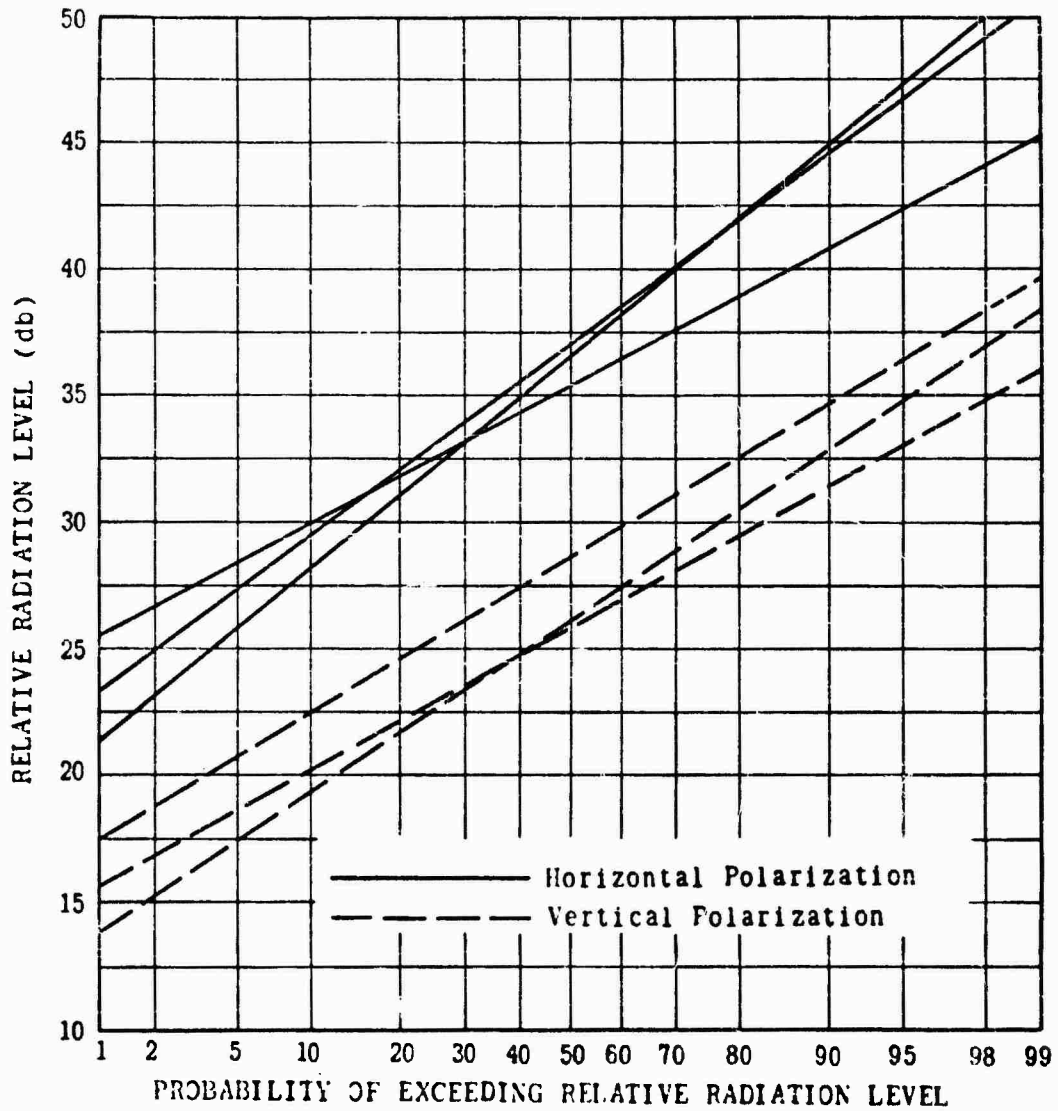

Figure 5-7. PDF at 1st Harmonic for all Serial Numbers.

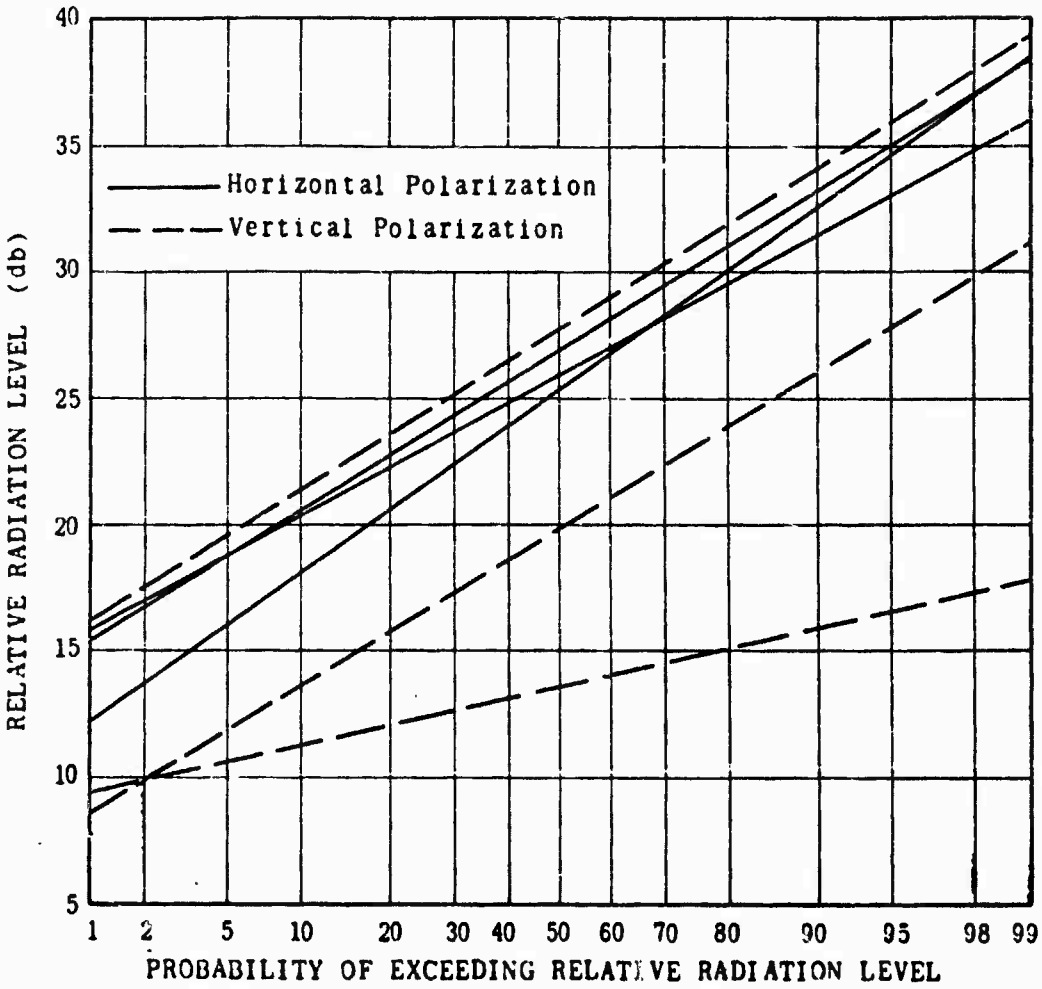

Figure 5-8. PDF at 2nd Harmonic for all Serial Numbers.

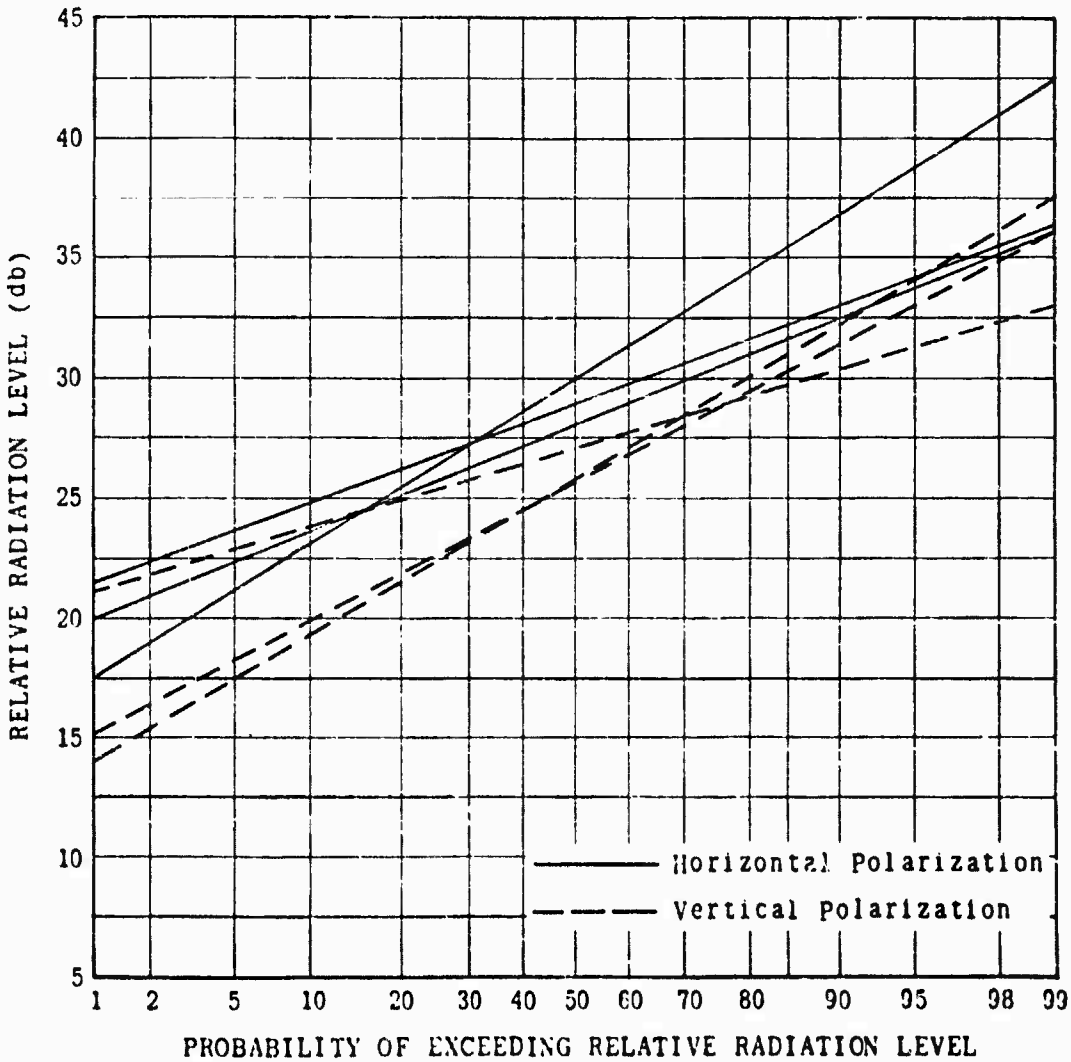

Figure 5-9. PDF at 3rd Harmonic for all Serial Numbers.

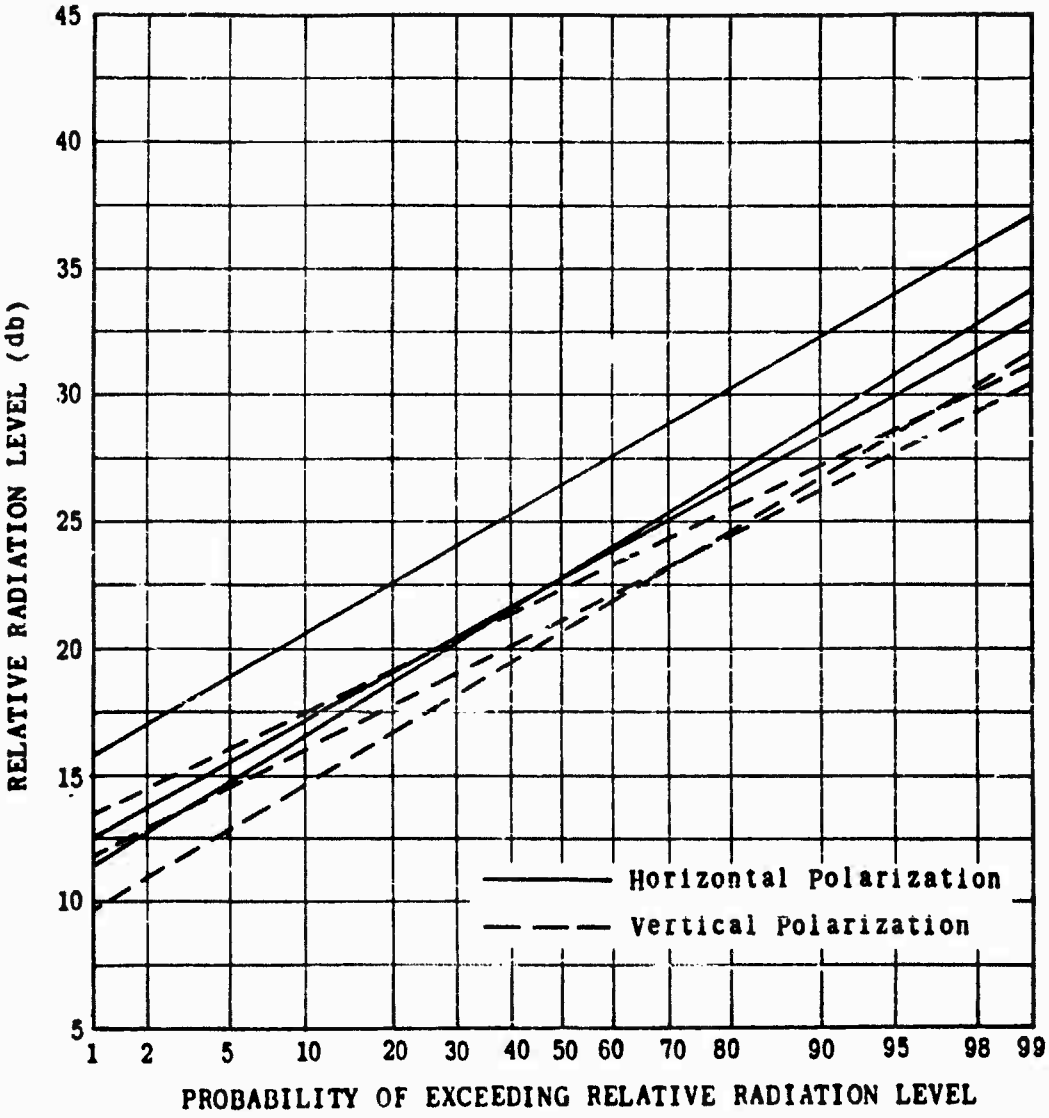

Figure 5-10. PDF at 4th Harmonic for all Serial Numbers.

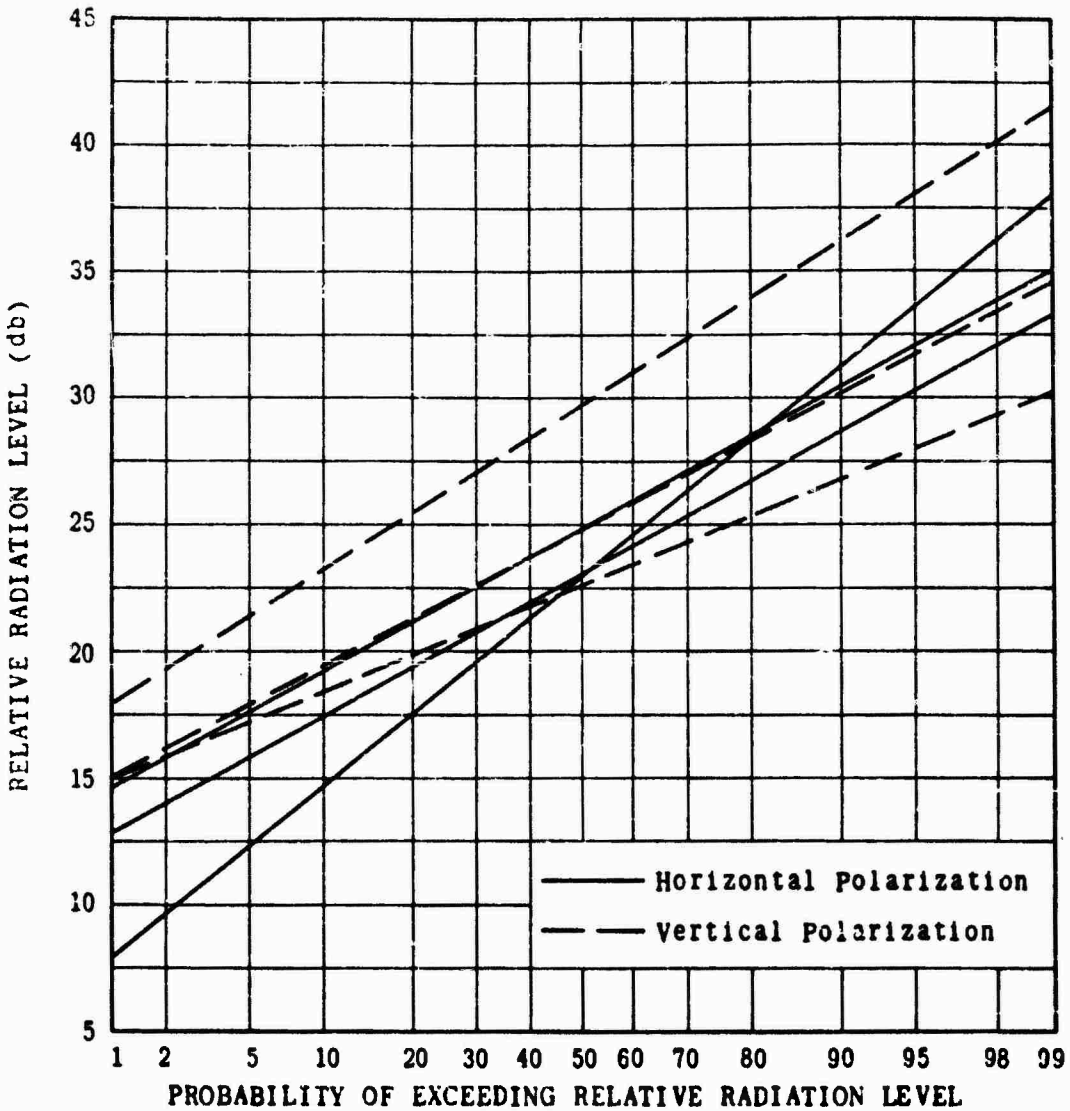

Figure 5-11. PDF at 5th Harmonic for all Serial Numbers.

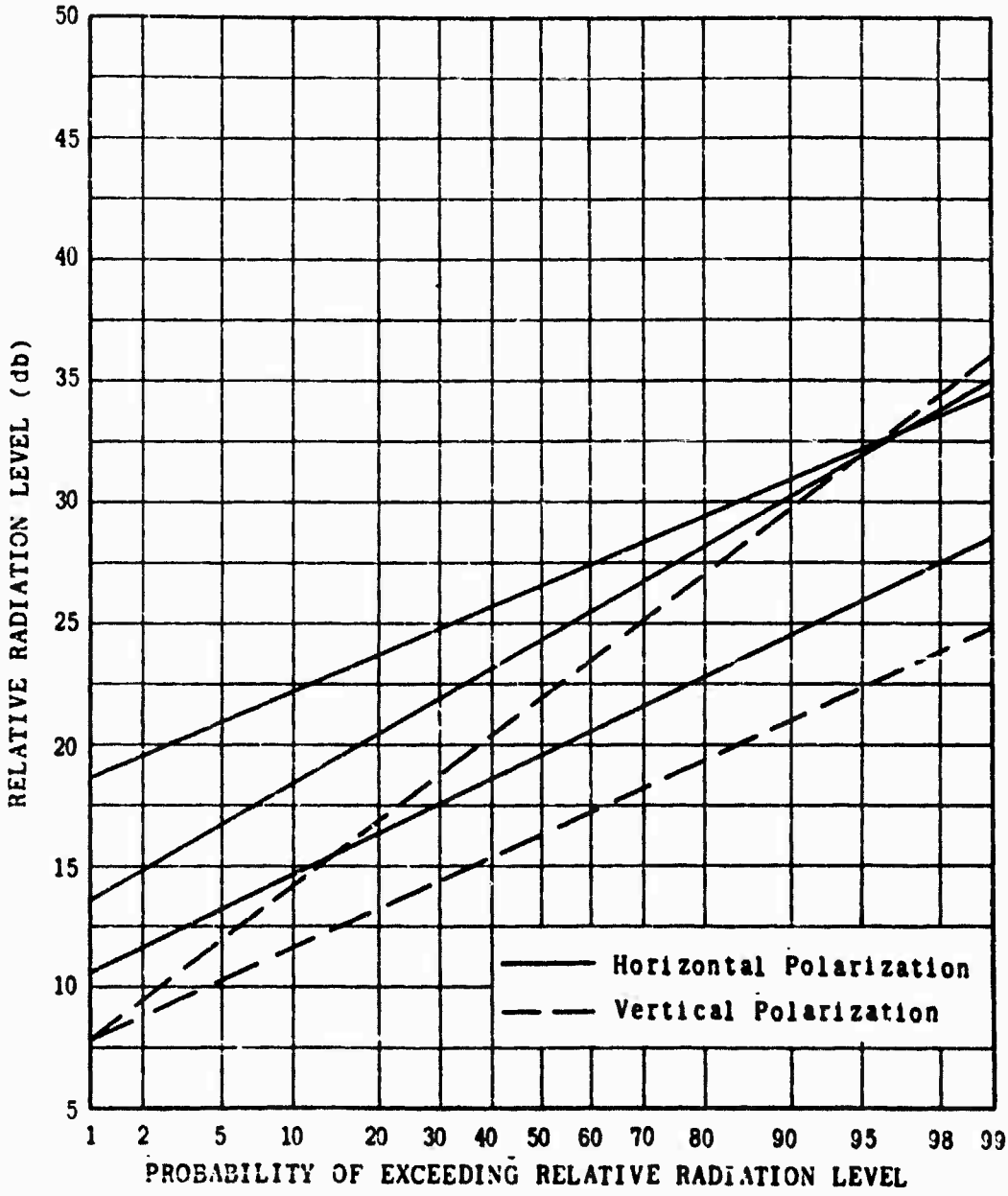

Figure 5-12. PDF at 6th Harmonic for all Serial Numbers.

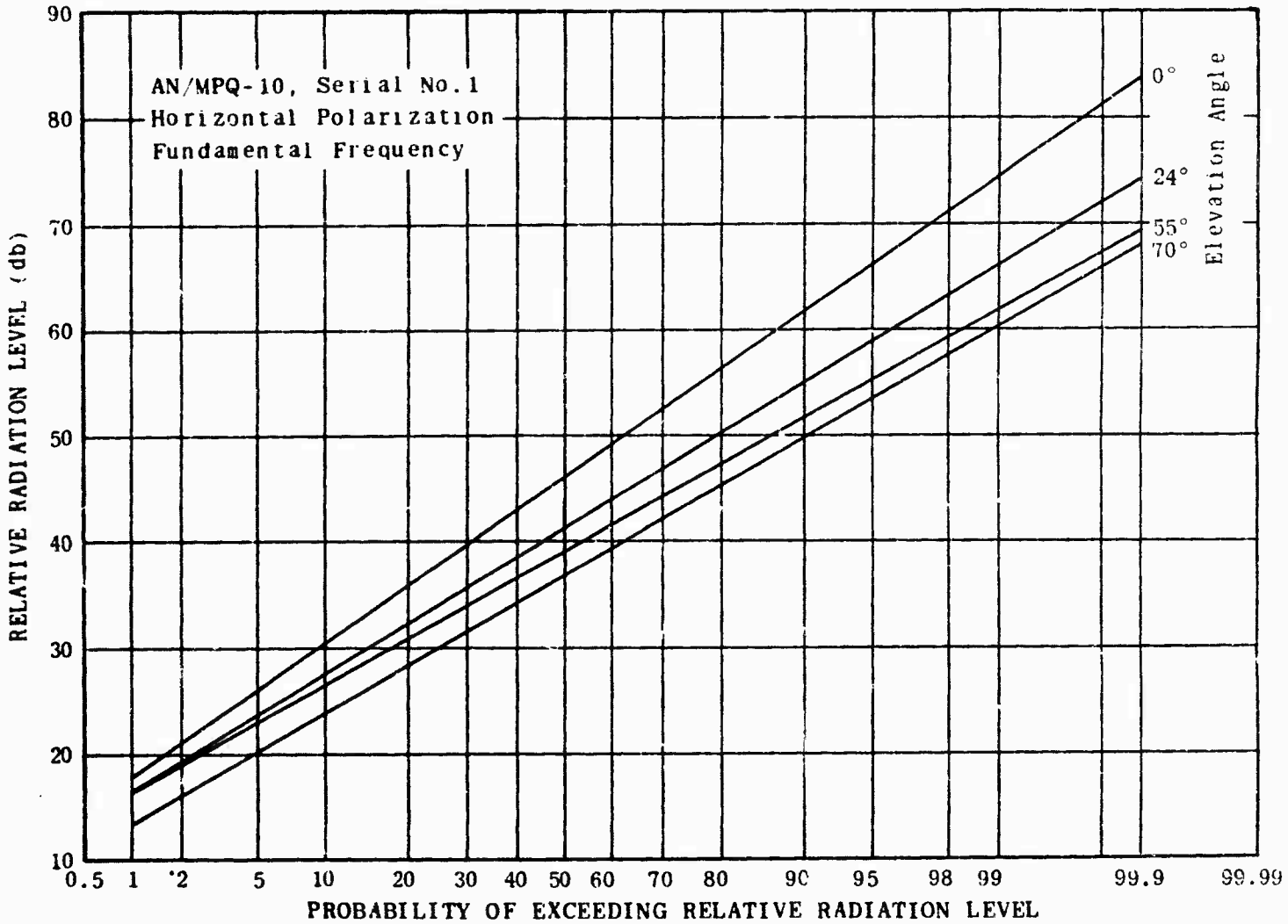

Figure 5-13. Pattern Distribution Functions.

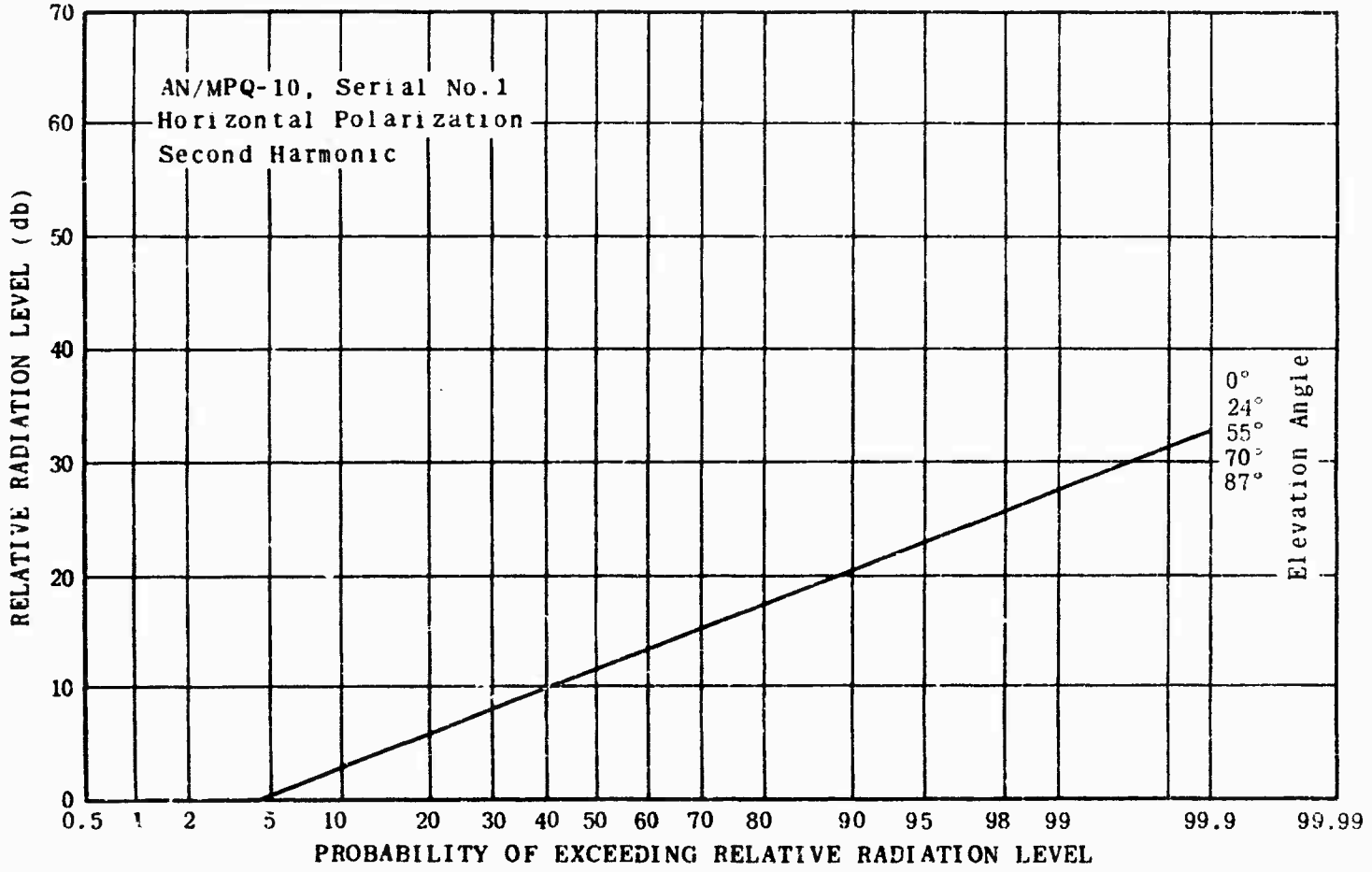

Figure 5-14. Pattern Distribution Functions.

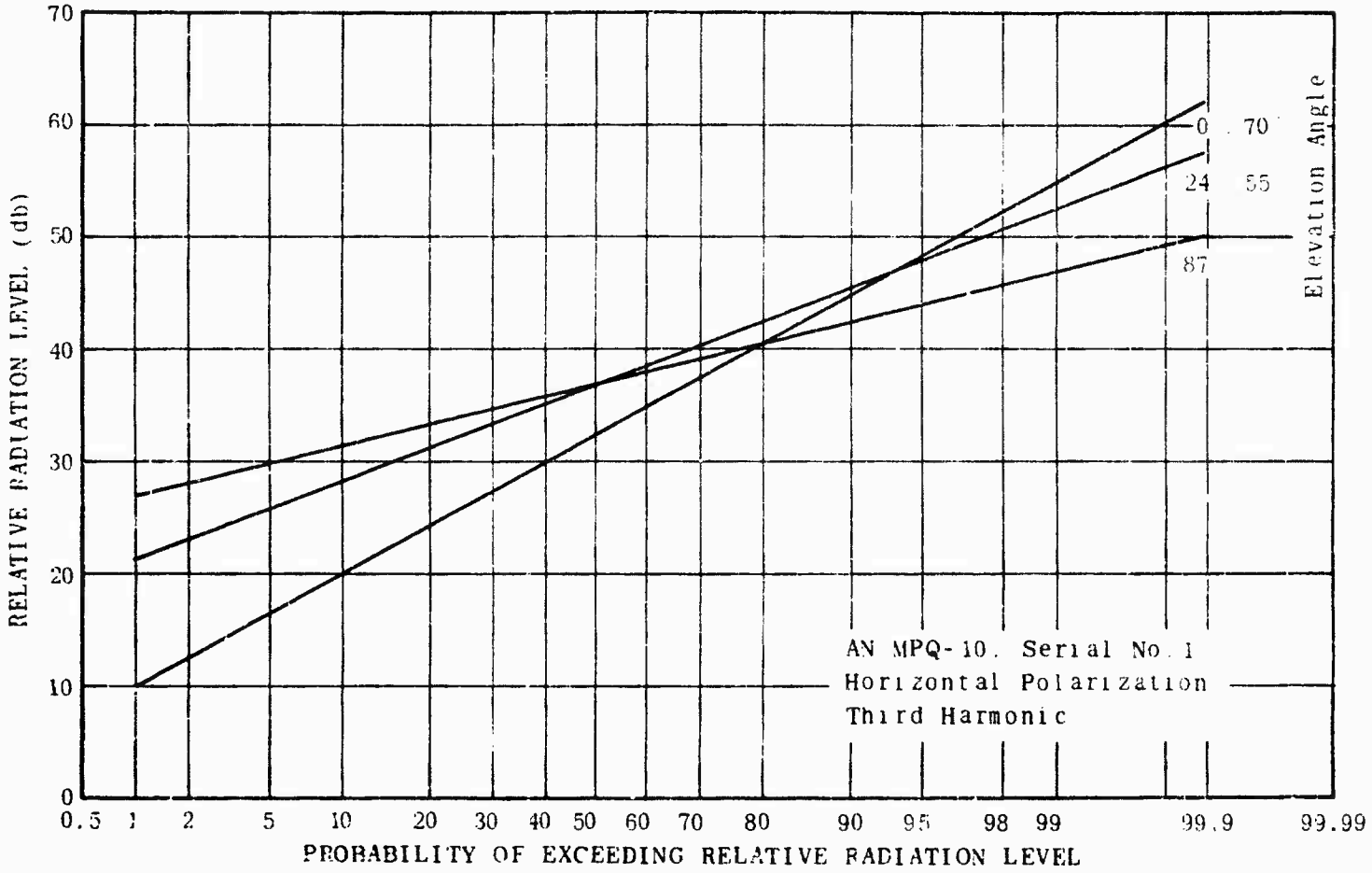

Figure 5-15. Pattern Distribution Functions.

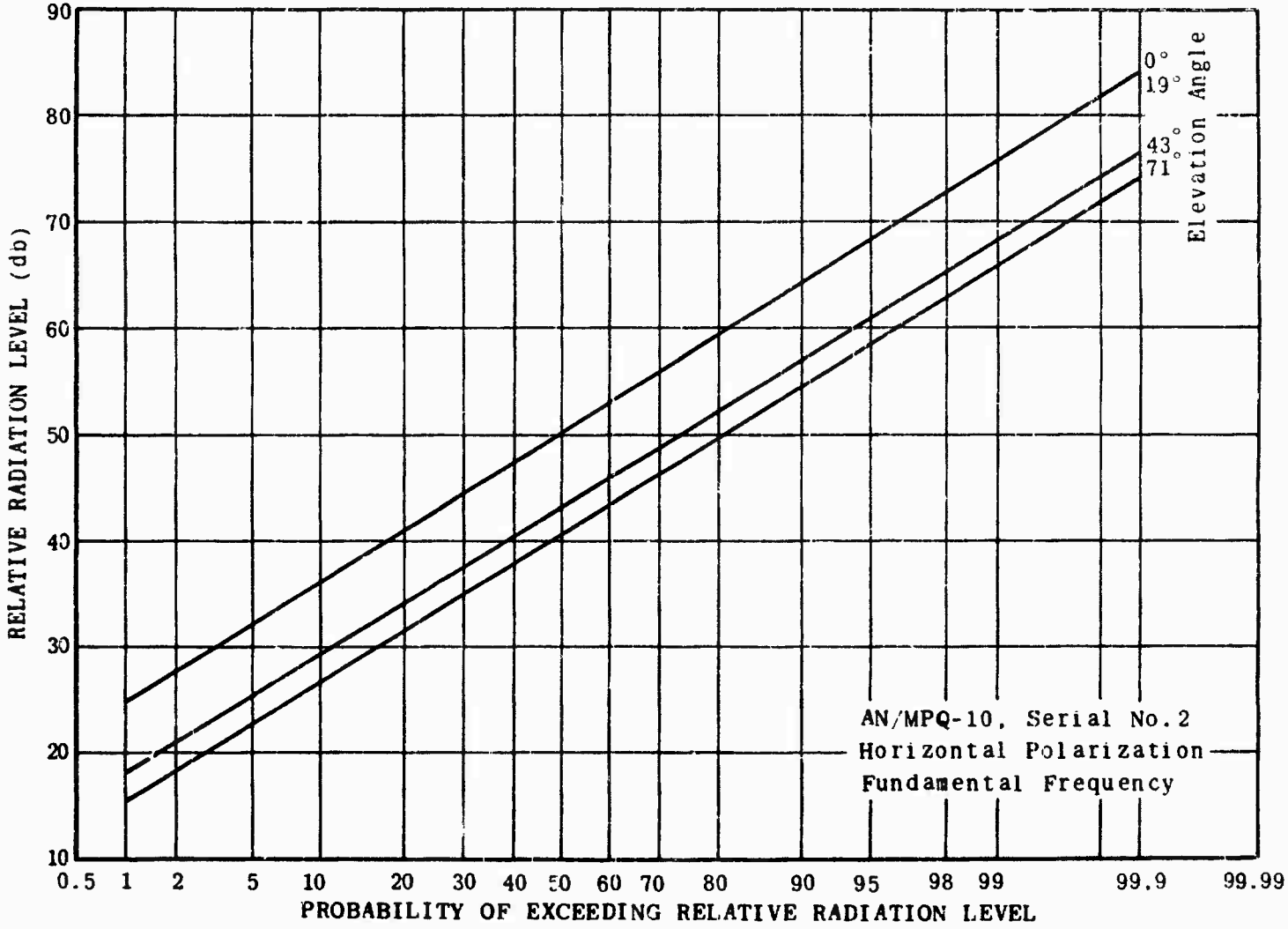

Figure 5-16. Pattern Distribution Functions.

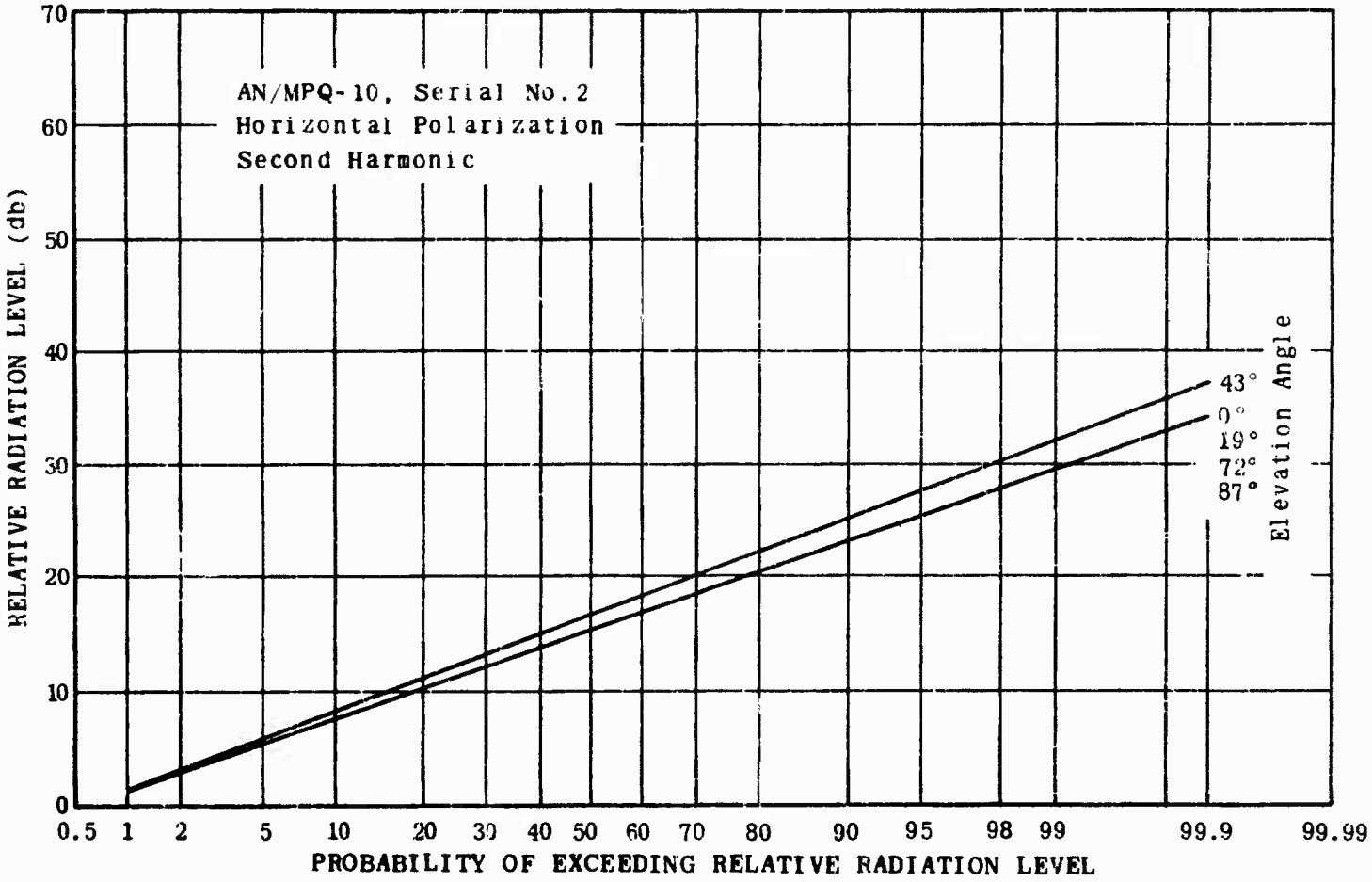

Figure 5-17. Pattern Distribution Functions.

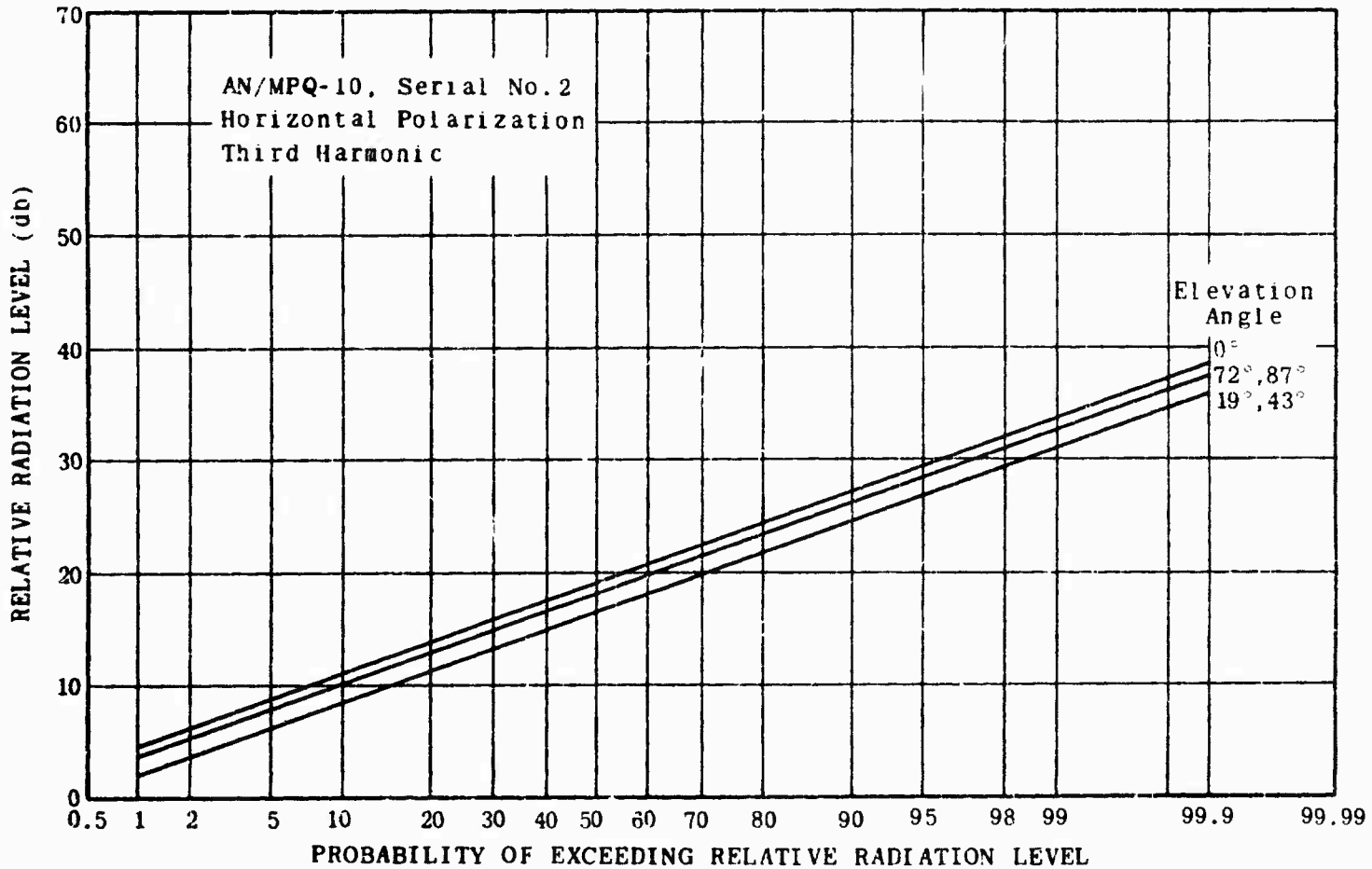

Figure 5-18. Pattern Distribution Functions.

Similarily, the vertically polarized plots, Figures 5-19 through 5-24, show little effect from a change in elevation angle. In fact, in some cases such as Figure 5-14, the pattern distribution funtion was completely unchanged for all elevation angles.

5.2 Site Effect Statistic

The site effect may be defined as the difference between an antenna pattern as it would appear in free space and the antenna pattern as it appears when the antenna is emersed in an actual operating configuration. For the purposes of interference prediction the antenna pattern is considered to be a statistic and the pattern is expressed in terms of a pattern distribution function, (PDF). Figures 5-1 through 5-12, which were just presented in Section 5 may be considered to be typical examples of the pattern distribution.

Since the antenna pattern is treated as a statistic, it then becomes logical to consider a site effect statistic. The site effect statistic is defined as the difference between the PDF for an antenna in free space and the PDF for the same antenna emersed in an actual operating configuration.

Site effects arise from the many and diverse reflecting objects which are generally in the vicinity of any operational antenna. For relatively high-gain antennas the pattern for an antenna within a site displays higher apparent radiation levels in the side and back lobes on the average than the same antenna in free space. The higher apparent radiation levels are caused by the relatively large level of energy available in the main lobe for reflection and then reception in directions from the antenna which are different from the main beam direction. The presence of reflecting and scattering objects within the site is in general least noticeable in the main beam region of the antenna. The effects of the site become more and more noticeable as the lower radiation levels from the antenna are considered. Thus, the site effect statistic may be treated as an adjustment factor for the theoretical pattern distribution function. The adjustment factor is small for the higher levels of radiation from the antenna and becomes increasingly larger for lower levels of radiation from the antenna. The adjustment factor is also significantly larger for those sites which are capable of supporting many

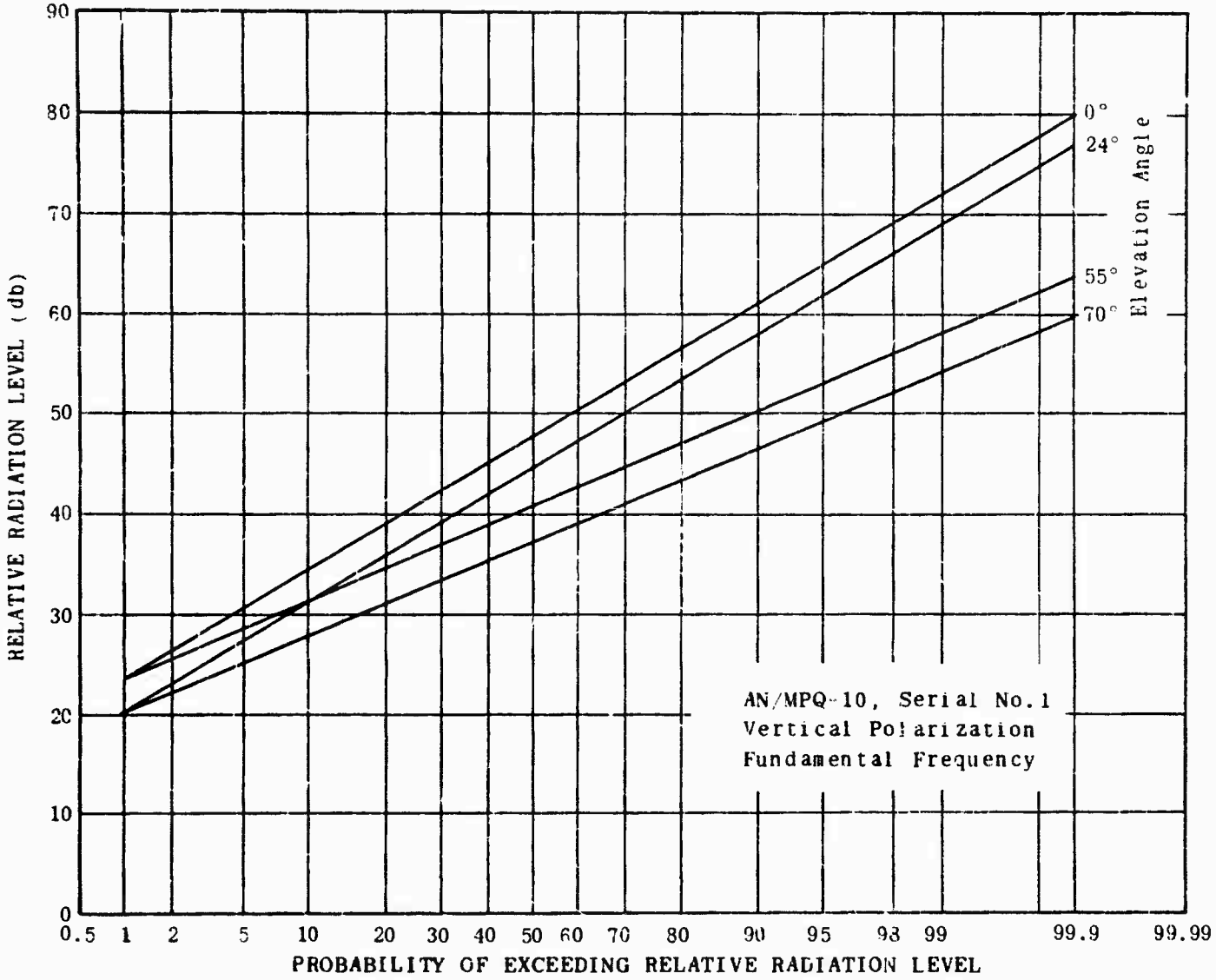

Figure 5-19. Pattern Distribution Functions.

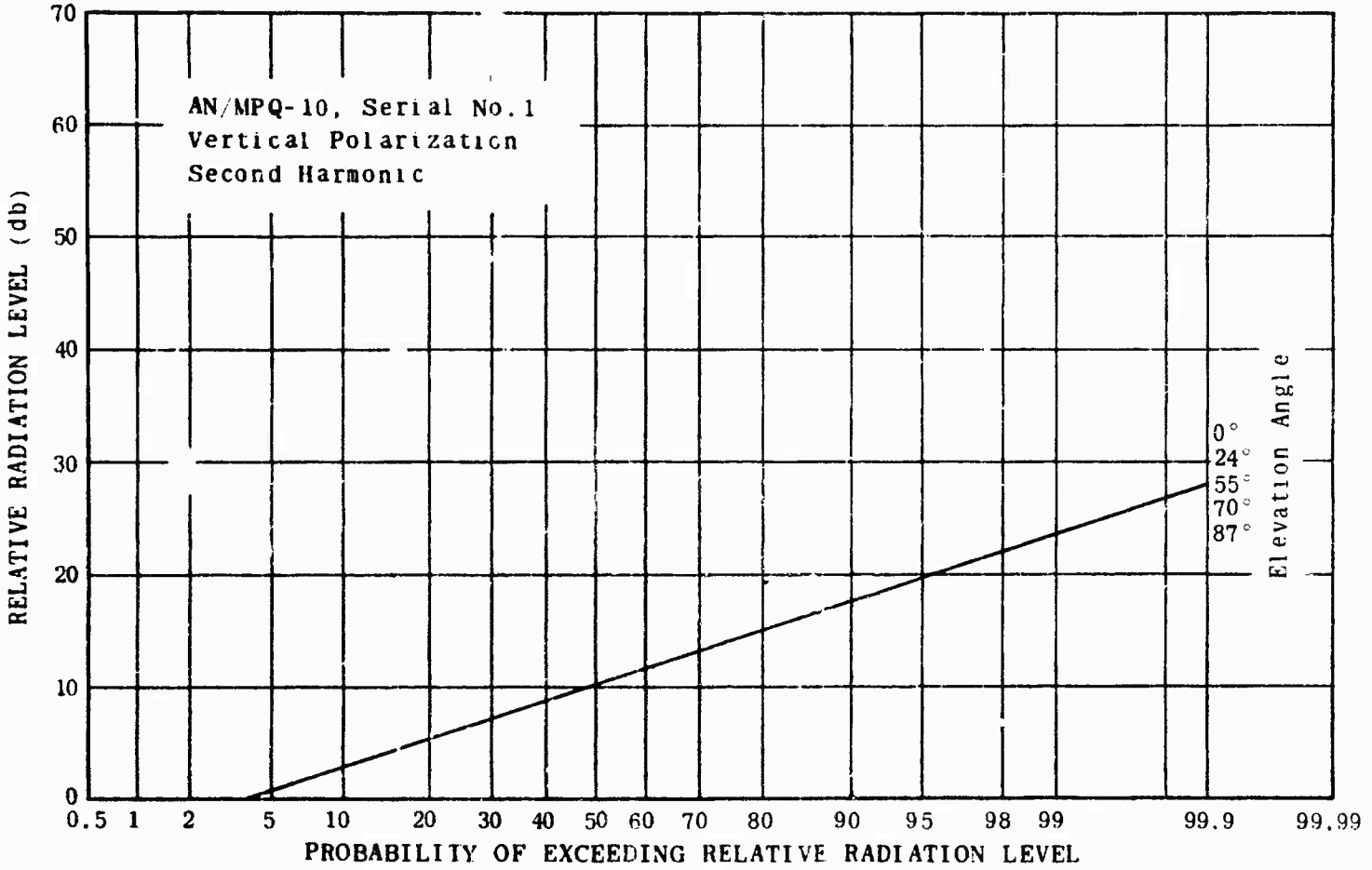

Figure 5-20. Pattern Distribution Functions.

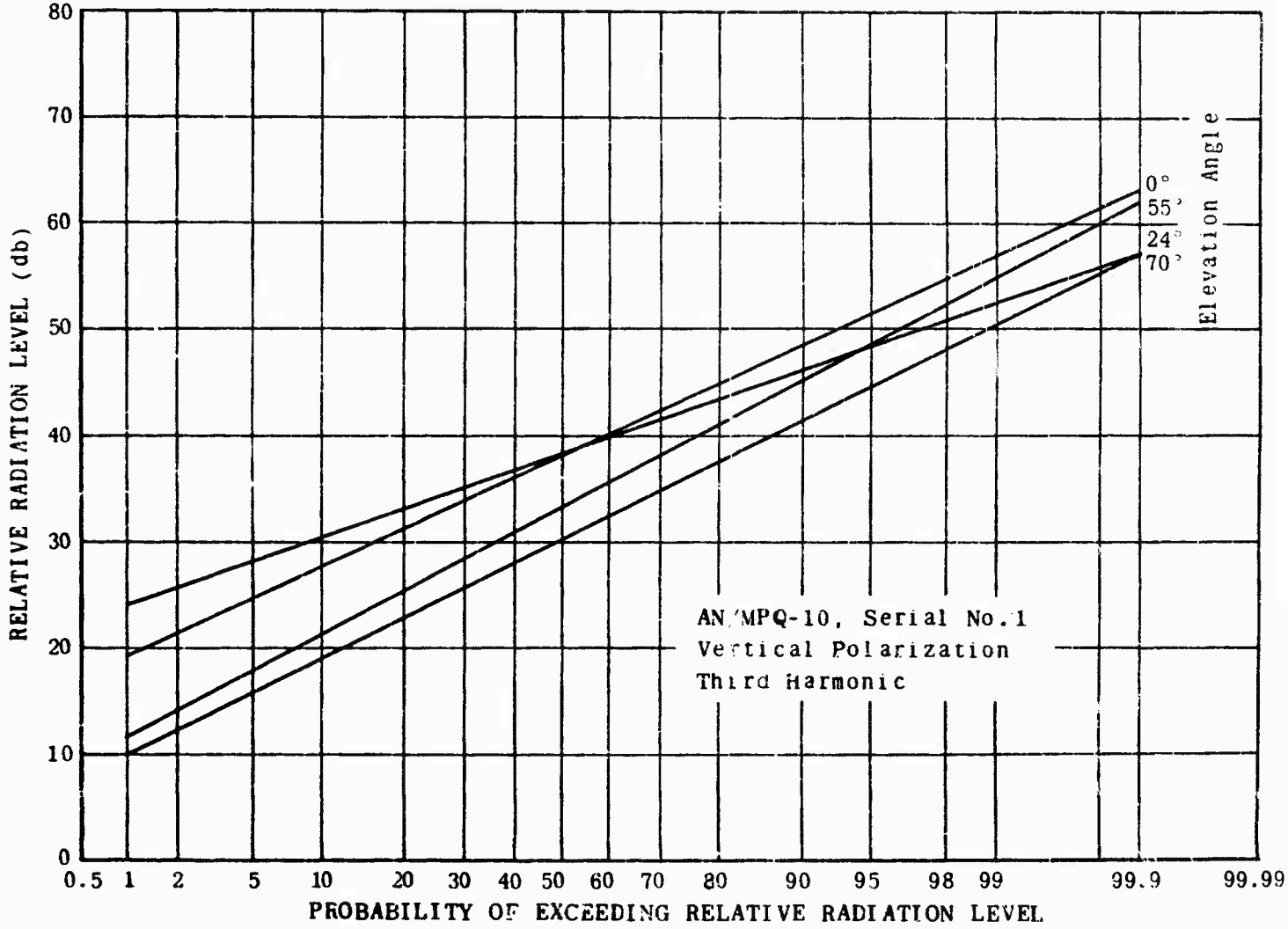

Figure 5-21. Pattern Distribution Functions.

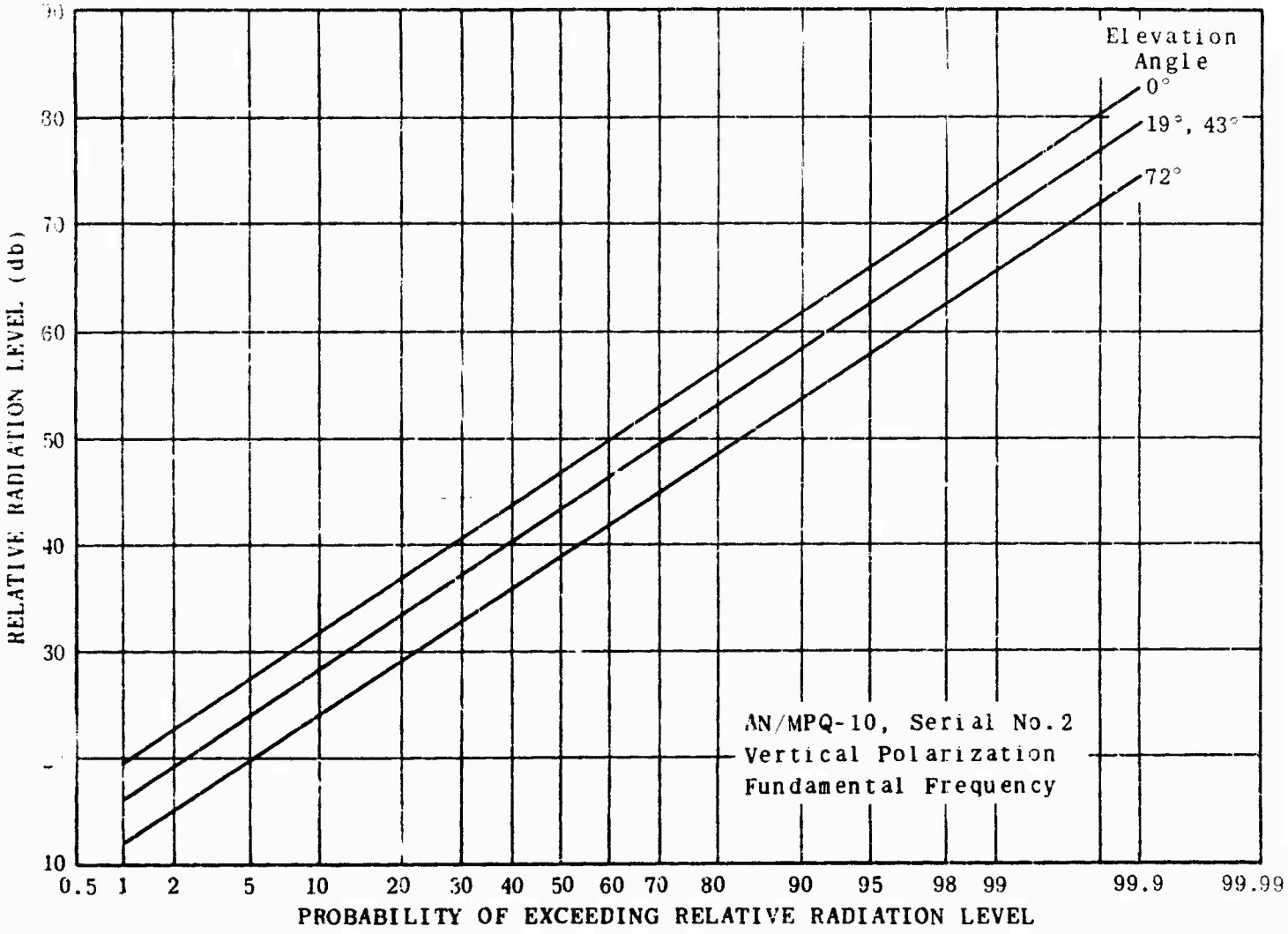

Figure 5-22. Pattern Distribution Functions.

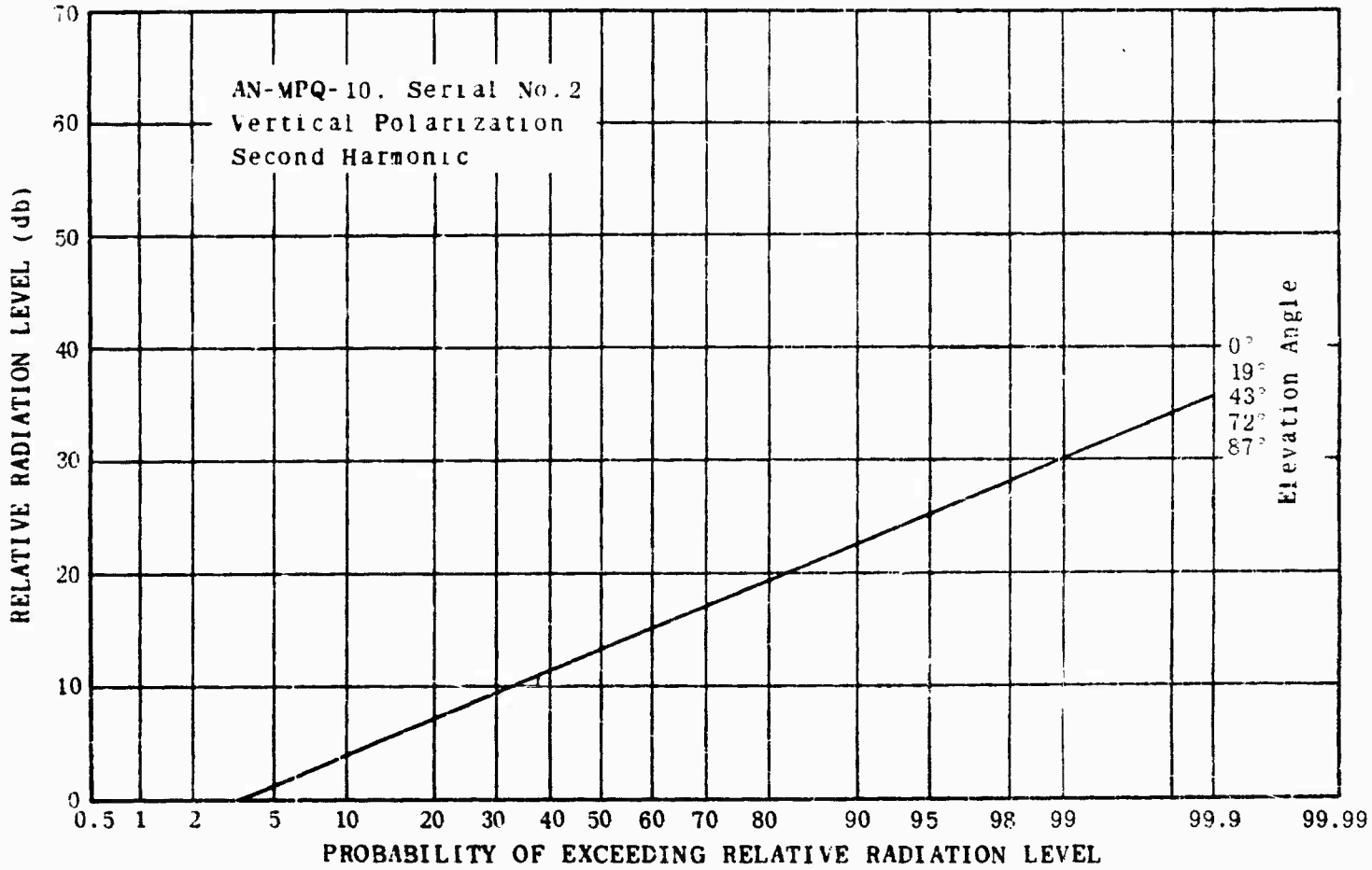

Figure 5-23. Pattern Distribution Functions.

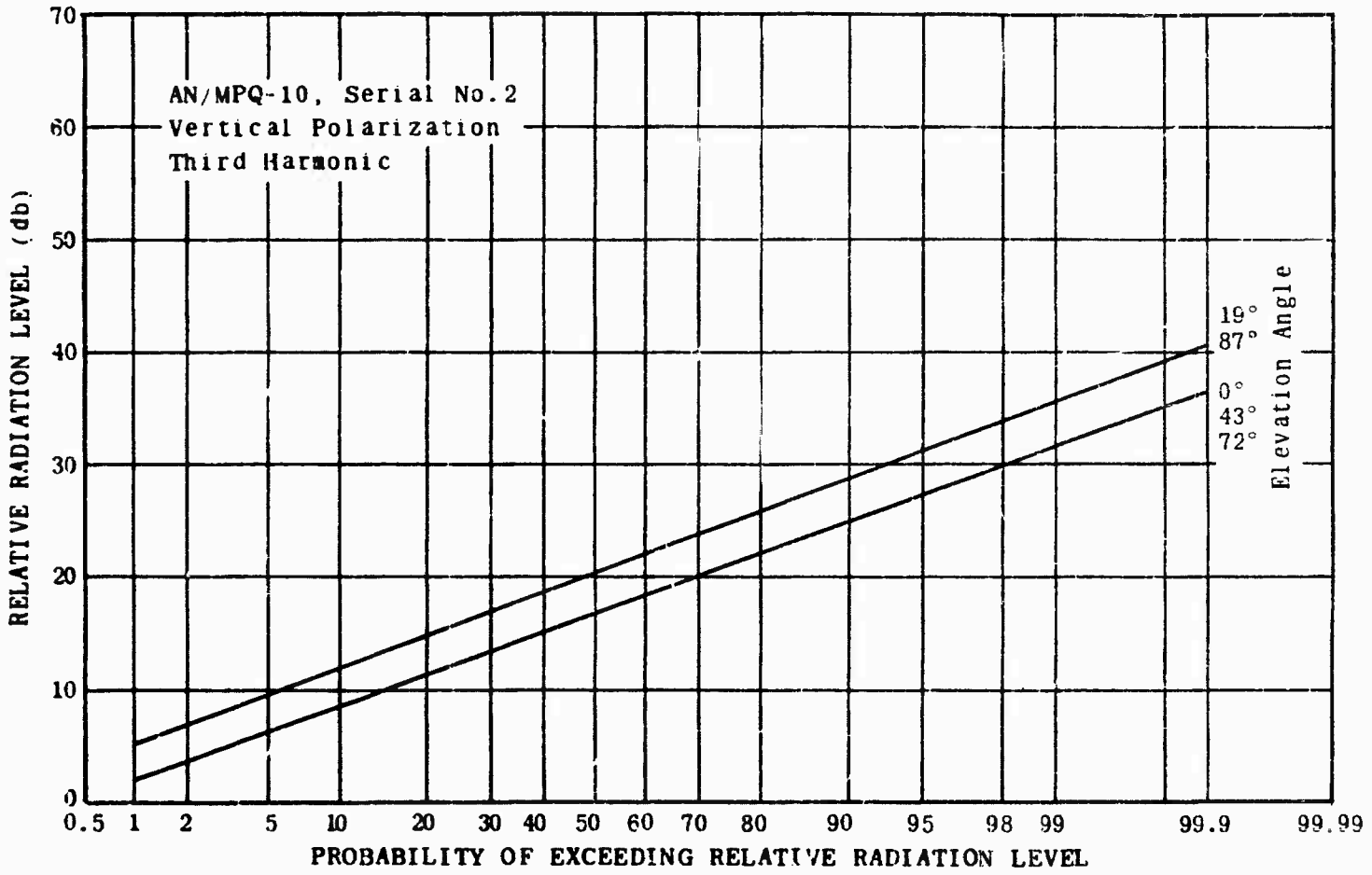

Figure 5-24. Pattern Distribution Functions.

reflection paths and significantly smaller for those sites which are capable of supporting only a few reflection paths.

Figure 5-25 depicts a typical site effect function for three general types of site conditions. The functions shown on Figure 5-25 are used in interference prediction as a correction to the theoretical pattern distribution functions. The adjustment amplitude is added point-by-point to each appropriate theoretical pattern distribution function. As the curves on Figure 5-25 indicate, the site effect statistic for a relatively open site, that is a site within which only a few reflection paths are possible, is small. The site effect statistic for a crowded site is relatively large, while the site effect statistic for an average site falls between the two extremes.

The functions plotted in Figure 5-25 show the general form of the site effect statistic. The actual numerical values are gross estimates based on past experience with measured patterns at various types of antenna sites. Measured information is presently being gathered in order to update the actual numerical values presented in Figure 5-25.

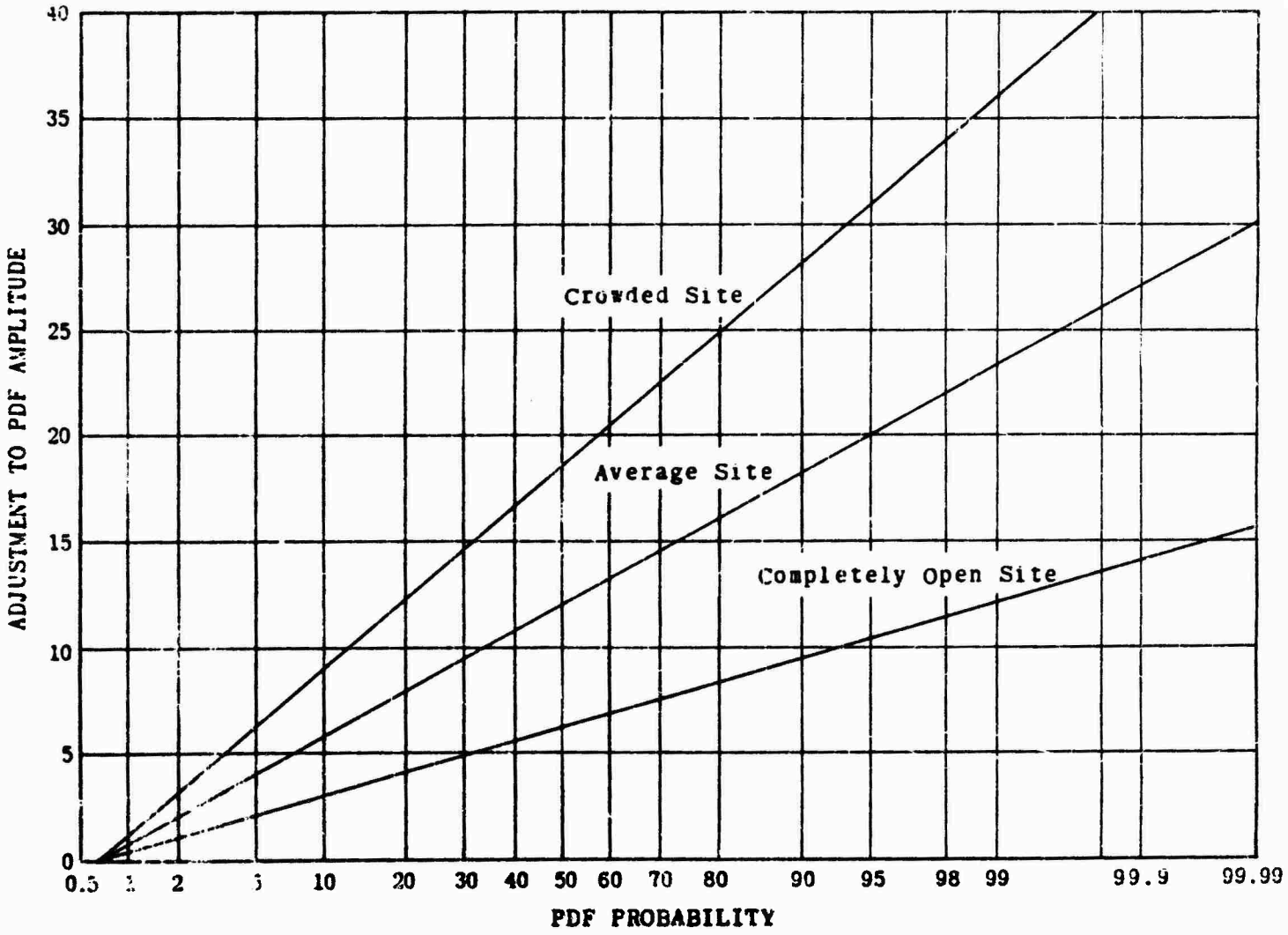

Figure 5-25. Site Statistics for Large Aperture Antennas.